UNIVERSITÉ DU LUXEMBOURG

PhD-FSTM-2023-040
The Faculty of Science, Technology and Medicine

DISSERTATION

Defence held on 10/05/2023 in Esch-sur-Alzette

to obtain the degree of

DOCTEUR DE L'UNIVERSITÉ DU LUXEMBOURG

EN *BIOLOGIE*

by

Patrycja MULICA
Born on 22 March 1992 in Mrągowo (Poland)

STUDYING THE IMPACT OF A53T α-SYNUCLEIN ON ASTROCYTIC FUNCTIONS AND ACTIVATION IN HUMAN IPSC-DERIVED CULTURES

Dissertation defence committee

Prof. Dr Anne Grünewald, dissertation supervisor
Université du Luxembourg, LCSB

Prof. Dr Alexander Skupin, chairman
Université du Luxembourg, LCSB

Dr Johannes Meiser
Luxembourg Institute of Health

Prof. Dr Tiago Outeiro
Georg-August-Universität Göttingen

Dr Philip Seibler
Universität zu Lübeck, Institut für Neurogenetik

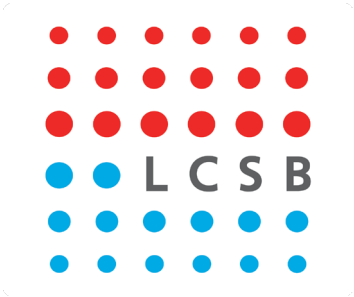

A dissertation by

Patrycja Mulica

submitted to the University of Luxembourg

in fulfillment of the requirements for the degree of

DOCTOR of PHILOSOPHY

Affidavit

I hereby confirm that the PhD thesis entitled “Studying the impact of A53T α-synuclein on astrocytic functions and activation in human iPSC-derived cultures” has been written independently and without any other sources than cited.

Luxembourg, 10th of May 2023
Patrycja Mulica

Abstract

With its high prevalence among the elderly, the movement disorder Parkinson's disease (PD) poses a major challenge for our society. Unfortunately, despite continuous efforts from the research community, we still lack the disease-modifying treatments for this condition. Therefore, it is of great importance to develop suitable models, which can be employed to better understand the molecular mechanisms underlying PD. In this context, iPSC technology offers a possibility to study the disease pathogenesis using patient-derived brain cells.

In recent years, astrocytes have come into the spotlight as potential major contributors to PD development. Yet, there is a limited number of studies utilizing iPSC-derived models to examine PD-linked mutations at endogenous levels.

This thesis aims to address the described gap by studying the effect of the A53T α-synuclein on the physiology of human iPSC-derived astrocytes. To identify a suitable model, we first compared two published protocols for the generation of iPSC astrocytes, referred to as Oksanen and Palm method, respectively. A transcriptomic analysis revealed higher maturation characteristics for Oksanen astrocytes. Furthermore, these astrocytes showed a higher similarity to their human postmortem counterparts.

Applying the Oksanen protocol, we generated astrocytes derived from a healthy individual and a patient carrying the G209A mutation in *SNCA*, corresponding to p.A53T substitution in α-synuclein. The utilization of single-cell RNA sequencing allowed us to identify perturbed molecular mechanisms exclusively in pure astrocytic populations. We could demonstrate that astrocytes have a decreased capacity to differentiate. Furthermore, we observed a distinct response of the two cell lines to triggers of activation. Interestingly, activated patient astrocytes also showed changes in pathways related to mitochondrial homeostasis.

Taken together, we show that A53T α-synuclein has a profound effect on the function of iPSC-derived astrocytes. In particular, we could demonstrate that patient astrocytes differ from healthy control cells in their activation status and with respect to mitochondrial biology. Further investigation will be required to elucidate the impact of the identified perturbations on the astrocyte-neuron interplay in the context of PD.

Acknowledgements

Now when my PhD journey comes to an end, I would like to acknowledge people whose support was of great importance for the completion of this thesis.

First and foremost, I would like to thank Prof. Dr. Anne Grünewald and Prof. Dr. Rejko Krüger for giving me a chance to explore the neurobiology field. I am truly grateful for all the advice and guidance given me throughout these years.

I would like to thank Dr. Johannes Meiser for the stimulating discussions during my yearly CET meetings. Your pieces of advice helped me to stay on track with my project.

Furthermore, I would like to thank Dr. Sandro Pereira and Dr. Peter Barbuti for introducing me to the world of iPSC-derived cultures and for all the discussions and mentorship. Additionally, I would like to express my gratitude for the help received from Dr. Carmen Venegas who generously shared her knowledge whenever needed.

I received substantial support from my colleagues from the group. I am grateful for all the moments I shared with Jenny Ghelfi, Maria Tziortziou, Soraya Hezzaz, Gideon Agyeah and Dr Kobi Wasner. You created a unique atmosphere where we can trust and support each other. Thank you for that. In particular, I would like to thank Dr. Sylvie Delcambre for working with me on various projects and her substantial contributions. I would like to also acknowledge the Translational Neuroscience group which assisted me during my initial years.

Special thanks I would like to direct to Dr. Katja Badanjak and Dr. Semra Smajic, who shared with me the majority of this journey. Thank you for all the discussions, sharing your knowledge and giving me emotional support. It really meant a lot to me.

Importantly, I would like to thank all the collaborators, both from LCSB and other institutes. In particular, I would like to acknowledge the group of Prof. Alexander Skupin, Prof. Jari Koistinaho, Dr. Enrico Glaab and Prof. Malte Spielmann. Working with you was a great experience which really taught me a lot. Furthermore, I am really grateful for the help received from Dr. Paul Antony whose skills always inspired me to explore my data further.

I would like to also acknowledge my soul siblings, Agnieszka and Karol. Thank you for supporting me since we first met during our studies till these days, thank you for listening to my long stories and for everything you do for me.

I would like to thank my colleagues Elle, Vanessa and Joanna, who took their time to read this thesis. I am also grateful for the support from the whole Polonium Foundation team. Your insights helped me to see the light at the end of the tunnel. I would like to thank my other friends in Poland and Germany. Our friendships often started at work and then you always supported me in my struggles and doubts.

Finally, I would like to thank my parents and other members of my family for their unconditional love and for always trusting my decisions. With your support I managed to believe that a girl from a small town can fulfill her big dreams of becoming a scientist. This transition wouldn’t be possible without you Bogdan, thank you for sharing with me all the ups and downs during my PhD and critically assessing all my newest discoveries.

Dissemination

The presented work is in the form of cumulative thesis. During my PhD I contributed to 5 publications mentioned below.

Introduction

My first-author review is a part of an introduction to the thesis.

Patrycja Mulica, Anne Grünewald, Sandro L. Pereira. 2021. Astrocyte-Neuron Metabolic Crosstalk in Neurodegeneration: A Mitochondrial Perspective. Front Endocrinol, 7;12:668517

Results

In the Results section there are included two first-author manuscripts.

Patrycja Mulica, Carmen Venegas, Zied Landoulsi, Katja Badanjak, Semra Smajic, Sylvie Delcambre, Jens Schwamborn, Rejko Krüger, Paul Antony, Patrick May, Enrico Glaab, Anne Grünewald, Sandro L. Pereira. Assessing the suitability of iPSC-derived human astrocytes for disease modeling. Submitted to Biological Procedures Online

Patrycja Mulica, Varun Sreenivasan, Sandro L. Pereira, Paul Antony, Kristian Händler, Kamil Grzyb, Sylvie Delcambre, Maria Tziortziou, Carmen Venegas, Semra Smajic, Katja Badanjak, Marja Koskuvi, Taisia Rolova, Rejko Krüger, Jari Koistinaho, Alexander Skupin, Malte Spielmann, Anne Grünewald. Impact of A53T α-synuclein on astrocytic functions and activation in human iPSC-derived cultures. In preparation to be submitted to the Journal of Neuroinflammation

Appendix

I contributed to two more published articles.

Kobi Wasner, Semra Smajic, Jenny Ghelfi, Sylvie Delcambre, Cesar A. Prada-Medina, Evelyn Knappe, Giuseppe Arena, Patrycja Mulica, Gideon Agyeah, Aleksandar Rakovic, Ibrahim Boussaad, Katja Badanjak, Jochen Ohnmacht, Jean-Jacques Gérardy, Masashi Takanashi, Joanne Trinh, Michel Mittelbronn, Nobutaka Hattori, Christine Klein, Paul Antony, Philip Seibler, Malte Spielmann, Sandro L Pereira, Anne Grünewald. 2022. Parkin

Deficiency Impairs Mitochondrial DNA Dynamics and Propagates Inflammation. Mov Disord., 37(7):1405-1415

Katja Badanjak, Patrycja Mulica, Semra Smajic, Sylvie Delcambre, Leon-Charles Tranchevent, Nico Diederich, Thomas Rauen, Jens C Schwamborn, Enrico Glaab, Sally A Cowley, Paul M. A. Antony, Sandro L. Pereira, Carmen Venegas, Anne Grünewald. 2021. iPSC-derived Microglia as a Model to Study Inflammation in Idiopathic Parkinson's Disease. Front Cell Dev Biol., 9:740758

Table of contents

List of abbreviations

AD	Alzheimer’s disease
ATP	adenosine triphosphate
BMP	Bone Morphogenetic Protein
CBP	CREB-binding protein
cDNA	complementary deoxyribonucleic acid
CNS	Central Nervous System
CNTF	Ciliary Neurotrophic Factor
CRISPR	Clustered Regularly Interspaced Short Palindromic Repeats
CSF	cerebrospinal fluid
CT-1	Cardiotrophin-1
2,4-D	2,4-Dichlorophenoxyacetic acid
DNA	deoxyribonucleic acid
ELISA	enzyme-linked immunosorbent assay
FGF2	fibroblast growth factor 2
IL-1β	Interleukin-1 beta
iPSCs	Induced Pluripotent Stem Cells
L-DOPA	l-3,4-dihydroxyphenylalanine
LIF	Leukemia Inhibitory Factor
mtDNA	mitochondrial deoxyribonucleic acid
MuSiC	MUlti-Subject SIngle Cell deconvolution
NFIA	Nuclear Factor I A
NF-κB	Nuclear Factor Kappa B
PD	Parkinson’s disease
qPCR	quantitative real-time polymerase chain reaction
RNA	ribonucleic acid
ROS	reactive oxygen species
SHP-2	SH2 domain-containing protein tyrosine phosphatase-2
SNARE	soluble N-ethylmaleimide-sensitive factor attachment protein receptors
SNCA	Synuclein alpha
TCA	tricarboxylic acid cycle
TNF-α	Tumor Necrosis Factor alpha

1 Introduction

1.1 Parkinson's disease

1.1.1 Epidemiology

Parkinson's disease (PD) is the second most frequent cause of neurodegeneration after Alzheimer's disease [1]. The prevalence of PD is estimated to reach 1% among people older than 60 years and 0.3% in the total population [2]. The typical age of onset is between 65 and 70 years, with symptoms occurring before the age of 40 in less than 5% of cases [3]. According to recent estimations, the prevalence of PD will further surge due to the drastically aging population [4].

Strikingly, the risk of developing PD is twice as high in men than in women [5]. Furthermore, the mortality rate is increased among the men which further underlines the sex-related differences [6].

1.1.2 Symptoms and diagnosis

PD is characterized by motor symptoms, which encompass rigidity, resting tremor and bradykinesia and which typically manifest asymmetrically [7]. Aside from these motor impairments, patients can present various non-motor symptoms such as dysautonomia, rapid eye movement sleep behavior disorder (RBD), depression and olfactory impairments. Notably, these signs may occur long before the typical motor symptoms [8]. PD is also associated with mood disorders, dementia and chronic pain [9], as well as shortened life expectancy [1].

The proper diagnosis of PD still remains a challenge, given the fact that it is frequently confused with other forms of parkinsonism such as progressive supranuclear palsy, multisystem atrophy and corticobasal degeneration [10]. To avert such mistakes, the Movement Disorder Society prepared guidelines to ensure a reliable diagnosis [11]. Accordingly, the assessment is based on the presence of cardinal symptoms such as tremor, rigidity and bradykinesia, as well as the identification of supportive criteria and a lack of absolute exclusion criteria or red flags [12]–[14]. To assist in the patient examination, genetic testing, assessment of responsiveness to L-DOPA treatment and neuroimaging may be applied [10].

1.1.3 Etiology

The majority of PD cases are described as idiopathic due to the lack of known genetic cause of the disease. However, around 20-30% of PD patients present with a familial form of the disease [15], [16]. 5-10% of all cases are linked to mutations in a single gene [15]. An autosomal recessive mode of inheritance together with an early disease onset was described for mutations in *Parkin* (*PRKN*), *PTEN Induced Kinase 1* (*PINK1*), and *DJ-1* (*PARK7*) [17]. In contrast, an autosomal dominant pattern was observed for carriers of mutations in the *Synuclein Alpha* (*SNCA*), *Leucine Rich Repeat Kinase 2* (*LRRK2*) and *Vacuolar Protein Sorting associated Protein 35* (*VPS35*) genes [18]. Furthermore, additional genes have been described in association with PD [19]. For the remaining familial cases, a genetic cause is still unknown but it is hypothesized that the missing heritability might be attributed to non-coding variants and interaction of several genes which require further studies [15].

Besides genetic factors, there is a strong body of evidence suggesting the importance of environmental factors in PD development [20]. Exposure to pesticides such as paraquat, rotenone, 2,4-D, as well as dithiocarbamates and organochlorines was linked to a higher probability of developing PD. A similar positive correlation was also observed for individuals suffering from head injuries [4]. In contrast, cigarette smoking, fruit and vegetable consumption and the use of statins have been associated with a reduced risk of PD development [1], [4], [9].

1.1.4 Pathology

The hallmark of PD is the degeneration of dopaminergic neurons, which are located in the *substantia nigra pars compacta* of the midbrain [4] and have projections to the basal ganglia [21]. Another typical feature of the disorder is the presence of Lewy bodies composed of misfolded α-synuclein, which can be found in the patients' brains [22]. Despite the dopaminergic system being mostly affected by abnormal α-synuclein aggregation, numerous studies have shown the presence of such deposits in cardiac, gastrointestinal, and other body parts [23].

The reasons for the specific vulnerability of dopaminergic neurons in PD are still poorly understood. One possible explanation might be their autonomous pace-making activity and calcium homeostasis [12]. In addition, numerous reports implicated mitochondrial

dysfunction, oxidative stress, excitotoxicity, apoptosis, the ubiquitin-proteasome system, reactive oxygen species formation and neuroinflammation in the PD pathogenesis [7], [8].

1.1.5 Treatment

To date, no disease-modifying treatments effective against PD are available [12]. However, several drugs have been established to treat PD symptoms and thus improve the quality of life of patients. In the early phase of the disease, anticholinergic drugs are frequently applied to control motor symptoms [7]. As PD progresses, typical treatment regimes involve the administration of levodopa or of dopamine agonists. Levodopa is the most widely used drug to alleviate motor symptoms and considered to be the most effective one [12]. As non-motor symptoms constitute a substantial part of the PD spectrum, they are targeted in the therapy as well [2]. Furthermore, deep-brain stimulation can be used when PD has already progressed substantially in patients [12].

One may envisage that therapies targeting the disease mechanism will gain importance in the near future [4].

1.2 Pathophysiology of α-synuclein

1.2.1 Protein structure and function

α-synuclein is a 14 kDa protein encoded by *SNCA* gene located on chromosome 4 [24]–[26]. Its abundance in the brain is striking, accounting for 1% of the total protein content in cytosolic brain fractions [27]. The localization of α-synuclein is mainly described as presynaptic [28], [29], however, numerous reports showed its presence in the nucleus as well, in particular under stress conditions [30]–[36]. Furthermore, α-synuclein was found in neurons in their cell soma and axons [27].

With respect to protein structure, α-synuclein consists of three distinct domains [37], [38]. On its N-terminus it possesses seven copies of 11-residue imperfect repeats, which have the tendency to form an amphipathic helix, when bound to lipid membranes [39]–[44]. The central domain of the protein is called the “non-A beta component of AD amyloid (NAC)” [38], since it was originally discovered as a component of amyloid plaques [45]. This part of α-synuclein was shown to be instrumental in the aggregation process observed in synucleinopathies [46]. In contrast, the C-terminus remains natively unfolded [47] and was

shown to be involved in numerous functions such as calcium binding [48], chaperone activity of α-synuclein [49], oxidative stress [50] and most importantly, the prevention from aggregation [51]. Apart from the α-helix formed on the N-terminus upon lipid binding, α-synuclein is generally considered a natively unfolded protein in aqueous solutions [40], [47], [52], [53].

Although substantial progress has been made in elucidating the function of α-synuclein, its role remains ambiguous [54]. Among the most prominent functions exerted by α-synuclein is its link to synaptic vesicle recycling (Figure 1). There is a strong body of evidence suggesting that the protein plays a role in the majority of the steps constituting the process [55]. Its involvement was explained by various mechanisms. α-synuclein might inhibit the activity of phospholipase D2, which is implicated in vesicle trafficking [56]–[58]. Additionally, it might influence vesicle recycling by modulating actin polymerisation [59]. Another function linked to α-synuclein's involvement in vesicle recycling is its chaperone activity [60]. The protein was shown to facilitate proper folding of proteins forming the SNARE complex [61], [62].

Furthermore, α-synuclein can regulate neurotransmitter synthesis, storage and release, which is in particular observed for dopaminergic neurons [55], [63]. Modulation of the activity of the dopamine transporter as well as of tyrosine hydroxylase might result in altered dopaminergic neurotransmission [64]–[69].

There is still a major controversy regarding the role of α-synuclein in the brain. Deletion of both α-synuclein and β-synuclein do not affect the survival of mice or their brain function [70]. Nevertheless, it seems that α-synuclein is crucially involved in synaptic plasticity and in the regulation of neuronal activity during development [55], [71], [72].

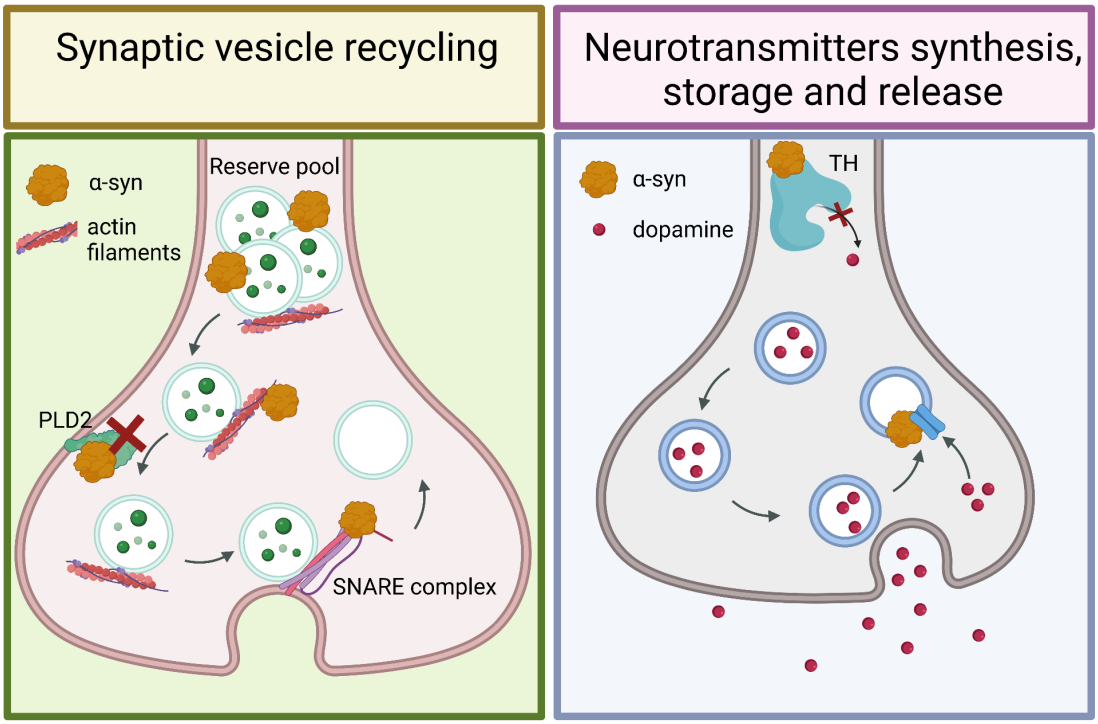

Figure 1. α-synuclein functions at the synapse. α-synuclein is involved in all steps of synaptic vesicle recycling as well as neurotransmitter synthesis, storage and release as it was described in the studies on dopaminergic neurons. PLD2, phospholipase D2, TH, tyrosine hydroxylase. Figure was generated using BioRender.

1.2.2 α-synuclein pathology

α-synuclein has attracted considerable attention as a potential trigger of PD pathology [73]. This hypothesis became especially prevalent after several point mutations and multiplications of the *SNCA* gene were discovered, which all lead to the development of PD [74]–[80]. Importantly, in the majority of cases these mutations cause relatively early-onset disease with an autosomal dominant pattern of inheritance and affect several α-synuclein properties, in particular its propensity to aggregate [81], [82]. The premise of α-synuclein relevance for the disease pathology was further strengthened by the identification of α-synuclein as the main component of Lewy bodies [22], [83]. However, α-synuclein deposition does not occur only in Lewy bodies but also in neurites, with the latter being affected in the initial phase of the disorder [84]. Inspired by this observation, the famous theory of α-synuclein spreading was introduced. In brief, six stages of PD were proposed, where α-synuclein accumulation starts at the olfactory bulb and the dorsal vagal nucleus, reaching the substantia nigra at stage 3 and the cortex in the final phase [85].

Generally, it is believed that there is a direct link between α-synuclein aggregation and PD pathology. However, it is still unclear which species is the most toxic form [73]. α-synuclein usually aggregates gradually, forming oligomers at first, then protofibrils and finally fibrils [86]. There is a growing body of evidence supporting the concept of oligomers representing the most toxic form [87]–[91]. Importantly, this standpoint is supported by the identification of oligomers in the brains of patients suffering from synucleinopathies [92]–[94]. In contrast, the toxicity status of fibrils is very controversial. Numerous reports showed their link to PD pathogenesis [95]–[98], whereas others described them as protective [99], [100]. The picture is further confounded by the different propensity of various *SNCA* point mutations to form either fibrils or oligomers. Whereas the A53T mutation was reported to support the tendency of the protein to fibrilize, A30P causes oligomerization [101], [102].

α-synuclein was reported to be post-translationally modified, which might also affect its propensity to aggregate [103]–[107]. The most studied post-translational modification is phosphorylation at serine 129. In brains of patients suffering from dementia with Lewy bodies, it was shown that 90% of aggregated α-synuclein is phosphorylated [108]. Yet, it is still unclear what the relationship is between phosphorylation, α-synuclein aggregation and toxicity [109]. Additionally, glycation has been also shown to be associated with higher toxicity of α-synuclein [110].

Despite a pivotal focus being placed on understanding the dynamics of α-synuclein aggregation, there is still an ongoing debate about the mechanisms of protein-mediated toxicity. The question remains if it is caused by a pathological gain of function associated with aggregates or rather loss of function. The latter scenario presumably occurs when functional α-synuclein is accumulated in inclusions and thus can no longer fulfill its role in the cell [111].

Importantly, α-synuclein can be found not only in the cytosol but also in various organelles such as the nucleus, mitochondria and the endoplasmic reticulum (ER) [74]. In particular, numerous studies link α-synuclein to mitochondrial impairments in PD. Initially, in various patient-derived samples including nigral tissue, a defect in respiratory chain complex I was detected, which suggested that mitochondrial dysfunction is of great importance for the pathogenesis of PD [74], [112]–[114]. This finding was supported by data obtained from experiments in transgenic mice and in vitro cultures of human neurons showing the presence of α-synuclein in mitochondria and the concomitant impairment of complex I [115]–[117]. Other studies demonstrated that α-synuclein might promote fragmentation of mitochondria [118], [119] and mtDNA damage [119]. Interestingly, it was also shown that

α-synuclein might regulate mitochondrial biogenesis by indirect means. Under oxidative stress conditions the protein was detected in the nucleus, where it was bound to the promoter of PGC-1alpha [120], the main controller of mitochondrial biogenesis [121]. Conversely, a defect in these organelles associated with increased ROS production can also affect the aggregation process of α-synuclein [122], [123]. Underlining the importance of the interplay between α-synuclein and mitochondria in PD pathology, the A53T α-synuclein mutation caused the protein to translocate to mitochondria, which coincides with decreased complex I activity and increased fragmentation of the organelles [124].

1.2.3 α-synuclein pathology in glial cells

Historically, PD was regarded as a disorder that primarily affected neurons. However, accumulated evidence suggests that the dysfunction of glial cells might be an important contributing factor to the disease [125], [126]. α-synuclein inclusions are frequently detected in glial cells of PD patients, both in the regions affected by neuronal pathology and reactive gliosis and in areas without clear signs of such pathologies [127], [128]. Since α-synuclein is primarily known as a neuronal protein, numerous studies focused on investigating protein release and uptake by neighboring glial cells [129]. Indeed, it was reported that α-synuclein can pass through the cell membrane and emerge in the extracellular space [130]–[132]. This release can be mediated by exosomes and nanotubes [133]–[138]. Subsequently, the protein may be taken up by astrocytes, microglia or oligodendrocytes [139]–[145]. Interestingly, inter-glial transfer of α-synuclein has also been observed - a feature that is currently understudied, but which might contribute to PD pathology [146], [147].

Regarding the effects of endogenous α-synuclein on astrocytic physiological functions and their contribution to PD, our knowledge is still limited. Yet, there are first reports using mice selectively expressing human A53T α-synuclein in astrocytes. Using this approach, it was shown that dysfunctional α-synuclein can trigger reactive astrogliosis, impairs astrocytic functions and causes neuronal demise [148]. These findings support the notion that astrocytes constitute important players in the pathogenesis of PD, although further studies will be needed to elucidate the various levels of their involvement in the disease.

1.3 Manuscript I

Astrocyte-Neuron Metabolic Crosstalk in Neurodegeneration: a Mitochondrial Perspective

Patrycja Mulica[1], Anne Grünewald[1,2]*, Sandro L. Pereira[1]

[1]Luxembourg Centre for Systems Biomedicine, University of Luxembourg, Esch-sur-Alzette, Luxembourg

[2]Institute of Neurogenetics, University of Lübeck, Lübeck, Germany

This article was published in the Frontiers of Endocrinology.

1.3.1 Preface

Astrocytes are fundamental for maintaining brain homeostasis by supporting the physiological functions of neurons [149]. Therefore, it becomes increasingly clear that studying the astrocyte-neuron interplay might be key for understanding the development of numerous neurodegenerative diseases, in particular PD [125]. Furthermore, with the advent of novel protocols to generate iPSC-derived model systems, we can study PD-associated protein at the endogenous level, which provides novel insights into the mechanisms underlying the pathogenesis of the movement disorder [150].

In this review, we aimed at summarizing the current knowledge of the contribution of astrocytes to neurodegeneration. In particular, we focused on their metabolic support function for neurons. We compiled the literature, which explores the importance of astrocyte-neuron crosstalk in AD and PD. Moreover, since mitochondria play a key role in cellular metabolism, we discussed their involvement in this crosstalk. Finally, we highlighted the relevance of iPSC-derived cellular models for studying astrocytic metabolic functions in AD and PD.

Regarding my contribution to the manuscript, I was responsible for writing the following chapters: Introduction, Heterogeneity of Astrocytes, Cellular Functions of Astrocytes and iPSC-derived Astrocyte Models to Study Metabolism in Neurodegenerative Diseases. Additionally, I wrote two sub-chapters in the section entitled Astrocyte-Neuron Metabolic Crosstalk in Health and Neurodegenerative Diseases, namely Mitochondria and Astrocyte-Neuron Coupling as well as Astrocytic Calcium Signaling and Astrocyte-Neuron Crosstalk. Moreover, I prepared figures 1 and 3 and I contributed to the writing of the abstract.

1.3.2 Manuscript

frontiers in Endocrinology

REVIEW
published: 07 May 2021
doi: 10.3389/fendo.2021.668517

Astrocyte-Neuron Metabolic Crosstalk in Neurodegeneration: A Mitochondrial Perspective

Patrycja Mulica[1], *Anne Grünewald*[1,2*] *and Sandro L. Pereira*[1]

[1] Luxembourg Centre for Systems Biomedicine, University of Luxembourg, Esch-sur-Alzette, Luxembourg, [2] Institute of Neurogenetics, University of Lübeck, Lübeck, Germany

Converging evidence made clear that declining brain energetics contribute to aging and are implicated in the initiation and progression of neurodegenerative disorders such as Alzheimer's and Parkinson's disease. Indeed, both pathologies involve instances of hypometabolism of glucose and oxygen in the brain causing mitochondrial dysfunction, energetic failure and oxidative stress. Importantly, recent evidence suggests that astrocytes, which play a key role in supporting neuronal function and metabolism, might contribute to the development of neurodegenerative diseases. Therefore, exploring how the neuro-supportive role of astrocytes may be impaired in the context of these disorders has great therapeutic potential. In the following, we will discuss some of the so far identified features underlining the astrocyte-neuron metabolic crosstalk. Thereby, special focus will be given to the role of mitochondria. Furthermore, we will report on recent advancements concerning iPSC-derived models used to unravel the metabolic contribution of astrocytes to neuronal demise. Finally, we discuss how mitochondrial dysfunction in astrocytes could contribute to inflammatory signaling in neurodegenerative diseases.

Keywords: metabolism, astrocytes, neurons, neurodegeneration, Parkinson's disease, Alzheimer's disease

OPEN ACCESS

Edited by:
Effie Tozzo,
Cellarity, United States

Reviewed by:
Jeni Sideris,
Astellas Pharma, United States
Tamas Kozicz,
Mayo Clinic, United States

****Correspondence:***
Anne Grünewald
anne.gruenewald@uni.lu

Specialty section:
This article was submitted to Translational Endocrinology, a section of the journal Frontiers in Endocrinology

Received: *16 February 2021*
Accepted: *22 April 2021*
Published: *07 May 2021*

Citation:
Mulica P, Grünewald A and Pereira SL (2021) Astrocyte-Neuron Metabolic Crosstalk in Neurodegeneration: A Mitochondrial Perspective. Front. Endocrinol. 12:668517. doi: 10.3389/fendo.2021.668517

INTRODUCTION

Neurodegenerative diseases can be grouped into a large class of disorders characterized by the gradual loss of various neuronal populations (1). The symptoms can be diverse depending on the cell types being affected, ranging from dementia and motor dysfunction to behavioral alterations (2). The incidence of Alzheimer's (AD) and Parkinson's disease (PD) was estimated in 2016 to reach globally over 43 and 6 million cases respectively, which positions them among the most common neurodegenerative disorders to date (3). Both of these diseases are associated with an extensive accumulation of protein aggregates; in AD patient brains such abnormalities are formed mainly by amyloid-beta (Aβ) and Tau proteins, whereas α-synuclein (α-SYN) is linked to the pathology of PD (2). So far, neurodegenerative diseases have been regarded primarily as neuronal pathologies, however, recent findings suggest that glial cells might play an important role in the disease formation and progression (4). In particular, astrocytes, as the cells supporting neuronal function, seem to be of great importance for our understanding of underlying disease mechanisms (5). In our review, we will focus on astrocytic metabolism as a key aspect of the astrocyte-neuron interplay

(**Figure 1**), which, when disturbed, likely accelerates neuronal demise. In this context, we will illuminate recent advances concerning the role of mitochondria - organelles that are not only crucial for cellular metabolism, but also involved in inflammatory signaling. In addition, to highlight the need for research on neurodegeneration at the endogenous level, we compare the current literature on iPSC models used to study astrocytic metabolism.

HETEROGENEITY OF ASTROCYTES

Astrocytes represent the most abundant population among glial cells residing in the human brain (6). The classification of this highly heterogeneous group poses a major challenge, given the limited number of studies exploring the variability of astrocytes. Based on neuroanatomical studies and analysis of their morphology, astrocytes have been traditionally subdivided into four distinct classes such as (i) interlaminar, (ii) varicose projection, (iii) protoplasmic and (iv) fibrous. Interlaminar astrocytes are located in the layer I of the human cortex and are characterized by a round cell body and, in general, a short length of their processes. Nevertheless, they also possess a few processes, which expand to layers II-IV of the cortex but the function of those, as well as of interlaminar astrocytes on the whole, remains elusive. Despite being more uncommon, varicose projection astroglia, found in layers V-VI, attract attention due to the fact that they are specific to humans and higher-order primates. They typically develop short spiny processes together with one to five longer ones, which extend to the deep layers of the cortex and might terminate in the neuropil or on the blood vessels (7). Similarly to interlaminar astrocytes, the role played by varicose projection astrocytes is not yet fully understood. However, it was hypothesized that both of these subtypes might be involved in long-distance communication within the cortex (7). Layers II to VI of the cerebral cortex are populated by the most abundant group of astroglia, namely the protoplasmic astrocytes. They form numerous processes, which are homogeneously distributed and typically described as bulbous, creating overall a bushy morphology. Organized in distinct domains with minimum overlap between individual astrocytes, protoplasmic astroglia were suggested to influence neuronal activity in spatially and temporally coordinated units. Their involvement in metabolic support is also widely reported, similarly to their contribution to the regulation of blood flow (7, 8). The last group of astroglia, fibrous astrocytes, reside in the white matter and are typically larger in size, although containing less processes. As protoplasmic astrocytes, fibrous astroglia seem to be involved in the metabolic support but not in the modulation of neuronal activity due to the lack of synapses in the white matter (7, 9). Apart from the cells described above, other astroglia types were identified such as Bergmann glia in the cerebellum and Müller cells in the retina (10).

Most of the above-described neuroanatomical studies aiming at classifying astrocytic populations relied primarily on GFAP as a potent astrocytic marker - although its widespread application has recently been called into question. In the meantime, it became apparent that GFAP is not expressed in all mature and non-activated astrocytes in the central nervous system.

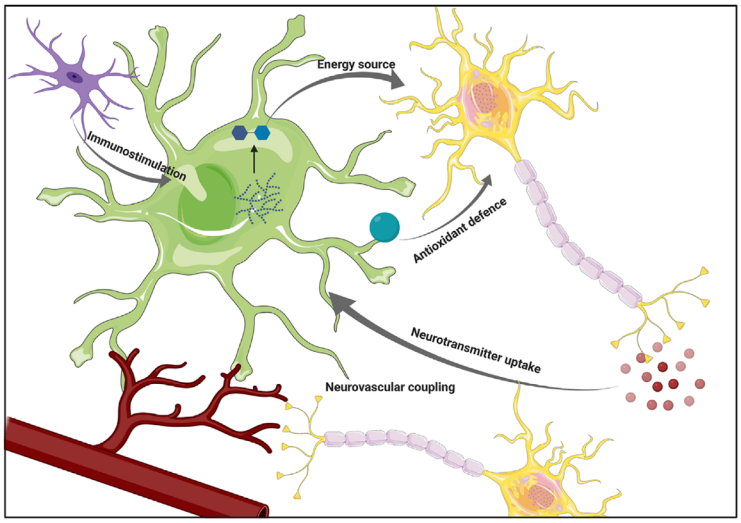

FIGURE 1 | The overview of astrocytic functions. Astrocytes support neuronal functions by providing energy substrates and supporting antioxidant defense. Their ability to participate in the immune response by sensing cytokines secreted by microglia, as well as participation in neurovascular coupling positions them as a crucial component of the interplay between various brain cell types. Figure created with BioRender.com using images adapted from Servier Medical Art by Servier, licensed under a Creative Common Attribution 3.0 Unported License http://smart.servier.com/.

Moreover, it was postulated that GFAP expression patterns might present regional differences (11). Accordingly, recent studies tried to overcome this limitation by using different markers such as Aldh1l1. Based on the observation that Aldh1l1 might serve as a general marker for astrocytes in the central nervous system (12), Lin et al. discovered five subpopulations of astrocytes in mouse brain, which were molecularly and functionally distinct, and suggested that similar types might be found in human brain. Interestingly, synaptogenesis was observed to be differently modulated by various identified subtypes suggesting functional heterogeneity of astrocytes (13). Recent developments in single-cell transcriptomics allowed identification of five to seven astrocytic subpopulations in the mouse nervous system, presenting various morphologies and functions (14, 15). This finding highlights that more research is needed to unravel the full spectrum of astrocytic heterogeneity.

CELLULAR FUNCTIONS OF ASTROCYTES

Astrocytes are involved in a myriad of functions, mostly attributed to their supporting role for neurons. During development, they appear after completed neurogenesis and contribute to synapse pruning (16, 17). Besides their role in brain development, astrocytic processes extensively ensheath synapses and participate in neurotransmitter removal from the synaptic cleft, preventing excitotoxicity and direct contact of the neurotransmitter with neighboring synapses. In a similar fashion, astrocytes are pivotal for maintaining an ionic balance at the synapse, which is required for synaptic transmission (6). A strong body of evidence supports the idea of the 'tripartite synapse'. Accordingly, astrocytes play not only a supportive role in synaptic functions, but also actively modulate neurotransmission. This hypothesis was supported by the observation that astrocytes can react to neuronal activity by increasing their intracellular Ca^{2+} levels, which in turn leads to the secretion of numerous gliotransmitters including glutamate, purines, GABA and D-serine (11). Such gliotransmitters are believed to participate in the feedback regulation of synaptic activities (18). Besides the perisynaptic processes that participate in tripartite synapses, astrocytes extend vascular processes (end-feet) that ensheath capillary endothelium and pericytes, giving rise to the blood-brain barrier (BBB), a selectively permeable structure that tightly controls the movement of molecules and cells between the vascular compartment and the brain parenchyma (19). This unique anatomic position, structurally mediating blood vessels and neurons, is influential for astrocytic roles in surveilling and buffering local environmental changes to nurture neurons with appropriate metabolites in a spatial-temporal manner, a process named neurovascular-coupling (NC), which will be discussed in more detail below (20). Furthermore, the recent discovery of the glymphatic system (21), a waste clearance system relying on perivascular tunnels defined by astrocytes, broadens the scope of astroglial involvement in CNS homeostasis. This system supports the elimination of byproducts of brain metabolism including neurotoxic proteins such as Aβ, countering their noxious accumulation in the brain parenchyma (22).

An important aspect of astrocytic physiology is their ability to respond to brain injury or CNS disease, a phenomenon known as reactive astrogliosis. The term collectively describes various molecular and cellular processes, which are highly heterogeneous and therefore challenging to summarize under a definitive classification. The response might range from mild astrogliosis, typically characterized by altered gene expression and occasional cell hypertrophy without astrocytic proliferation, to severe astrogliosis, which is accompanied by the increase of GFAP expression, cell hypertrophy and substantial proliferation. Pronounced reactive astrogliosis might lead to the formation of scar tissue, composed of proliferating astrocytes (23). Astrocytes also play an important role in neuroinflammation, since they can react to cytokines released by activated microglia (24) and secrete cytokines and chemokines (25) contributing to the ongoing inflammation process. This aspect is further discussed in section *Astrocytes and Mitochondria in Inflammation*.

ASTROCYTE-NEURON METABOLIC CROSSTALK IN HEALTH AND NEURODEGENERATIVE DISEASES

Despite accounting only for 2% of the body mass, the relative oxygen consumption of the adult human brain under resting conditions rises up to 20% of whole-body oxygen consumption (26, 27). Furthermore, when focusing on glucose oxidation rates in awake resting conditions, a figure that was broadly accepted, attributed 70-80% of those rates to neurons and approximately 20-30% to astrocytes. However, a re-examination of these proportions taking into account cell type volume fractions results in astrocytic glucose oxidation rates that exceed those of neurons (28). This assessment brought to light astrocytic energy demands that were not previously accounted for. In fact, the intricacies of the astrocyte-neuron metabolic dialogue are still under intense debate. Nevertheless, it is well appreciated that astrocytes play a central role in brain metabolic homeostasis, particularly concerning brain energetics and redox balance. Astrocytes serve as active regulators of their microenvironment and coordinate substrate availability with neuronal activity in a spatial-temporal manner. In the following sections, we discuss the most relevant biochemical processes that account for the astrocyte-neuron metabolic interplay. After a brief introduction of each process [for more details please refer to references (28, 29)], we will focus on known pathological mechanisms which disrupt the astrocyte-neuron dialogue in AD and PD (**Figure 2**).

Cerebral Blood Flow and Neurovascular Coupling

The brain's activity is sustained by a timely modulation of regional hemodynamics. The co-regulation of cerebral blood flow (CBF) and neuronal activity is known as neurovascular coupling (NC) or functional hyperemia and comprehends a complex set of regulatory steps performed by distinct cells

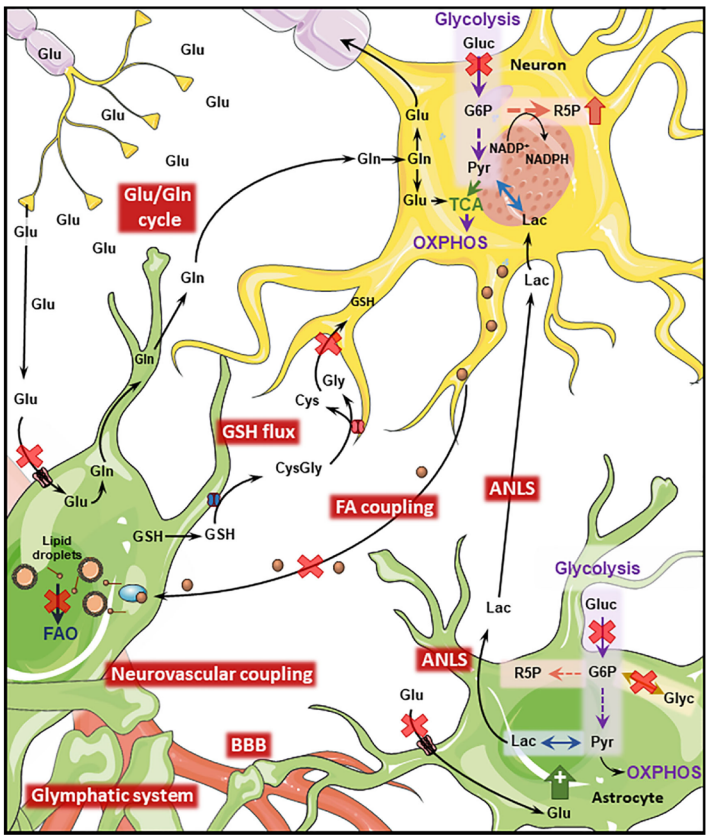

FIGURE 2 | Disrupted Astrocyte-Neuron metabolic interplay in PD and AD. Metabolic interaction between astrocytes and neurons is disrupted in AD and PD. Both diseases present cerebral hypoperfusion with associated degradation of BBB integrity which might impact the function of the glymphatic system. Neurovascular coupling is impaired in AD. Cerebral hypoperfusion is accompanied by reduced glucose metabolism which will transversely affect downstream pathways such as the ANLS. Astrocytic glycogen metabolism is regulated by noradrenaline and insulin being impaired in both diseases. Neuronal PPP is upregulated in AD and late PD as a response to increased oxidative stress. Oxidative stress is further exacerbated by disruption of the GSH flux from astrocytes to neurons. The transfer of neuronal peroxidated FA to astrocytes where they are degraded through FAO is impaired by the AD-related ApoE4 isoform, leading to the accumulation of such toxic FA. The Glu/GLn cycle is impaired in both conditions, due to defective removal of glutamate from the synaptic cleft which leads to excitotoxicity-induced neuronal loss. (Gluc, glucose; Glu, glutamate; Gln, glutamine; Lac, lactate; Pyr, pyruvate; Glyc, glycogen; R5P, ribose 5-phosphate; G6P, glucose 6-phosphate; GSH, glutathione; Cys, cysteine; Gly, glycine; FAO, fatty acid oxidation; TCA, tricarboxylic acid cycle). Figure created with images adapted from Servier Medical Art by Servier; licensed under a Creative Common Attribution 3.0 Unported License http://smart.servier.com/.

including astrocytes (20). The molecular basis of NC is complex and results from a conjunction of feedback and feedforward mechanisms. While feedback regulation aims at supplying the target region with depleted energy substrates and removing by-products of intense neuronal activity (some of which have vasodilator properties), feedforward signaling is based on the release of vasoactive molecules [e.g. K^+, prostanoids, nitric oxide (NO)]. The astrocytic participation in NC differs throughout the cerebrovascular tree, being more prevalent at the level of capillaries (20) and less important in arterioles (30). Astrocytes sense local increases in extracellular glutamate (the main excitatory transmitter) through metabotropic receptors resulting in the activation of a Ca^{2+}-dependent signaling pathway, which will generate arachidonic acid and downstream vasodilating metabolites (such as prostaglandins and epoxyeicosatrienoic acids). Conversely, arachidonic acid itself can diffuse to vascular endothelial cells, where it can be transformed to vasoconstricting molecules such as 20-HETE (31, 32). These opposing roles of astrocyte activation on cerebral hemodynamics are dependent on NO levels, which regulate the routes of arachidonic acid conversion. The molecular orchestration regulating neurovascular coupling is much more complex and also includes adaptation to low O_2 levels (20, 31).

Cerebral hypoperfusion caused by a combination of abnormalities in the cerebrovascular architecture as well as non-structural alterations was suggested as a prodromal feature of AD (30). BOLD fMRI studies investigating stimuli and task-triggered local cerebrovascular reactivity in AD patients and in cognitively normal individuals with an increased genetic risk for AD (APOE4 allele) revealed that neurovascular coupling is disrupted in preclinical stages of AD (32–34). Moreover, Aβ - the prime component of amyloid plaques - has vasculotoxic and vasoactive properties that mediate cerebrovascular deficiency (20, 30, 32).

Cerebral hemodynamics are also impacted in PD, with reduced CBF being reported in early stages of the disease (35). Moreover, in distinct regions of PD post-mortem brain tissue, degradation of vascular integrity was observed (20, 36). By contrast, several studies suggest that neurovascular coupling is sustained in PD (20, 37). Impaired nutrient input and accumulation of toxic metabolic sub-products due to cerebral hypoperfusion are worsened by the loss of BBB integrity, a well-recognized feature of early AD, which was also suggested to occur in PD (38–40). Furthermore, the disruption of BBB integrity is likely to enable the contamination of the brain parenchyma with blood-borne immunogenic molecules and to negatively impact the function of the glymphatic system, contributing in that manner to the build-up of toxic protein aggregates as seen in both pathologies (41, 42).

Astrocyte-Neuron Energetic Coupling

Efficient exchange of energy substrates between the blood and the brain is sustained by the expression of distinct transporters, including GLUT1 for glucose, MCTs for monocarboxylates (such as lactate, pyruvate and ketone bodies) and FAT for fatty acids, at the level of the BBB (43). From these various molecules, glucose is the prime energetic substrate for the adult human brain, and its catabolism through primary (e.g. glycolysis and mitochondrial tricarboxylic acid (TCA) cycle) or secondary [e.g. pentose phosphate shunt pathway (PPP)] metabolic pathways not only generates ATP to fulfill the brain's energy demands, but also provides critical precursors for the synthesis of neurotransmitters, neuromodulators and cellular components. In addition, glucose is important to sustain cellular antioxidant systems (28). Nevertheless, under specific circumstances, brain cells can rely upon other substrates that are imported from the blood (e.g. ketones bodies during starvation and lactate during intense activity) or produced locally (e.g. lactate, glutamine). Out of these alternative substrates, lactate was identified as a key player mediating the metabolic interplay between astrocytes and neurons. Both these cell types can efficiently metabolize glucose and lactate, however, while astrocytes present a more pronounced glycolytic profile, neurons preferentially rely on oxidative metabolism *via* mitochondrial oxidative phosphorylation (OXPHOS) (29). This notion was central to the formulation of the astrocyte-neuron lactate shuttle (ANLS) hypothesis (44), which was supported by studies suggesting incomplete glucose oxidation and/or increased lactate production following neuronal activity (26, 45).

Astrocyte-Neuron Lactate Shuttle (ANLS)

This model, which was first introduced in the early nineties (44), postulates that extracellular glutamate increase during intense neuronal activity leads to active astrocytic glutamate uptake, which in turn triggers Na^+/K^+ ATPase activation in astrocytes (to maintain Na^+/K^+ homeostasis) with an associated energy consumption and a drop in cellular ATP levels (46). To counteract this effect, astrocytic glucose uptake and glycolysis is elevated, secondarily increasing lactate production and excretion, which will then be available as a fuel to neuronal cells (47, 48). However, this concept is not consensual and evidence has been raised to dispute some of its premises (28). Interestingly, an alternative neuron-astrocyte lactate shuttle was also proposed (28).

Brain hypoperfusion is accompanied by reduced glucose and oxygen metabolic rates. This hypometabolism of glucose characterizes the normal aging process, with glucose metabolic rates decreasing by 26% from age 18 to 78 (49), but is further accentuated in pathological conditions such as AD and PD (38). In early AD, fluorodeoxyglucose-PET showed a characteristic reduction of total glucose metabolism in the parietotemporal association cortices, posterior cingulate cortex and the precuneus (49). Interestingly, aerobic glycolysis, which corresponds to the fraction of glycolysis not coupled to oxidative phosphorylation and which was previously associated with biosynthetic and neuroprotective roles, was found to be reduced in brain regions with higher levels of Tau deposition (50). Contrariwise, AD postmortem brain-derived data points to an overall upregulation of glycolytic enzymes, which was interpreted as a compensatory mechanism to mitochondrial dysfunction and to the reduced levels of glucose transporters that accompanies disease progression (51).

Alterations in glucose metabolism were also identified in brains from early- and late-stage PD patients (51). Several PD studies reported an extensive cortical hypometabolism of glucose, while only some of these investigations concomitantly show increased glucose metabolism in diverse subcortical regions (35, 52). Overall, disease-associated changes in glucose metabolism in both AD and PD are expected to profoundly disrupt brain cellular function, ultimately contributing to impaired neurotransmission, inefficient antioxidant defenses and neuronal death.

Glutamate/GABA-Glutamine Cycle

Astrocytes participate in the fast removal of neurotransmitters from the synaptic cleft, which is important for efficient signal termination (53). In the case of glutamate, this fast removal warrants the prevention of excitotoxicity. Astrocytes take up extracellular glutamate through high affinity sodium-dependent glutamate transporters (EAAT2) and the glutamate aspartate transporter (EAAT1). Astrocytic recycling of glutamate is instrumental to restore neuronal pools of this neurotransmitter, since neurons are deprived of key enzymes for glutamate *de novo* synthesis (53). Astrocytic glutamate can be converted to glutamine by the astrocyte-exclusive glutamine synthetase (54). Non-neuroactive glutamine is then safely redirected to neurons, where it can be converted back to glutamate through phosphate-activated glutaminase activity (53). Similar to this process, but at the level of GABAergic synapses, astrocytes take up part of the released GABA, which is processed through the TCA cycle in mitochondria.

Glutamine released by astrocytes can equally be recovered by inhibitory GABAergic neurons to be used in the synthesis of GABA (53). Of note, both neurons and astrocytes can divert glutamate and glutamine for other uses such as oxidation in the TCA cycle or release from the brain for the maintenance of nitrogen balance across the BBB (29, 55). This net removal is compensated for *via* anaplerosis through the astrocyte-specific pyruvate carboxylase enzyme (55).

The previously mentioned hypometabolism of glucose occurring in AD and PD has a transversal effect on brain metabolism not only affecting directly communicating pathways such as the PPP, but also impairing downstream mechanisms such as the Glutamate/GABA-Glutamine cycle (56). Furthermore, neuronal loss in AD was linked to dysregulation of the glutamatergic system. A process that involves excitotoxicity, due to impaired glutamate uptake from the synaptic cleft. This impaired glutamate removal was further linked to lower activation of astrocytic glutamate transporters secondary to Aβ action (57, 58). Extensive evidence from distinct acute and genetic PD models identified an analogous glutamatergic dysfunction in this condition. Similarly, a defective glutamate uptake by astrocytes is instrumental for neuronal demise caused by glutamate excitotoxicity (59).

Astrocyte-Neuron Fatty Acid Coupling

Recently, an elegant mechanism coupling fatty acids (FA) metabolism in neurons and astrocytes was exposed (60). Extended periods of enhanced neuronal activity result in augmented generation of reactive oxygen species (ROS) and consequential accumulation of peroxidated FA (pFA). This poses an oxidative risk to the cell, since neurons have limited capacity to isolate those toxic species within lipid droplets. Instead, neurons release these pFA to the extracellular milieu in the form of ApoE-positive lipid particles, which are endocytosed by neighboring astrocytes and incorporated in lipid droplets. As a response to increased neuronal activity, astrocytes upregulate the expression of detoxification genes and initiate the breakdown of the lipid droplets, further catabolizing the released pFA to fuel oxidative phosphorylation in the mitochondria. Remarkably, this entire protective coupling mechanism is ApoE-isoform-dependent, and was shown to be seriously disrupted in mice knocked-in for the AD-relevant ApoE4 variant. This model presented compromised FA sequestration in neurons and decreased mobilization and energetic degradation in astrocytes (61). Interestingly, altered lipid metabolism has also been reported in PD, for instance in astrocytes derived from α-SYN KO mice (62).

Glycogen Storage

The astrocytic compartment is the most prominent site of glycogen storage in the brain, with accumulation of these energetic reserves being minute or inexistent in neurons (63). Interestingly, neuronal activity was shown to regulate astrocytic glycogen metabolism even in the presence of adequate glucose supply, disproving the idea that glycogen serves uniquely as an emergency energy reserve (29, 63). Further investigations are required to unravel the metabolic fates engaged in glycogen mobilization under distinct conditions. However, diversion of glycogen-derived glucose-6-phosphate into pathways such as the PPP have been observed under oxidative stress (64). Glycogen-derived lactate released by astrocytes is taken up by neurons and operates in the mechanism of long term memory consolidation (65) - a process that is hindered in AD. Indeed, decreased glycogenesis due to the inhibition of glycogen synthase was linked to overactivation of glycogen synthase kinase 3 (GSK-3) in AD (66). Furthermore, the dynamics of glycogen metabolism are regulated by factors such as noradrenaline (which stimulates the mobilization of glycogen stores, i.e. glycogenolysis) and insulin (which promotes glycogenesis) (26). Therefore, the degeneration of the noradrenergic system characteristic of AD (67) and the unbalanced insulin signaling occurring in AD and PD (26) will likely further contribute to the metabolic impairment found in these conditions.

Antioxidant System

The elevated cerebral metabolic rate along with an environment rich in unsaturated fatty acids and iron content and an inefficient antioxidant system renders the brain highly susceptible to oxidative stress (68). Also at this level, the astrocyte-neuron metabolic dialogue reveals its importance, since astrocytes, which are endowed with an intrinsically competent antioxidant system, convey some of this antioxidant potential to neurons (29). A good example of this is the shuttling of glutathione (GSH) precursors, the most prevalent antioxidant molecule in the brain, from astrocytes to neurons. Both cell types are capable of producing GSH, which might act as an independent ROS scavenger or as a substrate for antioxidant enzymes. However, neuronal cells strictly depend on astrocyte-derived GSH. Neurons express minimal levels of the System xc- cystine/glutamate antiporter, rendering them unable to efficiently capture cystine from the extracellular milieu. Cystine is the oxidized form of cysteine and is indispensable for the synthesis of GSH (68). Thus, neurons are dependent on the release of GSH by astrocytes. At the plasma membrane, GSH is converted by enzymes into glycine and cysteine, which are readily usable by neurons (29). The significance of this shuttling process is highlighted by the fact that neuronal GSH levels are dramatically increased when they are co-cultured with astrocytes (69).

Oxidative and nitrosative stress contributes to the pathogenesis of PD and AD (70), with robust evidence showing augmented oxidative stress markers in postmortem brain samples (71). Studies in PD patients showed significantly reduced glutathione levels in the substantia nigra (72), increased lipid peroxidation in the plasma and decreased activity of antioxidant enzymes (73). Moreover, the accumulation of Aβ in early AD results in increased oxidative stress (74). Under physiological and acute stress, astrocytes mediate neuroprotection by detoxifying the microenvironment from ROS and reactive nitrogen species (RNS), while providing neurons with precursors for glutathione synthesis. An example of a neuroprotective action performed upon astrogliosis is found in PD patients, in which reactive astrocytes elevate DJ-1 expression (75, 76). However, chronic reactive astrogliosis renders astrocytes neurotoxic, namely by the persistent production of ROS/RNS and release of immunogenic molecules (as discussed below) (70). Remarkably, disruption of

normal brain metabolism can fuel this imbalanced oxidative status, since diminished levels of key PPP enzymes have been identified in the putamen of early-stage PD patients (71). This decreased flux through the PPP impairs the production of nicotinamide adenine dinucleotide phosphate (NADPH), which is a mandatory substrate for the regeneration of GSH pools by glutathione reductase. The decreased PPP flux was interpreted as a contributor to oxidative stress in early PD, while in later stages of the disease, the PPP flux would be upregulated in an attempt to counteract sustained oxidative stress (71). Interestingly, an increased PPP flux has been widely documented in AD as a metabolic adaptation to oxidative conditions (77). Furthermore, a recent mouse study showed that physiological ROS levels in astrocytes are needed to regulate metabolic rewiring, which modulates the PPP flux with potential implications on neuronal survival and cognitive impairment. This mechanism engaged the function of nuclear factor E2-related factor 2 (NRF2) and consequently, contributed to prevent disproportionate ROS release outside of the cell (78).

Moreover, a recent study associates PD with the hypermethylation and consequent downregulation in blood cells of *SLC7A11*, the gene coding for the System xc- cystine/glutamate antiporter. If maintained at the brain level, this dysregulation might account for a disruption of glutathione metabolism and glutamate neurotransmission (79).

Further examples of the causal relation between augmented oxidative stress and metabolic alterations in neurodegeneration can be found in the mitochondrial TCA cycle, were the activity of enzymes such as aconitase (80) and the α-ketoglutarate dehydrogenase complex (KGDHC) are impacted by reactive oxygen species (81). Paradoxically, these and other enzymes equally contribute to the production of ROS, further unbalancing the cellular redox status and aggravating disease mechanisms. KGDHC is a heteromeric enzyme that catalyzes the conversion of α-ketoglutarate to succinyl-CoA in a process that generates NADH and therefore supports ATP generation *via* OXPHOS. The regulatory process behind KGDHC activity is intricate and involves ADP/ATP, NAD^+/NADH ratios, succinyl-CoA, Ca^{2+} and ROS levels (82). α-ketoglutarate is a metabolic precursor in the synthesis of glutamate, glutamine and GABA in diverse cell types, therefore the large scope of KGDHC functions, make this complex a leading molecular player integrating diverse cellular functions such as energy production, neurotransmission and redox homeostasis (83). Remarkably, changes in the activity of brain KGDHC have been reported in multiple neurodegenerative conditions, including PD (84). Moreover, such changes were extensively detailed in AD, where reduced KGDHC activity correlates with declined cognition (85).

Noteworthy, attempts to enhance defense mechanisms by specifically increasing the activity of ROS-sensing NRF2 has proven to be an efficient approach to maintain neuronal viability in both AD and PD models (74, 77, 86). NRF2 is a transcription factor primarily active in astrocytes, where it orchestrates cellular antioxidant responses and remodeling of intermediary metabolism. This example stresses the therapeutic potential that interventions targeting the astrocyte-neuron metabolic interaction have in the context of neurodegeneration (78).

Mitochondria and Astrocyte-Neuron Coupling

As previously mentioned, astrocytes and neurons fundamentally differ in their dependence on the mitochondrial oxidative phosphorylation. While ATP in astrocytes is mostly produced *via* aerobic glycolysis, they still possess functional mitochondria. However, the composition and organization of OXPHOS complexes in astrocytes is strikingly distinct from the respiratory chain structure in neurons. Initially, variations in complex I activity were observed when analyzing mitochondria in astrocytes and neurons from multiple species (87). Furthermore, it was shown that astrocytes contain a smaller percentage of complex I assembled into supercomplexes. These changes were correlated with an increase in ROS production in astrocytes (88). Overall, differences in the respiratory chain complex composition between astrocytic and neuronal cells, together with distinctive transcriptional and molecular regulation of key metabolic enzymes and substrate transporters (29), might explain higher glycolysis rates in astrocytes and their well-developed antioxidant defense system (88).

Multiple lines of evidence implicate PD-associated proteins in the regulation of mitochondrial function. One of the most prominent examples is α-SYN, which is relevant for both familial and idiopathic forms of PD. α-SYN effects on neuronal function can be either of primary or secondary nature. When localized to the mitochondria, the protein was shown to interfere with mitochondrial bioenergetics and biogenesis (89). By contrast, some studies also suggest that mitochondrial impairment can occur prior to α-SYN aggregation and potentially contribute to this phenomenon [reviewed in (89)]. Although predominantly expressed in neurons, α-SYN can be engulfed by astrocytes and affect their function. Notably, it was reported that such an uptake was more efficient for astrocytes than neurons, as demonstrated in murine co-cultures of astrocytes and neurons. Following the exposure to α-SYN, alterations in mitochondrial morphology and increased cell death were observed in the co-cultured neurons. Interestingly, neuronal death did not occur directly after the treatment, suggesting a neuronal response to the astrocytic dysfunction, presumably mediated by the release of astrocytic cytokines. Astrocytes could still survive in culture several days after exposure, underlining the importance of glycolysis for maintaining their function and neuronal dependence from undisturbed astrocytic metabolism (90). α-SYN is not the only PD protein, which may have a role in regulating mitochondrial processes in neurons as well as astrocytes. The relevance of PINK1 for mitochondrial homeostasis was explored in astrocytes from *PINK1*-knockout mice, which exhibited severe mitochondrial impairments (91). Another example is Parkin, which, when depleted in mice, caused stronger mitochondrial phenotypes in astrocytes than in neurons. Furthermore, Parkin-deficient astrocytes were not able to promote neuronal differentiation *in vitro* (92). Additionally, the PD protein DJ-1, which is highly abundant in astrocytes and involved in the oxidative stress defense, was shown to play a key role in maintaining proper mitochondrial function in astrocytes (93). In the absence of DJ-1, these cells lose their ability to protect

neighboring neurons from oxidative stress (94). Since data on the role of astrocytic mitochondria in PD is still sparse [reviewed in (76, 95)] further experiments will be required to assess how astrocyte metabolism as well as astrocyte-neuron coupling may contribute to the development of the movement disorder.

Similar to the scenario described above for α-SYN in PD, Aβ has been shown to affect mitochondrial function and metabolism in AD neurons. Thus, some authors argue that mitochondrial impairment precedes Aβ pathology in AD (95). Overall, the available mitochondrial function data in astrocytes from AD mouse or patient models is very limited (96). Therefore, more studies will be required to shed light on possible effects of this dysfunction on astrocyte-neuron coupling.

Astrocytic Calcium Signaling and Astrocyte-Neuron Crosstalk

Interestingly, mitochondria were shown to be involved in intracellular calcium signaling in astrocytes (97). Calcium release from mitochondria can trigger spontaneous Ca^{2+} oscillations in astrocytic processes - a phenomenon attributed to the opening of the mitochondrial permeability transition pore when oxidative phosphorylation is particularly active. This suggests a direct connection between metabolic demand and calcium signaling (98). Spontaneous Ca^{2+} waves can be propagated to other astrocytes and ultimately cause neuronal activity. Furthermore, it was proposed that the described process might play an important role in brain development, by supporting the formation of synaptic connections and the regulation of the neurotransmission (99).

Although astrocytes have been considered passive bystanders in neurotransmission events, this view was recently challenged. It became clear that astrocytes are able to respond to neurotransmitters as manifested by changes in Ca^{2+} levels. Based on this response, astrocytes were shown to react to glutamate, acetylcholine, ATP, GABA, and endocannabinoids. In return, they are able to release glutamate, D-serine, ATP, and GABA influencing activity of the neighboring neurons (100).

Alterations in Ca^{2+} signaling were identified in reactive astrocytes in the context of neurodegeneration. Generally, these changes were characterized by an enhanced amplitude, duration and frequency of these signals (97). In an AD mouse model, it was shown that astrocytes surrounding Aβ plaques might generate aberrant Ca^{2+} signals, which can be further propagated to other astrocytes (101, 102). It was hypothesized that changes in Ca^{2+} signaling might be one of the mechanisms, which play a role in the contribution of reactive astrocytes to the pathology of neurodegenerative diseases, however, this possibility requires further examination (97).

As discussed in the previous sections, neuronal activity marked by glutamate release can elicit metabolic changes in astrocytes as evidenced by considerably higher glucose uptake (103). Recently it became clear that such metabolic modulation is elicited by dual Na^{+} and Ca^{2+} signaling, which triggers glucose mobilization and subsequent aerobic glycolysis to support neuronal functions by providing lactate. In contrast, spontaneous calcium spikes in astrocytes do not trigger a similar response, suggesting that astrocytic metabolism is mainly focused on meeting high metabolic demands of neurons (104, 105).

iPSC-DERIVED ASTROCYTE MODELS TO STUDY METABOLISM IN NEURODEGENERATIVE DISEASES

In recent years, we have witnessed major breakthroughs in modeling human diseases after the iPSC technology was implemented. Since then, we observed the development of numerous protocols for the generation of iPSC-derived astrocytes (106–110) [for an extensive review of earlier protocols see (111)], allowing researchers to shed light on the involvement of astroglia in the pathogenesis of human neurodegenerative diseases. Such tools proved to be also useful in studying metabolic alterations in the brain (**Table 1**), in particular taking into account the above-mentioned contribution of astrocytic metabolism to the maintenance of neuronal function. In astrocytes derived from AD patients harboring *PSEN1* mutations, fatty acid oxidation was compromised (112), in line with earlier reports showing decreased levels of fatty acid oxidation products in AD patients (122) and the studies regarding the astrocyte-neuron FA-coupling mentioned above. Importantly, Konttinen and colleagues identified a plausible target for AD treatment, since the fatty acid oxidation impairment was rescued with a compound (GW0742), which triggered the activation of PPARβ/δ, a ligand-inducible transcription factor controlling lipid and glucose metabolism (112, 123). Another variant linked to AD, *APOE4*, was shown to cause altered expression of various lipid metabolism genes in iPSC-derived astrocytes. Furthermore, the intra- and extracellular levels of cholesterol were increased in these cultures (115). Changes in cholesterol levels were also observed in another study using iPSC-derived astrocytes harboring the Swedish mutation in the amyloid precursor protein (APP) gene (117). These findings suggest that cholesterol metabolism might be implicated in the pathogenesis of AD.

In the context of PD, several metabolic changes were detected in astrocytes derived from patients harboring *LRRK2* mutations. The secretion to the medium was increased for several polyamines, such as putrescine and spermidine and the levels of their precursors, arginine and ornithine, were elevated in astrocytes. Polyamines are important for various cellular processes, such as cell proliferation and differentiation, gene transcription and translation, as well as regulation of ion channel and receptor activity (119). Notably, changes in polyamine levels were also detected in the cerebrospinal fluid (CSF) of PD patients supporting the relevance of the data obtained in the iPSC models (124). Moreover, in the same study from Sonninen et al., a decline in phospholipids levels, in particular lysophosphatidylethanolamine, was observed in PD astrocytes, which is again in agreement with data obtained from the analysis of CSF from PD patients (119, 125). Another important aspect of astrocytic metabolism, namely glutamine

TABLE 1 | The summary of patient-derived models used to elucidate the effects of neurodegeneration-linked mutations on astrocytic metabolism.

Disease	Study	Gene	Mutation/ variant	Type of cells	Main finding	Astrocytic protocol used	Comments
AD	Konttinen et al. (112)	*PSEN1*	Deletion of exon 9	Astrocytes, murine neuroprogenitor cells	Impaired fatty acid oxidation, rescued by GW0742 treatment	Krencik et al. (113); modified in Oksanen et al. (114)	Isogenic controls included
AD	Lin et al. (115)	*APOE*	*APOE4, APOE3*	Astrocytes, neurons, microglia, organoids	Increased levels of cholesterol and reduced Aβ uptake in *APOE4* astrocytes	Chen et al. (116)	Isogenic controls included
AD	Fong et al. (117)	*APP*	KO, V717F, Swedish	Astrocytes, neurons, neuroprogenitor cells	Decreased lipoprotein endocytosis and increased SREBP levels in APP-KO astrocytes, accompanied by reduced Aβ uptake, astrocytes harboring Swedish mutation mimic this phenotype	Yuan et al. (118); modified in the study	Isogenic controls included
PD	Sonninen et al. (119)	LRRK2, GBA	LRRK2 G2019S, GBA N370S	Astrocytes	Increased α-SYN levels, changes in metabolism, particularly in polyamines and lysophosphatidylethanolamine levels, altered calcium signaling	Krencik et al. (113); modified in Oksanen et al. (114)	Isogenic controls included
FTD	Aldana et al. (120)	*CHMP2B*	H150, H151, H242	Neurons, astrocytes	Altered glutamine-glutamate related pathways in neurons, in astrocytes enhanced glutamate uptake	Shaltouki et al. (121); modified in the study	Isogenic controls included

AD, Alzheimer's disease; PD, Parkinson's disease; FTD, frontotemporal dementia.

uptake and conversion, was studied in the context of frontotemporal dementia. In this case iPSC-derived astrocytes presented substantial changes in glutamate uptake (120).

Although mainly implemented to study metabolic changes in human diseases, iPSC models of astrocytes proved their uttermost importance in elucidating molecular pathways governing metabolism of valine and medium-chain fatty acids in the brain. These findings might be useful to determine an optimal ketogenic diet, which was shown to have a positive impact on the health of patients suffering from traumatic brain injury, glucose transporter I deficiency, AD and epileptic seizures (126–128).

ASTROCYTES AND MITOCHONDRIA IN INFLAMMATION

As touched on in the third section of this review, astrocytes are immunocompetent cells. Accordingly, stimulation with interferon (IFN) γ and/or tumor necrosis factor (TNF) α can trigger the expression of major histocompatibility complex (MHC) class II molecules, which are required for antigen presentation (129). Moreover, *in vitro* studies in human immortalized astrocytes and primary mouse astrocytes have shown that, in response to IFN-γ, astrocytes are able to activate naïve T cells. However, there is conflicting evidence as to whether class II MHC+ astrocytes can stimulate the proliferation of activated T-helper (Th) type 1 or 2 cells (129).

While the antigen-presenting properties of astrocytes are still under debate, there are a myriad of studies (130) highlighting that astrocytes can release cytokines including IL-1, -6 and -10; TNF-α, transforming growth factor (TGF) β as well as IFN-α and -β in response to molecular triggers (129). Such signals can be of extra- or intracellular nature and are detected by pattern recognition receptors (PRR). Contrary to acute injury models, in neurodegenerative disease it is suspected that mild but progressive cues trigger astrocyte reactivity. Situated at the tripartite synapse, astrocytes have the capacity to sense altered neurotransmission patterns and neuronal stress signals (131). As previously mentioned, astrocytes can engulf neurotoxic proteins such as α-SYN (132) and Aβ (133). These aggregates can then be transferred from diseased to healthy cells *via* tunneling nanotubes (134) (**Figure 3**). Moreover, experiments with iPSC-derived astrocyte-neuron co-cultures revealed that astrocytes rapidly internalize neuronal α-SYN. By contrast, this intercellular transfer was prohibited in cultures from PD patients with mutations in the lysosomal storage protein ATP13A2 (135). This data not only suggests that astrocytes contribute to the neuronal α-SYN pathology in genetic PD, but that they may also act as mediators in neuroinflammatory processes. In line with this hypothesis, selective overexpression of A53T-mutant α-SYN in murine astrocytes induced rapidly progressing paralysis, which was the result of an overshooting inflammatory response. Astrocytic expression of A53T α-SYN triggered microglial activation and neurodegeneration in this PD mouse model (136). As discussed in sub-section *Mitochondria and Astrocyte-Neuron Coupling*, α-SYN likely interferes with astroglial and neuronal mitochondria. Thus, the proinflammatory action of α-SYN may be amplified by mitochondrial impairment in both cell types. In fact, in mice, depletion of the mitochondrial transcription factor A (TFAM), which controls transcription, replication and 3D structure of the mitochondrial genome, caused the activation of the cGAS-STING inflammatory pathway. With regard to PD, our own research revealed that, in post-mortem nigral dopaminergic neurons from sporadic patients with α-SYN pathology, TFAM deficiency is associated with reduced respiratory chain complex I protein levels (137). In the absence of TFAM, mitochondrial DNA (mtDNA) is released into the cytosol and the extracellular space, where it acts as damage-associated molecular pattern (DAMP) (138).

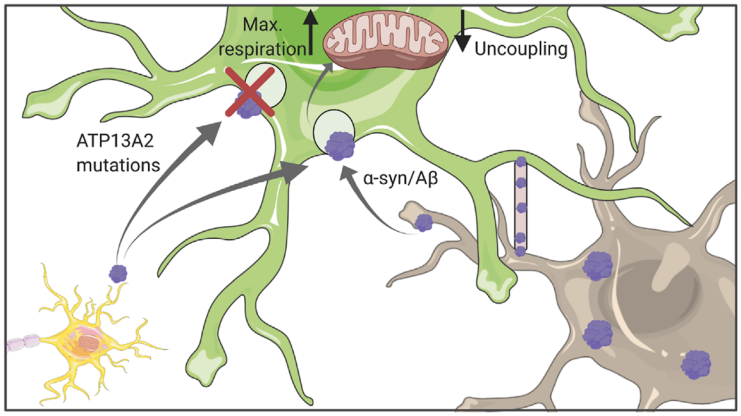

FIGURE 3 | Astrocytic uptake of protein aggregates. Astrocytes can internalize both Aβ and α-synuclein which might originate either from other astrocytes or neurons. Uptaken aggregates were shown to affect mitochondrial function, in particular their respiration capacity and coupling status. Figure created with BioRender.com using images adapted from Servier Medical Art by Servier, licensed under a Creative Common Attribution 3.0 Unported License http://smart.servier.com/.

As mitochondrial DAMP, mtDNA does not only have the capacity to initiate cGAS-STING signaling, but also to activate the NLRP3 inflammasome. In fact, CMPK2 - the rate-limiting enzyme supplying deoxyribonucleotides for mtDNA synthesis - is required for the generation of oxidized mtDNA fragments that are recognized by the NLRP3 complex in the cytosol (139). Supporting these observations, single-cell RNA sequencing and quantitative immunofluorescence analyses of control and IPD midbrain sections indicated an upregulation and activation of astroglial cells in the patient tissue (140). To test whether α-SYN accumulation, mitochondrial dysfunction, neurodegeneration and astroglial immune response are indeed causally linked in PD, iPSC-derived (co-culture) models will be useful. First experiments in astrocytes derived from healthy controls suggest that treatment with high-molecular-weight α-SYN fibrils reduces the secretion of pro-inflammatory cytokines. Similar to the situation in neurons, mitochondrial respiration in these cells was impaired in response to α-SYN exposure. This effect was even more pronounced in PD patient astrocytes harboring *PRKN* mutations (141).

Beyond DAMPs of neuronal (or even astroglial) origin, molecules released from microglia can initiate signaling cascades that mediate astrocyte reactivity (131). Liddelow and colleagues identified two classes of reactive astrocytes, which they termed A1 and A2 in analogy to the nomenclature of macrophages. While A1 astrocytes act neurotoxically, A2 astrocytes have neuroprotective function (25). A1 astrocytes are activated by cytokines such as Il-1α, TNF or C1q secreted from microglia. As a consequence, they promote neuronal death by hampering outgrowth, synaptogenesis and phagocytosis. Consistent with these properties, A1 astrocyte numbers are elevated in various neurodegenerative disorders including PD (24). Interestingly, mitochondria (as a source of DAMPs) are not only involved in the initiation of inflammation (142), they are also crucial for the modulation of the inflammatory response. Experiments in mouse cortical astrocytes suggest a transient change in mitochondrial dynamics coinciding with elevated ROS levels and autophagy induction in response to proinflammatory stimuli (143). This spontaneous upregulation of mitochondrial clearance ensures astrocyte survival and may, in turn, influence neuronal metabolism (143).

DISCUSSION

Taken together, there is increasing evidence that mitochondrial dysfunction and disrupted metabolism impact on astrocyte-neuron coupling in AD as well as PD. Moreover, a multitude of studies indicate that the oxidative stress defense system is impaired in both disorders. By contrast, the sequence of events causing these phenotypes currently remains elusive. Further experimental work will be required to clarify whether (i) primary mitochondrial dysfunction due to mutations in (one or multiple) proteins relevant for mitochondrial homeostasis could lead to oxidative stress and metabolic disruptions or whether (ii) protein aggregation and metabolic imbalances cause secondary mitochondrial dysfunction thereby aggravating neuronal pathology. Ultimately, faulty mitochondria may release DAMPs that could trigger inflammation - a less explored aspect of astroglial metabolism and function. Equally, it should be noted that, to date, very few metabolic findings from mouse models have been validated in human astrocytes. By contrast, various protocols for the generation of pure astrocyte cultures from iPSCs have been published in the recent years. In-depth characterization experiments indicate that these cultures may not only serve as models to study disease mechanisms but that they could be used

for drug-screening approaches in the future. By combining mutant neurons with isogenic control astrocytes and vice versa, we may be able to better define the predominant metabolic role and cell type of action for proteins associated with AD or PD. Thus, patient-derived astrocyte-neuron co-culture systems hold great potential for the exploration of metabolic modulation strategies in neurodegenerative disorders.

AUTHOR CONTRIBUTIONS

PM, AG, and SP designed the structure of the review. PM, AG, and SP performed literature search, wrote the draft and edited the manuscript. The figures were prepared by PM and SP. All authors contributed to the article and approved the submitted version.

FUNDING

PM, SP, and AG were supported by the Luxembourg National Research Fund (FNR) within the CORE (CAMeSyn, C19/BM/13688526) and ATTRACT programs (Model-IPD, FNR9631103). In addition, PM was supported by the FNR *via* the PARK-QC DTU (PRIDE17/12244779/PARK-QC). AG and SP were supported by a donation from Le Foyer Assurances Luxembourg, which was matched by the FNR within the framework of the PARK-QC DTU program.

REFERENCES

1. Dugger BN, Dickson DW. Pathology of Neurodegenerative Diseases. *Cold Spring Harb Perspect Biol* (2017) 9. doi: 10.1101/cshperspect.a028035
2. Erkkinen MG, Kim M-O, Geschwind MD. Clinical Neurology and Epidemiology of the Major Neurodegenerative Diseases. *Cold Spring Harb Perspect Biol* (2018) 10. doi: 10.1101/cshperspect.a033118
3. GBD 2016 Neurology Collaborators. Global, Regional, and National Burden of Neurological Disorders, 1990-2016: A Systematic Analysis for the Global Burden of Disease Study 2016. *Lancet Neurol* (2019) 18:459–80. doi: 10.1016/S1474-4422(18)30499-X
4. Verkhratsky A, Parpura V, Pekna M, Pekny M, Sofroniew M. Glia in the Pathogenesis of Neurodegenerative Diseases. *Biochem Soc Trans* (2014) 42:1291–301. doi: 10.1042/BST20140107
5. Phatnani H, Maniatis T. Astrocytes in Neurodegenerative Disease. *Cold Spring Harb Perspect Biol* (2015) 7. doi: 10.1101/cshperspect.a020628
6. Allen NJ, Eroglu C. Cell Biology of Astrocyte-Synapse Interactions. *Neuron* (2017) 96:697–708. doi: 10.1016/j.neuron.2017.09.056
7. Oberheim NA, Takano T, Han X, He W, Lin JHC, Wang F, et al. Uniquely Hominid Features of Adult Human Astrocytes. *J Neurosci Off J Soc Neurosci* (2009) 29:3276–87. doi: 10.1523/JNEUROSCI.4707-08.2009
8. Kimelberg HK. Supportive or Information-Processing Functions of the Mature Protoplasmic Astrocyte in the Mammalian CNS? A Critical Appraisal. *Neuron Glia Biol* (2007) 3:181–9. doi: 10.1017/S1740925X08000094
9. Vasile F, Dossi E, Rouach N. Human Astrocytes: Structure and Functions in the Healthy Brain. *Brain Struct Funct* (2017) 222:2017–29. doi: 10.1007/s00429-017-1383-5
10. Haim LB, Rowitch DH. Functional Diversity of Astrocytes in Neural Circuit Regulation. *Nat Rev Neurosci* (2017) 18:31–41. doi: 10.1038/nrn.2016.159
11. Sofroniew MV, Vinters HV. Astrocytes: Biology and Pathology. *Acta Neuropathol (Berl)* (2010) 119:7–35. doi: 10.1007/s00401-009-0619-8
12. Yang Y, Vidensky S, Jin L, Jie C, Lorenzini I, Frankl M, et al. Molecular Comparison of GLT1+ and ALDH1L1+ Astrocytes *In Vivo* in Astroglial Reporter Mice. *Glia* (2011) 59:200–7. doi: 10.1002/glia.21089
13. Lin C-CCJ, Yu K, Hatcher A, Huang T-W, Lee HK, Carlson J, et al. Identification of Diverse Astrocyte Populations and Their Malignant Analogs. *Nat Neurosci* (2017) 20:396–405. doi: 10.1038/nn.4493
14. Batiuk MY, Martirosyan A, Wahis J, de Vin F, Marneffe C, Kusserow C, et al. Identification of Region-Specific Astrocyte Subtypes At Single Cell Resolution. *Nat Commun* (2020) 11:1220. doi: 10.1038/s41467-019-14198-8
15. Zeisel A, Hochgerner H, Lönnerberg P, Johnsson A, Memic F, van der Zwan J, et al. Molecular Architecture of the Mouse Nervous System. *Cell* (2018) 174:999–1014.e22. doi: 10.1016/j.cell.2018.06.021
16. Molofsky AV, Deneen B. Astrocyte Development: A Guide for the Perplexed. *Glia* (2015) 63:1320–9. doi: 10.1002/glia.22836
17. Fossati G, Matteoli M, Menna E. Astrocytic Factors Controlling Synaptogenesis: A Team Play. *Cells* (2020) 9. doi: 10.3390/cells9102173
18. Araque A, Parpura V, Sanzgiri RP, Haydon PG. Tripartite Synapses: Glia, the Unacknowledged Partner. *Trends Neurosci* (1999) 22:208–15. doi: 10.1016/s0166-2236(98)01349-6
19. Daneman R, Prat A. The Blood-Brain Barrier. *Cold Spring Harb Perspect Biol* (2015) 7:a020412. doi: 10.1101/cshperspect.a020412
20. Iadecola C. The Neurovascular Unit Coming of Age: A Journey Through Neurovascular Coupling in Health and Disease. *Neuron* (2017) 96:17–42. doi: 10.1016/j.neuron.2017.07.030
21. Iliff JJ, Wang M, Liao Y, Plogg BA, Peng W, Gundersen GA, et al. A Paravascular Pathway Facilitates CSF Flow Through the Brain Parenchyma and the Clearance of Interstitial Solutes, Including Amyloid β. *Sci Transl Med* (2012) 4:147ra111. doi: 10.1126/scitranslmed.3003748
22. Jessen NA, Munk ASF, Lundgaard I, Nedergaard M. The Glymphatic System: A Beginner's Guide. *Neurochem Res* (2015) 40:2583–99. doi: 10.1007/s11064-015-1581-6
23. Anderson MA, Ao Y, Sofroniew MV. Heterogeneity of Reactive Astrocytes. *Neurosci Lett* (2014) 565:23–9. doi: 10.1016/j.neulet.2013.12.030
24. Liddelow SA, Guttenplan KA, Clarke LE, Bennett FC, Bohlen CJ, Schirmer L, et al. Neurotoxic Reactive Astrocytes are Induced by Activated Microglia. *Nature* (2017) 541:481–7. doi: 10.1038/nature21029
25. Rothhammer V, Quintana FJ. Control of Autoimmune CNS Inflammation by Astrocytes. *Semin Immunopathol* (2015) 37:625–38. doi: 10.1007/s00281-015-0515-3
26. Morita M, Ikeshima-Kataoka H, Kreft M, Vardjan N, Zorec R, Noda M. Metabolic Plasticity of Astrocytes and Aging of the Brain. *Int J Mol Sci* (2019) 20. doi: 10.3390/ijms20040941
27. Dienel GA. Brain Glucose Metabolism: Integration of Energetics With Function. *Physiol Rev* (2019) 99:949–1045. doi: 10.1152/physrev.00062.2017
28. Dienel GA, Rothman DL. Reevaluation of Astrocyte-Neuron Energy Metabolism With Astrocyte Volume Fraction Correction: Impact on Cellular Glucose Oxidation Rates, Glutamate-Glutamine Cycle Energetics, Glycogen Levels and Utilization Rates vs. Exercising Muscle, and Na+/K+ Pumping Rates. *Neurochem Res* (2020) 45:2607–30. doi: 10.1007/s11064-020-03125-9
29. Bélanger M, Allaman I, Magistretti PJ. Brain Energy Metabolism: Focus on Astrocyte-Neuron Metabolic Cooperation. *Cell Metab* (2011) 14:724–38. doi: 10.1016/j.cmet.2011.08.016
30. Love S, Miners JS. Cerebrovascular Disease in Ageing and Alzheimer's Disease. *Acta Neuropathol (Berl)* (2016) 131:645–58. doi: 10.1007/s00401-015-1522-0
31. Carmignoto G, Gómez-Gonzalo M. The Contribution of Astrocyte Signalling to Neurovascular Coupling. *Brain Res Rev* (2010) 63:138–48. doi: 10.1016/j.brainresrev.2009.11.007
32. Kisler K, Nelson AR, Montagne A, Zlokovic BV. Cerebral Blood Flow Regulation and Neurovascular Dysfunction in Alzheimer Disease. *Nat Rev Neurosci* (2017) 18:419–34. doi: 10.1038/nrn.2017.48
33. Michels L, Warnock G, Buck A, Macauda G, Leh SE, Kaelin AM, et al. Arterial Spin Labeling Imaging Reveals Widespread and Aβ-Independent

Reductions in Cerebral Blood Flow in Elderly Apolipoprotein Epsilon-4 Carriers. *J Cereb Blood Flow Metab Off J Int Soc Cereb Blood Flow Metab* (2016) 36:581–95. doi: 10.1177/0271678X15605847
34. Sperling RA, Bates JF, Chua EF, Cocchiarella AJ, Rentz DM, Rosen BR, et al. fMRI Studies of Associative Encoding in Young and Elderly Controls and Mild Alzheimer's Disease. *J Neurol Neurosurg Psychiatry* (2003) 74:44–50. doi: 10.1136/jnnp.74.1.44
35. Borghammer P, Chakravarty M, Jonsdottir KY, Sato N, Matsuda H, Ito K, et al. Cortical Hypometabolism and Hypoperfusion in Parkinson's Disease is Extensive: Probably Even At Early Disease Stages. *Brain Struct Funct* (2010) 214:303–17. doi: 10.1007/s00429-010-0246-0
36. Guan J, Pavlovic D, Dalkie N, Waldvogel HJ, O'Carroll SJ, Green CR, et al. Vascular Degeneration in Parkinson's Disease. *Brain Pathol Zurich Switz* (2013) 23:154–64. doi: 10.1111/j.1750-3639.2012.00628.x
37. Rosengarten B, Dannhardt V, Burr O, Pöhler M, Rosengarten S, Oechsner M, et al. Neurovascular Coupling in Parkinson's Disease Patients: Effects of Dementia and Acetylcholinesterase Inhibitor Treatment. *J Alzheimers Dis JAD* (2010) 22:415–21. doi: 10.3233/JAD-2010-101140
38. Camandola S, Mattson MP. Brain Metabolism in Health, Aging, and Neurodegeneration. *EMBO J* (2017) 36:1474–92. doi: 10.15252/embj.201695810
39. Lee H, Pienaar IS. Disruption of the Blood-Brain Barrier in Parkinson's Disease: Curse or Route to a Cure? *Front Biosci Landmark Ed* (2014) 19:272–80. doi: 10.2741/4206
40. Carvey PM, Zhao CH, Hendey B, Lum H, Trachtenberg J, Desai BS, et al. 6-Hydroxydopamine-induced Alterations in Blood-Brain Barrier Permeability. *Eur J Neurosci* (2005) 22:1158–68. doi: 10.1111/j.1460-9568.2005.04281.x
41. Reeves BC, Karimy JK, Kundishora AJ, Mestre H, Cerci HM, Matouk C, et al. Glymphatic System Impairment in Alzheimer's Disease and Idiopathic Normal Pressure Hydrocephalus. *Trends Mol Med* (2020) 26:285–95. doi: 10.1016/j.molmed.2019.11.008
42. Keir LHM, Breen DP. New Awakenings: Current Understanding of Sleep Dysfunction and its Treatment in Parkinson's Disease. *J Neurol* (2020) 267:288–94. doi: 10.1007/s00415-019-09651-z
43. Pierre K, Pellerin L. Monocarboxylate Transporters in the Central Nervous System: Distribution, Regulation and Function. *J Neurochem* (2005) 94:1–14. doi: 10.1111/j.1471-4159.2005.03168.x
44. Pellerin L, Magistretti PJ. Glutamate Uptake Into Astrocytes Stimulates Aerobic Glycolysis: A Mechanism Coupling Neuronal Activity to Glucose Utilization. *Proc Natl Acad Sci USA* (1994) 91:10625–9. doi: 10.1073/pnas.91.22.10625
45. Li B, Freeman RD. Neurometabolic Coupling Between Neural Activity, Glucose, and Lactate in Activated Visual Cortex. *J Neurochem* (2015) 135:742–54. doi: 10.1111/jnc.13143
46. Magistretti PJ, Chatton J-Y. Relationship Between L-Glutamate-Regulated Intracellular Na+ Dynamics and ATP Hydrolysis in Astrocytes. *J Neural Transm Vienna Austria* (2005) 1996:112. doi: 10.1007/s00702-004-0171-6
47. Pellerin L, Bouzier-Sore A-K, Aubert A, Serres S, Merle M, Costalat R, et al. Activity-Dependent Regulation of Energy Metabolism by Astrocytes: An Update. *Glia* (2007) 55:1251–62. doi: 10.1002/glia.20528
48. Magistretti PJ. Role of Glutamate in Neuron-Glia Metabolic Coupling. *Am J Clin Nutr* (2009) 90:875S–80S. doi: 10.3945/ajcn.2009.27462CC
49. Marcus C, Mena E, Subramaniam RM. Brain PET in the Diagnosis of Alzheimer's Disease. *Clin Nucl Med* (2014) 39:e413–422; quiz e423-426. doi: 10.1097/RLU.0000000000000547
50. Vlassenko AG, Gordon BA, Goyal MS, Su Y, Blazey TM, Durbin TJ, et al. Aerobic Glycolysis and Tau Deposition in Preclinical Alzheimer's Disease. *Neurobiol Aging* (2018) 67:95–8. doi: 10.1016/j.neurobiolaging.2018.03.014
51. Bell SM, Burgess T, Lee J, Blackburn DJ, Allen SP, Mortiboys H. Peripheral Glycolysis in Neurodegenerative Diseases. *Int J Mol Sci* (2020) 21. doi: 10.3390/ijms21238924
52. Meles SK, Renken RJ, Pagani M, Teune LK, Arnaldi D, Morbelli S, et al. Abnormal Pattern of Brain Glucose Metabolism in Parkinson's Disease: Replication in Three European Cohorts. *Eur J Nucl Med Mol Imaging* (2020) 47:437–50. doi: 10.1007/s00259-019-04570-7
53. Leke R, Schousboe A. The Glutamine Transporters and Their Role in the Glutamate/GABA-Glutamine Cycle. *Adv Neurobiol* (2016) 13:223–57. doi: 10.1007/978-3-319-45096-4_8
54. Anlauf E, Derouiche A. Glutamine Synthetase as an Astrocytic Marker: its Cell Type and Vesicle Localization. *Front Endocrinol* (2013) 4:144. doi: 10.3389/fendo.2013.00144
55. Rothman DL, De Feyter HM, de Graaf RA, Mason GF, Behar KL. 13c MRS Studies of Neuroenergetics and Neurotransmitter Cycling in Humans. *NMR BioMed* (2011) 24:943–57. doi: 10.1002/nbm.1772
56. Hertz L, Chen Y. Integration Between Glycolysis and Glutamate-Glutamine Cycle Flux may Explain Preferential Glycolytic Increase During Brain Activation, Requiring Glutamate. *Front Integr Neurosci* (2017) 11:18. doi: 10.3389/fnint.2017.00018
57. Huang S, Tong H, Lei M, Zhou M, Guo W, Li G, et al. Astrocytic Glutamatergic Transporters are Involved in Aβ-Induced Synaptic Dysfunction. *Brain Res* (2018) 1678:129–37. doi: 10.1016/j.brainres.2017.10.011
58. Conway ME. Alzheimer's Disease: Targeting the Glutamatergic System. *Biogerontology* (2020) 21:257–74. doi: 10.1007/s10522-020-09860-4
59. Iovino L, Tremblay ME, Civiero L. Glutamate-Induced Excitotoxicity in Parkinson's Disease: The Role of Glial Cells. *J Pharmacol Sci* (2020) 144:151–64. doi: 10.1016/j.jphs.2020.07.011
60. Ioannou MS, Jackson J, Sheu S-H, Chang C-L, Weigel AV, Liu H, et al. Neuron-Astrocyte Metabolic Coupling Protects Against Activity-Induced Fatty Acid Toxicity. *Cell* (2019) 177:1522–35. doi: 10.1016/j.cell.2019.04.001
61. Qi G, Mi Y, Shi X, Gu H, Brinton RD, Yin F. Apoe4 Impairs Neuron-Astrocyte Coupling of Fatty Acid Metabolism. *Cell Rep* (2021) 34:108572. doi: 10.1016/j.celrep.2020.108572
62. Castagnet PI, Golovko MY, Barceló-Coblijn GC, Nussbaum RL, Murphy EJ. Fatty Acid Incorporation is Decreased in Astrocytes Cultured From Alpha-Synuclein Gene-Ablated Mice. *J Neurochem* (2005) 94:839–49. doi: 10.1111/j.1471-4159.2005.03247.x
63. DiNuzzo M, Schousboe A. *Brain Glycogen Metabolism*. Cham, Switzerland: Springer International Publishing (2019). doi: 10.1007/978-3-030-27480-1
64. Rahman B, Kussmaul L, Hamprecht B, Dringen R. Glycogen is Mobilized During the Disposal of Peroxides by Cultured Astroglial Cells From Rat Brain. *Neurosci Lett* (2000) 290:169–72. doi: 10.1016/s0304-3940(00)01369-0
65. Suzuki A, Stern SA, Bozdagi O, Huntley GW, Walker RH, Magistretti PJ, et al. Astrocyte-Neuron Lactate Transport is Required for Long-Term Memory Formation. *Cell* (2011) 144:810–23. doi: 10.1016/j.cell.2011.02.018
66. Bak LK, Walls AB, Schousboe A, Waagepetersen HS. Astrocytic Glycogen Metabolism in the Healthy and Diseased Brain. *J Biol Chem* (2018) 293:7108–16. doi: 10.1074/jbc.R117.803239
67. Gannon M, Che P, Chen Y, Jiao K, Roberson ED, Wang Q. Noradrenergic Dysfunction in Alzheimer's Disease. *Front Neurosci* (2015) 9:220. doi: 10.3389/fnins.2015.00220
68. Dringen R. Metabolism and Functions of Glutathione in Brain. *Prog Neurobiol* (2000) 62:649–71. doi: 10.1016/s0301-0082(99)00060-x
69. Scheiber IF, Mercer JFB, Dringen R. Metabolism and Functions of Copper in Brain. *Prog Neurobiol* (2014) 116:33–57. doi: 10.1016/j.pneurobio.2014.01.002
70. Rizor A, Pajarillo E, Johnson J, Aschner M, Lee E. Astrocytic Oxidative/Nitrosative Stress Contributes to Parkinson's Disease Pathogenesis: The Dual Role of Reactive Astrocytes. *Antioxid Basel Switz* (2019) 8. doi: 10.3390/antiox8080265
71. Dunn L, Allen GF, Mamais A, Ling H, Li A, Duberley KE, et al. Dysregulation of Glucose Metabolism is an Early Event in Sporadic Parkinson's Disease. *Neurobiol Aging* (2014) 35:1111–5. doi: 10.1016/j.neurobiolaging.2013.11.001
72. Sian J, Dexter DT, Lees AJ, Daniel S, Agid Y, Javoy-Agid F, et al. Alterations in Glutathione Levels in Parkinson's Disease and Other Neurodegenerative Disorders Affecting Basal Ganglia. *Ann Neurol* (1994) 36:348–55. doi: 10.1002/ana.410360305
73. Baillet A, Chanteperdrix V, Trocmé C, Casez P, Garrel C, Besson G. The Role of Oxidative Stress in Amyotrophic Lateral Sclerosis and Parkinson's Disease. *Neurochem Res* (2010) 35:1530–7. doi: 10.1007/s11064-010-0212-5
74. Kim GH, Kim JE, Rhie SJ, Yoon S. The Role of Oxidative Stress in Neurodegenerative Diseases. *Exp Neurobiol* (2015) 24:325–40. doi: 10.5607/en.2015.24.4.325
75. Bandopadhyay R, Kingsbury AE, Cookson MR, Reid AR, Evans IM, Hope AD, et al. The Expression of DJ-1 (PARK7) in Normal Human CNS and Idiopathic Parkinson's Disease. *Brain J Neurol* (2004) 127:420–30. doi: 10.1093/brain/awh054

76. Booth HDE, Hirst WD, Wade-Martins R. The Role of Astrocyte Dysfunction in Parkinson's Disease Pathogenesis. *Trends Neurosci* (2017) 40:358–70. doi: 10.1016/j.tins.2017.04.001
77. Allaman I, Bélanger M, Magistretti PJ. Astrocyte-Neuron Metabolic Relationships: for Better and for Worse. *Trends Neurosci* (2011) 34:76–87. doi: 10.1016/j.tins.2010.12.001
78. Vicente-Gutierrez C, Bonora N, Bobo-Jimenez V, Jimenez-Blasco D, Lopez-Fabuel I, Fernandez E, et al. Astrocytic Mitochondrial ROS Modulate Brain Metabolism and Mouse Behaviour. *Nat Metab* (2019) 1:201–11. doi: 10.1038/s42255-018-0031-6
79. Vallerga CL, Zhang F, Fowdar J, McRae AF, Qi T, Nabais MF, et al. Analysis of DNA Methylation Associates the Cystine-Glutamate Antiporter SLC7A11 With Risk of Parkinson's Disease. *Nat Commun* (2020) 11:1238. doi: 10.1038/s41467-020-15065-7
80. Khodagholi F, Shaerzadeh F, Montazeri F. Mitochondrial Aconitase in Neurodegenerative Disorders: Role of a Metabolism- Related Molecule in Neurodegeneration. *Curr Drug Targets* (2018) 19:973–85. doi: 10.2174/1389450118666170816124203
81. Chen H, Denton TT, Xu H, Calingasan N, Beal MF, Gibson GE. Reductions in the Mitochondrial Enzyme α-Ketoglutarate Dehydrogenase Complex in Neurodegenerative Disease - Beneficial or Detrimental? *J Neurochem* (2016) 139:823–38. doi: 10.1111/jnc.13836
82. Gibson GE, Starkov A, Blass JP, Ratan RR, Beal MF. Cause and Consequence: Mitochondrial Dysfunction Initiates and Propagates Neuronal Dysfunction, Neuronal Death and Behavioral Abnormalities in Age-Associated Neurodegenerative Diseases. *Biochim Biophys Acta* (2010) 1802:122–34. doi: 10.1016/j.bbadis.2009.08.010
83. Fernandez E, Bolaños JP. α-Ketoglutarate Dehydrogenase Complex Moonlighting: ROS Signalling Added to the List: An Editorial Highlight for "Reductions in the Mitochondrial Enzyme α-Ketoglutarate Dehydrogenase Complex in Neurodegenerative Disease - Beneficial or Detrimental?" *J Neurochem* (2016) 139:689–90. doi: 10.1111/jnc.13862
84. Gibson GE, Kingsbury AE, Xu H, Lindsay JG, Daniel S, Foster OJF, et al. Deficits in a Tricarboxylic Acid Cycle Enzyme in Brains From Patients With Parkinson's Disease. *Neurochem Int* (2003) 43:129–35. doi: 10.1016/s0197-0186(02)00225-5
85. Bubber P, Haroutunian V, Fisch G, Blass JP, Gibson GE. Mitochondrial Abnormalities in Alzheimer Brain: Mechanistic Implications. *Ann Neurol* (2005) 57:695–703. doi: 10.1002/ana.20474
86. Tufekci KU, Civi Bayin E, Genc S, Genc K. The Nrf2/ARE Pathway: A Promising Target to Counteract Mitochondrial Dysfunction in Parkinson's Disease. *Park Dis* (2011) 2011:314082. doi: 10.4061/2011/314082
87. Stewart VC, Land JM, Clark JB, Heales SJ. Comparison of Mitochondrial Respiratory Chain Enzyme Activities in Rodent Astrocytes and Neurones and a Human Astrocytoma Cell Line. *Neurosci Lett* (1998) 247:201–3. doi: 10.1016/s0304-3940(98)00284-5
88. Lopez-Fabuel I, Le Douce J, Logan A, James AM, Bonvento G, Murphy MP, et al. Complex I Assembly Into Supercomplexes Determines Differential Mitochondrial ROS Production in Neurons and Astrocytes. *Proc Natl Acad Sci USA* (2016) 113:13063–8. doi: 10.1073/pnas.1613701113
89. Grünewald A, Kumar KR, Sue CM. New Insights Into the Complex Role of Mitochondria in Parkinson's Disease. *Prog Neurobiol* (2019) 177:73–93. doi: 10.1016/j.pneurobio.2018.09.003
90. Lindström V, Gustafsson G, Sanders LH, Howlett EH, Sigvardson J, Kasrayan A, et al. Extensive Uptake of α-Synuclein Oligomers in Astrocytes Results in Sustained Intracellular Deposits and Mitochondrial Damage. *Mol Cell Neurosci* (2017) 82:143–56. doi: 10.1016/j.mcn.2017.04.009
91. Choi I, Kim J, Jeong H-K, Kim B, Jou I, Park SM, et al. PINK1 Deficiency Attenuates Astrocyte Proliferation Through Mitochondrial Dysfunction, Reduced AKT and Increased P38 MAPK Activation, and Downregulation of EGFR. *Glia* (2013) 61:800–12. doi: 10.1002/glia.22475
92. Schmidt S, Linnartz B, Mendritzki S, Sczepan T, Lübbert M, Stichel CC, et al. Genetic Mouse Models for Parkinson's Disease Display Severe Pathology in Glial Cell Mitochondria. *Hum Mol Genet* (2011) 20:1197–211. doi: 10.1093/hmg/ddq564
93. Larsen NJ, Ambrosi G, Mullett SJ, Berman SB, Hinkle DA. DJ-1 Knock-Down Impairs Astrocyte Mitochondrial Function. *Neuroscience* (2011) 196:251–64. doi: 10.1016/j.neuroscience.2011.08.016
94. Mullett SJ, Di Maio R, Greenamyre JT, Hinkle DA. DJ-1 Expression Modulates Astrocyte-Mediated Protection Against Neuronal Oxidative Stress. *J Mol Neurosci MN* (2013) 49:507–11. doi: 10.1007/s12031-012-9904-4
95. Swerdlow RH. Mitochondria and Mitochondrial Cascades in Alzheimer's Disease. *J Alzheimers Dis JAD* (2018) 62:1403–16. doi: 10.3233/JAD-170585
96. McAvoy K, Kawamata H. Glial Mitochondrial Function and Dysfunction in Health and Neurodegeneration. *Mol Cell Neurosci* (2019) 101:103417. doi: 10.1016/j.mcn.2019.103417
97. Shigetomi E, Saito K, Sano F, Koizumi S. Aberrant Calcium Signals in Reactive Astrocytes: A Key Process in Neurological Disorders. *Int J Mol Sci* (2019) 20. doi: 10.3390/ijms20040996
98. Agarwal A, Wu P-H, Hughes EG, Fukaya M, Tischfield MA, Langseth AJ, et al. Transient Opening of the Mitochondrial Permeability Transition Pore Induces Microdomain Calcium Transients in Astrocyte Processes. *Neuron* (2017) 93:587–605.e7. doi: 10.1016/j.neuron.2016.12.034
99. Parri HR, Gould TM, Crunelli V. Spontaneous Astrocytic Ca2+ Oscillations *In Situ* Drive NMDAR-mediated Neuronal Excitation. *Nat Neurosci* (2001) 4:803–12. doi: 10.1038/90507
100. Durkee CA, Araque A. Diversity and Specificity of Astrocyte-neuron Communication. *Neuroscience* (2019) 396:73–8. doi: 10.1016/j.neuroscience.2018.11.010
101. Kuchibhotla KV, Lattarulo CR, Hyman BT, Bacskai BJ. Synchronous Hyperactivity and Intercellular Calcium Waves in Astrocytes in Alzheimer Mice. *Science* (2009) 323:1211–5. doi: 10.1126/science.1169096
102. Delekate A, Füchtemeier M, Schumacher T, Ulbrich C, Foddis M, Petzold GC. Metabotropic P2Y1 Receptor Signalling Mediates Astrocytic Hyperactivity *In Vivo* in an Alzheimer's Disease Mouse Model. *Nat Commun* (2014) 5:5422. doi: 10.1038/ncomms6422
103. Loaiza A, Porras OH, Barros LF. Glutamate Triggers Rapid Glucose Transport Stimulation in Astrocytes as Evidenced by Real-Time Confocal Microscopy. *J Neurosci Off J Soc Neurosci* (2003) 23:7337–42. doi: 10.1523/JNEUROSCI.23-19-07337.2003
104. Porras OH, Ruminot I, Loaiza A, Barros LF. Na(+)-Ca(2+) Cosignaling in the Stimulation of the Glucose Transporter GLUT1 in Cultured Astrocytes. *Glia* (2008) 56:59–68. doi: 10.1002/glia.20589
105. Horvat A, Muhič M, Smolič T, Begić E, Zorec R, Kreft M, et al. Ca2+ as the Prime Trigger of Aerobic Glycolysis in Astrocytes. *Cell Calcium* (2021) 95:102368. doi: 10.1016/j.ceca.2021.102368
106. Li X, Tao Y, Bradley R, Du Z, Tao Y, Kong L, et al. Fast Generation of Functional Subtype Astrocytes From Human Pluripotent Stem Cells. *Stem Cell Rep* (2018) 11:998–1008. doi: 10.1016/j.stemcr.2018.08.019
107. Tcw J, Wang M, Pimenova AA, Bowles KR, Hartley BJ, Lacin E, et al. An Efficient Platform for Astrocyte Differentiation From Human Induced Pluripotent Stem Cells. *Stem Cell Rep* (2017) 9:600–14. doi: 10.1016/j.stemcr.2017.06.018
108. Janssen K, Bahnassawy L, Kiefer C, Korffmann J, Terstappen GC, Lakics V, et al. Generating Human Ipsc-Derived Astrocytes With Chemically Defined Medium for In Vitro Disease Modeling. *Methods Mol Biol Clifton NJ* (2019) 1994:31–9. doi: 10.1007/978-1-4939-9477-9_3
109. Santos R, Vadodaria KC, Jaeger BN, Mei A, Lefcochilos-Fogelquist S, Mendes APD, et al. Differentiation of Inflammation-Responsive Astrocytes From Glial Progenitors Generated From Human Induced Pluripotent Stem Cells. *Stem Cell Rep* (2017) 8:1757–69. doi: 10.1016/j.stemcr.2017.05.011
110. Tchieu J, Calder EL, Guttikonda SR, Gutzwiller EM, Aromolaran KA, Steinbeck JA, et al. NFIA is a Gliogenic Switch Enabling Rapid Derivation of Functional Human Astrocytes From Pluripotent Stem Cells. *Nat Biotechnol* (2019) 37:267–75. doi: 10.1038/s41587-019-0035-0
111. Chandrasekaran A, Avci HX, Leist M, Kobolák J, Dinnyés A. Astrocyte Differentiation of Human Pluripotent Stem Cells: New Tools for Neurological Disorder Research. *Front Cell Neurosci* (2016) 10:215. doi: 10.3389/fncel.2016.00215
112. Konttinen H, Gureviciene I, Oksanen M, Grubman A, Loppi S, Huuskonen MT, et al. Pparβ/δ-Agonist GW0742 Ameliorates Dysfunction in Fatty Acid Oxidation in PSEN1ΔE9 Astrocytes. *Glia* (2019) 67:146–59. doi: 10.1002/glia.23534
113. Krencik R, Zhang S-C. Directed Differentiation of Functional Astroglial Subtypes From Human Pluripotent Stem Cells. *Nat Protoc* (2011) 6:1710–7. doi: 10.1038/nprot.2011.405

114. Oksanen M, Petersen AJ, Naumenko N, Puttonen K, Lehtonen Š, Gubert Olivé M, et al. Psen1 Mutant Ipsc-Derived Model Reveals Severe Astrocyte Pathology in Alzheimer's Disease. *Stem Cell Rep* (2017) 9:1885–97. doi: 10.1016/j.stemcr.2017.10.016
115. Lin Y-T, Seo J, Gao F, Feldman HM, Wen H-L, Penney J, et al. Apoe4 Causes Widespread Molecular and Cellular Alterations Associated With Alzheimer's Disease Phenotypes in Human Ipsc-Derived Brain Cell Types. *Neuron* (2018) 98:1141–54.e7. doi: 10.1016/j.neuron.2018.05.008
116. Chen C, Jiang P, Xue H, Peterson SE, Tran HT, McCann AE, et al. Role of Astroglia in Down's Syndrome Revealed by Patient-Derived Human-Induced Pluripotent Stem Cells. *Nat Commun* (2014) 5:4430. doi: 10.1038/ncomms5430
117. Fong LK, Yang MM, Dos Santos Chaves R, Reyna SM, Langness VF, Woodruff G, et al. Full-Length Amyloid Precursor Protein Regulates Lipoprotein Metabolism and Amyloid-β Clearance in Human Astrocytes. *J Biol Chem* (2018) 293:11341–57. doi: 10.1074/jbc.RA117.000441
118. Yuan SH, Martin J, Elia J, Flippin J, Paramban RI, Hefferan MP, et al. Cell-Surface Marker Signatures for the Isolation of Neural Stem Cells, Glia and Neurons Derived From Human Pluripotent Stem Cells. *PloS One* (2011) 6: e17540. doi: 10.1371/journal.pone.0017540
119. Sonninen T-M, Hämäläinen RH, Koskuvi M, Oksanen M, Shakirzyanova A, Wojciechowski S, et al. Metabolic Alterations in Parkinson's Disease Astrocytes. *Sci Rep* (2020) 10:14474. doi: 10.1038/s41598-020-71329-8
120. Aldana BI, Zhang Y, Jensen P, Chandrasekaran A, Christensen SK, Nielsen TT, et al. Glutamate-Glutamine Homeostasis is Perturbed in Neurons and Astrocytes Derived From Patient iPSC Models of Frontotemporal Dementia. *Mol Brain* (2020) 13:125. doi: 10.1186/s13041-020-00658-6
121. Shaltouki A, Peng J, Liu Q, Rao MS, Zeng X. Efficient Generation of Astrocytes From Human Pluripotent Stem Cells in Defined Conditions. *Stem Cells Dayt Ohio* (2013) 31:941–52. doi: 10.1002/stem.1334
122. Ciavardelli D, Piras F, Consalvo A, Rossi C, Zucchelli M, Di Ilio C, et al. Medium-Chain Plasma Acylcarnitines, Ketone Levels, Cognition, and Gray Matter Volumes in Healthy Elderly, Mildly Cognitively Impaired, or Alzheimer's Disease Subjects. *Neurobiol Aging* (2016) 43:1–12. doi: 10.1016/j.neurobiolaging.2016.03.005
123. Palomer X, Barroso E, Pizarro-Delgado J, Peña L, Botteri G, Zarei M, et al. Pparβ/δ: A Key Therapeutic Target in Metabolic Disorders. *Int J Mol Sci* (2018) 19. doi: 10.3390/ijms19030913
124. Paik M-J, Ahn Y-H, Lee PH, Kang H, Park CB, Choi S, et al. Polyamine Patterns in the Cerebrospinal Fluid of Patients With Parkinson's Disease and Multiple System Atrophy. *Clin Chim Acta Int J Clin Chem* (2010) 411:1532–5. doi: 10.1016/j.cca.2010.05.034
125. Manyam BV, Ferraro TN, Hare TA. Cerebrospinal Fluid Amino Compounds in Parkinson's Disease. Alterations Due to Carbidopa/Levodopa. *Arch Neurol* (1988) 45:48–50. doi: 10.1001/archneur.1988.00520250054021
126. Sonnay S, Christinat N, Thevenet J, Wiederkehr A, Chakrabarti A, Masoodi M. Exploring Valine Metabolism in Astrocytic and Liver Cells: Lesson From Clinical Observation in TBI Patients for Nutritional Intervention. *Biomedicines* (2020) 8. doi: 10.3390/biomedicines8110487
127. Thevenet J, De Marchi U, Domingo JS, Christinat N, Bultot L, Lefebvre G, et al. Medium-Chain Fatty Acids Inhibit Mitochondrial Metabolism in Astrocytes Promoting Astrocyte-Neuron Lactate and Ketone Body Shuttle Systems. *FASEB J Off Publ Fed Am Soc Exp Biol* (2016) 30:1913–26. doi: 10.1096/fj.201500182
128. Sonnay S, Chakrabarti A, Thevenet J, Wiederkehr A, Christinat N, Masoodi M. Differential Metabolism of Medium-Chain Fatty Acids in Differentiated Human-Induced Pluripotent Stem Cell-Derived Astrocytes. *Front Physiol* (2019) 10:657. doi: 10.3389/fphys.2019.00657
129. Dong Y, Benveniste EN. Immune Function of Astrocytes. *Glia* (2001) 36:180–90. doi: 10.1002/glia.1107
130. Lee H-J, Kim C, Lee S-J. Alpha-Synuclein Stimulation of Astrocytes: Potential Role for Neuroinflammation and Neuroprotection. *Oxid Med Cell Longev* (2010) 3:283–7. doi: 10.4161/oxim.3.4.12809
131. Haim BL, Carrillo-de Sauvage M-A, Ceyzériat K, Escartin C. Elusive Roles for Reactive Astrocytes in Neurodegenerative Diseases. *Front Cell Neurosci* (2015) 9:278. doi: 10.3389/fncel.2015.00278
132. Lee H-J, Suk J-E, Patrick C, Bae E-J, Cho J-H, Rho S, et al. Direct Transfer of Alpha-Synuclein From Neuron to Astroglia Causes Inflammatory Responses in Synucleinopathies. *J Biol Chem* (2010) 285:9262–72. doi: 10.1074/jbc.M109.081125
133. Söllvander S, Nikitidou E, Brolin R, Söderberg L, Sehlin D, Lannfelt L, et al. Accumulation of Amyloid-β by Astrocytes Result in Enlarged Endosomes and Microvesicle-Induced Apoptosis of Neurons. *Mol Neurodegener* (2016) 11:38. doi: 10.1186/s13024-016-0098-z
134. Rostami J, Holmqvist S, Lindström V, Sigvardson J, Westermark GT, Ingelsson M, et al. Human Astrocytes Transfer Aggregated Alpha-Synuclein *via* Tunneling Nanotubes. *J Neurosci Off J Soc Neurosci* (2017) 37:11835–53. doi: 10.1523/JNEUROSCI.0983-17.2017
135. Tsunemi T, Ishiguro Y, Yoroisaka A, Valdez C, Miyamoto K, Ishikawa K, et al. Astrocytes Protect Human Dopaminergic Neurons From α-Synuclein Accumulation and Propagation. *J Neurosci Off J Soc Neurosci* (2020) 40:8618–28. doi: 10.1523/JNEUROSCI.0954-20.2020
136. Gu X-L, Long C-X, Sun L, Xie C, Lin X, Cai H. Astrocytic Expression of Parkinson's Disease-Related A53T Alpha-Synuclein Causes Neurodegeneration in Mice. *Mol Brain* (2010) 3:12. doi: 10.1186/1756-6606-3-12
137. Grünewald A, Rygiel KA, Hepplewhite PD, Morris CM, Picard M, Turnbull DM. Mitochondrial DNA Depletion in Respiratory Chain-Deficient Parkinson Disease Neurons. *Ann Neurol* (2016) 79:366–78. doi: 10.1002/ana.24571
138. West AP, Khoury-Hanold W, Staron M, Tal MC, Pineda CM, Lang SM, et al. Mitochondrial DNA Stress Primes the Antiviral Innate Immune Response. *Nature* (2015) 520:553–7. doi: 10.1038/nature14156
139. Zhong Z, Liang S, Sanchez-Lopez E, He F, Shalapour S, Lin X-J, et al. New Mitochondrial DNA Synthesis Enables NLRP3 Inflammasome Activation. *Nature* (2018) 560:198–203. doi: 10.1038/s41586-018-0372-z
140. Smajic S, Prada-Medina CA, Landoulsi Z, Dietrich C, Jarazo J, Henck J, et al. Single-Cell Sequencing of the Human Midbrain Reveals Glial Activation and a Neuronal State Specific to Parkinson's Disease. *medRxiv* (2020). doi: 10.1101/2020.09.28.20202812
141. Russ K, Teku G, Bousset L, Redeker V, Piel S, Savchenko E, et al. Tnf-α and α-Synuclein Fibrils Differently Regulate Human Astrocyte Immune Reactivity and Impair Mitochondrial Respiration. *Cell Rep* (2021) 34:108895. doi: 10.1016/j.celrep.2021.108895
142. Grazioli S, Pugin J. Mitochondrial Damage-Associated Molecular Patterns: From Inflammatory Signaling to Human Diseases. *Front Immunol* (2018) 9:832. doi: 10.3389/fimmu.2018.00832
143. Motori E, Puyal J, Toni N, Ghanem A, Angeloni C, Malaguti M, et al. Inflammation-Induced Alteration of Astrocyte Mitochondrial Dynamics Requires Autophagy for Mitochondrial Network Maintenance. *Cell Metab* (2013) 18:844–59. doi: 10.1016/j.cmet.2013.11.005

Conflict of Interest: The authors declare that the research was conducted in the absence of any commercial or financial relationships that could be construed as a potential conflict of interest.

Copyright © 2021 Mulica, Grünewald and Pereira. This is an open-access article distributed under the terms of the Creative Commons Attribution License (CC BY). The use, distribution or reproduction in other forums is permitted, provided the original author(s) and the copyright owner(s) are credited and that the original publication in this journal is cited, in accordance with accepted academic practice. No use, distribution or reproduction is permitted which does not comply with these terms.

2. Aims

Despite years of extensive research, there are still no disease-modifying treatments available for PD. Instead, numerous therapies have been introduced to alleviate patients' symptoms [22]. The quest for the ultimate cure for PD has been intensified with the discovery of iPSC technology, which allows researchers to study disease pathologies at the endogenous level. Importantly, the usage of patient-derived cell models offers a possibility to assess disease progression over time and to uncover the underlying molecular mechanisms [151].

While PD was initially primarily considered a neuronal disease, this neuro-centric view has lately seen a shift. In recent years, more and more studies also explore the contribution of glial cells to neuronal demise in PD. In particular, as key supporters of neuronal functions, astrocytes attract substantial attention as possible contributors to PD pathogenesis [125]. In this context, astrocytic metabolism might serve as an interesting target to develop novel disease-modifying therapies.

Genetic models are an important tool to dissect the molecular mechanisms underlying PD. In particular, mutations in the PD gene *SNCA,* which codes for the main protein component of Lewy bodies (that constitute pathological hallmark of PD), may help to gain a better understanding of the cellular processes leading to the movement disorder [17]. Studying the effect of such mutations at the endogenous level provides the additional advantage that also the contribution of the genetic background of a patient can be considered.

Taking all of this into consideration, I identified several study aims:

- identification of a suitable protocol to generate mature iPSC-derived astrocytes

- generation and characterisation of iPSC-derived astrocytes harboring A53T α-synuclein mutation

- assessment of perturbed genes and pathways in PD astrocytes under resting and activated conditions

- analysis of the effect of A53T α-synuclein on astrocytic physiological functions

3. Results

3.1 Manuscript II

Assessing the suitability of iPSC-derived human astrocytes for disease modeling

Patrycja Mulica[1], Carmen Venegas[1], Zied Landoulsi[1], Katja Badanjak[1], Semra Smajic[1], Sylvie Delcambre[1], Jens Schwamborn[1], Rejko Krüger[1,2], Paul Antony[1], Patrick May[1], Enrico Glaab[1], Anne Grünewald[1,3,#,*], Sandro L. Pereira[1,2,#]

[1]Luxembourg Centre for Systems Biomedicine, University of Luxembourg, Esch-sur-Alzette, Luxembourg
[2]Luxembourg Institute of Health, Strassen, Luxembourg
[3]Institute of Neurogenetics, University of Lübeck, Lübeck, Germany

[#]These two authors share last-authorship.

***Correspondence:** Anne Grünewald, PhD, Luxembourg Centre for Systems Biomedicine, University of Luxembourg, 6 avenue du Swing, L-4367 Belvaux, Luxembourg, phone: (+352) 46 66 44 9793, e-mail: anne.gruenewald@uni.lu

This article has been submitted to Biological Procedures Online.

3.1.1 Preface

In the context of neurodegeneration, the typical disease modeling and novel drugs testing has been based so far on the animal models. However, due to fundamental differences in the biological pathways between humans and other species, the identified drugs typically have low success rates in clinical studies [152]. The implementation of iPSC modeling offers the possibility of overcoming these challenges [150]. Yet, in light of the plethora of published protocols for the generation of iPSC-derived cultures, it is frequently problematic to identify the right method for the given research question.

Therefore, in this study we compared two protocols for obtaining iPSC-derived astrocytes. Both of the methods have been previously published [153], [154] and they differ substantially in their duration. We applied bulk RNA sequencing to delineate the major differences in the transcriptome of the generated cells. After analyzing the expression of astrocytic markers known from the literature, we could show that Oksanen astrocytes display a greater maturation status. This finding was further confirmed by the assessment of cellular morphology using high-content imaging followed by automated analysis in Matlab. To compare iPSC-derived astrocytes obtained in two studied methods with human astrocytes from the human postmortem tissue, we applied the MuSiC method. Using this approach, we could demonstrate the higher similarity between postmortem human astrocytes and Oksanen astrocytes. Finally, we evaluated the activation status of the cells in both methods by analyzing the gene expression of typical markers for astrocytic pan-reactivity as well as A1 and A2 activation states.

My contribution to this study includes mostly the experimental part. I was responsible for the generation of astrocytes using both protocols. Furthermore, I performed the RNA isolation and imaging. I was also involved in data analysis. Moreover, I contributed to the preparation of figures and writing of the manuscript.

3.1.2 Manuscript

Assessing the suitability of iPSC-derived human astrocytes for disease modeling

Patrycja Mulica[1], Carmen Venegas[1], Zied Landoulsi[1], Katja Badanjak[1], Semra Smajic[1], Sylvie Delcambre[1], Jens Schwamborn[1], Rejko Krüger[1,2], Paul Antony[1], Patrick May[1], Enrico Glaab[1], Anne Grünewald[1,3,#,*], Sandro L. Pereira[1,2,#]

[1]Luxembourg Centre for Systems Biomedicine, University of Luxembourg, Esch-sur-Alzette, Luxembourg

[2]Luxembourg Institute of Health, Strassen, Luxembourg

[3]Institute of Neurogenetics, University of Lübeck, Lübeck, Germany

[#]These two authors share last-authorship.

***Correspondence:** Anne Grünewald, PhD, Luxembourg Centre for Systems Biomedicine, University of Luxembourg, 6 avenue du Swing, L-4367 Belvaux, Luxembourg, phone: (+352) 46 66 44 9793, e-mail: anne.gruenewald@uni.lu

Running title: Comparison of iPSC-astrocytes protocols

Keywords: iPSC, astrocytes, disease modeling

Word count: Title: 79 characters; Abstract: 181 words; Manuscript: 4202 words; Figures: 5; References: 61

Abstract

Background

Disease modeling with iPSC-derived cultures has proved to be particularly useful, although the selection of an appropriate protocol for a given research question remains challenging. In particular, numerous methods for the generation of iPSC-derived astrocytes have been reported. Yet, the properties of the obtained cells are frequently inconsistent, which complicates the choice between protocols. Therefore, we compared two approaches for the generation of iPSC-derived astrocytes. We phenotyped glia that were obtained using the differentiation protocols by Oksanen or Palm and colleagues, respectively.

Results

We employed high-throughput imaging and RNA sequencing to deep-characterize the cultures. Oksanen and Palm astrocytes differ considerably in their properties: while the former cells are more labor-intense in their generation (5 vs 2 months), they are also more mature. This notion was strengthened by data resulting from cell type deconvolution analysis that was applied to bulk transcriptomes from the cultures to assess their similarity with human postmortem astrocytes.

Conclusions

Overall, our analyses highlight the need to consider the advantages and disadvantages of a given differentiation protocol, when designing functional or drug discovery studies involving iPSC-derived astrocytes.

Introduction

Astrocytes constitute the largest cell population among glial cells residing in the mammalian brain and play a crucial role in maintaining its proper functioning[1]. Astrocytes are involved in synapse formation, the regulation of brain blood flow, ion and neurotransmitter homeostasis and, most importantly, metabolic support of neuronal functions[2]. Moreover, astrocytes are acknowledged as being critical for the regulation of neuroinflammation, with their ability to recognize inflammatory signals and subsequently react to them through the production of numerous chemokines and cytokines[3–5].

Astrocytes originate from neural stem cells, also known as radial glia[6]. Astrocytic development is a highly regulated process, which is initiated after neurogenesis and controlled by a myriad of intrinsic and extrinsic factors[7]. Key cues for the initiation of gliogenesis are the JAK-STAT, Notch and BMP signaling pathways[8,9]. Furthermore, the transcription factors NFIA and Sox9 have been shown to be fundamental for the commitment to the astrocytic lineage[10,11]. After having populated different regions of the central nervous system, astrocytic precursors begin to mature, i.e. they acquire an expression profile typical for fully differentiated astrocytes. In addition to the upregulation of the established astrocyte marker *GFAP*, the mature state of astrocytes was correlated with the overexpression of genes such as *S100B*, *SLC1A2*, *GJB6*, *GJA1*, *KCNJ10* and *ALDH1L1*. Furthermore, astrocytes develop highly branched processes, which form non-overlapping domains and their proliferation ceases[8,12,13]. In line with the paramount importance of metabolism for maintaining astrocytic functions, it has been reported that metabolic pathways are subject to a substantial remodeling during cell maturation. In particular, despite relying on pronounced glycolysis as a source of energy[14], astrocytes require a transient upregulation of mitochondrial biogenesis and likely the consequent increase in oxidative phosphorylation to halt proliferation and complete their maturation[15].

Recently, astrocytes have gained attention as key contributors to the pathogenesis of numerous neurodegenerative diseases[5]. One of the hallmarks of these disorders is an astrocytic transition from a resting to a reactive state[16,17]. Reactive astrogliosis is a term coined to describe transcriptional, biochemical, physiological and morphological changes that astrocytes undergo when facing brain pathology. Specifically, they may increase *GFAP* levels and drastically modify

the morphology of both their soma and processes[18]. Furthermore, reactive astrocytes change their transcriptome[4], in particular their cytokine expression and secretion profiles[3]. Importantly, changes in activation status might exert a profound effect on astrocytic physiological functions, including their crucial role in energetic coupling with neurons[19].

To unravel the role of astrocytes in neurodegenerative diseases, appropriate and reliable models must be implemented. This is especially true as drug discovery approaches increasingly rely on iPSC-derived cells given the limitations of rodent models in mirroring key phenotypes of neurodegenerative disorders such as Alzheimer's and Parkinson's disease. Since the advent of iPSC technology, numerous protocols have been developed for the generation of patient-derived astrocytes. However, they vary substantially in terms of labor-intensiveness, yield and maturation status of the resulting cells, making it difficult to opt for the appropriate protocol for a given research question[20,21].

Here, we aimed to explore two astrocyte differentiation paradigms, using either iPSCs or neural precursor cells as a starting point and which are substantially different in terms of media composition and the duration of the procedure. We compared one of the most widely used differentiation protocols - a method established by Oksanen et al.[22] that represents a slightly modified version of Krencik and colleagues' method paper[23] - against a "quick" differentiation protocol that was previously established in-house by Palm et al.[24]. By applying RNA sequencing (RNA-seq) and high-content imaging methods, we were able to thoroughly assess maturity and activation status of the obtained astrocytes. Additionally, we compared iPSC-derived astrocytes with their postmortem human counterparts to have a better understanding of the relevance of the generated cultures for disease modeling.

Materials and methods

Cell culture

The study was conducted in accordance to the institutional ethics rules (reference number of the ethics approval: ERP20-038). Human iPSC lines CTRL1 and CTRL2, which were previously generated as described[25,26], were maintained in mTeSR™ Plus medium. Astrocytes differentiated directly

from iPSCs (herein referred to as "Oksanen method") were generated as previously described[22,23]. In short, iPSCs were converted to neuroepithelial cells by maintenance for 11 days in neurodifferentiation medium (NDM) containing 10 µM SB431542 (Sigma) and 200 nM LDN-193189 (Sigma). NDM consisted of DMEM-F12 (Gibco) and Neurobasal (Gibco) in 50:50 ratio supplemented with 1% B27 without vitamin A (Gibco), 0.5% N2 (Gibco), 1% GlutaMAX (Gibco) and 0.5% penicillin/streptomycin (Gibco). Next, cells were kept for two additional days in NDM supplemented with 25 ng/ml bFGF (Peprotech). Subsequently, cells were dissociated by scraping, plated on ultra-low attachment plates (Corning) and grown for two days in NDM without the addition of growth factors. Under these conditions, cells formed spheres and were maintained in astrodifferentation medium (ADM) for five months, and manually dissociated by cutting once per week. ADM was comprised of DMEM-F12 supplemented with 1% non-essential amino acids (Gibco), 1% N2, 1% GlutaMAX, 0.5% penicillin/streptomycin, 2 µg/ml heparin (Sigma), as well as 10 ng/ml bFGF and 10 ng/ml EGF (Peptrotech). Terminal differentiation was achieved by dissociating the spheres with accutase (Merck Millipore) and plating them on matrigel (Corning)-coated plates, followed by cultivation for 7 days in ADM containing 10 ng/ml CNTF (Peprotech) and 10 ng/ml BMP4 (Peprotech).

The alternative two-step protocol referred to as "Palm method" is initiated by the conversion of iPSCs into small molecule neural precursor cells (smNPCs), by means of dual-SMAD inhibition and induction of WNT and SHH signaling. These cells correspond to neuroepithelial cells that retain the potential to give rise to neural tube and neural crest lineages[26]. After conversion, smNPCs were expanded in N2B27 medium consisting of DMEMF-12 (Gibco)/Neurobasal (Gibco) in 50:50 ratio, supplemented with 1% B27 without vitamin A (Gibco), 0.5% N2 (Gibco), 1% GlutaMAX (Gibco) and 1% penicillin/streptomycin (Gibco). Additionally, 3 µM CHIR99201 (Sigma), 0.75 µM purmorphamine (Sigma) and 150 µM ascorbic acid (Sigma) were added to the medium. The second step in this protocol corresponds to the generation of astrocytes from smNPCs, as published before[24]. In brief, smNPCs were plated and kept in the standard medium for two days. Afterwards, the medium was changed to N2B27 medium containing 3 µM CHIR, 0.75 µM PMA, 150 µM ascorbic acid and 20 ng/ml bFGF (Peprotech) for two additional days. At day four, cells were dissociated using accutase and plated in DMEMF-12 supplemented with 1% penicillin/streptomycin, 1% GlutaMAX, 1% N2, 2% B27 with vitamin A (Gibco), 40 ng/ml EGF (Peprotech), 40 ng/ml bFGF and 1.5 ng/ml hLIF (Peprotech). Cells were maintained in this medium

for three passages and for terminal differentiation grown in DMEM-F12 containing 1% penicillin/streptomycin, 1% GlutaMAX and 1% FBS (Gibco) for 60 days.

Immunocytochemistry and image analysis

To perform immunocytochemistry analysis, cells were fixed using 4% paraformaldehyde in PBS (ThermoScientific). Subsequently, cells were permeabilized and blocked with 0.25% Triton X-100 and 1% BSA in PBS for 1 h. The same solution was used to prepare dilutions of primary and secondary antibodies. Primary antibodies were incubated overnight at four degree at the given dilutions: Oct4 (abcam, 1:1000), TRA-1-60 (Merck Millipore, 1:1000), Sox2 (Santa Cruz Biotechnology, 1:1000), Nestin (Novus, 1:1000), Musashi1 (Abcam, 1:500), Pax6 (Imtec Diagnostics, 1:1000), Sox1 (R&D Systems, 1:100), GFAP (Dako, 1:500). On the following day, after several washing steps, secondary antibodies were applied for three hours and subsequently washed again with PBS. Afterwards, nuclei were stained with 20 µM Hoechst (LifeTechnologies), cells were washed and subjected to imaging. Images of iPSCs and smNPCs were acquired with a Zeiss Axio Imager M2, whereas astrocytes were imaged using a Yokogawa CV8000 microscope.

To perform image analysis of astrocytes in a quantitative manner, custom-made code was prepared using Matlab 2020a. The analysis was run using the High-Performance Computing Platform available at the University of Luxembourg. The code can be shared upon request of the computer vision scripts with IDs 906 and 907 (contact person: Dr. Paul Antony). Briefly, cellular morphometrics were quantified based on nuclei and GFAP signals. GFAP reporter fluorescence intensity signals were quantified in the perinuclear zone of single cells. Morphometric features from the GFAP channel were analyzed by segmenting soma and $GFAP^{+}$ protrusions and extracting multiple shape descriptors including perimeter, area, and their ratio.

RNA-seq analysis

RNA extraction was carried out with the RNeasy Plus Kit (Qiagen) following the manufacturer's instructions. Library preparation and sequencing were performed by the Beijing Genomics Institute (BGI) in Copenhagen, Denmark, using the BGISEQ-500 platform.

Raw RNA-seq reads were quality-filtered with the removal of adaptor sequences and contaminating low-quality reads. Furthermore, the base percentage distribution and distribution of quality scores along the reads was checked. Data was subsequently pre-processed, applying the software package "Rsubread"[27]. Gene-level differential expression analysis to compare the two astrocytic protocols, Oksanen and Palm, was conducted in the R statistical programming software using the package "DESeq2"[28]. Genes with low expression counts were excluded with the "filterByExpr-function" using the package edgeR[29] with default parameters. To determine P-value significance scores for differential expression we used the Wald test followed by an adjustment for multiple hypothesis testing with the Benjamini and Hochberg method[30]. Heat maps were generated using the "heatmap.2" function from the R package "gplots"[31].

Pathway enrichment analyses were performed in the GeneGo MetaCore™ software[32] using standard enrichment analysis workflow. As input, the gene-level differential expression analysis results were used. The statistics for pathway over-representation analysis, including false-discovery rate (FDR) scores based on the method by Benjamini and Hochberg, were calculated for the GeneGo collections of cellular pathway maps, process networks and Gene Ontology gene set terms.

Deconvolution analysis

Deconvolution analysis of bulk RNA-seq data was conducted using the "Multi-subject Single Cell deconvolution" method (MuSiC[33]). MuSiC uses cross-subject cell type-specific gene expression from single-cell RNA sequencing (scRNA-seq) data to estimate the relative cell type composition in bulk RNA-seq data. We used three different reference scRNA-seq datasets that were downloaded from the Gene expression Omnibus (GEO): (i) single-nuclei RNA seq (snRNA-seq) from *substantia nigra* and cortex of five control human donors[34] (GSE140231), (ii) snRNA-seq of postmortem midbrain of six controls and five idiopathic PD cases[35] (GSE157783) and (iii) sc-RNAseq data of human embryo ventral midbrain cells between 6 and 11 weeks of gestation[36] (GSE76381). Cell type annotations included in the published metadata were used as reference for cell type proportion inference.

Quantitative PCR

After RNA isolation, cDNA was synthesized using SuperScript III Reverse Transcriptase Kit (Invitrogen). To perform quantitative PCR (qPCR), PowerTrack SYBR Green Master Mix (Thermofisher) was used and the reaction was run on the LightCycler 480 (Roche), with the primer annealing step at 60 degree. The expression of the genes of interest was normalized to the housekeeping genes *ACTB* and *L27*.

Statistical analysis

To perform statistical analyses, GraphPad Prism (version 9.4.0) was used. Typically, two-way ANOVA was applied for grouped analysis. Differences with p-value below 0.05 were considered as significant.

Results

Astrocytes generated using the Oksanen protocol resemble morphologically mature astrocytes

Despite having been neglected for decades, the key role of astrocytes in neurodegeneration has become increasingly evident[37]. To study astrocytic involvement in pathological mechanisms in more detail, disease modeling using iPSC-derived cultures has become a mainstream procedure. However, with the constantly growing number of available protocols[20,21], the question remains how to select the right approach for a particular research question. To address this point, we applied two distinct protocols to generate iPSC-derived astrocytes (Figure 1A) from two healthy control lines. The first protocol, here referred to as “Oksanen protocol”, is based on the generation of neuroepithelial cells, which grow as spheres, and after prolonged maintenance in the presence of EGF and bFGF and manual weekly titration give rise to glial progenitors. As a final step, cells are terminally differentiated by inducing the JAK-STAT pathway and BMP signaling with CNTF and BMP4, respectively[22,23] (Figure 1B). The second method, denominated here as “Palm protocol”, utilizes neural stem cells derived from small molecule neural precursor cells (smNPCs), which present neuroepithelial features and retain the ability to generate neural tube and neural crest lineages. Astrocytic differentiation is achieved by the cultivation in a medium containing fetal bovine serum[24].

Firstly, we characterized both the iPSC and smNPC lines to ensure their differentiation potential. The iPSC lines did not show any chromosomal aberrations (Figure S1), thus validating their use for posterior generation of smNPCs and astrocytes. Furthermore, we assessed the expression of several iPSC and smNPC markers using immunocytochemistry. Both iPSC lines expressed typical pluripotency markers such as Oct4, TRA-1-60 and Sox2 (Figure S2A). Moreover, the expression of neural progenitor cell markers, such as Musashi1, Nestin, Pax6 and Sox1, was identified in the smNPC lines (Figure S2B) rendering them suitable for differentiation.

Next, astrocytes were generated applying the Oksanen and Palm protocols to iPSCs and smNPCs, respectively. The obtained cultures were characterized by employing high-content imaging screening and custom-made scripts prepared in Matlab (Figure 2A), with GFAP as an astrocytic marker. This approach allowed us to assess the efficiency of the protocols, as well as the morphology of the generated astrocytes. In general, Oksanen astrocytes differed substantially in their morphology from Palm astrocytes (Figure 2B) and showed higher consistency between the two cell lines used, both in terms of morphology and $GFAP^+$ cell numbers. Contrariwise, when using the Palm protocol, we observed a discrepancy between the two control cell lines, with CTRL1 showing an impairment in differentiation as indicated by a reduced number of $GFAP^+$ cells. Furthermore, the Oksanen protocol yielded a higher percentage of $GFAP^+$ cells (Figure 2C), when analyzing both cell lines together. After preparing a Matlab code, which specifically recognized soma and astrocytic processes, we quantified multiple morphological features (Figure 2D). Interestingly, Oksanen astrocytes consistently presented longer and finer branches and a smaller somal area. Overall, cells generated with this protocol more closely resembled the prototypical astrocyte morphology[38].

Oksanen astrocytes present more mature expression profile

To thoroughly evaluate the differences between astrocytes generated using the Oksanen and Palm protocols, we utilized bulk RNA-seq. First, we compared differentially expressed genes between the two protocols for each line separately. The analysis revealed in total 16491 differentially expressed genes, when comparing CTRL1 in two methods and 14625 genes for the comparison of CTRL2. Altogether, we identified 12485 genes, which were differentially expressed between the two protocols for both cell lines (Figure 3A). Moreover, we plotted the expression Z-score values of the top 50 differentially expressed genes as a heatmap. Among the upregulated

genes in the Palm astrocytes, we identified several genes involved in the regulation and promotion of cell proliferation such as *PLK2*[39] and *CCN1*[40] (Figure 3B), which might suggest a lower degree of maturation of these cells.

To gain more mechanistic insight into the obtained datasets, we performed pathway enrichment analysis. Among the upregulated pathways in Oksanen astrocytes, we detected Notch signaling (Figure 3C), which is known to be involved in gliogenesis[41]. Contrariwise, these cells downregulated pathways linked to cell cycle regulation (Figure 3D).

Next, we assessed astrocytic maturity and the purity of the cultures by analyzing the expression of commonly used astrocytic and neuronal marker genes[12,13,42]. Generally, Oksanen astrocytes presented a higher expression of astrocytic markers, however, the same tendency was shown for neuronal markers (Figure 4A). We confirmed our findings by quantifying multiple analyzed targets by means of qPCR (Figure 4B). Interestingly, the expression of mature astrocytic markers such as *AQP4*, *SLC1A3* and *ALDH1L1*, was comparatively upregulated in Oksanen astrocytes, suggesting that cells attain a more advanced maturation status under these culture conditions.

To further characterize the cultures, we employed the bulk tissue cell type deconvolution method "MuSiC"[33]. Using this approach and applying multiple published human datasets[34–36], we were able to estimate the percentage of cells sharing the characteristics of various brain cell types. When compared to data obtained from postmortem midbrain, Oksanen cultures showed a higher proportion of cells resembling human mature astrocytes (Figure 4C). Similarly, Oksanen cells more closely resembled cortical astrocytes from the human brain than the cells obtained with the Palm protocol (Figure 4D). Of note, when assessing the cell composition of cultures obtained with the Oksanen protocol, we did not identify cells that matched the gene expression profile of mature neurons as identified in postmortem midbrain scRNA-seq studies[34,35]. Regarding the cells generated with Palm protocol, they resembled to a high extent the expression profile of oligodendrocytes, both cortical and midbrain ones.

Thus, we hypothesized that the higher expression of neuronal markers in Oksanen cultures might be caused by the presence of neuronal precursors rather than highly developed neurons. For a more detailed assessment of the cell type composition, we then additionally utilized a dataset generated from human embryonal midbrain tissue[36]. Based on the expression profiles of embryonal midbrain at week 8 of development, we identified a higher proportion of cells resembling neuroblasts with the Oksanen compared to the Palm protocol (Figure 4E). Furthermore, the Oksanen protocol yielded a higher proportion of cells resembling radial glia than the cultures obtained with the Palm method (Figure S3A, B).

Oksanen and Palm astrocytes differ in their activation profiles

The two applied protocols differ greatly in their media composition used to generate astrocytes. Since it has been reported that FBS presence might lead to astrocytic activation[43], we analyzed the expression of several activation markers known from the literature[4,44]. Astrocytes generated with the Oksanen protocol, in particular for CTRL1, showed increased expression of pan reactive markers. However, several of these markers are known to change their expression not only during astrocytic reactivity but also during cell maturation[45]. Furthermore, to establish an analogy to the neurotoxic (A1) and neuroprotective (A2) astrocytic profiles described by Liddelow and colleagues, we assessed the expression of a panel of genes known to be differently regulated in each of these reactive states. The studied genes were non-specifically expressed with none of the protocols exclusively engaging in one of the two activation profiles. Nevertheless, a significantly higher number of these activation markers was upregulated under the Palm protocol (Figure 5B).

Discussion

With the advent of iPSC technology and the growing recognition of the importance of astrocytes in the pathogenesis of PD, the number of available protocols used to generate iPSC-derived astrocytes is growing. In our study, we aimed to compare two of such methods to understand what their potential advantages and limitations could be. The first method, referred to as Oksanen protocol, is one of the most widely employed astrocyte differentiation methods based on long-term expansion of astrocytic progenitors generated from iPSCs[22,23] (both papers together were cited more than 500 to date). The second method, i.e. the Palm protocol, is a straightforward differentiation method that was established in-house and which uses neural precursor cells as the

starting point together with FBS-containing medium for astrocytic differentiation and maturation[24]. Both protocols vary greatly in their duration and yield of generated cells, posing the question about their applicability for different research projects. Therefore, we performed an in-depth imaging and transcriptomic analysis of both methods to unravel the morphological and gene expression profiles of these astrocytes.

Human mature astrocytes possess a distinctive morphology that allows differentiating between cellular soma and highly ramified processes, which account for 80% of the cell volume[38]. The finest processes, known as perisynaptic astrocytic processes (PAPs), develop later during cell maturation[46] and were shown to play a role in an array of brain functions, most importantly in synapse function and maturation[47–49]. Astrocytes are subject to profound changes during reactive gliosis, a phenomenon in which the processes were reported to increase the thickness of their main branches, accompanying an enlargement of the cell soma[50,51]. High-throughput imaging analyses of iPSC-derived astrocytes generated in this study, revealed remarkable morphological changes between both protocols. Oksanen astrocytes presented a more pronounced stellate shape with smaller soma but an increased relative area of the processes. The increased somal area and less defined shape observed for Palm astrocytes (particularly for CTRL2) is in line with a fibroblast-like morphology previously reported for human astrocytes grown in FBS-containing medium[43]. Furthermore, for all morphological parameters assessed in the study, there was a higher consistency between the cell lines for the Oksanen protocol. Image analysis also revealed a higher percentage of $GFAP^+$ cells in the Oksanen cultures, when compared to Palm cultures. Since GFAP is a widely recognized astrocytic marker[52] used to assess differentiation efficiency[53], the decreased number of cells expressing this protein in the Palm cultures (Palm: 22% of $GFAP^+$ cells; Oksanen: 74% of $GFAP^+$ cells) suggests an impaired astrocytic differentiation and maturation process. This hypothesis was supported by the evaluation of mature astrocyte markers[13], which were consistently elevated in Oksanen astrocytes. However, in cells generated with the Oksanen method, we could also identify a comparatively higher expression of several neuronal markers, suggestive of a contaminant neuronal population.

To study the cellular composition of the generated cultures in more detail, we applied bulk tissue cell type deconvolution using the MuSiC method[33]. With this approach, we compared our bulk RNA-seq data with several datasets produced using scRNA- or snRNA-seq[34–36]. In general, we could observe a higher similarity between cells generated with the Oksanen protocol and postmortem human astrocytes. The similarity was particularly striking when compared with cortical astrocytes. These results further strengthen the notion that Oksanen astrocytes are more mature than Palm

cells. Furthermore, the increased transcriptomic resemblance of Oksanen astrocytes to cortical rather than midbrain astrocytes can be explained by the lack of added morphogens responsible for regional patterning[54]. Thus, these findings suggest that the Oksanen protocol is of particular interest for disease modeling, in which mature and functional models are preferred to avoid masking disease phenotypes[55]. This protocol also showed increased reproducibility between the distinct lines used, as demonstrated by similar morphology and the percentage of obtained $GFAP^+$ cells. However, a limitation of the method was the identification of a residual non-glial population based on the expression of neuronal marker genes. Despite this fact, Oksanen cultures did not show a high degree of similarity to any mature neuronal populations identified in postmortem datasets. This discrepancy could be partially explained by the changed activation status of Oksanen cells, as reactive astrocytes were shown to express MAP2[56]. We also hypothesized that the expression of neuronal markers in these cultures could rather be explained by the presence of immature neuronal progenitors. Indeed, we observed a portion of cells in the Oksanen cultures that resembled radial glia and neuroblasts as identified in embryonal datasets[36]. The cellular heterogeneity within the iPSC-derived cultures poses a major challenge for scientists aiming at high reproducibility of their research. Nevertheless, our microscopy data indicate that the Oksanen protocol yields over 74% of $GFAP^+$ cells.

Next, we assessed the activation status of the generated astrocytes. FBS usage in the astrocytic differentiation protocols was frequently criticized as a driving factor for astrocytic reactivity[43]. Furthermore, FBS is prone to batch inconsistencies and its unknown amount of growth factors and hormones might lead to lower experimental reproducibility[21]. Therefore, we studied the expression of several activation markers known from the literature[4,44]. Oksanen astrocytes showed a higher expression of pan reactive markers, when compared to Palm astrocytes. However, it is worth noting that a few of these markers, such as *GFAP*, *CD44* and *VIM*, are also considered general astrocytic markers[57,58] and therefore the observed expression differences could also correlate with the relative number of astrocytes in the culture. The expression of marker genes belonging to A1 and A2 activation states was higher in the cells produced with the Palm method. This observation is in accordance with previous studies reporting a profound effect of serum-containing media on astrocytic reactivity[59]. Interestingly, the same study associated the FBS-induced reactivity with fibroblast-like morphology, which we also observed for Palm astrocytes, as previously mentioned.

Disease modeling is an important application of iPSC-derived cultures. Together with the technological development of high-throughput devices for drug screening, iPSC-derived cellular

models have the potential to advance personalized medicine approaches for neurodegenerative disorders[60]. However, to harness the full potential of iPSC-derived cells in drug screenings, the fast generation of highly homogenous cultures would be a major advantage. The two protocols analyzed here differ greatly in their efficiency and workload required to generate human astrocytes. While the Palm method produces a considerable number of cells in a relatively short time (2 months), the Oksanen protocol requires prolonged culturing of cells (for 5-6 months) together with manual cutting of the produced spheres. This experimental challenge will likely hamper a potential automation of Oksanen cultures, whereas Palm astrocytes might be easily obtained using automated platforms[61]. Nevertheless, the Oksanen protocol seems to be more suitable for initial disease modeling, given the high degree of maturity of the resulting cells as shown in this study.

Taken together, we showed that astrocytes generated with the Oksanen method express typical astrocytic markers and resemble their postmortem human counterparts to a higher extent than cells obtained with the Palm protocol. However, the cultures are not purely astrocytic and their generation is more time-consuming, which makes them less suitable for drug screenings. We presented an extensive transcriptomic comparison of the protocols, which will provide researchers with relevant information, when choosing the optimal protocol for their research questions.

Declarations

Ethic approval and consent to participate

The study was conducted in accordance with the institutional ethics rules (reference number of the ethics approval: ERP20-038, granted by the Ethics Review Panel of the University of Luxembourg).

Consent for publication

Not applicable.

Availability of data and materials

The raw data for this manuscript is not publicly available due to its sensitive nature. The datasets analyzed during the current study, including the scripts used during analyses, are publicly available. Detailed information on how to access the data and the code can be found at https://doi.org/10.17881/4jvc-fq34.

Competing interests

The authors declare no conflicts of interests.

Funding

PM and SS were supported by the Luxembourg National Research Fund (FNR) within the framework of the PARK-QC DTU (PRIDE17/12244779/PARK-QC). KB was supported by the FNR within the framework of the CriTICS DTU (FNR10907093). CV was funded by an FNR CORE Junior Grant ("NeuroFlame", C20/BM/14548100). AG received funding through an FNR ATTRACT grant ("Model-IPD", FNR9631103). AG, ZL, PMa were supported by the FNR within the CORE/Inter grant ("ProtectMove",INTER/DFG/19/14429377). In addition, AG, SLP and SD were supported by the FNR within the framework of a CORE grant ("CAMeSyn", C19/BM/13688526). Work of RK is supported by the Fonds National de Recherche (FNR) within the following projects: National Centre for Excellence in Research on Parkinson's disease (NCER-PD), MotaSYN, MAMaSyn, and i2TRON DTU. Moreover, RK is supported by the Michael J Fox Foundation, and the European Union's Horizon Europe research and innovation program (Orchestra). EG received support from the Fonds National de Recherche (FNR) as part of the National Centre for Excellence in Research on Parkinson's disease (NCER-PD) and the European Union's Horizon 2020 research and innovation program under the grant no. ERAPERMED 2020-314 for the project DIGI-PD.

Authors' contributions

PM, CV, KB and SD performed experiments. PM, ZL, SS, PA, PMa, EG performed the analysis. PM, ZL, PA, EG, AG and SLP wrote the manuscript, which was reviewed by all the authors. JS contributed to iPSC generation. AG and RK acquired funding for this study and together with PMa supervised the work.

Acknowledgements

We would like to thank Dr. Marja Koskuvi and Prof. Jari Koistinaho for the practical introduction to the Oksanen protocol. In addition, we thank the group of Prof. Jens Schwamborn, Center for Regenerative Therapies at TU Dresden, Integrated Biobank of Luxembourg, Max Planck Institute for Molecular Biomedicine in Münster and Hertie Institute for Clinical Brain Research in Tübingen for providing the cell lines used in the study.

Figures

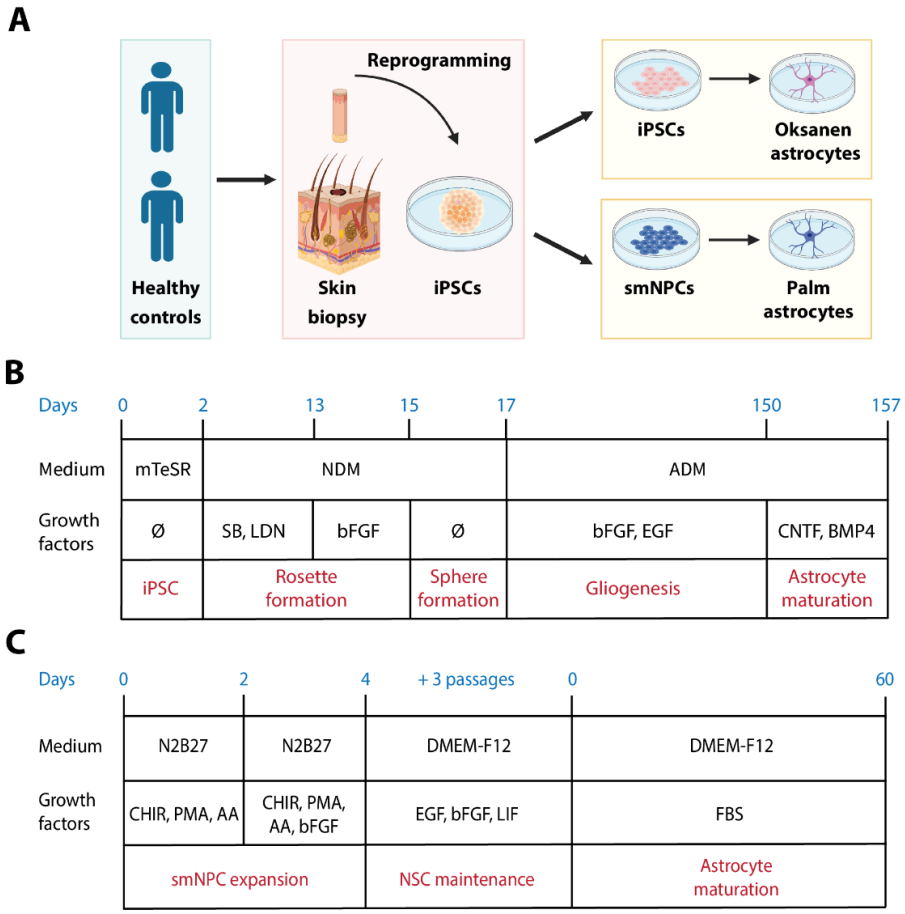

Figure 1. Generation of the astrocytic cultures in this study. A. Scheme representing main steps required to obtain astrocytes with the different protocols. **B.** Overview of the Oksanen protocol. NDM, neurodifferentiation medium (see Methods section); ADM, astrodifferentiation medium (see Methods section); SB, SB431542; LDN, LDN-193189; CNTF, Ciliary Neurotrophic Factor; BMP4, Bone Morphogenetic Factor 4. **C.** Overview of the Palm protocol. N2B27, medium comprised of DMEM-F12, Neurobasal and supplements (see Methods section), CHIR, CHIR99021; PMA, purmorphamine; AA, ascorbic acid; EGF, Epidermal Growth Factor; bFGF, basic Fibroblast Growth Factor; LIF, Leukemia Inhibitory Factor; FBS, Fetal Bovine Serum; smNPCs, small molecule Neural Progenitor Cells; NSCs, Neural Stem Cells. The figure was generated using Biorender.

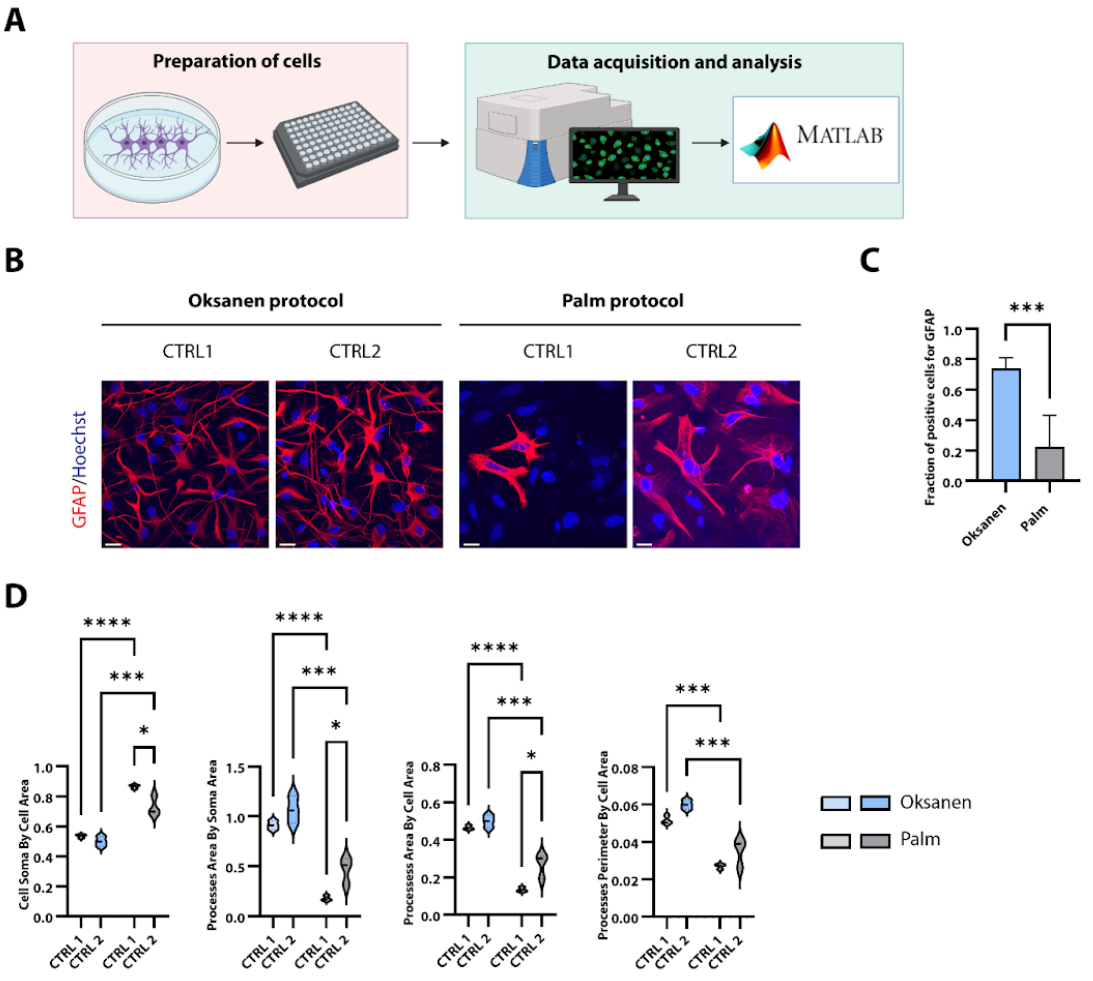

Figure 2. Morphological analysis of the generated astrocytes. A. Scheme summarizing the experimental procedure. **B.** Representative images for both astrocytic protocols. Scale bar: 20 µm. CTRL1, healthy control line 1; CTRL2, healthy control line 2. The brightness and contrast for the image of CTRL2 in the Palm protocol was adjusted. **C.** Quantification of GFAP^{+} cells in astrocytic cultures using high content imaging. For each protocol and cell line, 3 biological replicates were used. Data are presented as the mean ± SD, ***P ≤0.001. SD, standard deviation. **D.** Assessment of astrocytic morphology. The summed area of astrocytic soma was normalized to the summed cell area. The summed area of astrocytic processes was normalized to the summed soma area. The summed area of astrocytic processes was normalized to the summed cell area. The summed perimeter of astrocytic processes was normalized to the summed cell area. CTRL1, healthy control 1; CTRL2, healthy control line 2. *P ≤0.05, **P ≤0.01, ***P ≤0.001, ***P ≤0.0001. Part of the figure was generated using Biorender.

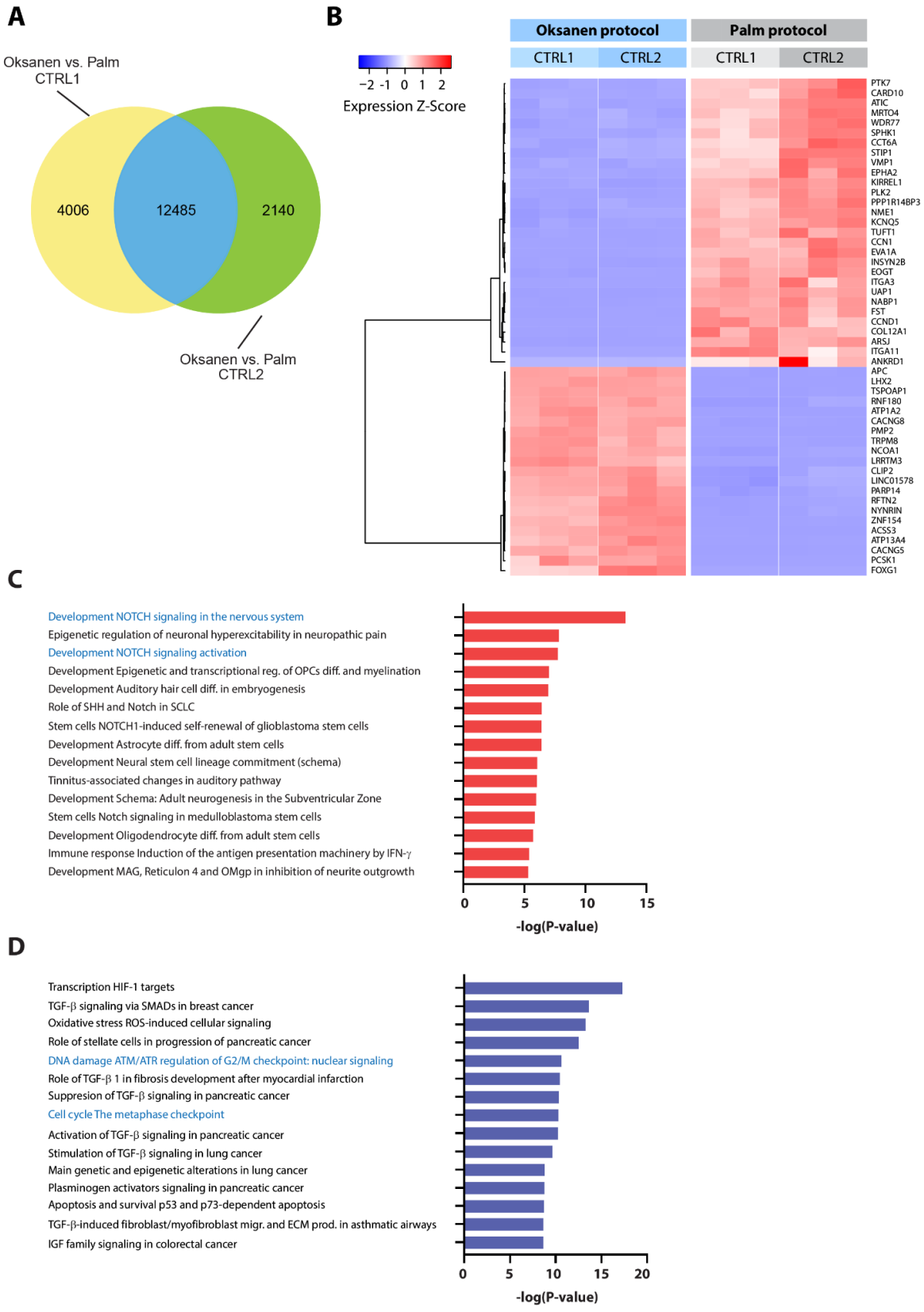

Figure 3. Transcriptomic analysis of astrocytes. A. Venn diagram showing the number of overlapping differentially expressed genes (DEGs) when comparing both differentiation protocols.

B. Heatmap showing 50 top differentially expressed genes between astrocytes obtained with Oksanen vs Palm protocols. **C.** Pathway enrichment analysis showing the upregulated pathways in Oksanen protocol. **D.** Pathway enrichment analysis showing the downregulated pathways in Oksanen protocol.

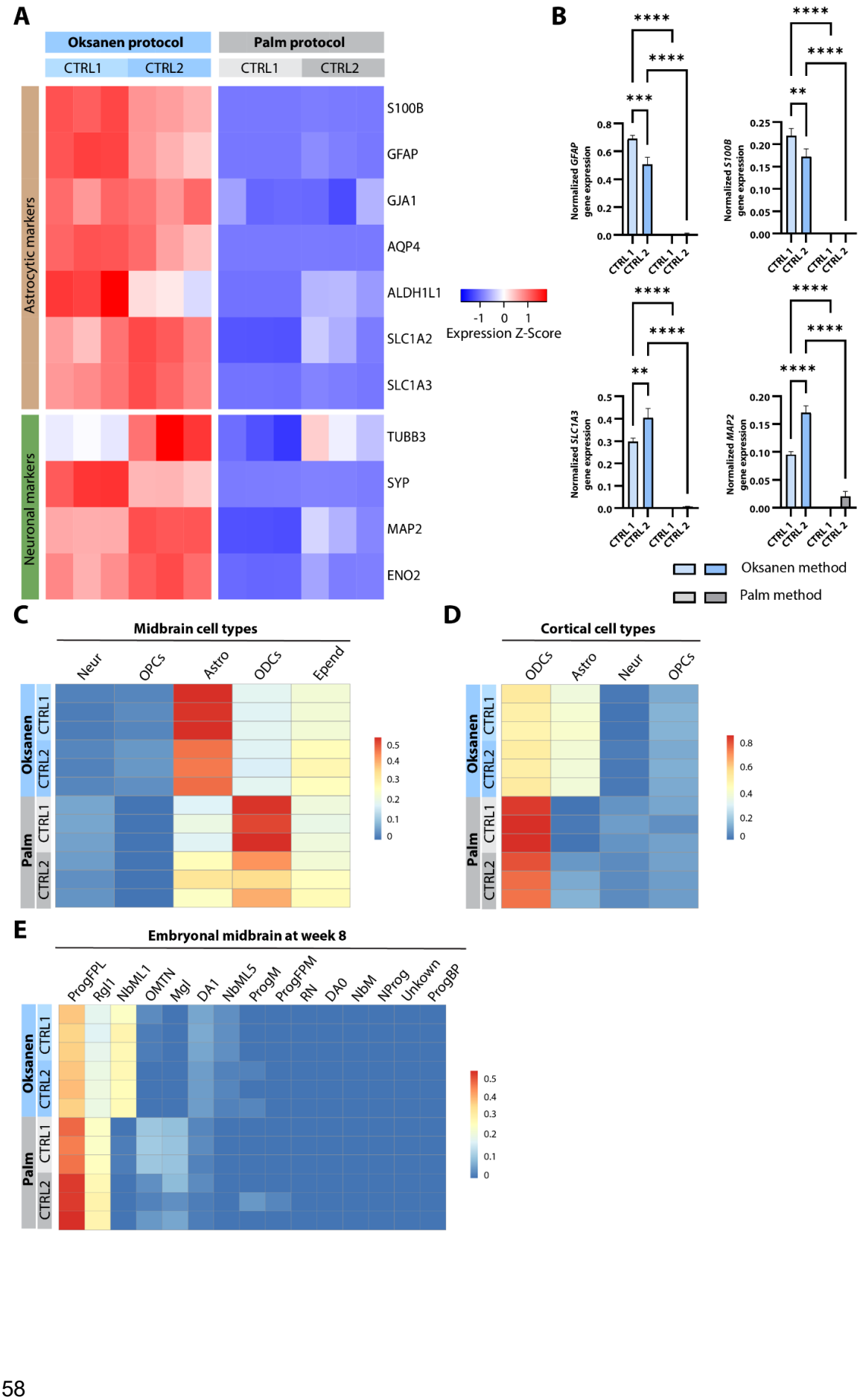
A
Oksanen protocol
Palm protocol
CTRL1
CTRL2
CTRL1
CTRL2
Astrocytic markers
Neuronal markers
S100B
GFAP
GJA1
AQP4
ALDH1L1
SLC1A2
SLC1A3
TUBB3
SYP
MAP2
ENO2
-1
0
1
Expression Z-Score
B
Normalized GFAP gene expression
Normalized S100B gene expression
Normalized SLC1A3 gene expression
Normalized MAP2 gene expression
Oksanen method
Palm method
C
Midbrain cell types
Neur
OPCs
Astro
ODCs
Ependy
Oksanen
Palm
D
Cortical cell types
ODCs
Astro
Neur
OPCs
E
Embryonal midbrain at week 8
ProgFPL
Rgl1
NbML1
OMTN
Mgl
DA1
NbML5
ProgM
ProgFPM
RN
DA0
NbM
NProg
Unkown
ProgBP

Figure 4. Characterization of cell type composition. A. Heatmap displaying expression values for astrocytic and neuronal markers. **B.** Validation of *GFAP*, *S100B*, *SLC1A3* and *MAP2* expression profiles using qPCR. CTRL1, healthy control 1; CTRL2, healthy control line 2. For each protocol and cell line, 3 biological replicates were used. Data are presented as the mean ± SD,*P ≤0.05, **P ≤0.01, ***P ≤0.001, ***P ≤0.0001. **C.** Heatmap showing the percentage of iPSC-derived cells in astrocytic cultures sharing the expression profile with the cell types identified in Smajic et al.[35]. **D.** Heatmap showing the percentage of generated astrocytic cultures sharing the expression signatures with the cortical cell types identified in Agarwal et al.[34]. **E.** Heatmap displaying the comparison of the generated astrocytes with the dataset from human embryonal midbrain at week 8[36]. CTRL1, healthy control1; CTRL2, healthy control 2; Mgl, Microglia; Astro, Astrocytes; Epend, Ependymal cells; ODCs, Oligodendrocytes; Neur, Neurons; OPCs, Oligodendrocyte Precursor Cells; ProgFPL, lateral floorplate progenitor; Rgl1, Radial glia-like cell type 1; NbML1, Mediolateral neuroblast type 1; OMTN, Oculomotor and Trochlear Nucleus; DA1, Dopaminergic neurons 1; NbML5, Mediolateral neuroblast type 5; ProgM, midline neuronal progenitor; ProgFPM, medial floorplate progenitor; RN, red nucleus; DA0, Dopaminergic neurons 0; NbM, medial neuroblasts; NProg, Neuronal progenitor; ProgBP, basal plate progenitor.

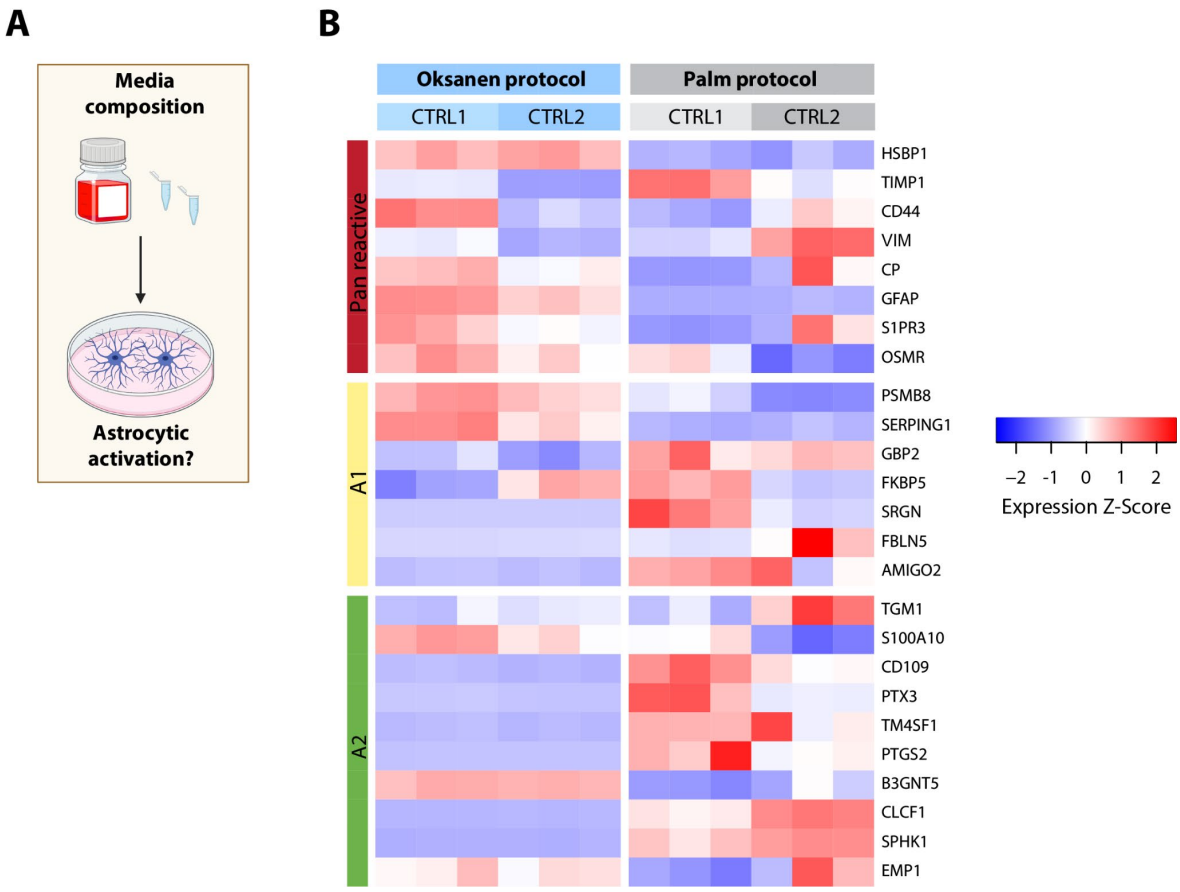

Figure 5. Activation status of astrocytes generated in the study using cell culture media with and without FBS. A. Scheme visualizing the research idea. B. Heatmap representing the expression Z-score values for the genes associated with pan reactive, A1 and A2 reactivity states[4,44]. Part of the figure was prepared using Biorender.

Supplementary information

Assessing the suitability of iPSC-derived human astrocytes for disease modeling

Patrycja Mulica[1], Carmen Venegas[1], Zied Landoulsi[1], Katja Badanjak[1], Semra Smajic[1], Sylvie Delcambre[1], Jens Schwamborn[1], Rejko Krüger[1,2], Paul Antony[1], Patrick May[1], Enrico Glaab[1], Anne Grünewald[1,3,#,*], Sandro L. Pereira[1,2,#]

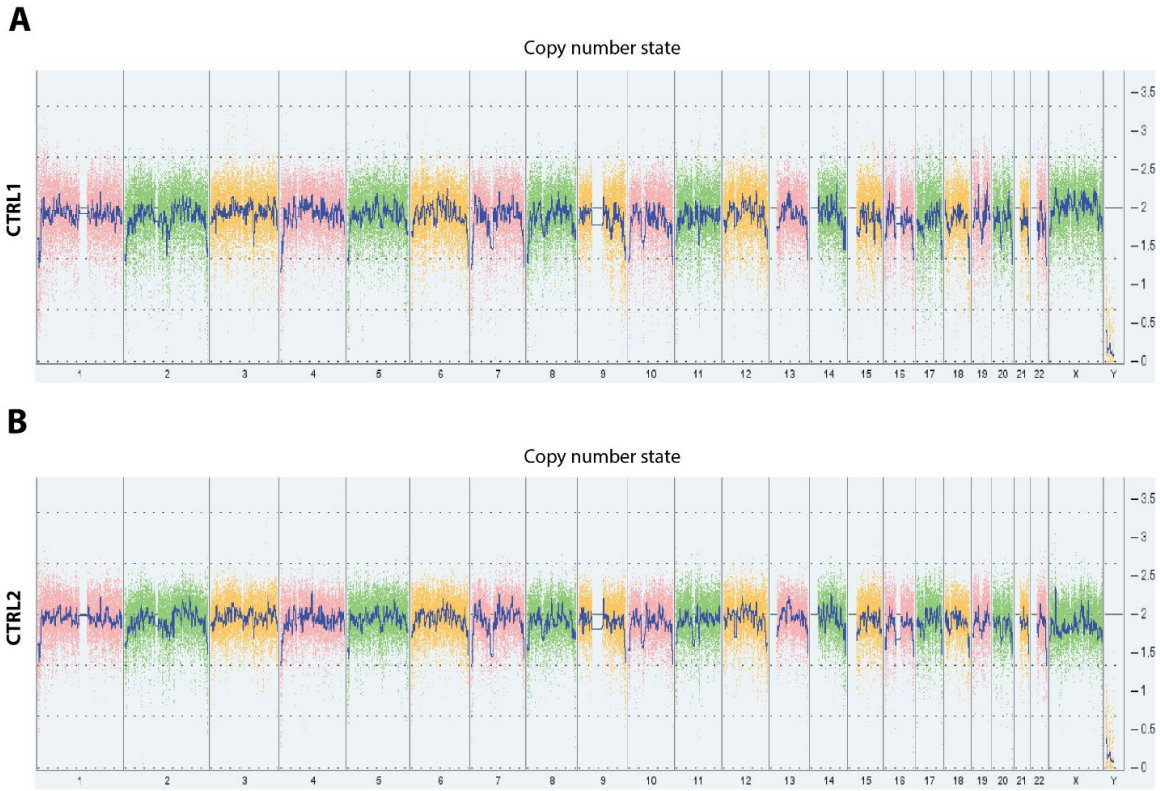

Figure S1. The analysis of karyotypes. A. The whole genome view of healthy control 1. B. The whole genome view of healthy control 2. The karyotype analysis was performed using Karyostat™ service from Thermofisher.

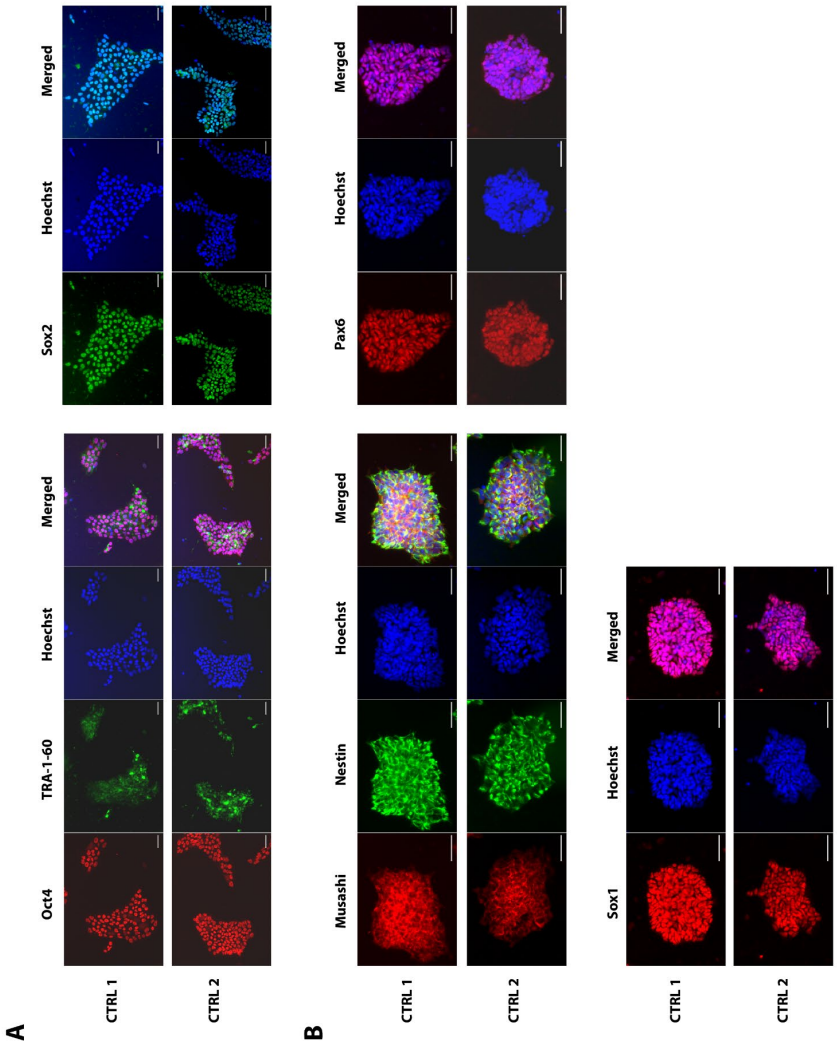

Figure S2. The analysis of iPSC and smNPC markers in immunocytochemistry. A. Two healthy iPSC controls were analyzed for the expression of Oct4, TRA-1-60 and Sox2. B. Two healthy smNPC controls were assessed for the expression of Musashi, Nestin, Pax6 and Sox1. Scale bar: 50 µm.

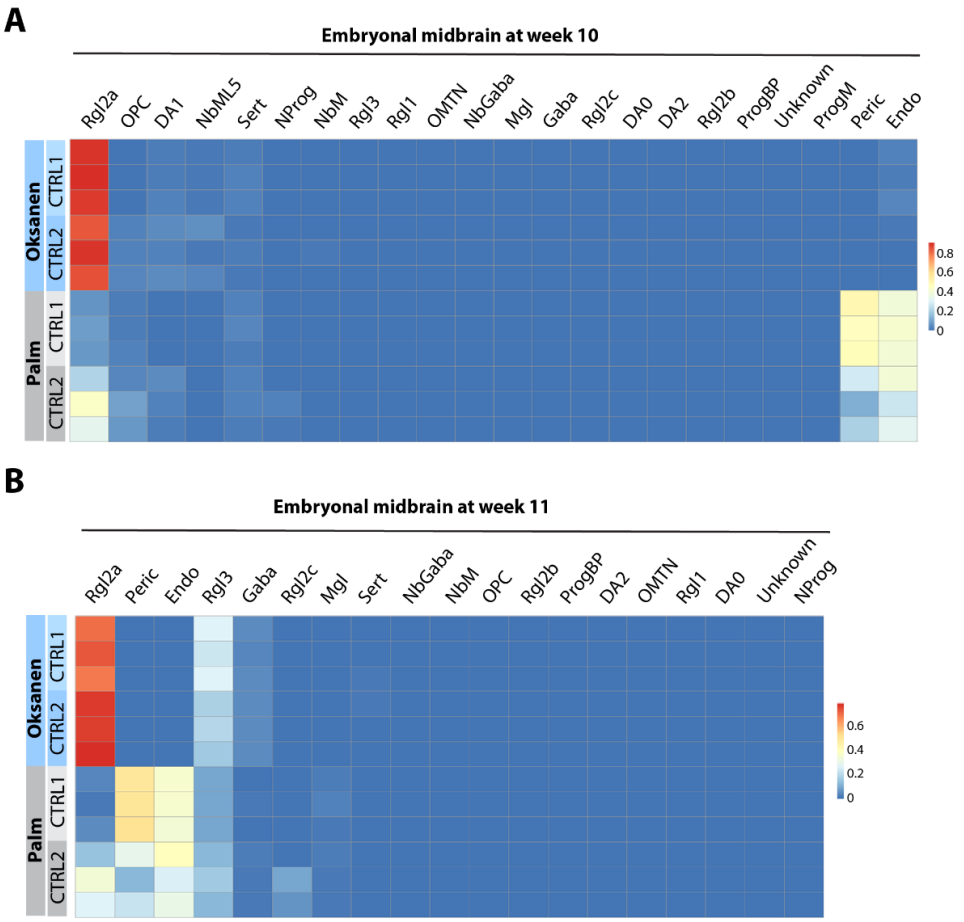

Figure S3. Heatmaps showing the percentage of cells in the generated cultures resembling cell types identified in human postmortem midbrain and human embryonal midbrains. As a reference the human embryonal midbrain datasets[36] from week 10 (panel A) and week 11 (panel B) of development. Endo, Endocytes; Gaba, GABAergic neurons; OPC, Oligodendrocyte Precursor Cells; OMTN, oculomotor and trochlear nucleus; NbM, medial neuroblasts; NProg, Neuronal Progenitors; ProgBP, basal plate progenitor; ProgFPL, lateral floorplate progenitor; ProgM, midline neuronal progenitor; Peric, Pericytes; NbML5, mediolateral neuroblasts type 5; DA0, dopaminergic neurons 0; Rgl1, radial glia type 1; DA1, dopaminergic neurons 1; Rgl2a, radial glia type 2a; Rgl2b, radial glia type 2b; Mgl, microglia, NbGaba, neuroblasts GABAergic; Sert, serotonergic neurons; DA2, dopaminergic neurons 2; Rgl3, radial glia type 3; Rgl2c, radial glia type 2c.

Bibliography

1. Allen, N. J. & Eroglu, C. Cell Biology of Astrocyte-Synapse Interactions. *Neuron* **96**, 697–708 (2017).

2. Sofroniew, M. V. & Vinters, H. V. Astrocytes: biology and pathology. *Acta Neuropathol. (Berl.)* **119**, 7–35 (2010).

3. Colombo, E. & Farina, C. Astrocytes: Key Regulators of Neuroinflammation. *Trends Immunol.* **37**, 608–620 (2016).

4. Liddelow, S. A. *et al.* Neurotoxic reactive astrocytes are induced by activated microglia. *Nature* **541**, 481–487 (2017).

5. Mulica, P., Grünewald, A. & Pereira, S. L. Astrocyte-Neuron Metabolic Crosstalk in Neurodegeneration: A Mitochondrial Perspective. *Front. Endocrinol.* **12**, 668517 (2021).

6. Kanski, R., van Strien, M. E., van Tijn, P. & Hol, E. M. A star is born: new insights into the mechanism of astrogenesis. *Cell. Mol. Life Sci. CMLS* **71**, 433–447 (2014).

7. Molofsky, A. V. & Deneen, B. Astrocyte development: A Guide for the Perplexed. *Glia* **63**, 1320–1329 (2015).

8. Zarei-Kheirabadi, M., Vaccaro, A. R., Rahimi-Movaghar, V., Kiani, S. & Baharvand, H. An Overview of Extrinsic and Intrinsic Mechanisms Involved in Astrocyte Development in the Central Nervous System. *Stem Cells Dev.* **29**, 266–280 (2020).

9. de Majo, M., Koontz, M., Rowitch, D. & Ullian, E. M. An update on human astrocytes and their role in development and disease. *Glia* **68**, 685–704 (2020).

10. Deneen, B. *et al.* The transcription factor NFIA controls the onset of gliogenesis in the developing spinal cord. *Neuron* **52**, 953–968 (2006).

11. Kang, P. *et al.* Sox9 and NFIA coordinate a transcriptional regulatory cascade during the initiation of gliogenesis. *Neuron* **74**, 79–94 (2012).

12. Molofsky, A. V. *et al.* Astrocytes and disease: a neurodevelopmental perspective. *Genes Dev.* **26**, 891–907 (2012).

13. Jurga, A. M., Paleczna, M., Kadluczka, J. & Kuter, K. Z. Beyond the GFAP-Astrocyte Protein Markers in the Brain. *Biomolecules* **11**, 1361 (2021).

14. Bonvento, G. & Bolaños, J. P. Astrocyte-neuron metabolic cooperation shapes brain activity. *Cell Metab.* **33**, 1546–1564 (2021).

15. Zehnder, T. *et al.* Mitochondrial biogenesis in developing astrocytes regulates astrocyte maturation and synapse formation. *Cell Rep.* **35**, 108952 (2021).

16. Vandenbark, A. A., Offner, H., Matejuk, S. & Matejuk, A. Microglia and astrocyte involvement in neurodegeneration and brain cancer. *J. Neuroinflammation* **18**, 298 (2021).

17. Bennett, M. L. & Viaene, A. N. What are activated and reactive glia and what is their role in neurodegeneration? *Neurobiol. Dis.* **148**, 105172 (2021).

18. Escartin, C. *et al.* Reactive astrocyte nomenclature, definitions, and future directions. *Nat. Neurosci.* **24**, 312–325 (2021).

19. Escartin, C., Guillemaud, O. & Carrillo-de Sauvage, M.-A. Questions and (some) answers on reactive astrocytes. *Glia* **67**, 2221–2247 (2019).

20. Chandrasekaran, A., Avci, H. X., Leist, M., Kobolák, J. & Dinnyés, A. Astrocyte Differentiation of Human Pluripotent Stem Cells: New Tools for Neurological Disorder Research. *Front. Cell. Neurosci.* **10**, 215 (2016).

21. Kumar, M., Nguyen, N. T. P., Milanese, M. & Bonanno, G. Insights into Human-Induced Pluripotent Stem Cell-Derived Astrocytes in Neurodegenerative Disorders. *Biomolecules* **12**, 344 (2022).

22. Oksanen, M. *et al.* PSEN1 Mutant iPSC-Derived Model Reveals Severe Astrocyte Pathology in Alzheimer's Disease. *Stem Cell Rep.* **9**, 1885–1897 (2017).

23. Krencik, R. & Zhang, S.-C. Directed differentiation of functional astroglial subtypes from human pluripotent stem cells. *Nat. Protoc.* **6**, 1710–1717 (2011).

24. Palm, T. *et al.* Rapid and robust generation of long-term self-renewing human neural stem cells with the ability to generate mature astroglia. *Sci. Rep.* **5**, 16321 (2015).

25. Badanjak, K. *et al.* iPSC-Derived Microglia as a Model to Study Inflammation in Idiopathic Parkinson's Disease. *Front. Cell Dev. Biol.* **9**, 740758 (2021).

26. Reinhardt, P. *et al.* Derivation and expansion using only small molecules of human neural progenitors for neurodegenerative disease modeling. *PloS One* **8**, e59252 (2013).

27. Liao, Y., Smyth, G. K. & Shi, W. The R package Rsubread is easier, faster, cheaper and better for alignment and quantification of RNA sequencing reads. *Nucleic Acids Res.* **47**, e47 (2019).

28. Love, M. I., Huber, W. & Anders, S. Moderated estimation of fold change and dispersion for RNA-seq data with DESeq2. *Genome Biol.* **15**, 550 (2014).

29. Robinson, M. D., McCarthy, D. J. & Smyth, G. K. edgeR: a Bioconductor package for differential expression analysis of digital gene expression data. *Bioinforma. Oxf. Engl.* **26**, 139–140 (2010).

30. Benjamini, Y. & Hochberg, Y. Controlling the False Discovery Rate: A Practical and Powerful Approach to Multiple Testing. *J. R. Stat. Soc. Ser. B Methodol.* **57**, 289–300 (1995).

31. Warnes, G. R. *et al.* gplots: Various R Programming Tools for Plotting Data. (2022).

32. MetaCore Login | Clarivate. https://portal.genego.com/.

33. Wang, X., Park, J., Susztak, K., Zhang, N. R. & Li, M. Bulk tissue cell type deconvolution with multi-subject single-cell expression reference. *Nat. Commun.* **10**, 380 (2019).

34. Agarwal, D. *et al.* A single-cell atlas of the human substantia nigra reveals cell-specific pathways associated with neurological disorders. *Nat. Commun.* **11**, 4183 (2020).

35. Smajić, S. *et al.* Single-cell sequencing of human midbrain reveals glial activation and a Parkinson-specific neuronal state. *Brain J. Neurol.* awab446 (2021) doi:10.1093/brain/awab446.

36. La Manno, G. *et al.* Molecular Diversity of Midbrain Development in Mouse, Human, and Stem Cells. *Cell* **167**, 566-580.e19 (2016).

37. Jiwaji, Z. & Hardingham, G. E. Good, bad, and neglectful: Astrocyte changes in neurodegenerative disease. *Free Radic. Biol. Med.* **182**, 93–99 (2022).

38. Oberheim, N. A. *et al.* Uniquely hominid features of adult human astrocytes. *J. Neurosci. Off. J. Soc. Neurosci.* **29**, 3276–3287 (2009).

39. Cao, F. *et al.* Knocking down of Polo-like kinase 2 inhibits cell proliferation and induced cell apoptosis in human glioma cells. *Life Sci.* **270**, 119084 (2021).

40. Sakamoto, S. *et al.* Induction and function of CYR61 (CCN1) in prostatic stromal and epithelial cells: CYR61 is required for prostatic cell proliferation. *The Prostate* **61**, 305–317 (2004).

41. Lasky, J. L. & Wu, H. Notch Signaling, Brain Development, and Human Disease. *Pediatr. Res.* **57**, 104–109 (2005).

42. Sarnat, H. B. Immunocytochemical markers of neuronal maturation in human diagnostic neuropathology. *Cell Tissue Res.* **359**, 279–294 (2015).

43. Magistri, M. *et al.* A comparative transcriptomic analysis of astrocytes differentiation from human neural progenitor cells. *Eur. J. Neurosci.* **44**, 2858–2870 (2016).

44. Zamanian, J. L. *et al.* Genomic analysis of reactive astrogliosis. *J. Neurosci. Off. J. Soc. Neurosci.* **32**, 6391–6410 (2012).

45. Gorina, Y. V. *et al.* Astrocyte Activation Markers. *Biochem. Biokhimiia* **87**, 851–870 (2022).

46. Bushong, E. A., Martone, M. E. & Ellisman, M. H. Maturation of astrocyte morphology and the establishment of astrocyte domains during postnatal hippocampal development. *Int. J. Dev. Neurosci. Off. J. Int. Soc. Dev. Neurosci.* **22**, 73–86 (2004).

47. Perez-Alvarez, A., Navarrete, M., Covelo, A., Martin, E. D. & Araque, A. Structural and functional plasticity of astrocyte processes and dendritic spine interactions. *J. Neurosci. Off. J. Soc. Neurosci.* **34**, 12738–12744 (2014).

48. Bernardinelli, Y. *et al.* Activity-dependent structural plasticity of perisynaptic astrocytic domains promotes excitatory synapse stability. *Curr. Biol. CB* **24**, 1679–1688 (2014).

49. Oliet, S. H., Piet, R. & Poulain, D. A. Control of glutamate clearance and synaptic efficacy by glial coverage of neurons. *Science* **292**, 923–926 (2001).

50. Wilhelmsson, U. *et al.* Redefining the concept of reactive astrocytes as cells that remain within their unique domains upon reaction to injury. *Proc. Natl. Acad. Sci.* **103**, 17513–17518 (2006).

51. JI, F., LIANG, J., LIU, L., CAO, M. & LI, F. Curcumin exerts antinociceptive effects by inhibiting the activation of astrocytes in spinal dorsal horn and the intracellular extracellular signal-regulated kinase signaling pathway in rat model of chronic constriction injury. *Chin. Med. J. (Engl.)* **126**, 1125–1131 (2013).

52. Middeldorp, J. & Hol, E. M. GFAP in health and disease. *Prog. Neurobiol.* **93**, 421–443 (2011).

53. Booth, H. D. E. *et al.* RNA sequencing reveals MMP2 and TGFB1 downregulation in LRRK2 G2019S Parkinson's iPSC-derived astrocytes. *Neurobiol. Dis.* **129**, 56–66 (2019).

54. Krencik, R., Weick, J. P., Liu, Y., Zhang, Z.-J. & Zhang, S.-C. Specification of transplantable astroglial subtypes from human pluripotent stem cells. *Nat. Biotechnol.* **29**, 528–534 (2011).

55. Liu, C., Oikonomopoulos, A., Sayed, N. & Wu, J. C. Modeling human diseases with induced pluripotent stem cells: from 2D to 3D and beyond. *Dev. Camb. Engl.* **145**, dev156166 (2018).

56. Geisert, E. E., Johnson, H. G. & Binder, L. I. Expression of microtubule-associated protein 2 by reactive astrocytes. *Proc. Natl. Acad. Sci. U. S. A.* **87**, 3967–3971 (1990).

57. Moretto, G., Xu, R. Y. & Kim, S. U. CD44 expression in human astrocytes and oligodendrocytes in culture. *J. Neuropathol. Exp. Neurol.* **52**, 419–423 (1993).

58. O'Leary, L. A. *et al.* Characterization of Vimentin-Immunoreactive Astrocytes in the Human Brain. *Front. Neuroanat.* **14**, (2020).

59. Zhang, Y. *et al.* Purification and Characterization of Progenitor and Mature Human Astrocytes Reveals Transcriptional and Functional Differences with Mouse. *Neuron* **89**, 37–53 (2016).

60. Kim, C. iPSC technology--Powerful hand for disease modeling and therapeutic screen. *BMB Rep.* **48**, 256–265 (2015).

61. Boussaad, I. *et al.* Integrated, automated maintenance, expansion and differentiation of 2D and 3D patient-derived cellular models for high throughput drug screening. *Sci. Rep.* **11**, 1439 (2021).

3.2 Manuscript III

The impact of A53T α-synuclein on astrocytic function and activation in human iPSC-derived cultures

Patrycja Mulica[1], Varun Sreenivasan[2], Sandro Pereira[1], Paul Antony[1], Kristian Händler[2], Kamil Grzyb[1], Sylvie Delcambre[1], Maria Tziortziou[1], Carmen Venegas[1], Semra Smajic[1], Katja Badanjak[1], Maria Koskuvi[3], Taisia Rolova[3], Rejko Krüger[1 4], Jari Koistinaho[3], Alexander Skupin[1], Malte Spielmann[2], Anne Grünewald[1 5]

[1]Luxembourg Centre for Systems Biomedicine, University of Luxembourg, Esch-sur-Alzette, Luxembourg
[2]Institute of Human Genetics, University of Lübeck, Lübeck, Germany
[3]Neuroscience Center, University of Helsinki, Helsinki, Finland
[4]Luxembourg Institute of Health, Strassen, Luxembourg
[5]Institute of Neurogenetics, University of Lübeck, Lübeck, Germany

***Correspondence:** Anne Grünewald, PhD, Luxembourg Centre for Systems Biomedicine, University of Luxembourg, 6 avenue du Swing, L-4367 Belvaux, Luxembourg, phone: (+352) 46 66 44 9793, e-mail: anne.gruenewald@uni.lu

This publication is in preparation to be submitted to the Journal of Neuroinflammation.

3.2.1 Preface

α-synuclein is one of the most widely recognized potential contributors to PD pathology [73]. This notion is supported by the existence of *SNCA* mutations which typically cause early-onset PD [155]. Therefore, these variants are frequently employed as a model to study fundamental disease mechanisms. Recently, dysfunctional astrocytes have become increasingly recognized as one of the driving factors for neurodegeneration [156]. In this context, it is of great importance to employ genetic models of PD as a tool to clarify disease related processes. Yet, our knowledge gained from these models derived from iPSC-cultures is still limited despite the multiple advantages brought by studying patient material [152].

Therefore, in this study we aimed to explore the impact of *SNCA* mutation on iPSC-derived astrocytes. To meet this aim, we generated iPSC-derived astrocytes harboring A53T mutation in α-synuclein and compared them with a healthy control. We employed a single-cell sequencing technique to study molecular pathways in the pure astrocytic populations. Using this approach, we could show that PD astrocytes are characterized by a decreased differentiation potential. Moreover, they differ profoundly from the healthy control in their activation status following the treatment with IL-1β and TNF-α cytokines. We could also demonstrate modifications in mitochondrial pathways in A53T α-synuclein astrocytes.

Concerning my contribution to this work, I was involved in both the experimental and analytical parts. I maintained and differentiated the human iPSCs into astrocytes. Furthermore, I performed experiments such as immunocytochemistry followed by high-content imaging, RNA isolation, cDNA generation. I also contributed to qPCRs and data analysis. Moreover, I was responsible for the preparation of figures and manuscript writing.

3.2.2 Manuscript

Impact of A53T α-synuclein on astrocytic function and activation in human iPSC-derived cultures

Patrycja Mulica[1], Varun Sreenivasan[2], Sandro L. Pereira[1], Paul Antony[1], Kristian Händler[2], Kamil Grzyb[1], Sylvie Delcambre[1], Maria Tziortziou[1], Carmen Venegas[1], Semra Smajic[1], Katja Badanjak[1], Marja Koskuvi[3], Taisia Rolova[3], Rejko Krüger[1 4], Jari Koistinaho[3], Alexander Skupin[1], Malte Spielmann[2 5 6], Anne Grünewald[1 7]

[1]Luxembourg Centre for Systems Biomedicine, University of Luxembourg, Esch-sur-Alzette, Luxembourg

[2]Institute of Human Genetics, Universitätsklinikum Schleswig-Holstein, University of Lübeck and University of Kiel, Lübeck 23562, Germany

[3]Neuroscience Center, HILIFE, University of Helsinki, Helsinki, Finland

[4]Luxembourg Institute of Health, Strassen, Luxembourg

[5]Human Molecular Genomics Group, Max Planck Institute for Molecular Genetics, Berlin 14195, Germany

[6]German Centre for Cardiovascular Research (DZHK), partner site Hamburg/Lübeck/Kiel, Lübeck 23562, Germany

[7]Institute of Neurogenetics, University of Lübeck, Lübeck, Germany

***Correspondence:** Anne Grünewald, PhD, Luxembourg Centre for Systems Biomedicine, University of Luxembourg, 6 avenue du Swing, L-4367 Belvaux, Luxembourg, phone: (+352) 46 66 44 9793, e-mail: anne.gruenewald@uni.lu

Running title: Effects of α-synuclein on astrocytes

Keywords: iPSC, astrocytes, α-synuclein, single-cell RNA sequencing

Word count: Title: 67 characters; Abstract: 242 words; Manuscript: 5783 words; Figures: 7; References: 87

Abstract

α-synuclein accumulation is one of the most established histological hallmarks of Parkinson's disease (PD). While substantial research efforts have been made to elucidate its role in neurons, the protein's impact on astrocytic function remains poorly understood. Thus, in the current study, we aimed to deep-phenotype human iPSC-derived astrocytes harboring the PD-linked mutation p.A53T in α-synuclein (*SNCA* c.209G>A) by applying a combination of single-cell RNA sequencing, high-throughput imaging and inflammatory profiling. To induce reactive astrogliosis - a pathological phenomenon that has been widely described in brain tissues from PD patients - cultures were treated with the microglial cytokines IL-1β and TNF-α. Our multimodel approach revealed several mutation-specific transcriptomic changes; first, in the patient cultures, we observed a reduction in the expression of genes that regulate the inflammatory response. Second, single-cell population and entropy analyses suggested that A53T α-synuclein limits the astrocytic differentiation potential. Third, the reduced capacity of A53T astrocytes to react to inflammatory stimuli was linked to a disruption in the glycolytic pathway. Fourth, gene enrichment analysis implicated mitochondrial pathways such as fission and mitophagy regulation in A53T α-synuclein-mediated astrocytic dyshomeostasis. Finally, to functionally validate our findings, we studied mitochondrial morphology and detected an increase in mitochondrial size and mass in activated patient cells. In conclusion, here we showed that A53T α-synuclein interferes with the inflammatory response capacity of astrocytes, likely due to a disruption in the glycolytic pathway, further highlighting the critical involvement of glia in the pathogenesis of PD.

Introduction

Parkinson's disease (PD) is a neurodegenerative disorder, which affects about 1% of the population above the age of 60 [1]. It is characterized by the progressive demise of dopaminergic neurons in the substantia nigra pars compacta [2]. Affected individuals suffer from motor symptoms such as bradykinesia, resting tremor and rigidity [3]. Typically, in PD brains, there is a deposition of Lewy bodies, which are composed mainly of aggregated α-synuclein [4]. Although the majority of PD cases are of idiopathic nature, i.e. with unknown etiology, in 5-10% of patients a mutation in an established PD gene can be found [5].

The mutational spectrum of PD includes pathogenic variants in the *α-synuclein* gene (*SNCA)*. To date, nine different point or multiplication mutations have been identified in *SNCA*. The majority of patients carrying *SNCA* mutations, which are inherited in an autosomal dominant manner, develop PD during their 4th decade of life [6–8]. The first ever discovered mutation in *SNCA* was the single-nucleotide change c.209G>A (p.A53T) [9], which has been reported to enhance the propensity of α-synuclein to aggregate [10].

The discovery of mutations in *SNCA* and the detection of α-synuclein in Lewy bodies led to the hypothesis that dysfunctional α-synuclein can act as a trigger of PD pathology [11]. α-synuclein is a small 14 kDA protein, which is unfolded under physiological conditions [12,13]. It localizes mainly to the presynapse, where it was shown to regulate synaptic vesicle recycling [14,15]. Furthermore, it was demonstrated that α-synuclein can affect neurotransmitter synthesis, storage and release [16]. Moreover, there is evidence that aggregated forms of α-synuclein, such as oligomers and fibrils, have a toxic effect on the cell [11].

Interestingly, α-synuclein was reported to localize not only to the cytosol but also to several organelles, including mitochondria [17]. α-synuclein can aggregate at the outer mitochondrial membrane, thereby disrupting protein import, calcium homeostasis and fusion/fission processes. Moreover, it has been shown to enter mitochondria. When localized at the inner mitochondrial membrane, α-synuclein interferes with respiratory chain function, which induces excessive reactive oxygen species (ROS) formation, and, in turn, causes mtDNA damage [18].

Until recently, PD was regarded as a pathology, which primarily affects neurons. However, glial cells have started to gain attention as potential contributors to the etiology of the movement disorder. In light of their neuro-supportive role, astrocytes are of particular relevance in the context of PD [19]. Interestingly, several histopathological reports described reactive astrogliosis in the substantia nigra pars compacta of patients, which likely contributes to neuroinflammatory signaling in this brain region [20,21].

While α-synuclein is mostly localized to neurons, low levels of the protein can also be found in astrocytes [22,23]. In mouse models, it was demonstrated that even minor α-synuclein quantities are critical for the maintenance of normal astrocytic function. α-synuclein was shown to bind to fatty acids in the brain [24]. In line with this finding, in astrocytes, a knockout of the protein disrupts fatty acid metabolism [25]. Moreover, the selective expression of A53T α-synuclein in astrocytes can trigger reactive astrogliosis and neurodegeneration [26].

While the aforementioned studies offer first insights into the role of α-synuclein in astrocytes, our knowledge about its endogenous regulatory functions in these cells remains limited. With the recent advancements in iPSC technologies there is now a plethora of protocols available that enable the generation of patient-derived astrocytes [27]. These model systems allow elucidating the effects of mutant α-synuclein on astrocytic physiology, while preserving the genetic background of the patient. By contrast, the various differentiation protocols vary considerably in terms of astrocyte purity and maturity, necessitating single-cell analysis approaches. Single-cell RNA sequencing can provide valuable insights into disease-associated molecular pathways specifically occuring in the astrocytic populations of a culture [28].

Taking advantage of state-of-the-art methodology, we generated iPSC-derived astrocytes harboring A53T-mutant α-synuclein and compared these to cultures from a healthy age- and gender-matched control. To explore the impact of the A53T mutation in α-synuclein on the astrocyte transcriptome, we performed single-cell RNA sequencing. Using this approach as well as high-throughput imaging and functional analyses, we demonstrated that A53T α-synuclein causes profound changes in the astrocytic differentiation potential, inflammatory pathways and mitochondrial biology.

Methods

Cell culture

An iPSC line derived from a healthy control was generated in the group of Prof. Gasser as previously described [29]. The iPSC line harboring p.A53T mutation in α-synuclein was purchased from the biobank of the National Institute of Neurological Disorders and Stroke (cell line ID: 50050). Both cell lines were maintained in mTeSR™ Plus medium (StemCell Technologies).

Astrocyte differentiation from iPSCs was performed as previously reported [30,31]. In brief, iPSCs were plated on Matrigel-coated (Corning) plates in mTeSR™ Plus medium supplemented with 10 µM ROCK inhibitor (Abcam). The following day, the medium was changed to mTeSR™ Plus without the inhibitor. The next day, conversion to neuroepithelial cells was initiated by adding

neurodifferentiation medium (NDM) containing 10 µM SB431542 (Sigma) and 200 nM LDN-193189 (Sigma). NDM was composed of DMEM-F12 (Gibco) and Neurobasal (Gibco) in a 1:1 ratio with an addition of 1% B27 without vitamin A (Gibco), 0.5% N2 (Gibco), 1% GlutaMAX (Gibco) and 0.5% penicillin/streptomycin (Gibco). Cells were kept in this medium for 11 days. After that, cells were maintained for 2 days in NDM containing 25 ng/ml bFGF (Peprotech) in order to expand the formed rosettes. Next, rosettes were detached by scraping and transferred to ultra-low attachment plates (Corning). For 2 days, they were maintained in NDM in the absence of additional growth factors until they formed clear spheres. Astrospheres were grown in astrodifferentation medium (ADM) for five months. ADM consisted of DMEM-F12 containing 1% non-essential amino acids (Gibco), 1% N2, 1% GlutaMAX, 0.5% penicillin/streptomycin, 2 µg/ml heparin (Sigma), supplemented with 10 ng/ml bFGF and 10 ng/ml EGF (Peprotech). Spheres were split manually by cutting once per week. To terminally differentiate astrocytic progenitors, spheres were treated with accutase (Merck Millipore) and the resulting cells were plated on Matrigel (Corning)-coated plates, followed by their maintenance for seven days in ADM with an addition of 10 ng/ml CNTF (Peprotech) and 10 ng/ml BMP4 (Peprotech).

Immunocytochemistry and image analysis

For immunocytochemistry experiments, cells were fixed with 4% paraformaldehyde in PBS (ThermoScientific). Afterwards, they were permeabilized and blocked for 1 h in PBS containing 0.25% Triton X-100 and 1% BSA. Primary and secondary antibodies were diluted in the same buffer. Overnight incubation at four degrees was applied with the primary antibodies at the following dilutions: Oct4 (Abcam, 1:1000), TRA-1-60 (Merck Millipore, 1:1000), Sox2 (Santa Cruz Biotechnology, 1:1000), GFAP (Dako, 1:500), Tom20 (Santa Cruz, 1:250). The next day, cells were washed several times with PBS and incubated with secondary antibodies for three hours. Subsequently, the washing step was repeated and the solution containing 20 µM Hoechst (LifeTechnologies) was applied to stain nuclei. As the final step, cells were washed with PBS and imaged using either a Zeiss Axio Imager M2 or a Yokogawa CV8000 microscope.

Image analysis for astrocytic and mitochondrial morphology was performed in a quantitative manner, using a custom-made code prepared in Matlab 2020a and Matlab 2021a. The High-Performance Computing Platform at the University of Luxembourg was utilized to run the analysis. The code is available upon request of the computer vision scripts with IDs 905 and 1797.

Quantitative PCR

RNA was isolated using the RNeasy Plus Kit (Qiagen) and following the procedure described in the manufacturer's manual. To synthesize cDNA from the obtained RNA, SuperScript III Reverse Transcriptase Kit (Invitrogen) was applied. To quantify genes of interest (Supplementary Table 1), quantitative PCR (qPCR) was performed using iQ SYBR Green Supermix (BioRad) and the reaction was run on the LightCycler 480 (Roche). For all studied genes, the annealing temperature was 60 degrees. Normalization of gene expression values was done using the housekeeping genes *ACTB* and *L27* in the experiments for Figure 1 and 4, whereas in Figure 7 *ACTB* was used for normalization.

Cytometric bead array

The levels of human MCP1 (CCL2), RANTES (CCL5) and IL-6 in the conditioned astrocytic media were analyzed by applying the Cytometric Bead Array (CBA) Flex and Human Soluble Protein Master Buffer Kit (BD Biosciences) according to manufacturer's protocol. The samples were measured on the BD Accuri C6 Plus flow cytometer using BD CSampler Plus software (BD Biosciences). Mean PE-Height fluorescence intensity values were used to define the standard curves. Sample concentrations were calculated based on the standard curves using log-log regression.

Single-cell RNA sequencing: library preparation and sequencing

Cells were counted using the C-Chip Disposable Haemocytometer (NanoEnTek) to determine the concentration and viability. Single-cell samples with final cell viability above 90% were resuspended in defined volumes of 0.2% BSA (in PBS), with a final concentration of 1000 cells per µL. The whole procedure was performed on ice whenever possible. Single cells were processed with the Chromium Next GEM Single Cell 3' Bead, Chip and Library Kits v3.1 (10x Genomics) following the manufacturer's protocol. For mid-range cell recovery, we used 12 PCR cycles for cDNA amplification. Libraries were purified using SPRIselect magnetic beads (Beckman Coulter) and their quality evaluated with the High Sensitivity D5000 ScreenTape Assay on a 4200 TapeStation device (Agilent). Single-cell library fragments between 560-600 bp were sequenced with the NextSeq 2000 device (Illumina) using the P2 2000 (200 cycles) NextSeq kit. The sequencing setup was designed to reach 20,000 reds per cell with a paired-end configuration. Sequenced libraries were mapped to the GRCh38 human reference genome.

Single-cell RNA sequencing: generation of featurevbarcode count matrix, quality control, and filtering

The fastq files were processed using Cell Ranger 5.0.1 to generate single-nuclei feature-barcode count matrices by aligning to the human transcriptome version GRCh38-2020-A (10X Genomics) using the *cellranger count* pipeline, with the option to include intronic reads. Across the entire dataset containing four sequenced samples, the cellranger output resulted in 21325 barcodes being classified as nuclei, with a median number of genes ranging between 2600 - 4500 per nuclei. Downstream quality control and filtering were performed using R v4.1.3 with Seurat v4. The following filtering criteria were applied: minimum cutoffs of 1000 UMI counts per barcode and 750 distinct genes per barcode as well as a maximum per-barcode threshold of 25% mitochondrial and 25% ribosomal reads. These criteria, in addition to filtering out doublets using Scrublet 0.2.3 with a maximum cut off of a 0.15, resulted in a total of 18453 nuclei-associated barcodes across all samples.

Single-cell RNA sequencing: normalization, merging of samples, cell clustering, and annotation

Normalization, merging, cell-clustering and annotation were carried out using R v4.1.3 with Seurat v4. The data corresponding to the four samples/conditions were log-normalized using the *NormalizeData* function and merged using the *merge* function in Seurat. To identify cell types, the dimensionality of the dataset was reduced to the top 2500 highly variable genes (*FindVariableFeatures*), the resulting data was scaled (*ScaleData*) and further reduced in dimensionality using principal component analysis (*RunPCA*). The top 30 principle components were used to cluster the data (*FindClusters*) using the Louvain clustering algorithm at a resolution of 0.055. Differentially expressed (DE) genes of each of the identified clusters against the remaining cells were calculated (*FindAllMarkers*) and filtered using the following parameters: *min.cell.group*=5, *min.pct*=0.05 and *logfc_threshold*=0.2. To test for statistical significance (bonferroni-adjusted p-value < 0.05) the Wilcoxon Rank Sum test was used. The differentially expressed genes obtained in this fashion were used to annotate the cell types of the clusters.

Single-sample gene set enrichment analysis

Single-sample Gene Set Enrichment Analysis (ssGSEA) was carried out in R v4.1.3 using msigdbr v7.5.1, escape 1.4.0. The *msigdbr* and *getGeneSets* functions were used to fetch and filter the all the Hallmark genesets (50 gene sets) as well as a subset of C5 ontology gene sets containing the phrase “GOBP…mitocho…” in order to limit the analysis to mitochondria-related pathways (103 gene sets) from the MSigDB. *enrichIt* function was used to calculate the enrichment score per cell

for every gene set. Wilcoxon test (*wilcox_test* in rstatix v0.7.1 library) was used to compare the enrichment scores between groups of cells, where Bonferroni correction was applied during multiple comparisons.

Statistical analysis of qPCR and imaging data

Statistical analyses were performed using GraphPad Prism (version 9.4.0). Generally, for grouped analyses, two-way ANOVA was utilized. The threshold for statistical significance was set to a p-value below 0.05.

Results

Patient-derived astrocytes show decreased expression of GFAP and S100B

In this study, we used cell lines derived from a healthy individual and a patient harboring the p.A53T (c.209G>A) mutation in α-synuclein. Initially, we performed a karyotype analysis, which revealed no chromosomal aberrations in the patient line (Fig. S1) as well as in the healthy control (see first manuscript of the thesis for more details). Furthermore, we confirmed the pluripotent potential of both lines by assessing the expression of typical stemness markers such as Oct4, TRA-1-60 and Sox2. All studied markers were expressed in both iPSC lines used here (Fig. S2).

Following this initial characterization, we applied an established differentiation protocol to generate iPSC-derived astrocytes as described previously [30,31]. To control for the purity and differentiation efficiency of the cultures, we performed immunocytochemistry using GFAP as an astrocyte marker and assessed the percentage of positive cells using an automated image analysis approach. With our method, we exclusively considered the GFAP signal in the perinuclear zone of the cell (Fig. 1B). As a result, we observed comparable percentages of cells expressing GFAP in the two lines (Fig. 1C). Interestingly, while the majority of cells presented an astrocytic morphology, not all cells expressed GFAP (PD, 57%; CTRL, 66%).

Next, to evaluate the maturity of the astrocyte cultures, we studied the expression of several astrocytic markers. We observed no significant differences in the expression levels of *SLC1A3* and *AQP4* between the two cell lines. However, the expression of *GFAP* and *S100B* was downregulated in A53T α-synuclein astrocytes (Fig. 1D). To control for the presence of neurons, we assessed the mRNA levels of *MAP2*. Although based on this marker, a minor neuronal contamination of the cultures was observed, no significant difference in terms of expression was detected between the two lines (Fig. 1D).

Despite the primarily neuronal localization of α-synuclein, the protein was also detected in glial cells [22,23]. We determined the mRNA abundance of *SNCA* in both astrocytic cell lines and observed overall low expression levels, with no difference between healthy control and A53T-mutant astrocytes (Fig. 1D).

A53T α-synuclein astrocytes show reduced differentiation potential

To study the impact of A53T α-synuclein on the astrocytic expression profile, we applied single-cell RNA sequencing to the cultures using 10xGenomics technology. With this technique, we were able to distinguish mature astrocytes from other cell populations for downstream analyses.

Since reactive astrocytes are known as important players in the neuroinflammation process [32], we mimicked their activation by exposing them to two cytokines, namely IL-1β and TNF-α for 48h. We sequenced both, untreated and treated cells, of the healthy control and the patient line, obtaining data from around 2800-8100 cells after filtering out doublets and cells with transcripts of poor quality. We embedded the generated transcriptomes into two dimensions using the UMAP algorithm. With this approach, we identified five distinct clusters: (i) resting astrocytes, (ii) activated astrocytes #1, (iii) activated astrocytes #2, (iv) radial glia, and (v) neural progenitors (Fig. 2A). The annotation of these clusters was achieved using markers reported in the literature. In particular, we used *GFAP* [33], *AQP4* [34] and *S100B* [35] as genes defining astrocytes, whereas *CXCL10* [36] and *CCL2* [37] were selected as additional markers for activated astrocytes. *DCX* was identified as a gene typically expressed by neural progenitors [38] and the radial glia cluster was established using *PAX6* [39] and *MKI67* as proliferation markers [39,40].

Interestingly, we observed that while untreated cells derived from the healthy control and the patient clustered together, activated cells separated based on their genotype (Fig. 2C). Hence, the cluster denominated as “Activated astrocytes #1” comprised almost exclusively treated cells from patients, whereas the cluster named “Activated astrocytes #2” was composed mainly of treated control cells. In addition, also the proportions of the other identified cell clusters were different between the patient and the control. In particular, the A53T-mutant cultures contained larger numbers of radial glia (PD, 60%; control, 40%) and neural progenitor cells (PD, 60.9%; control, 39.1%). Moreover, we performed an analysis of single-cell entropy as a means to assess the differentiation potential of the studied cultures. While at baseline, we did not detect any significant differences between control and A53T-mutant astrocytes, upon treatment, PD cells presented a lower differentiation capacity (Fig. 2D).

A53T α-synuclein astrocytes overexpress gene linked to mitochondrial biogenesis

Next, we determined the top differentially expressed genes across all the identified clusters (Fig. 2E). The "Activated astrocytes #1" cluster was characterized by overexpression of *IMMP2L*, which encodes a protein responsible for the processing of cytosolic protein precursors that are targeted to the mitochondrial intermembrane space [41]. Furthermore, this cluster was characterized by elevated expression levels of *PRDX6* - a gene linked to the cellular anti-oxidative defense [42]. In contrast, the "Activated astrocytes #2" cluster, which is primarily composed of treated control cells, showed high expression levels of genes encoding cytokines such as CXCL11, CCL5 or CXCL10 [43,44].

Cellular morphology of activated A53T α-synuclein astrocytes differs from activated control cells

To assess the impact of reactivity on astroglial morphology, we employed high-content imaging followed by automated image analysis with custom-made Matlab scripts. The applied masks allowed to separately assess various morphometric parameters for the cellular soma and the processes (Fig. 3A). Our analysis revealed that the normalized area of the processes was significantly decreased for activated A53T-mutant astrocytes compared to activated control cells (Fig. 3B). A similar trend was observed for the summed perimeter of all processes when normalized to nuclei count. Furthermore, the normalized soma area was increased in case of activated A53T α-synuclein astrocytes. In line with these findings, the ratio of the process area to soma area was decreased for activated A53T-mutant astrocytes.

A53T alpha-synuclein alters activation profile of astroglial cultures

Next, to determine the activation status of the astrocytes, we analyzed the expression profile of a set of genes that were previously identified to define A1 or A2 reactivity states [32]. The analysis was performed for all cells that were part of any of the three astrocytic clusters, excluding radial glia and neural progenitors (Fig. 4A). Among the pan-reactive markers, we observed that at least 75% of cells were *HSBP1*-positive and that the expression of this gene was decreased in the patient culture, in particular upon treatment. *CXCL10* was almost exclusively expressed in treated cells, with lower mRNA levels in PD versus control astrocytes. Although the levels of *CD44* were higher in A53T-mutant astrocytes at baseline, upon treatment, this difference disappeared. Interestingly, compared to control cells, the expression of *GFAP* was reduced in A53T-mutant astrocytes under basal as well as treated conditions. In contrast, the mRNA levels of *VIM* were elevated in A53T α-synuclein astrocytes under basal and treated conditions. Most of the studied A1 and A2 activation

markers were not expressed to a high extent in the cultures. An exception was *S100A10*, which was expressed by >75% of cells with lower mRNA levels in the patient astrocytes (Fig. 4A).

To further explore potential differences in terms of activation between healthy control and PD astrocytes, we used quantitative PCR to assess the expression of a set of genes encoding cytokines, which have previously been shown to change their abundance in response to similar treatment conditions [31]. Interestingly, we could observe that, upon activation, the expression of *IL6* and *GMCSF* was upregulated in PD astrocytes, whereas in the same cells the mRNA levels of *CXCL10*, *CCL5* and *CCL2* were reduced when compared to healthy control cells (Fig. 4B). These findings were further supported by ELISA analyses of the corresponding cytokines in cell culture medium. Specifically, we could demonstrate that IL-6 levels in the extracellular space were upregulated in activated A53T-mutant astrocytes when compared to treated control cells, whereas CCL5 and CCL2 were released to a lesser extent (Fig. 4C).

To further strengthen these results, we assessed the activation status of the NF-κB pathway, which is stimulated by IL-1β and TNF-α. When analyzing the protein abundance of phosphorylated NF-κB p65 by means of Western blotting, we detected, upon treatment, a significant decrease in the activation of treated A53T-mutant astrocytes compared to activated control astrocytes (Fig. 4D).

Since we detected a reduction in the capacity of A53T-mutant astrocytes to respond to the inflammatory stimuli, we aimed to further explore the molecular cause of this dysfunction. Interestingly, glycolysis has been shown to be an important modulator of astrocytic reactivity [45,46]. In particular, it was demonstrated that aberrant glycolysis prevents astrocytes from transitioning into a reactive state [46]. Using our single-cell RNA sequencing dataset, we analyzed the expression of genes coding for glycolytic enzymes (Fig. 5A). Among the most abundantly expressed genes, we observed that the expression of *ENO1*, *PKM* and *TPI* was significantly downregulated in activated A53T-mutant astrocytes when compared to activated control cells, while the expression of *GAPDH* did not significantly differ between the patient and control cultures (Fig. 5A, Fig. 5B).

A53T-mutant astrocytes show lower enrichment in mitochondrial pathways

In light of a possible glycolysis disruption in A53T-mutant astrocytes, we decided to investigate mitochondria in more detail as oxidative phosphorylation may be a way to compensate for such metabolic deficit. In addition, we identified *IMMP2L* among the top differentially expressed genes

in the “Activated astrocytes #1” cluster, which further prompted us to analyze mitochondrial function.

In order to test for a mitochondrial involvement in *SNCA*-PD, we performed ssGSEA focussing on biological processes related to mitochondria in the gene-ontology database (Fig. S3A). With this approach, we identified a lower enrichment of genes coding for proteins involved in oxidative phosphorylation (Fig. 6B). Inspired by this finding, we next explored mitochondrial pathways in the ssGSEA and observed numerous differences between patient and control astrocytes (Fig. S3B). We then evaluated the three astrocytic clusters in more detail and uncovered nine pathways that revealed significant differences in the ssGSEA (Fig. 6C). Among the most altered pathways were gene sets related to the maintenance of protein localization to mitochondria, modulation of mitochondrial calcium ion homeostasis, regulation of mitophagy, mitochondrial fission and mitochondrial DNA (mtDNA) replication. Moreover, we also identified changes in pathways linked to apoptosis, regulation of mitochondrial organization and protein insertion into the inner mitochondrial membrane. Interestingly, all of these pathways were significantly less enriched in the “Activated astrocytes #1”, the cluster which is mainly composed of activated patient astrocytes (Figure 6C).

Aberrant mitochondrial morphology and increased mitochondrial mass in A53T-mutant astrocytes

To functionally validate our results from the gene enrichment analysis, we first assessed mitochondrial abundance and morphology as general read-outs of mitochondrial dyshomeostasis using high-content imaging. A custom-made code prepared in Matlab allowed us to define mitochondria based on the signal of Tom20 - an outer mitochondrial membrane protein. While astrocytes were labeled with an antibody against GFAP. To analyze mitochondrial morphometrics exclusively within astrocytes, we restricted our analysis to organelles localized within GFAP-positive cells (Fig. 7A). This approach revealed pronounced changes in mitochondrial morphology in activated PD patient astrocytes. Specifically, the average mitochondrial size, defined by the sum of mitochondrial pixels normalized to mitochondrial number (Fig. 7B), was significantly increased in activated A53T-mutant astrocytes when compared to treated control cells. Furthermore, mitochondrial mass, as calculated by the summed mitochondrial pixels normalized to nuclei pixels, was increased in activated A53T α-synuclein astrocytes. When performing a detailed analysis of mitochondrial branching, we could demonstrate that the normalized node number, average node degree and total link number was increased in activated A53T-mutant astrocytes. Lastly, as mtDNA replication was also nominated by the ssGSEA, we studied the expression of genes encoded by the mitochondrial genome as an indicator of impaired mtDNA maintenance. In line with the

ssGSEA results, we indeed detected a downregulation in the levels of mtDNA genes in activated A53T α-synuclein astrocytes compared to activated control cells (Fig. 6C).

Discussion

α-synuclein deposits are considered a key feature of PD pathology [11]. Hence, cell cultures derived from PD patients harboring mutations in α-synuclein are frequently employed as a genetic model system to study the underlying molecular mechanisms of PD [47]. Although there is a growing consensus that astrocytes contribute to the pathogenesis of PD [19], we still lack a deep understanding of how pathogenic α-synuclein alters glial physiology. In order to close this knowledge gap, we aimed to explore the impact of A53T α-synuclein on the function and activation status of human astrocytes.

iPSC technology proves to be particularly useful in modeling PD at the endogenous level [48]. Yet, to date, few studies have employed astrocytic differentiation protocols to investigate mutant α-synuclein in patient astrocytes. Thus, in this study, we employed an established protocol [31] to generate astrocytes from iPSCs derived from an A53T-mutant PD patient and a healthy age- and gender-matched control.

An immunocytochemistry characterization of these models revealed comparable percentages of astrocytes based on GFAP protein expression. Yet, this typical astrocytic marker was not expressed in all generated cells. This observation is in line with literature suggesting that not all resting astrocytes express GFAP [49]. In light of this limitation of GFAP as a marker protein, we additionally considered cell morphology as an important characterization criterion. In line with previous studies employing the same differentiation protocol [31], the absolute majority of cells in our cultures showed a morphology representative of human astrocytes [50]. Furthermore, mRNA analysis revealed high expression levels of the astrocytic marker genes *SLC1A3* and *AQP4* [51] when compared to neurons. Importantly, the expression of these genes did not vary significantly between the lines.

In addition, neuronal contamination is a frequently encountered challenge, when generating iPSC-derived astrocytes. Thus, we used the marker gene *MAP2* to test for the presence of neurons in our cultures. While we observed some residual levels of *MAP2*, the mRNA abundance of this gene was significantly lower in astrocytes than in neuronal cultures [52].

Another aspect of the model validation was the quantification of *SNCA* gene expression. Overall, we observed low levels of *SNCA* mRNA in astrocytes, which is in agreement with the literature [23]. Furthermore, *SNCA* expression was comparable between A53T-mutant and control

astrocytes. This finding corroborates results from iPSC-derived neuronal cultures, which suggested that the A53T mutation does not interfere with α-synuclein abundance [53–55]. Only in pure dopaminergic neurons an increase in the levels of A53T-mutant α-synuclein has been shown [55]. Based on these findings, we concluded that the generated astrocyte cultures expressed *SNCA* and were sufficiently pure and mature to serve as model systems in our study.

To delineate potential transcriptomic changes associated with A53T-mutant α-synuclein in astrocytes, we employed single-cell RNA sequencing. First, when exploring the different cellular populations in the cultures, we detected an increase in radial glia and neuronal progenitor cells in the mutant line. We hypothesized that this shift in terms of cell composition may be due to an A53T a-synuclein-mediated reduction in astrocytic differentiation capacity. Thus, to further explore this idea, we performed single-cell entropy analysis as a measure of the differentiation potential of the cultures. Indeed, this assessment uncovered a reduction in the differentiation capacity of A53T-mutant astrocytes under inflammatory conditions. Given that a study in iPSC-derived neurons with the *SNCA* triplication mutation previously reported impaired neurogenesis [56], we conclude that pathogenic α-synuclein interferes with cellular development in neurons as well as glia.

Astrocytic reactivity can be neuroprotective but may equally contribute to neurodegeneration [57]. Two reactive states, which are defined by diverse cellular programs, can be distinguished: A1 and A2 [58]. We decided to examine the reactivity of our cultures under basal conditions and after stimulation with IL-1β and TNF-α. These cytokines are typically secreted by activated microglia and can modulate the astrocytic response via the NF-kB pathway [45,59,60]. Interestingly, single-cell RNA sequencing revealed striking differences in the response of A53T-mutant and control astrocytes to the aforementioned treatment. The two lines clustered almost completely apart when activated, which suggested profound differences in their response to the stimulus. To further characterize the activation states of the cells, we examined the expression levels of genes that have previously been associated with pan-reactivity as well as A1 or A2 activation [32]. Exemplarily, single-cell transcriptomics revealed that the expression of *HSBP1* was downregulated in A53T-mutant astrocytes upon activation. *HSBP1* codes for a heat-shock protein, which was reported to be involved in neuroprotective mechanisms [61]. A similar decrease was observed for *CXCL10* - a chemokine that was shown to stimulate microglia migration as well as their activation [62]. A reduction in *CXCL10* expression in astrocytes may thus influence their crosstalk with microglia [63]. In addition, compared to treated control cells, activated A53T-mutant astrocytes

expressed lower mRNA levels of CD44. We recently observed an upregulation of *CD44* along the activation trajectory of postmortem astrocytes from sporadic PD patients [64]. Moreover, CD44 was implicated in the promotion of proinflammatory signaling in neurons [65]. Thus, from these results, we derived that the A53T mutation in alpha-synuclein renders astrocytes less responsive to inflammatory triggers.

In addition to investigating the reactive state (e.g. A1 vs A2) of the cultures, we also evaluated the expression of astrocytic cytokines and chemokines by means of qPCR. We focused on genes, which are known to be expressed in astrocytes after stimulation of the NF-kB pathway by IL-1β and TNF-α [45,60,66]. Importantly, neuroinflammation associated with the NF-kB pathway has been linked to neurodegeneration in PD [67]. Only in the case of *IL6* and *GM-CSF* expression, we detected an upregulation in activated A53T-mutant compared to control astrocytes. IL6 has been widely reported to be increased in the striatum, serum and CSF of PD patients and was thus proposed as a disease marker [68]. Furthermore, the cytokine IL6 was uncovered as the driving force of astrocytic reactivity [69]. Although GM-CSF is typically classified as a pro-inflammatory cytokine, there is evidence suggesting that it can also act anti-inflammatory and neuroprotective [70,71]. Among the remaining genes tested here, we observed a decrease in the expression of *CCL2*, *CCL5*, and *CXCL10* in A53T astrocytes. This result was in agreement with our previous analysis of A1 and A2 signature genes for which we generally observed decreased expression levels in activated patient astrocytes. These results were further strengthened by the detection of decreased levels of phosphorylated NF-kB p65 in activated A53T-mutant astrocytes. p65, which is also known as RelA, is a component of the NF-kB complex and acts as a transcriptional activator [72]. Phosphorylation at Ser536 enhances p65 transcriptional activity [73] and may therefore serve as a marker of NF-kB pathway activation. These findings further support our hypothesis that A53T astrocytes do not mount an efficient response to inflammatory stimuli.

Changes in astrocytic morphology are a key feature of astrogliosis [78]. Here, we show that activated A53T-mutant astrocytes are characterized by an increase in cell soma area, while at the same time they show fewer processes when compared to reactive control astrocytes. Although, typically, reactive astrocytes expand both their processes and soma in a process known as hypertrophy [79], in the context of Alzheimer's disease, it was shown that trimming of processes may also occur [80]. Thus, our transcriptomic and morphological analyses implicate A53T α-synuclein in aberrant astrocyte physiology in particular under inflammatory conditions.

Of note, astrocyte reactivity also depends on cellular metabolism [45,46]. In particular, glycolysis appears to be critical for efficient astrocyte activation [46]. Moreover, a recent study in 3xTg-AD mice linked alterations in the glycolytic flux of astrocytes to synaptic and behavioral deficits [74]. Hence, we examined the expression of genes encoding enzymes of the glycolysis pathway. Interestingly, for three out of the four most abundantly expressed genes of the pathway, namely *PKM*, *ENO1* and *TPI*, we observed a downregulated expression in treated A53T-mutant astrocytes, when compared to treated control cells. *PKM* codes for pyruvate kinase M1/2 - the enzyme, which is responsible for the conversion of phosphoenolpyruvate into pyruvate, thereby generating ATP [75]. *ENO1* and *TPI* encode so-called "moonlighting proteins", which play a pivotal role in the glycolytic pathway [76,77]. Together, these results may suggest that astrocytes harboring A53T α-synuclein have a defect in the glycolysis pathway, which likely contributes to the inability of these cells to respond to inflammation-inducing agents.

In light of the metabolic alterations in activated A53T-mutant astrocytes uncovered by single-cell transcriptomics, we became interested in mitochondria. While astrocytes are mostly dependent on glycolysis, mitochondria are critically involved in their homeostasis by regulating cellular calcium and Na+ levels among other processes [81]. Moreover, single-cell RNA analyses identified *IMMP2L* among the top differentially expressed genes in the cluster "Activated astrocytes #1". *IMMP2L* codes for the inner mitochondrial membrane peptidase 2 [82]. Mutations in *IMMP2L* caused hyperpolarization, increased ROS production and an ATP overload in mice [83]. Accordingly, we hypothesized that a multitude of mitochondrial functions may be disrupted in reactive A53T-mutant astrocytes.

SsGSEA indeed confirmed a lower enrichment for multiple mitochondria-associated pathways. Notably, in the "Activated astrocytes #1", we detected significant changes for pathways controlling the protein localization to mitochondria and mitochondrial organization. Previous studies demonstrated that α-synuclein can block mitochondrial protein import [84] and, more importantly, can itself be imported into mitochondria, where it is primarily localized at the inner membrane [85]. In addition, in the "Activated astrocytes #1" cluster, we identified a lower enrichment for pathways associated with calcium homeostasis, apoptosis-related fragmentation, mitophagy and fission - processes, which have previously been linked to α-synuclein in the context of neurodegeneration [86,87]. Finally, gene enrichment analysis revealed a deficit in oxidative phosphorylation in the "Activated astrocytes #1" cluster. This implies that activated patient astrocytes harboring A53T α-synuclein are unable to compensate for the observed glycolysis impairment by means of mitochondrial respiration.

To functionally validate the broad effects of A53T α-synuclein on astrocytic mitochondria, we applied a high-throughput imaging approach to investigate morphology and abundance as representative mitochondrial features. We detected an increase in mitochondrial size and mass, suggesting that the genetically nominated processes mitochondrial fission and clearance are indeed impaired in these cells. Furthermore, we also detected reduced expression of mtDNA-encoded genes. Thus, paralleling previous findings in neuronal models of *SNCA*-PD [18], A53T-mutant astrocytes show a wide range of mitochondrial impairments.

In conclusion, in the current study, we showed that A53T α-synuclein hampers the capacity of astrocytes to react to inflammatory stimuli. This reduced response may be due to an impairment in the glycolytic pathway. Furthermore, activated PD patient astrocytes harboring the A53T mutation in α-synuclein undergo extensive changes in mitochondrial morphology and function. Further studies will now be needed to characterize the exact metabolic profile of alpha-synuclein-mutant astrocytes. Moreover, experiments in co-culture systems will ultimately help to elucidate how metabolically induced astrocytic dysfunction contributes to neurodegeneration in PD. Such work building on our findings has the potential to uncover entry points for novel "glia-centric" disease-modifying therapy approaches in PD.

Code availability

The scripts used for the analysis of the single-nuclei RNA sequencing data set is made freely available through a public github repository (https://github.com/SpielmannLab/gruenewald_astrocytes).

Author contributions

PM, CV, KB, SD, SLP, KG, MT and TR performed experiments. PM, VS, PA, KH, SD, SS, TR performed the analysis. PM, VS and AG wrote the manuscript, which was reviewed by all the authors. MK gave training in the astrocytic differentiation protocol. AG and RK acquired funding for this study and together with JK, AS and MS supervised the work.

Acknowledgements

PM and SS were funded by the Luxembourg National Research Fund (FNR) within the framework of the PARK-QC DTU (PRIDE17/12244779/PARK-QC). KB was funded by the FNR within the framework of the CriTICS DTU (FNR10907093). CV was supported by an FNR CORE Junior Grant

(“NeuroFlame”, C20/BM/14548100). AG received funding through an FNR ATTRACT grant (“Model-IPD”, FNR9631103). Additionally, AG, SLP and SD were supported by the FNR within the framework of a CORE grant (“CAMeSyn”, C19/BM/13688526).

This work was in part funded by the German Research Foundation (DFG; Deutsche Forschungsgemeinschaft) within the framework of the Start-Up funding 01-21 to M.S. M.S. is a Deutsches Zentrum für Herz-Kreislaufforschung principal investigator and is supported by grants from the DFG (SP1532/3-2, SP1532/4-1 and SP1532/5-1), the Max-Planck-Gesellschaft and the Deutsches Zentrum für Luft- und Raumfahrt (DLR 01GM1925). Open Access funding provided by the Max Planck Society. Deposited in PMC for immediate release.

VKAS and KH thank Saranya Balachandran and Dr Cesar Prada for co-developing scripts for primary data analysis. We acknowledge the computational support from the OMICS compute cluster at the University of Lübeck.

Figure captions

Fig. 1 Characterization of iPSC-derived A53T-mutant and control astrocytes. A. Overview of the experimental set-up used in the study. This figure was generated using BioRender. **B.** Representative immunocytochemistry images of astrocytes stained with GFAP. Mask of the perinuclear zone generated using a Matlab script to assess the fraction of cells positive for GFAP. For each line, three biological replicates were analyzed. Scale bar, 20 µm. **C.** Quantification of cells positive for GFAP. Data are presented as mean ± standard deviation (SD). **D.** Analysis of gene expression using qPCR. Astrocytic mRNA levels of *SLC1A3*, *AQP4*, *GFAP*, *S100B,* and *SNCA* were quantified in relation to neurons. Three biological replicates were examined for each cell line. Data are presented as mean ± SD, **P ≤0.01, ***P ≤0.001, ***P ≤0.000.

Fig. 2 Single-cell RNA sequencing analysis of A53T-mutant and control astroglial cultures. A. UMAP embedding of obtained transcripts showing the cluster identification. **B.** Dot plot representing the expression of marker genes for each identified cluster. **C.** UMAP embedding showing the contribution of each generated sample to the identified clusters. **D.** The proportion of each sample per cluster. **E**. The single-cell entropy plot, which is indicative of differentiation potential. **F**. Heatmap showing the top differentially expressed genes for each cluster.

Fig. 3 Analysis of cellular morphology. A. Representative image showing the mask used for segmenting astrocytic soma and processes. Scale bar, 20 µm. **B.** Quantification of parameters used to assess cellular morphology.

Fig. 4 Astrocytic activation status in response to IL-1β and TNF-α treatment. A. Dot blot showing the percentage of cells expressing the indicated activation markers and their respective levels of expression. **B.** Analysis of cytokine gene expression by means of qPCR. The expression was normalized to the housekeeping genes *ACTB* and *L27*. Data are presented as mean ± SD, *P≤0.05, **P ≤0.01, ***P ≤0.001, ***P ≤0.000. **C.** Quantification of cytokines released into the medium. The concentration of the cytokines was normalized to the corresponding protein content of the cell extracts. Data are presented as mean ± SD, *P≤0.05, **P ≤0.01, ***P ≤0.001, ***P ≤0.000. **D.** Western blot analysis of phosphorylated NF-κB p65 protein levels in astrocytes. Data are presented as mean ± SD, *P≤0.05, **P ≤0.01, ***P ≤0.001, ***P ≤0.000. UT, untreated, TR, treated with IL-1β and TNF-α.

Fig. 5 Transcriptomic analysis of genes encoding enzymes of the glycolytic pathway. A. Dot blot showing the expression of genes involved in the glycolysis pathway. **B.** Violin plots showing the expression of the most abundantly expressed genes of the glycolytic pathway in the analyzed dataset.

Fig. 6 Single-sample gene enrichment analysis of mitochondria-related pathways. A. UMAP showing the identified clusters and color-coding. **B.** Single-sample gene enrichment analysis (ssGSEA) for the oxidative phosphorylation pathway. **C.** Single-sample GSEA for pre-selected mitochondrial pathways.

Fig. 7 Mitochondrial phenotyping in A53T-mutant and control astrocytes. A. Representative images of the mitochondrial morphology analysis with indicated mitochondrial and cellular masks. **B.** Quantification of morphological parameters related to mitochondria. Mito, mitochondria. Data are shown as mean ± SD, **P ≤0.01, ***P ≤0.001. **C.** The analysis of the gene expression of mitochondrially encoded genes. Data are shown as mean ± SD, **P ≤0.01, ***P ≤0.001. Expression is shown as a mean for the expression of *ND1*, *ND4*, *ND6*, *CYTB*, *COX1*, *ATP6/8* and normalized to *ACTB*.

Fig. 1

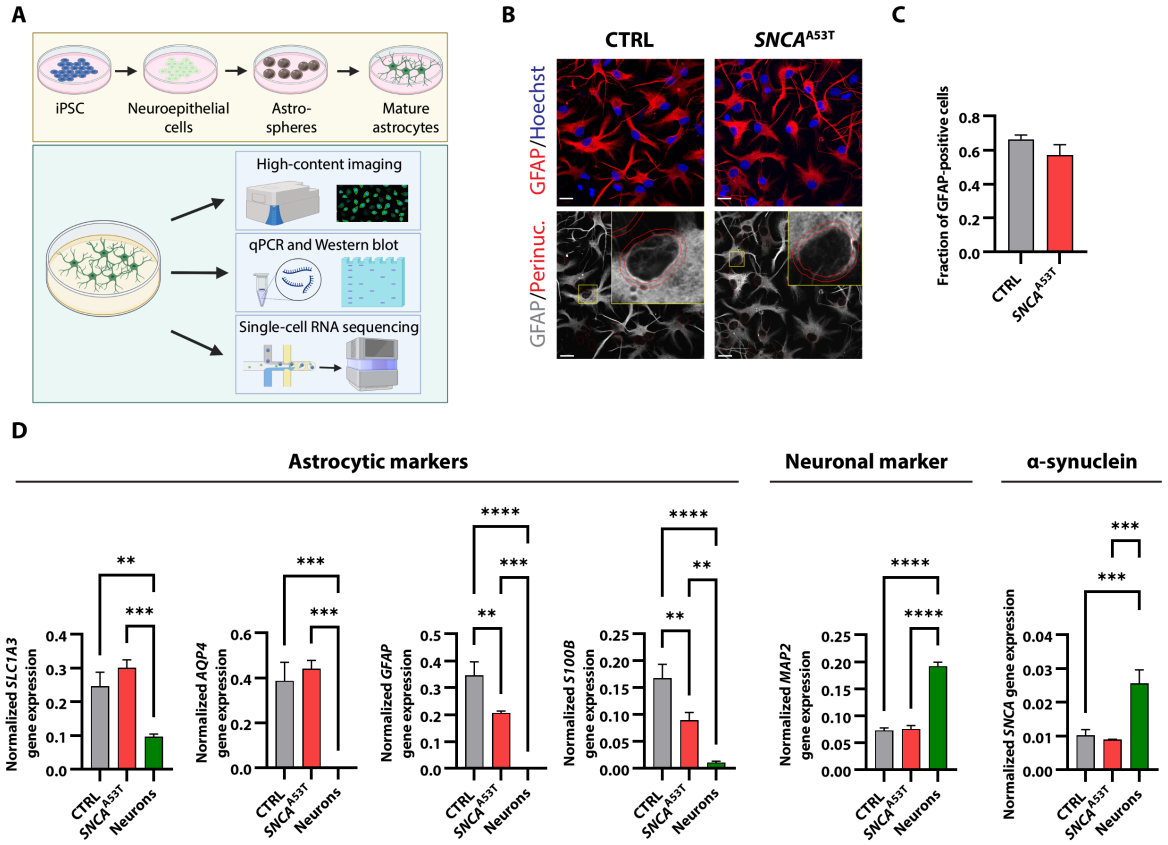
A
iPSC
Neuroepithelial cells
Astro-spheres
Mature astrocytes
High-content imaging
qPCR and Western blot
Single-cell RNA sequencing
B
CTRL
SNCA A53T
GFAP/Hoechst
GFAP/Perinuc.
C
Fraction of GFAP-positive cells
CTRL
SNCA A53T
D
Astrocytic markers
Neuronal marker
α-synuclein
Normalized SLC1A3 gene expression
Normalized AQP4 gene expression
Normalized GFAP gene expression
Normalized S100B gene expression
Normalized MAP2 gene expression
Normalized SNCA gene expression
CTRL
SNCA A53T
Neurons

Fig. 2

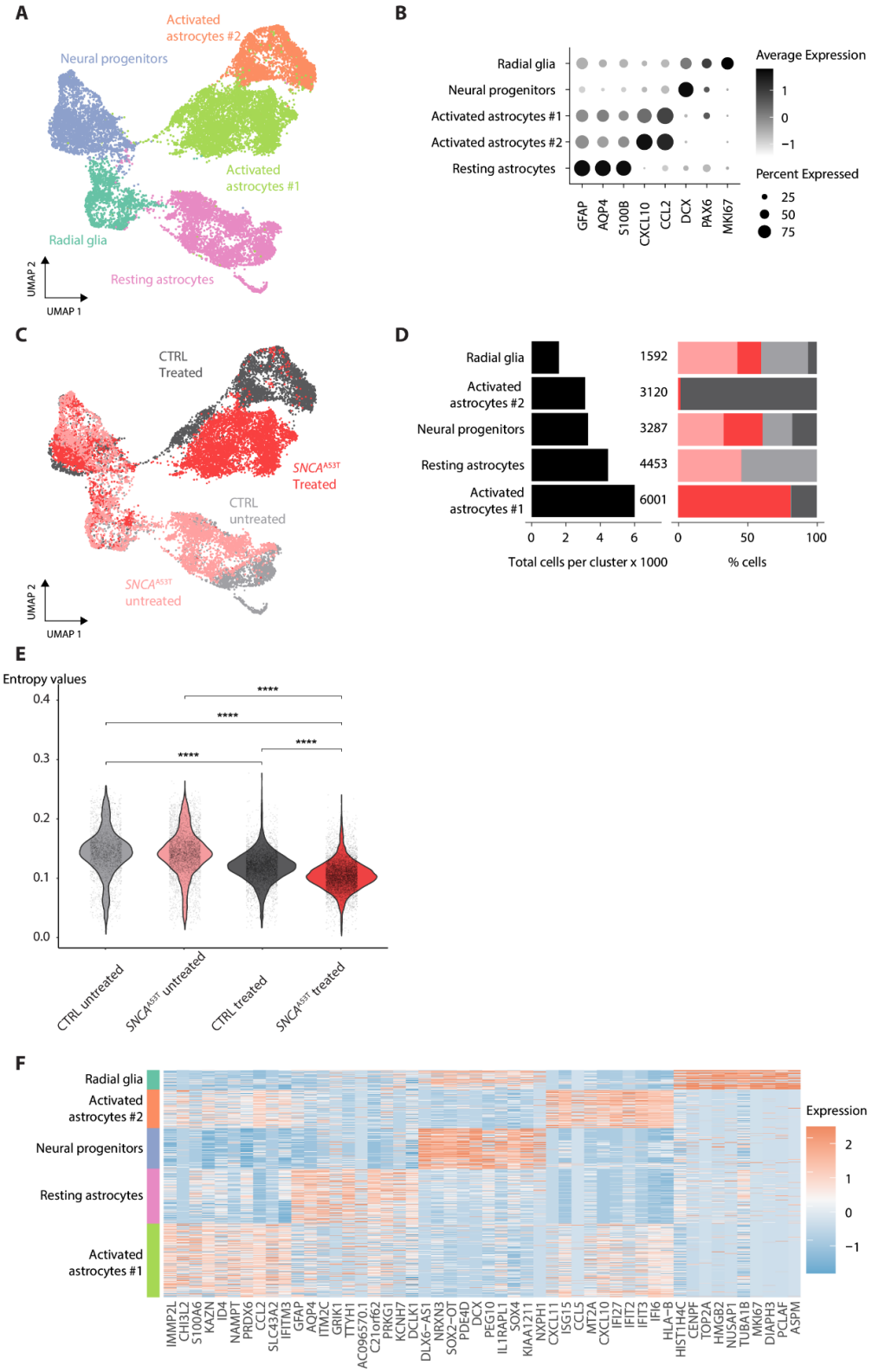
A
Activated astrocytes #2
Neural progenitors
Activated astrocytes #1
Radial glia
Resting astrocytes
UMAP 2
UMAP 1
B
Radial glia
Neural progenitors
Activated astrocytes #1
Activated astrocytes #2
Resting astrocytes
GFAP
AQP4
S100B
CXCL10
CCL2
DCX
PAX6
MKI67
Average Expression
1
0
−1
Percent Expressed
25
50
75
C
CTRL Treated
SNCA A53T Treated
CTRL untreated
SNCA A53T untreated
UMAP 2
UMAP 1
D
Radial glia
Activated astrocytes #2
Neural progenitors
Resting astrocytes
Activated astrocytes #1
1592
3120
3287
4453
6001
0
2
4
6
Total cells per cluster x 1000
0
50
100
% cells
E
Entropy values
0.4
0.3
0.2
0.1
0.0
****
****
****
****
CTRL untreated
SNCA A53T untreated
CTRL treated
SNCA A53T treated
F
Radial glia
Activated astrocytes #2
Neural progenitors
Resting astrocytes
Activated astrocytes #1
IMMP2L
CHI3L2
S100A6
KAZN
ID4
NAMPT
PRDX6
CCL2
SLC43A2
IFITM3
GFAP
AQP4
ITM2C
GRIK1
TTYH1
AC096570.1
C21orf62
PRKG1
KCNH7
DCLK1
DLX6-AS1
NRXN3
SOX2-OT
PDE4D
DCX
PEG10
IL1RAPL1
SOX4
KIAA1211
NXPH1
CXCL11
ISG15
CCL5
MT2A
CXCL10
IFI27
IFIT2
IFIT3
IFI6
HLA-B
HIST1H4C
CENPF
TOP2A
HMGB2
NUSAP1
TUBA1B
MKI67
DIAPH3
PCLAF
ASPM
Expression
2
1
0
−1

Fig. 3

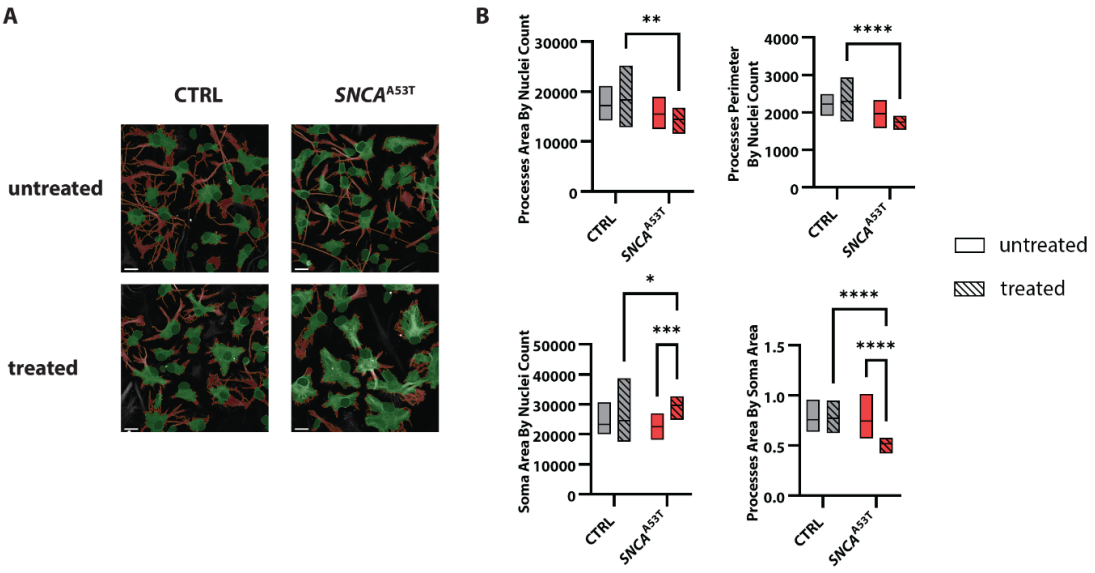
A
CTRL
SNCA A53T
untreated
treated
B
Processes Area By Nuclei Count
Processes Perimeter By Nuclei Count
Soma Area By Nuclei Count
Processes Area By Soma Area
CTRL
SNCA A53T
untreated
treated

Fig. 4

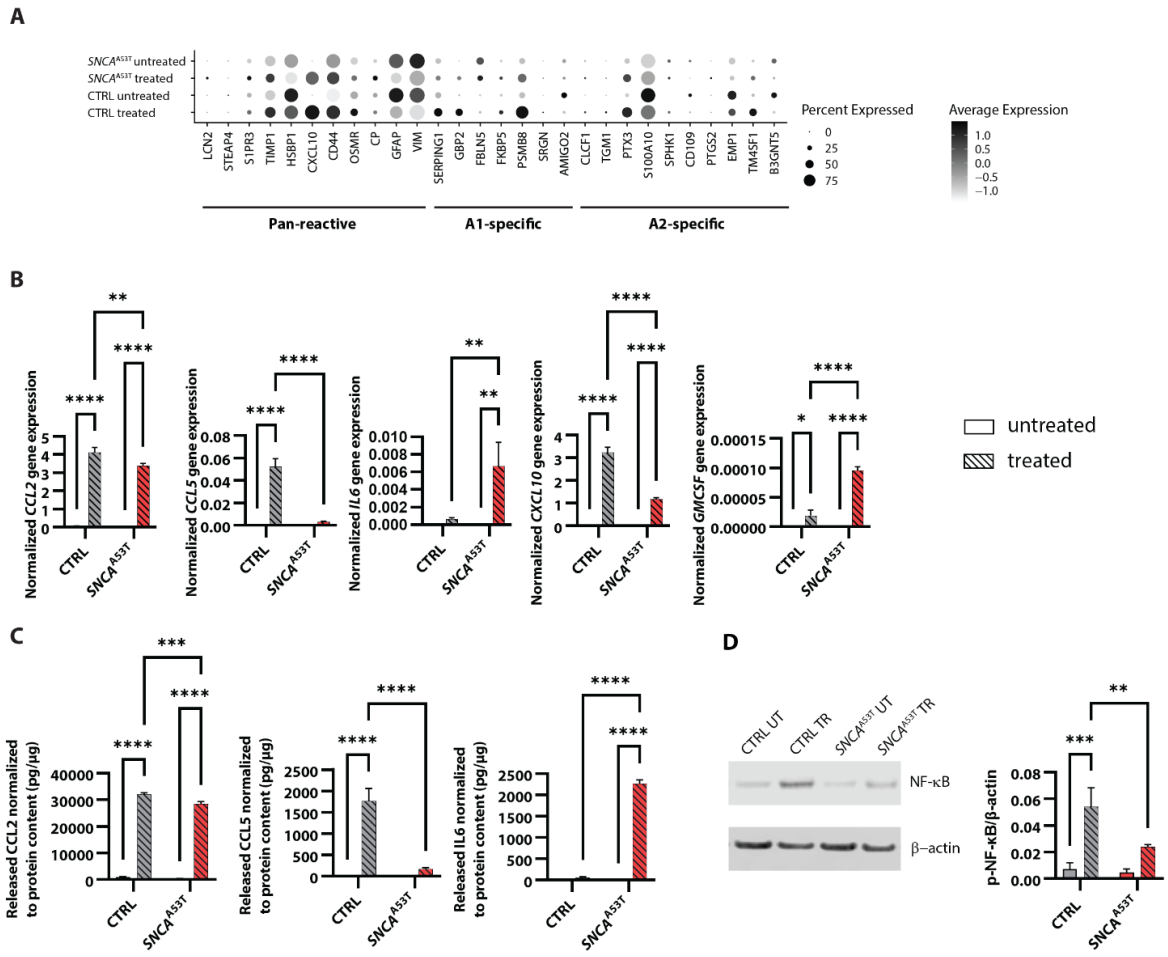
A
SNCA A53T untreated
SNCA A53T treated
CTRL untreated
CTRL treated
LCN2 STEAP4 S1PR3 TIMP1 HSBP1 CXCL10 CD44 OSMR CP GFAP VIM SERPING1 GBP2 FBLN5 FKBP5 PSMB8 SRGN AMIGO2 CLCF1 TGM1 PTX3 S100A10 SPHK1 CD109 PTGS2 EMP1 TM4SF1 B3GNT5
Pan-reactive
A1-specific
A2-specific
Percent Expressed
0 25 50 75
Average Expression
1.0 0.5 0.0 −0.5 −1.0
B
Normalized CCL2 gene expression
Normalized CCL5 gene expression
Normalized IL6 gene expression
Normalized CXCL10 gene expression
Normalized GMCSF gene expression
CTRL
SNCA A53T
untreated
treated
C
Released CCL2 normalized to protein content (pg/µg)
Released CCL5 normalized to protein content (pg/µg)
Released Il6 normalized to protein content (pg/µg)
D
CTRL UT
CTRL TR
SNCA A53T UT
SNCA A53T TR
NF-κB
β−actin
p-NF-κB/β-actin

Fig. 5

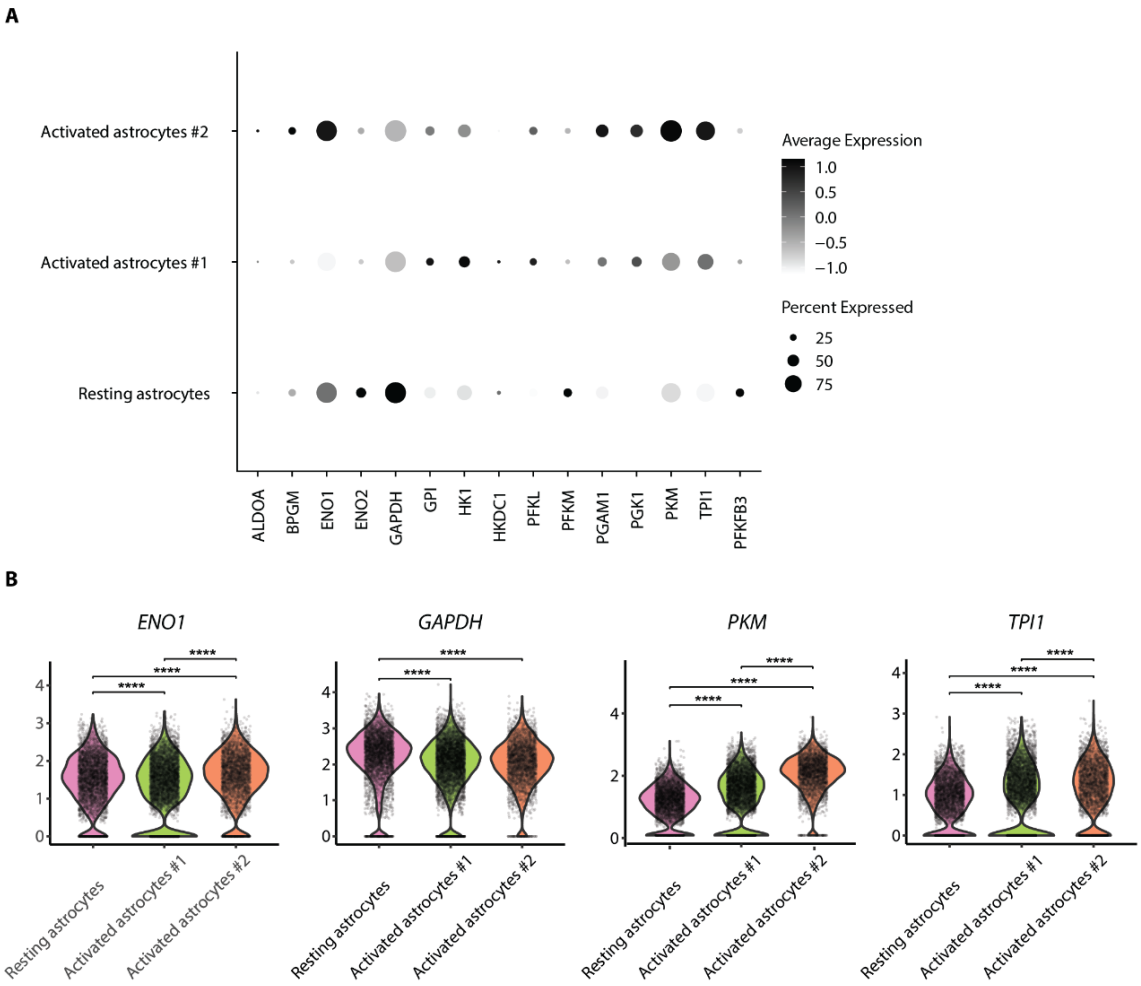
A
Activated astrocytes #2
Activated astrocytes #1
Resting astrocytes
ALDOA
BPGM
ENO1
ENO2
GAPDH
GPI
HK1
HKDC1
PFKL
PFKM
PGAM1
PGK1
PKM
TPI1
PFKFB3
Average Expression
1.0
0.5
0.0
−0.5
−1.0
Percent Expressed
25
50
75
B
ENO1
GAPDH
PKM
TPI1
****
Resting astrocytes
Activated astrocytes #1
Activated astrocytes #2

Fig. 6

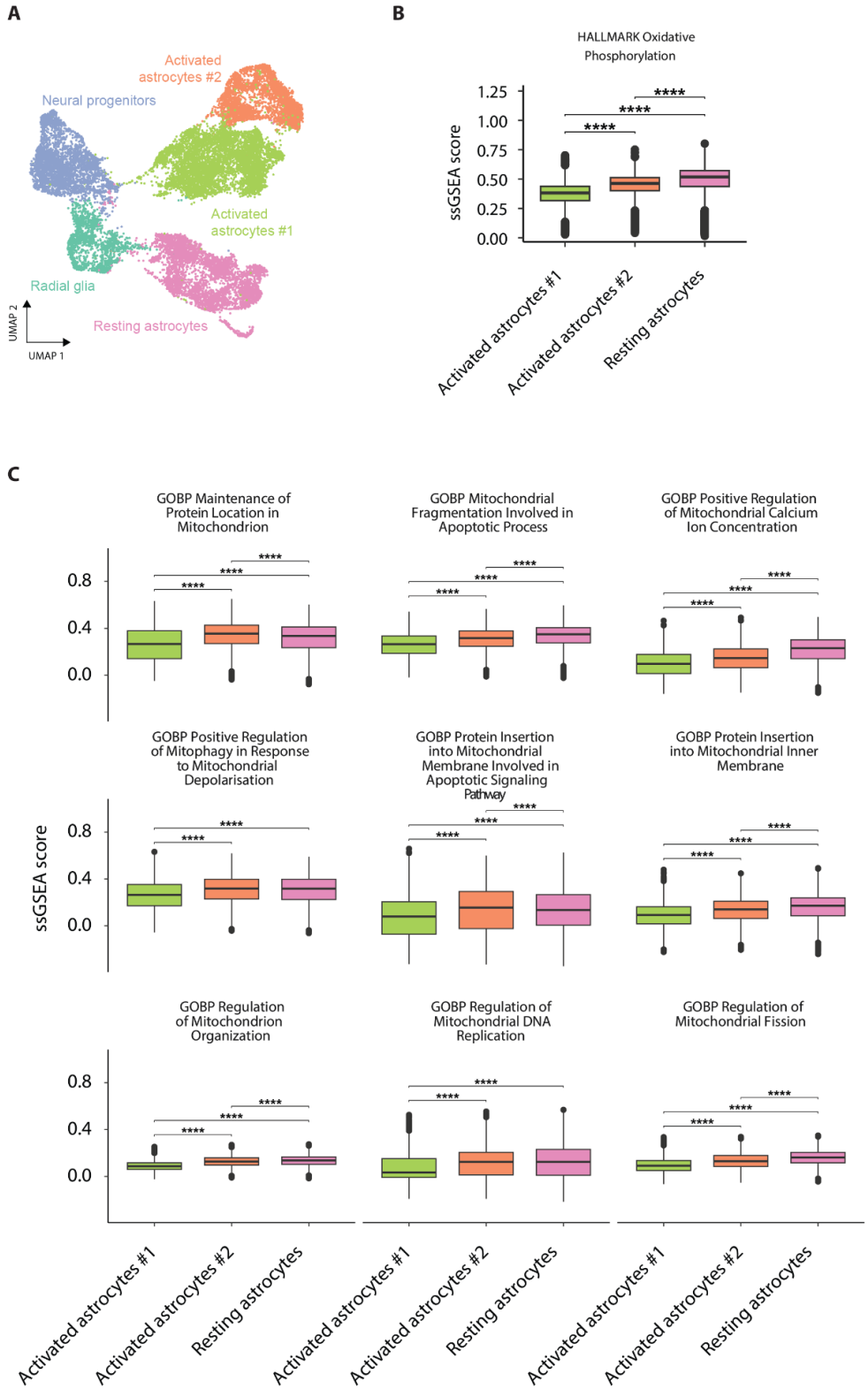
A
Activated astrocytes #2
Neural progenitors
Activated astrocytes #1
Radial glia
Resting astrocytes
UMAP 2
UMAP 1
B
HALLMARK Oxidative Phosphorylation
ssGSEA score
1.25
1.00
0.75
0.50
0.25
0.00
****
Activated astrocytes #1
Activated astrocytes #2
Resting astrocytes
C
GOBP Maintenance of Protein Location in Mitochondrion
GOBP Mitochondrial Fragmentation Involved in Apoptotic Process
GOBP Positive Regulation of Mitochondrial Calcium Ion Concentration
GOBP Positive Regulation of Mitophagy in Response to Mitochondrial Depolarisation
GOBP Protein Insertion into Mitochondrial Membrane Involved in Apoptotic Signaling Pathway
GOBP Protein Insertion into Mitochondrial Inner Membrane
GOBP Regulation of Mitochondrion Organization
GOBP Regulation of Mitochondrial DNA Replication
GOBP Regulation of Mitochondrial Fission
ssGSEA score
0.8
0.4
0.0
****
Activated astrocytes #1
Activated astrocytes #2
Resting astrocytes

Fig. 7

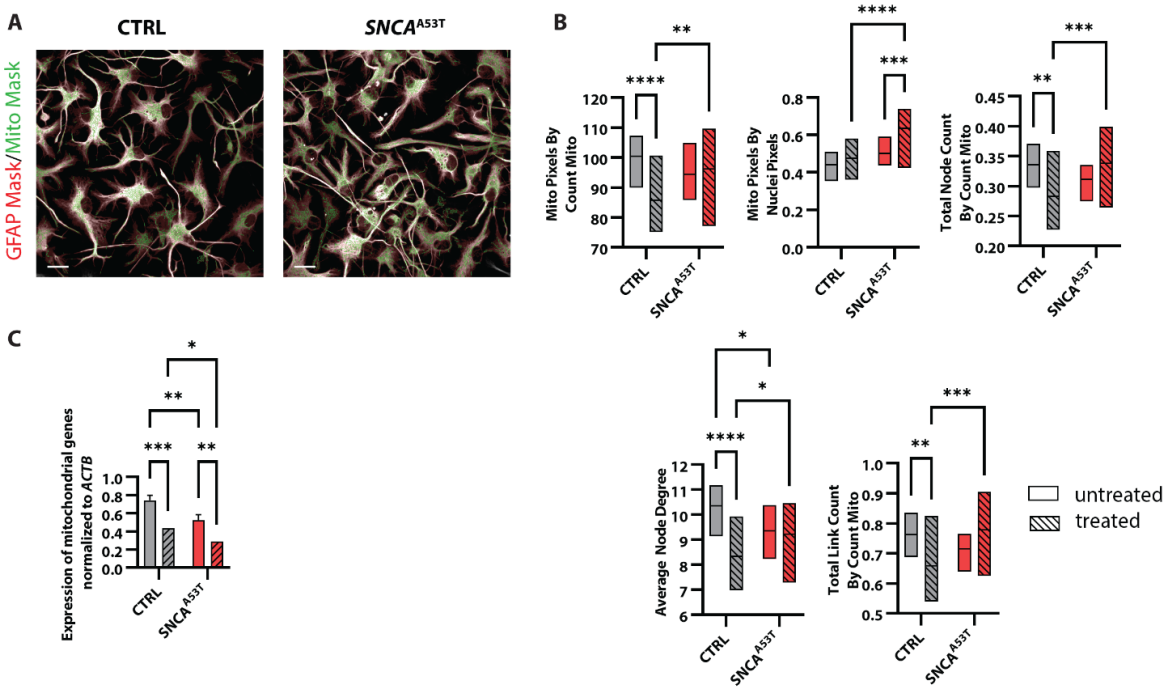
A
CTRL
SNCA A53T
GFAP Mask/Mito Mask
B
Mito Pixels By Count Mito
Mito Pixels By Nuclei Pixels
Total Node Count By Count Mito
Average Node Degree
Total Link Count By Count Mito
CTRL
SNCA A53T
C
Expression of mitochondrial genes normalized to ACTB
untreated
treated

Supplement

Supplementary Table 1. Primer sequences used in the qPCR approach

Gene of interest	FW primer	RV primer
SLC1A3	CTCACAGTCACCGCTGTCAT	CCTCATCAGAAGTTCCCCAGG
AQP4	TGGTGCCAGCATGAATCCC	CTCATAAAGGCCACCAGCGA
GFAP	GAGATCCGCACGCAGTATGA	TCTGCAAACTTGGAGCGGTA
S100B	AAGGAAGAGGATGTCTGAGCTG	AAGTCACATTCGCCGTCTCC
MAP2	CAGGTGGCGGACGTGTGAAAATTGAGAGTG	CACGCTGGATCTGCCTGGGGACTGTG
SNCA	AGAGGGTGTTCTCTATGTAGGCT	ACCCTTCCTCAGAAGGCATTT
ND1	GAGCAGTAGCCCAAACAATCTC	GGGTCATGATGGCAGGAGTAAT
ND4	ACCTACTGGGAGAACTCTCTGT	GGTGAGTGAGCCCCATTGTGTT
ND6	GGTCAGGGGTTGAGGTCTTG	ACTCTTTCACCCACAGCACC
CYTB	CTGATCCTCCAAATCACCACAG	GCGCCATTGGCGTGAAGGTA
COX1	GGAGCAGGAACAGGTTGAACAG	GTTGTGATGAAATTGATGGC
ATP6/8	CACAACACTAAAGGACGAACCT	GGGATGGCCATGGCTAGGTTTA

Figure S1. Karyotype analysis for the iPSC line harboring A53T α-synuclein. Whole genome view as depicted in the figure was obtained using Karyostat™ service (Thermofisher).

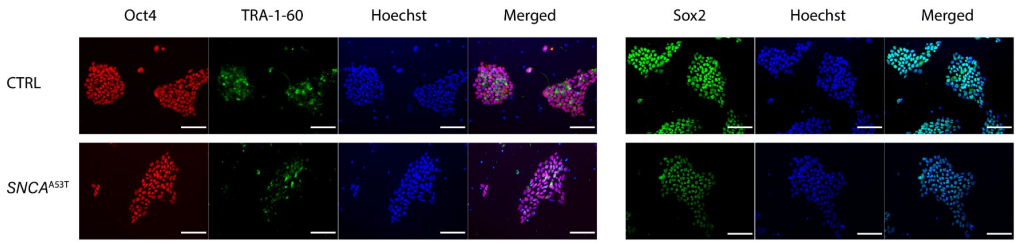

Figure S2. Analysis of pluripotency markers in iPSC lines by means of immunocytochemistry. Control iPSCs and a line harboring the A53T mutation in α-synuclein was analyzed for the abundance of Oct4, TRA-1-60 and Sox2. Scale bar: 100 µm.

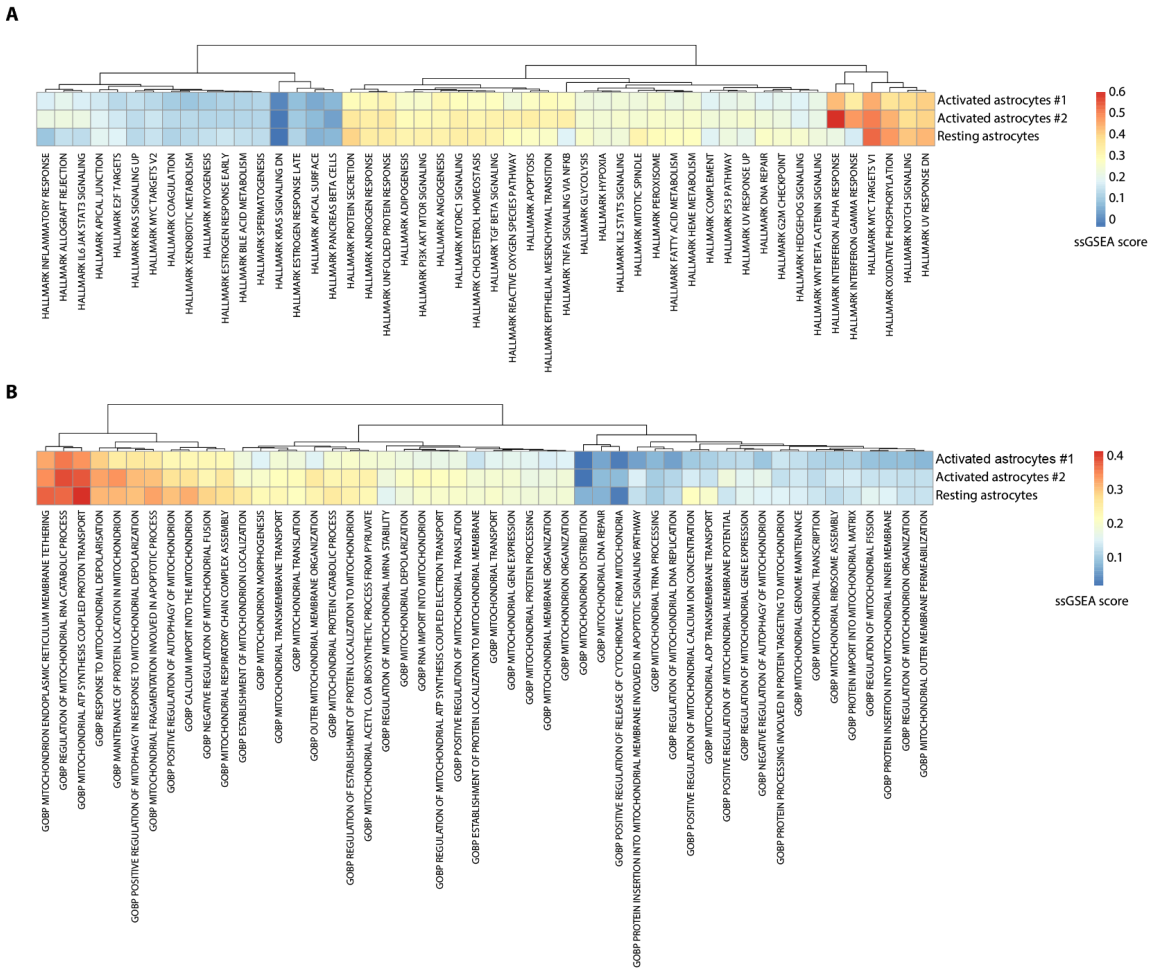

Figure S3. SsGSEA analysis for GOBP. A. The analysis performed on hallmark gene sets. **B.** Analysis for mitochondria-related pathways.

References

1. Alarcón TA, Presti-Silva SM, Simões APT, Ribeiro FM, Pires RGW. Molecular mechanisms underlying the neuroprotection of environmental enrichment in Parkinson's disease. Neural Regen Res. 2023;18:1450–6.

2. Simon DK, Tanner CM, Brundin P. Parkinson Disease Epidemiology, Pathology, Genetics, and Pathophysiology. Clin Geriatr Med. 2020;36:1–12.

3. Samii A, Nutt JG, Ransom BR. Parkinson's disease. Lancet Lond Engl. 2004;363:1783–93.

4. Kalia LV, Lang AE. Parkinson's disease. Lancet Lond Engl. 2015;386:896–912.

5. Ohnmacht J, May P, Sinkkonen L, Krüger R. Missing heritability in Parkinson's disease: the emerging role of non-coding genetic variation. J Neural Transm Vienna Austria 1996. 2020;127:729–48.

6. Brás IC, Outeiro TF. Alpha-Synuclein: Mechanisms of Release and Pathology Progression in Synucleinopathies. Cells. 2021;10:375.

7. Flagmeier P, Meisl G, Vendruscolo M, Knowles TPJ, Dobson CM, Buell AK, et al. Mutations associated with familial Parkinson's disease alter the initiation and amplification steps of α-synuclein aggregation. Proc Natl Acad Sci U S A. 2016;113:10328–33.

8. MDSGene [Internet]. [cited 2023 Mar 28]. Available from: https://www.mdsgene.org/

9. Polymeropoulos MH, Lavedan C, Leroy E, Ide SE, Dehejia A, Dutra A, et al. Mutation in the alpha-synuclein gene identified in families with Parkinson's disease. Science. 1997;276:2045–7.

10. Conway KA, Lee SJ, Rochet JC, Ding TT, Williamson RE, Lansbury PT. Acceleration of oligomerization, not fibrillization, is a shared property of both alpha-synuclein mutations linked to early-onset Parkinson's disease: implications for pathogenesis and therapy. Proc Natl Acad Sci U S A. 2000;97:571–6.

11. Stefanis L. α-Synuclein in Parkinson's disease. Cold Spring Harb Perspect Med. 2012;2:a009399.

12. Nakajo S, Tsukada K, Omata K, Nakamura Y, Nakaya K. A new brain-specific 14-kDa protein is a phosphoprotein. Its complete amino acid sequence and evidence for phosphorylation. Eur J Biochem. 1993;217:1057–63.

13. Weinreb PH, Zhen W, Poon AW, Conway KA, Lansbury PT. NACP, a protein implicated in Alzheimer's disease and learning, is natively unfolded. Biochemistry. 1996;35:13709–15.

14. Jakes R, Spillantini MG, Goedert M. Identification of two distinct synucleins from human brain. FEBS Lett. 1994;345:27–32.

15. Cheng F, Vivacqua G, Yu S. The role of α-synuclein in neurotransmission and synaptic

plasticity. J Chem Neuroanat. 2011;42:242–8.
16. Bendor JT, Logan TP, Edwards RH. The function of α-synuclein. Neuron. 2013;79:1044–66.
17. Brás IC, Xylaki M, Outeiro TF. Mechanisms of alpha-synuclein toxicity: An update and outlook. Prog Brain Res. 2020;252:91–129.
18. Malpartida AB, Williamson M, Narendra DP, Wade-Martins R, Ryan BJ. Mitochondrial Dysfunction and Mitophagy in Parkinson's Disease: From Mechanism to Therapy. Trends Biochem Sci. 2021;46:329–43.
19. Booth HDE, Hirst WD, Wade-Martins R. The Role of Astrocyte Dysfunction in Parkinson's Disease Pathogenesis. Trends Neurosci. 2017;40:358–70.
20. Miklossy J, Doudet DD, Schwab C, Yu S, McGeer EG, McGeer PL. Role of ICAM-1 in persisting inflammation in Parkinson disease and MPTP monkeys. Exp Neurol. 2006;197:275–83.
21. Koprich JB, Reske-Nielsen C, Mithal P, Isacson O. Neuroinflammation mediated by IL-1beta increases susceptibility of dopamine neurons to degeneration in an animal model of Parkinson's disease. J Neuroinflammation. 2008;5:8.
22. Zhang Y, Chen K, Sloan SA, Bennett ML, Scholze AR, O'Keeffe S, et al. An RNA-sequencing transcriptome and splicing database of glia, neurons, and vascular cells of the cerebral cortex. J Neurosci Off J Soc Neurosci. 2014;34:11929–47.
23. Zhang Y, Sloan SA, Clarke LE, Caneda C, Plaza CA, Blumenthal PD, et al. Purification and Characterization of Progenitor and Mature Human Astrocytes Reveals Transcriptional and Functional Differences with Mouse. Neuron. 2016;89:37–53.
24. Sharon R, Goldberg MS, Bar-Josef I, Betensky RA, Shen J, Selkoe DJ. alpha-Synuclein occurs in lipid-rich high molecular weight complexes, binds fatty acids, and shows homology to the fatty acid-binding proteins. Proc Natl Acad Sci U S A. 2001;98:9110–5.
25. Castagnet PI, Golovko MY, Barceló-Coblijn GC, Nussbaum RL, Murphy EJ. Fatty acid incorporation is decreased in astrocytes cultured from alpha-synuclein gene-ablated mice. J Neurochem. 2005;94:839–49.
26. Gu X-L, Long C-X, Sun L, Xie C, Lin X, Cai H. Astrocytic expression of Parkinson's disease-related A53T alpha-synuclein causes neurodegeneration in mice. Mol Brain. 2010;3:12.
27. Chandrasekaran A, Avci HX, Leist M, Kobolák J, Dinnyés A. Astrocyte Differentiation of Human Pluripotent Stem Cells: New Tools for Neurological Disorder Research. Front Cell Neurosci. 2016;10:215.
28. Kim HK, Ha TW, Lee MR. Single-Cell Transcriptome Analysis as a Promising Tool to Study

Pluripotent Stem Cell Reprogramming. Int J Mol Sci. 2021;22:5988.
29. Reinhardt P, Glatza M, Hemmer K, Tsytsyura Y, Thiel CS, Höing S, et al. Derivation and expansion using only small molecules of human neural progenitors for neurodegenerative disease modeling. PloS One. 2013;8:e59252.
30. Krencik R, Zhang S-C. Directed differentiation of functional astroglial subtypes from human pluripotent stem cells. Nat Protoc. 2011;6:1710–7.
31. Oksanen M, Petersen AJ, Naumenko N, Puttonen K, Lehtonen Š, Gubert Olivé M, et al. PSEN1 Mutant iPSC-Derived Model Reveals Severe Astrocyte Pathology in Alzheimer's Disease. Stem Cell Rep. 2017;9:1885–97.
32. Liddelow SA, Guttenplan KA, Clarke LE, Bennett FC, Bohlen CJ, Schirmer L, et al. Neurotoxic reactive astrocytes are induced by activated microglia. Nature. 2017;541:481–7.
33. Eng LF, Ghirnikar RS, Lee YL. Glial fibrillary acidic protein: GFAP-thirty-one years (1969-2000). Neurochem Res. 2000;25:1439–51.
34. Ikeshima-Kataoka H. Neuroimmunological Implications of AQP4 in Astrocytes. Int J Mol Sci. 2016;17:1306.
35. Boyes BE, Kim SU, Lee V, Sung SC. Immunohistochemical co-localization of S-100b and the glial fibrillary acidic protein in rat brain. Neuroscience. 1986;17:857–65.
36. Liang P, Zhang X, Zhang Y, Wu Y, Song Y, Wang X, et al. Neurotoxic A1 astrocytes promote neuronal ferroptosis via CXCL10/CXCR3 axis in epilepsy. Free Radic Biol Med. 2023;195:329–42.
37. Wang Y, Jin S, Sonobe Y, Cheng Y, Horiuchi H, Parajuli B, et al. Interleukin-1β induces blood-brain barrier disruption by downregulating Sonic hedgehog in astrocytes. PloS One. 2014;9:e110024.
38. Brown JP, Couillard-Després S, Cooper-Kuhn CM, Winkler J, Aigner L, Kuhn HG. Transient expression of doublecortin during adult neurogenesis. J Comp Neurol. 2003;467:1–10.
39. Penisson M, Ladewig J, Belvindrah R, Francis F. Genes and Mechanisms Involved in the Generation and Amplification of Basal Radial Glial Cells. Front Cell Neurosci. 2019;13:381.
40. Zhang X, Liu X, Zhu K, Zhang X, Li N, Sun T, et al. CD5L-associated gene analyses highlight the dysregulations, prognostic effects, immune associations, and drug-sensitivity predicative potentials of LCAT and CDC20 in hepatocellular carcinoma. Cancer Cell Int. 2022;22:393.
41. Kunová N, Havalová H, Ondrovičová G, Stojkovičová B, Bauer JA, Bauerová-Hlinková V, et al. Mitochondrial Processing Peptidases-Structure, Function and the Role in Human Diseases. Int J Mol Sci. 2022;23:1297.
42. Liao J, Zhang Y, Chen X, Zhang J. The Roles of Peroxiredoxin 6 in Brain Diseases. Mol

Neurobiol. 2021;58:4348–64.

43. Colombo E, Farina C. Astrocytes: Key Regulators of Neuroinflammation. Trends Immunol. 2016;37:608–20.

44. McColl SR, Mahalingam S, Staykova M, Tylaska LA, Fisher KE, Strick CA, et al. Expression of rat I-TAC/CXCL11/SCYA11 during central nervous system inflammation: comparison with other CXCR3 ligands. Lab Investig J Tech Methods Pathol. 2004;84:1418–29.

45. Pamies D, Sartori C, Schvartz D, González-Ruiz V, Pellerin L, Nunes C, et al. Neuroinflammatory Response to TNFα and IL1β Cytokines Is Accompanied by an Increase in Glycolysis in Human Astrocytes In Vitro. Int J Mol Sci. 2021;22:4065.

46. Robb JL, Hammad NA, Weightman Potter PG, Chilton JK, Beall C, Ellacott KLJ. The metabolic response to inflammation in astrocytes is regulated by nuclear factor-kappa B signaling. Glia. 2020;68:2246–63.

47. Delenclos M, Burgess JD, Lamprokostopoulou A, Outeiro TF, Vekrellis K, McLean PJ. Cellular models of alpha-synuclein toxicity and aggregation. J Neurochem. 2019;150:566–76.

48. Caiazza MC, Lang C, Wade-Martins R. What we can learn from iPSC-derived cellular models of Parkinson's disease. Prog Brain Res. 2020;252:3–25.

49. Sofroniew MV, Vinters HV. Astrocytes: biology and pathology. Acta Neuropathol (Berl). 2010;119:7–35.

50. Oberheim NA, Takano T, Han X, He W, Lin JHC, Wang F, et al. Uniquely hominid features of adult human astrocytes. J Neurosci Off J Soc Neurosci. 2009;29:3276–87.

51. Molofsky AV, Krencik R, Ullian EM, Tsai H, Deneen B, Richardson WD, et al. Astrocytes and disease: a neurodevelopmental perspective. Genes Dev. 2012;26:891–907.

52. DeGiosio RA, Grubisha MJ, MacDonald ML, McKinney BC, Camacho CJ, Sweet RA. More than a marker: potential pathogenic functions of MAP2. Front Mol Neurosci. 2022;15:974890.

53. Kouroupi G, Taoufik E, Vlachos IS, Tsioras K, Antoniou N, Papastefanaki F, et al. Defective synaptic connectivity and axonal neuropathology in a human iPSC-based model of familial Parkinson's disease. Proc Natl Acad Sci U S A. 2017;114:E3679–88.

54. Diao X, Wang F, Becerra-Calixto A, Soto C, Mukherjee A. Induced Pluripotent Stem Cell-Derived Dopaminergic Neurons from Familial Parkinson's Disease Patients Display α-Synuclein Pathology and Abnormal Mitochondrial Morphology. Cells. 2021;10:2402.

55. Zambon F, Cherubini M, Fernandes HJR, Lang C, Ryan BJ, Volpato V, et al. Cellular α-synuclein pathology is associated with bioenergetic dysfunction in Parkinson's iPSC-derived dopamine neurons. Hum Mol Genet. 2019;28:2001–13.

56. Oliveira LMA, Falomir-Lockhart LJ, Botelho MG, Lin K-H, Wales P, Koch JC, et al. Elevated

α-synuclein caused by SNCA gene triplication impairs neuronal differentiation and maturation in Parkinson's patient-derived induced pluripotent stem cells. Cell Death Dis. 2015;6:e1994.

57. Mulica P, Grünewald A, Pereira SL. Astrocyte-Neuron Metabolic Crosstalk in Neurodegeneration: A Mitochondrial Perspective. Front Endocrinol. 2021;12:668517.

58. Fan Y-Y, Huo J. A1/A2 astrocytes in central nervous system injuries and diseases: Angels or devils? Neurochem Int. 2021;148:105080.

59. Shinozaki Y, Shibata K, Yoshida K, Shigetomi E, Gachet C, Ikenaka K, et al. Transformation of Astrocytes to a Neuroprotective Phenotype by Microglia via P2Y1 Receptor Downregulation. Cell Rep. 2017;19:1151–64.

60. Choi SS, Lee HJ, Lim I, Satoh J, Kim SU. Human astrocytes: secretome profiles of cytokines and chemokines. PloS One. 2014;9:e92325.

61. Heilman PL, Song S, Miranda CJ, Meyer K, Srivastava AK, Knapp A, et al. HSPB1 mutations causing hereditary neuropathy in humans disrupt non-cell autonomous protection of motor neurons. Exp Neurol. 2017;297:101–9.

62. Tanuma N, Sakuma H, Sasaki A, Matsumoto Y. Chemokine expression by astrocytes plays a role in microglia/macrophage activation and subsequent neurodegeneration in secondary progressive multiple sclerosis. Acta Neuropathol (Berl). 2006;112:195–204.

63. Jha MK, Jo M, Kim J-H, Suk K. Microglia-Astrocyte Crosstalk: An Intimate Molecular Conversation. The Neuroscientist. SAGE Publications Inc STM; 2019;25:227–40.

64. Smajić S, Prada-Medina CA, Landoulsi Z, Ghelfi J, Delcambre S, Dietrich C, et al. Single-cell sequencing of human midbrain reveals glial activation and a Parkinson-specific neuronal state. Brain J Neurol. 2021;awab446.

65. Wang Y, Li L, Wu Y, Zhang S, Ju Q, Yang Y, et al. CD44 deficiency represses neuroinflammation and rescues dopaminergic neurons in a mouse model of Parkinson's disease. Pharmacol Res. 2022;177:106133.

66. Schreck R, Baeuerle PA. NF-kappa B as inducible transcriptional activator of the granulocyte-macrophage colony-stimulating factor gene. Mol Cell Biol. 1990;10:1281–6.

67. Kempuraj D, Thangavel R, Natteru PA, Selvakumar GP, Saeed D, Zahoor H, et al. Neuroinflammation Induces Neurodegeneration. J Neurol Neurosurg Spine. 2016;1:1003.

68. Liu T-W, Chen C-M, Chang K-H. Biomarker of Neuroinflammation in Parkinson's Disease. Int J Mol Sci. 2022;23:4148.

69. Woiciechowsky C, Schöning B, Stoltenburg-Didinger G, Stockhammer F, Volk H-D. Brain-IL-1 beta triggers astrogliosis through induction of IL-6: inhibition by propranolol and IL-10.

Med Sci Monit Int Med J Exp Clin Res. 2004;10:BR325-330.
70. Bhattacharya P, Budnick I, Singh M, Thiruppathi M, Alharshawi K, Elshabrawy H, et al. Dual Role of GM-CSF as a Pro-Inflammatory and a Regulatory Cytokine: Implications for Immune Therapy. J Interferon Cytokine Res Off J Int Soc Interferon Cytokine Res. 2015;35:585–99.
71. Mangano EN, Peters S, Litteljohn D, So R, Bethune C, Bobyn J, et al. Granulocyte macrophage-colony stimulating factor protects against substantia nigra dopaminergic cell loss in an environmental toxin model of Parkinson's disease. Neurobiol Dis. 2011;43:99–112.
72. Shabab T, Khanabdali R, Moghadamtousi SZ, Kadir HA, Mohan G. Neuroinflammation pathways: a general review. Int J Neurosci. 2017;127:624–33.
73. Chen L-F, Williams SA, Mu Y, Nakano H, Duerr JM, Buckbinder L, et al. NF-kappaB RelA phosphorylation regulates RelA acetylation. Mol Cell Biol. 2005;25:7966–75.
74. Le Douce J, Maugard M, Veran J, Matos M, Jégo P, Vigneron P-A, et al. Impairment of Glycolysis-Derived l-Serine Production in Astrocytes Contributes to Cognitive Deficits in Alzheimer's Disease. Cell Metab. 2020;31:503-517.e8.
75. Xiong X-Y, Tang Y, Yang Q-W. Metabolic changes favor the activity and heterogeneity of reactive astrocytes. Trends Endocrinol Metab. 2022;33:390–400.
76. Qiao G, Wu A, Chen X, Tian Y, Lin X. Enolase 1, a Moonlighting Protein, as a Potential Target for Cancer Treatment. Int J Biol Sci. 2021;17:3981–92.
77. Myers TD, Palladino MJ. Newly discovered roles of triosephosphate isomerase including functions within the nucleus. Mol Med. 2023;29:18.
78. Escartin C, Guillemaud O, Carrillo-de Sauvage M-A. Questions and (some) answers on reactive astrocytes. Glia. 2019;67:2221–47.
79. Zhou B, Zuo Y-X, Jiang R-T. Astrocyte morphology: Diversity, plasticity, and role in neurological diseases. CNS Neurosci Ther. 2019;25:665–73.
80. Tomimoto H, Akiguchi I, Wakita H, Suenaga T, Nakamura S, Kimura J. Regressive changes of astroglia in white matter lesions in cerebrovascular disease and Alzheimer's disease patients. Acta Neuropathol (Berl). 1997;94:146–52.
81. McAvoy K, Kawamata H. Glial mitochondrial function and dysfunction in health and neurodegeneration. Mol Cell Neurosci. 2019;101:103417.
82. Gokoolparsadh A, Fang Z, Braidy N, Lin P, Pardy CJ, Eapen V, et al. Transcriptional response to mitochondrial protease IMMP2L knockdown in human primary astrocytes. Biochem Biophys Res Commun. 2017;482:1252–8.
83. Lu B, Poirier C, Gaspar T, Gratzke C, Harrison W, Busija D, et al. A mutation in the inner mitochondrial membrane peptidase 2-like gene (Immp2l) affects mitochondrial function and

impairs fertility in mice. Biol Reprod. 2008;78:601–10.

84. Di Maio R, Barrett PJ, Hoffman EK, Barrett CW, Zharikov A, Borah A, et al. α-Synuclein binds to TOM20 and inhibits mitochondrial protein import in Parkinson's disease. Sci Transl Med. 2016;8:342ra78.

85. Devi L, Raghavendran V, Prabhu BM, Avadhani NG, Anandatheerthavarada HK. Mitochondrial import and accumulation of alpha-synuclein impair complex I in human dopaminergic neuronal cultures and Parkinson disease brain. J Biol Chem. 2008;283:9089–100.

86. Martinez JH, Alaimo A, Gorojod RM, Porte Alcon S, Fuentes F, Coluccio Leskow F, et al. Drp-1 dependent mitochondrial fragmentation and protective autophagy in dopaminergic SH-SY5Y cells overexpressing alpha-synuclein. Mol Cell Neurosci. 2018;88:107–17.

87. Nakamura K. α-Synuclein and mitochondria: partners in crime? Neurother J Am Soc Exp Neurother. 2013;10:391–9.

4. Discussion

PD poses a major challenge both for society as a whole and for the research community. Since high age is the primary risk factor for the disease development, in our aging population, we observe a continuous rise in PD cases [4]. Unfortunately, patients still await an effective cure as current therapies can only partially alleviate symptoms and are unable to halt disease progression [157]. The long-lasting pursuit for the discovery of disease-modifying drugs is hampered by PD complexity and its multifactorial nature. Although single gene mutations have been attributed to PD, the majority of cases are described as idiopathic [8]. Therefore, it is clear that we need to properly stratify patients and identify commonalities and differences in molecular mechanisms underlying the disease in each case. For that reason, PD modeling using iPSC-derived patient material could be utilized as a suitable tool to study the intricacy of the human system [158].

Another layer of complexity in studying PD pathogenesis is added by the multidirectional interactions between different cell types residing in the human brain. In particular, astrocytes, as essential supporters of neuronal functions, are proposed to play a key role in maintaining proper brain functions [159]. Consequently, studying astrocytes' role in PD may be fundamental for understanding the disease pathogenesis [160]. This could be achieved by utilizing genetic PD models which would help to explore driving factors for disease onset and progression [161].

Considering this, the research presented in the thesis summarizes the current knowledge about astrocyte-neuron crosstalk with special attention given to its role in neurodegeneration (Manuscript I). In the results section, we compared two differentiation protocols to identify the most relevant model for studying astrocytic functions (Manuscript II). By applying the suitable method, we generated iPSC-derived astrocytes harboring the A53T mutation in α-synuclein. After comparing them to healthy control astrocytes, we could determine perturbed molecular pathways, which might be important to consider in the context of PD pathogenesis (Manuscript III).

4.1 iPSC-derived astrocytes as a model to study PD

4.1.1 Relevance of iPSC-derived astrocytic models for PD research

Astrocytes are crucial in maintaining normal brain functions and contribute to CNS development [149]. In the latter, they act as important regulators of synapse development [162]. When the brain reaches maturity, astrocytes were shown to affect synaptic functions by the release of numerous gliotransmitters [163]. This discovery led to the “tripartite synapse” hypothesis, which suggests an active role of astrocytes in neurotransmission [164]. Besides their involvement in synaptic functions, astrocytes were demonstrated to affect blood flow in the brain and participate in neurovascular coupling [165]–[167]. Furthermore, astrocytes can influence the formation of the blood brain barrier and maintain the homeostasis of ions, fluids, pH and neurotransmitters [149]. Importantly, astrocytes can also support neuronal metabolic functions by providing lactate, which is utilized in the TCA cycle to supply energy for neurons [168].

Given the importance of the described interplay between astrocytes and neurons, astrocytes are now regarded as potential contributors to the pathology of PD [125]. As summarized in Manuscript I, defects in astrocytic metabolic pathways are frequently observed in the context of PD. Such impairments can profoundly affect astrocyte-neuron metabolic coupling and can be associated with PD pathogenesis. Moreover, dysfunctional astrocytes may be associated with PD pathology due to their significant contribution to inflammatory processes, oxidative stress, or α-synuclein-mediated toxicity [160]. In line with this, using genetic models of PD, it was demonstrated that mutations linked to early-onset disease could trigger astrocytic impairments, which further facilitate the demise of dopaminergic neurons [125].

Although the current knowledge about the astrocytic involvement in PD has advanced over the last years, we still lack a full understanding of the fine interplay between glial cells and neurons in the disease context. To explore perturbed mechanisms in more detail, one could employ novel tools such as iPSC lines, which offer numerous advantages over animal models. The biggest benefit of using iPSCs is an opportunity to differentiate them into any cell type of interest while preserving the patient’s genetic background [158]. This is particularly useful when studying the pathogenesis of idiopathic PD forms, in which the crosstalk of genetic and environmental factors still needs to be explored [169]. Genetic models of monogenic PD can also be examined using iPSC technology. When such

models are carefully compared with age- and gender-matched controls or cell lines with genetically corrected mutation, the impact of the studied mutations on the cellular processes can be assessed over time and at an endogenous level [158]. Furthermore, applying such models offers the possibility to test novel therapies efficiently. In contrast, testing drugs on animal models frequently proves to be inadequate due to pronounced differences in the biological processes between species [170]. The use of iPSC-derived models also brings us closer to the era of personalized medicine. Due to variations in the genetic background between patients, the applied therapies can cause numerous adverse effects [171]. Another challenge is a suboptimal efficacy of the designed treatment, which can be caused by genetic variations in patients [172]. This could be partially overcome by performing drug tests on a variety of iPSC lines, preferably derived from patients of various PD subsets, which would allow for matching the right treatment with individual patients [158]. Nonetheless, one should bear in mind the possible disadvantages of the system. iPSC models require meticulous quality checks to exclude lines carrying chromosomal aberrations [152]. As mentioned before, iPSC lines also have to be compared to the appropriate controls. When studying single gene mutations, it is advisable to include in the experimental set-up gene corrected lines which might prevent confounding the effects of the variant with the overall genetic background of the patient [152]. However, typically applied in such circumstances CRISPR-Cas9 method can produce off-targets which may further complicate the analysis [173]. Another challenge of the iPSC technology is linked to clonal variability. During the reprogramming of fibroblasts to iPSC, several colonies are chosen for further quality tests. Frequently, high variability is observed among the clones, partly due to the different integration sites of the vectors used to achieve reprogramming [169] – at least before the advent of reprogramming methods based on episomal vectors. Despite these potential limitations, iPSC modeling is considered one of the state-of-the-art methods that could help us achieve appropriate PD modeling, relevant for personalized medicine and discovery of efficient disease modifying treatments [158], [169].

In this context, in the Manuscript II, we explored two protocols to generate iPSC-derived astrocytes and assessed their relevance for disease modeling. While the Oksanen method is more suitable as a reliable tool to model PD, the Palm protocol could be more easily applied in an automated drug screening due to its shorter differentiation time. Furthermore, applying the Oksanen protocol in Manuscript III, we studied a genetic model of PD harboring the A53T mutation in α-synuclein. Importantly, in the iPSC-derived PD line, we were able to identify perturbed pathways, which could be further examined in the context of drug discovery. Yet, in light of the discussed challenges linked to utilizing iPSC-models it is important to mention limitations of our studies. Although we carefully assessed the

employed iPSC lines in Manuscript II and III to confirm the proper karyotypes and pluripotency status, we did not address the clonal variability. In both manuscripts, we employed only a limited number of cell lines which may be problematic when considering the genetic background variability between iPSC lines. Another major drawback of the study is the lack of a control line with corrected A53T α-synuclein mutation in Manuscript III. Initially, we used such a control provided by the biobank, however, a genotype assessment revealed that the isogenic line was not generated correctly. Consequently, we employed a line derived from an age and gender matched healthy control. Since genetic background could be an important confounding factor, the lack of isogenic control could challenge data interpretation.

4.1.2 Methods for the generation of iPSC-derived astrocytes

Astrocytic development is highly complex and still needs to be fully understood. In the human brain, the process commences with the gliogenic switch after the completed neurogenesis, with radial glia serving as a source for neurons and astrocytes [174]. The whole mechanism is tightly regulated by several intrinsic and extrinsic factors that control the activation of two key signaling pathways for astrocytic development, such as JAK/STAT and Notch [175], [176]. Astrocytic differentiation is prevented during neurogenesis by blocking the JAK/STAT pathway to allow for the sufficient generation of neurons. The control mechanism is driven by phosphatase SHP2 [177] and sequestration of the p300/CBP, which is important for activating JAK/STAT [178]. Furthermore, promoters of astrocytic signature genes are methylated, which prevents the binding of STAT3, the transcription factor involved in the JAK/STAT signaling [179]. The beginning of astrogenesis is marked by distinct changes in DNA methylation and histone acetylation associated with chromatin opening [176]. Acetylation is achieved by the acetyltransferase activity of p300/CBP, which is no longer sequestered by Ngn1 [180], [181]. Ngn1 is highly expressed during the preceding neurogenesis. However, at the onset of astrogenesis, its expression starts to be downregulated [181]. Due to the activity of p300/CBP the acetylation of histones is promoted at the binding sites of STAT3 within astrocytic gene promoters [180]. Decreased methylation of DNA necessary for opening the chromatin is linked to the activity of transcriptional factor NFIA as shown based on GFAP promoter [176], [182]. The described chromatin remodeling is initiated by extrinsic factors such as growth factor FGF2 and retinoic acid [183], [184]. The Notch pathway is another important player in controlling astrogenesis. The signaling is stimulated by the expression of Notch ligands by the newly generated neurons [185]. The mode of action of the pathway is based

on the decrease of DNA methylation pattern of the GFAP promoter through the activity of NF1A, one of the Notch targets [185]. Principally, Notch and JAK/STAT pathways cooperate to activate astrogenesis and regulate themselves. The Notch pathway can activate STAT3, which in turn is capable of inducing Notch signaling in the neighboring cells [176]. Moreover, JAK/STAT pathway can be regulated by the neuron-derived cytokines such as CT-1, LIF, CNTF and BMPs [176].

The described findings have been implemented in numerous protocols, which were developed to generate iPSC-derived astrocytes [186]. Yet, the abundance of developed methods presents a challenge when trying to identify a protocol that fits a particular research objective. Therefore, in Manuscript II, we compared two protocols used to obtain iPSC-derived astrocytes. The Oksanen protocol is based on the generation of neuroepithelial cells, which are further differentiated into glial progenitors in the presence of FGF2. As discussed, this growth factor potentiates cells for differentiation into astrocytes [183]. Interestingly, the Oksanen method mimics events during development, with neurogenesis proceeding with astrogenesis. As a result, the same method was used to generate astrocytes and neurons, with modifications introduced for final maturation [153], [187]. In contrast, the Palm protocol begins with neural stem cells, further differentiated using factors such as LIF and FGF2 [176].

To characterize iPSC-based models, the maturation status of the generated cells must be assessed. The aforementioned protocols differ in the use of factors that drive astrocytic maturation. While the Oksanen protocol applies CNTF and BMP4 to promote the JAK/STAT pathway [153], [176], the Palm method utilizes serum [154]. The latter method was shown to cause distinct changes in astrocytic morphology and activation status [188], [189]. By employing bulk RNA sequencing in Manuscript II, we could show that besides morphological differences, the Oksanen and Palm astrocytes present variations in their maturity. The Oksanen method generated more developed cells, which resembled to a higher extent human in vivo astrocytes. Therefore, we applied this protocol to model PD in astrocytes using A53T α-synuclein as described in Manuscript III. Further characterization of the generated models revealed that this method robustly produced astrocytes both in healthy control and mutant cell lines. Moreover, in this manuscript we further confirmed a high maturation status of Oksanen astrocytes as shown by the expression of genes associated with maturation.

4.2 Studying the effects of A53T α-synuclein on iPSC-derived astrocytes

4.2.1 *SNCA* mutations as a model to study PD

α-synuclein deposition is deemed not only a major hallmark of PD but also its fundamental contributor. The first evidence of the involvement of α-synuclein in PD pathology was observed in human postmortem brain tissue [73]. Further compelling evidence confirming α-synuclein related toxicity has been provided by the studies of cellular models, including over-expression of *SNCA* and treatments with α-synuclein oligomers or fibrils [190]. With the identification of genetic forms of PD associated with *SNCA* mutations, it became evident that genetic models could help to explore how α-synuclein contributes to the disease-onset and progression. Although transgenic mouse strains proved to be useful in modeling motor symptoms, variability in induced pathology is often observed [191]. Instead, iPSC models may be employed to unravel the contribution of *SNCA* mutations to PD development [192], [193]. Due to the primarily neuronal localization of α-synuclein, studies employing such models focused mainly on dopaminergic neurons [194].

Yet, astrocytes are also associated with PD pathology since glial deposits of α-synuclein were observed in IPD patients [195]. Furthermore, despite the low *SNCA* expression in astrocytes [189] the first transgenic mouse models expressing *SNCA* mutations revealed a selective expression of A53T α-synuclein in astrocytes, which led to paralysis accompanied by reactive astrogliosis and dopaminergic neuron death [148]. Yet, to our knowledge, no studies have explored the effects exerted by *SNCA* mutations on human iPSC-derived astrocytes. Therefore, in Manuscript III, we employed iPSC technology to examine the role of α-synuclein in patient-derived astrocytes. Our qPCR analysis revealed detectable levels of *SNCA* expression, although considerably lower than in neurons. Consequently, we concluded that we generated a suitable tool to study how *SNCA* mutations can influence astrocytic biology.

4.2.2 Astrocytic differentiation impairment

Surprisingly, multiple lines of evidence suggest a developmental component in PD despite its mainly neurodegenerative nature [196]. In particular, striking similarities in clinical symptoms have been observed for PD and autism spectrum disorder, a neurodevelopmental disease [197]. Furthermore, both conditions share the common mechanism of synaptic dysfunction, which was reported to occur already in the early phases of PD, before neuronal demise [198]. Further supporting the notion of PD having neurodevelopmental characteristics, it has been demonstrated that deletion of the *SNCA* gene can be associated with an impaired process of dopaminergic neurogenesis [199]. Similarly, a defect in neuronal differentiation was observed in iPSC-derived neurons harboring triplication of *SNCA* [200].

In agreement with the previously reported implications of α-synuclein in neuronal development, in Manuscript III, we detected changes in the composition of iPSC-derived astrocytic cultures between the PD line and healthy control. Specifically, our single-cell RNA sequencing analysis revealed a higher percentage of neuronal precursors and radial glia populations in the line harboring A53T mutation in α-synuclein. Moreover, we performed the analysis for single-cell entropy as an indicator of the differentiation potential. The assessment revealed lower capacity to differentiate in the activated PD astrocytes when compared with activated healthy control. Based on this observation, we concluded that α-synuclein dysfunction might affect both neurogenesis and astrogenesis.

4.2.3 Interplay of astrocytes and microglia under physiological and disease conditions

Microglia represent another important cell type for maintaining healthy brain functions. Their primary role constitutes an immune response classified as a component of innate immunity [201]. Furthermore, the role of microglia has also been implied in other cellular processes, such as synapse pruning and neurotransmission modulation, in which they cooperate with astrocytes [202]. Since both cell types are immune competent, the vital part of their communication is based on secreted cytokines and chemokines [201]. Such an interplay might have far-reaching consequences for brain homeostasis in the context of neurodegenerative diseases. The microglial response to pathogenic stimuli typically precedes astrocytic activation and directly contributes to the latter process [203]. Different

combinations of cytokines have been shown to elicit divergent astrocytic reactions, ranging from desirable tissue repair to neurotoxicity [204], [205]. Consequently, one may hypothesize that the fine interplay between astrocytes and microglia is involved in both the maintenance of brain homeostasis as well as disease onset and progression upon its dysregulation. Moreover, the described cascade of events has also been suggested to explain α-synuclein effects on innate immunity responses. The first studies demonstrated that α-synuclein might act as a damage-associated molecular pattern, leading to an upregulation of Toll-Like Receptors expression in microglia [206]. Astrocytic expression of most Toll-Like Receptors is considerably lower, which makes astrocytes dependent on the initial recognition of the stimulus by microglia [207]. Importantly, astrocyte-microglia crosstalk has also been shown to facilitate the clearance of α-synuclein fibrils, which further underlines the importance of the proper communication between these two cell types for PD pathogenesis [208].

Based on these findings, we decided to stimulate astrocytes with IL-1β and TNF-α cytokines to mimic microglia-induced inflammation. Indeed, these proteins have been shown previously to elicit astrocytic activation and the associated release of chemokines [209]. In Manuscript III, we treated both healthy control and PD patient iPSC-derived astrocytes and analyzed their activation profiles. As discussed in detail in the next chapters, our approach enabled us to identify changes in the activation states, which could be particularly relevant in the disease context, when multiple cell types interact and can jointly contribute to the disease.

4.2.4 The role of A53T α-synuclein in modulating astrocytic immune responses

Astrocyte reactivity, also known as reactive astrogliosis, is defined as a variety of morphological, molecular, and functional changes in astrocytes in response to the pathological stimulus [210]. Despite extensive research, the process is highly complex and poorly understood [211]. Although the major hallmark of reactive astrogliosis is considered to be an upregulation in GFAP levels [212], its widespread application has been lately called into question due to the regional variety of astrocytes [211]. The intricacy of the astrocytic responses further convolutes during their reactivity. Recently, it has been proposed that the diversity of the reactive astrocytes could be attributed to subtypes with more permanent reactive characteristics as opposed to states identified by transient

changes that could be reversible. Among the defined subtypes are proliferative astrocytes contributing to the border formation around the damaged tissue and non-proliferative cells showing a variable degree of molecular and morphological changes [213].

As discussed in the previous chapter, we modeled cytokine-induced astrocytic reactivity in Manuscript III using IL-1β and TNF-α. Surprisingly, our single-cell sequencing analysis showed major differences in astrocytic responses to the treatment as shown by separate clustering of reactive PD astrocytes and reactive healthy control cells. Furthermore, non-reactive astrocytes clustered independently from the treated cells, confirming that we generated reactive astrocytes defined as cells with distinct molecular changes [210].

Due to the complexity of astrocytic reactivity, numerous attempts have been made to describe astrocytic subtypes or states using expression profiles of particular genes. The identification of such patterns would enable easier identification of reactive types in the disease context. One of the most commonly used genetic signatures is the differentiation between A1 and A2 profiles [213]. Whereas A1 astrocytes have been associated with neurotoxic effects, A2 characteristics have been attributed to neuroprotection [214]. In Manuscript III, we analyzed the expression of genes linked to the A1 and A2 profiles and the expression of pan reactive markers. The analysis revealed the downregulation of several pan reactive, A1 and A2 markers in the reactive A53T α-synuclein astrocytes when compared to the activated healthy control. These results could suggest that overall PD astrocytes presented with a lower activation status.

To further explore the reactivity of astrocytes harboring A53T mutation in α-synuclein, we explored the activity of the NF-κB pathway. This signaling cascade is crucial for the understanding of glial cells activation and the related pathology of neurodegenerative diseases [215]. NF-κB is a protein complex consisting of several components in different configurations. In the glial cells, it typically exists as a homodimer of p65 (RelA) subunits or heterodimer of p50 and p65 [216]. The latter form is the most studied one, in which the DNA binding property has been assigned to p50 and the ability to activate transcription has been associated with p65 [215]. Before the activation, NF-κB is maintained in the cytoplasm by binding to its inhibitors known as IκB proteins. The pathway can be activated by numerous signals, e.g. TNF-α and IL-1β, which trigger the degradation of NF-κB inhibitors [217]. Consequently, the NF-κB complex can translocate to the nucleus, where it binds to the DNA at the NF-κB sites [218]. It is generally accepted that the NF-κB pathway is one of the most important regulators of inflammation since it modulates the expression of genes encoding the numerous pro-inflammatory cytokines and chemokines, including

IL-6, CXCL10, CCL5, CCL2 and GM-CSF [219], [220]. As mentioned before, in Manuscript III we used IL-1β and TNF-α to trigger astrocytic reactivity. Since these proteins activate the NF-κB pathway, we analyzed the expression of several target genes encoding the cytokines and chemokines. For *CCL2*, *CCL5* and *CXCL10* genes we observed a decrease in the expression in the activated PD astrocytes compared with reactive healthy control astrocytes. Only in the cases of *IL6* and *GMCSF* we observed an upregulation in the gene expression in the reactive PD astrocytes. IL-6 was frequently implicated in PD pathogenesis since its elevated levels have been detected in the CSF, blood serum as well as striatum of PD patients [221]. The fact that the expression of *IL6* and *GMCSF* was upregulated might suggest that it was also regulated by the activity of other pathways independent from NF-κB as shown for the *IL6* gene [222].

Since for most of the cytokines and marker genes for A1 and A2 reactive states we observed a decrease in their expression in activated PD astrocytes, we hypothesized that patient astrocytes have an impaired capacity to respond to the inflammatory stimulus. The analysis of the phosphorylation status of NF-κB p65 at serine 536 further supported this notion. Phosphorylation at this site was shown to be involved in the translocation of the cytosolic p65 to the nucleus. Furthermore, once p65 is already in the nucleus, the modification promotes DNA binding [223]. Therefore, we examined the levels of phosphorylated p65 levels as a readout of the NF-κB pathway activation. This analysis showed reduced pathway activity in the activated PD astrocytes compared to reactive healthy control cells. Moreover, the increase in the phosphorylated p65 levels in patient astrocytes was insignificant upon treatment. Therefore, we concluded that PD astrocytes indeed fail to respond efficiently to inflammatory stimuli.

Astrocytes are known for their dependence on glycolysis to produce energy. Interestingly, the glycolytic pathway has also been proposed as an important astrogliosis modulator [224]. Several reports have demonstrated that reactive responses of astrocytes and glycolytic metabolism are strictly interdependent since the concurrent increase in both processes was observed [225], [226]. Furthermore, efficient glycolysis seems to contribute directly to astrogliosis due to the fact that attenuating this metabolic pathway led to the decline in the cytokine production [225]. Considering it all, we analyzed the expression of the main glycolytic genes using our single-cell RNA sequencing data. Importantly, we confirmed that the majority of cells in both cell lines expressed the *PKM* gene, which encodes the brain isoform of pyruvate kinase [227]. This enzyme is responsible for a rate-limiting reaction, converting the phosphoenolpyruvate to pyruvate and ATP [224]. Interestingly, the reactive PD astrocytes showed a lower expression of *PKM* when

compared with the activated healthy control, which could lead to the decreased glycolytic activity. The same trend was observed for other glycolytic genes with high expression in our dataset, such as *ENO1* and *TPI*, while *GAPDH* showed no significant differences in the expression. In relation to the mentioned interplay between glycolysis and astrocytic reactivity [225], we concluded that the reduced capability of PD astrocytes to react to inflammatory stimuli could potentially be caused by a lower efficiency of the glycolytic pathway. Nevertheless, more experiments are needed to confirm the impairment in glycolysis.

Human astrocytes are characterized by a very complex and distinct morphology, possessing multiple branches known as astrocytic processes [228]. During astrogliosis, the cells undergo numerous morphological changes, such as cellular hypertrophy, defined as the expansion of the number and length of processes and the increase in soma size [214], [228]. However, other modifications have also been described in the literature, including swollen cell bodies and truncated astrocytic processes in AD patients [229]. Similarly, in our Manuscript III we observed that activated PD astrocytes reduce the area of their process while increasing the size of the cell body. This further suggests that patient astrocytes seem to have a major functional impairment along the dysfunctional responses to the applied treatment.

The question remains how the A53T α-synuclein mutation leads to the putative glycolytic impairment and ultimately a decrease in the astrocytic reactivity in our cultures. It has been shown that α-synuclein interaction with the PKM enzyme in microglia increases glycolytic activity [230]. However, additional biochemical validation will be required to explore the interplay between α-synuclein and pyruvate kinase in astrocytes. Importantly, there is accumulating evidence suggesting the direct role of α-synuclein in regulating gene expression [231], which could serve as a potential explanation for our findings.

4.2.5 α-synuclein effects on mitochondrial biology

Mitochondria are highly complex organelles that are surrounded by two membranes known as outer and inner membranes. Inside these structures, there is a compartment called a mitochondrial matrix containing mitochondrial DNA [232]. Mitochondria are pivotal for cellular physiology since they are involved in a myriad of functions. The primary role attributed to them is the generation of ATP in the process of oxidative phosphorylation carried out by the mitochondrial respiratory chain complexes [233]. However, mitochondria

also contribute to other metabolic pathways such as fatty acid β-oxidation, metabolism of amino acids, cofactors, heme and Fe-S clusters [232]. Furthermore, the organelles are also vital for calcium homeostasis and cell death [234].

As mentioned before, astrocytes rely mostly on glycolytic pathways as a source of energy. Interestingly, it has been shown for astrocytes that complex I of the mitochondrial respiratory chain is frequently uncoupled from the supercomplexes. Consequently, their respiration efficiency is relatively low when compared to neurons [235]. Nevertheless, it has been shown that other mitochondrial functions are critical for astrocytic physiology. Furthermore, there is a strong link between mitochondrial dysfunction in astrocytes and neurodegeneration [236] emphasizing the need for further research on the topic. Multiple lines of evidence suggest the α-synuclein-related pathology of mitochondria [237]. However, our knowledge about this relation in astrocytes still needs to be improved [238]. Still, the first studies suggested that α-synuclein might profoundly affect mitochondrial functions [142].

Taking all of this into account, in Manuscript III, we assessed mitochondrial pathways based on our single-cell RNA sequencing data. The first indication of potential mitochondrial dysfunction came from the analysis of the top differentially expressed genes. In the cluster composed of mainly reactive PD astrocytes and named Activated astrocytes #1 we identified *IMMP2L,* which encodes the subunit 2 of the inner mitochondrial membrane peptidase (IMP) [239]. IMP is responsible for the processing of several precursor proteins destined to be located in the mitochondrial intermembrane space [240]. This finding suggested a mitochondrial component of pathology in the studied PD astrocytes. For this reason, we performed gene set enrichment analysis to study the mitochondrial pathways in detail. This type of evaluation enables us to examine whole groups of genes linked to a certain pathway and, consequently, to draw less biased conclusions when compared with data derived from the single gene analyses [241]. The analysis identified in the cluster of Activated astrocytes #1 lower enrichment of several mitochondrial pathways including protein localization to mitochondria, protein insertion into the mitochondrial inner membrane, and regulation of mitochondrial organization. Furthermore, among the differentially enriched processes we identified mitochondria fragmentation related to apoptosis, regulation of mitochondrial calcium homeostasis, mitophagy, fission and mitochondrial DNA replication. This finding indicated potential damage in the analyzed organelles, so we performed additional validation for the initial data. After assessing mitochondria morphology using high content imaging, we could observe an increased size of the mitochondria and higher overall mitochondrial mass. The

first result could be connected to the reduced fission as our gene set enrichment analysis also suggested an impairment in this process. The second finding could imply the ongoing compensation process in response to mitochondrial damage. Interestingly, it has previously been reported in the literature that α-synuclein can affect most of the processes which were perturbed in our model [242], [243]. Regarding the mode of action of α-synuclein, it has been proposed that the protein can be translocated to the mitochondria and ultimately affect their functions [117]. Moreover, α-synuclein has also been shown to affect the expression of PGC-1α by binding directly to its promoter [120]. Since PGC-1α is a key regulator of mitochondrial biogenesis [244] such an interaction can have important implications for mitochondrial functions [120]. In the context of our research, additional experiments are required to confirm mitochondrial dysfunction and explore the pathological mechanisms contributing to the observed impairments.

5. Outlook

In my thesis, I presented the findings related to the effects of A53T α-synuclein on human iPSC-derived astrocytes. To ensure the usability and reproducibility of our research, we extensively compared two protocols that can be used for the generation of iPSC-derived astrocytes. After choosing the most appropriate model, we performed single-cell RNA sequencing on the patient's astrocytes and healthy control cells, both at baseline and inflammatory conditions. This approach revealed that the astrocytes harboring A53T mutation in α-synuclein are impaired in their immune responses which the defects in the glycolysis could cause. Furthermore, we observed profound changes in several mitochondrial pathways in PD astrocytes under inflammatory conditions, suggesting additional dysfunction in mitochondria.

In the future, more work has to be done to confirm and explain the initial findings presented in this thesis. While we showed the first data suggesting the glycolytic impairment in PD astrocytes, metabolomics-based approaches need to be taken to validate the data. The same holds true for our reports on putative mitochondrial dysfunction. Further experiments should be conducted to investigate their pathology, including measuring membrane potential, assessing mitophagy and mitochondrial calcium concentrations.

Significantly, the detected phenotypes should be correlated more carefully with the α-synuclein toxicity. Since α-synuclein can exert its pathological functions when localized either in the nucleus or in mitochondria, it would be advisable to study its localization in our model. This could be achieved by performing immunocytochemistry and biochemically in the cellular fractionations' experiments. Furthermore, a detailed analysis of α-synuclein levels should be done. So far, numerous antibodies have been published which can be applied to measure the levels of soluble and aggregated α-synuclein. Such studies can be performed using Western Blot and ELISA, however, additional validation using immunocytochemistry methods should be applied to confirm the α-synuclein detection, specifically in astrocytes.

An important aspect of astrocytic physiology is their supporting role in neuronal functions. Therefore, it would be of major significance to explore how the generated PD astrocytes affect the physiology of dopaminergic neurons. To meet this aim, one could use the conditioned medium from astrocytic cultures to apply it on the neurons. Another possibility

could be the co-culture system of astrocytes and neurons. Using these approaches, we could further explore the mechanisms behind the astrocytic contribution to Parkinson's disease onset and progression.

6. References

[1] L. M. L. de Lau and M. M. B. Breteler, “Epidemiology of Parkinson’s disease,” *Lancet Neurol.*, vol. 5, no. 6, pp. 525–535, Jun. 2006, doi: 10.1016/S1474-4422(06)70471-9.

[2] B. S. Connolly and A. E. Lang, “Pharmacological treatment of Parkinson disease: a review,” *JAMA*, vol. 311, no. 16, pp. 1670–1683, Apr. 2014, doi: 10.1001/jama.2014.3654.

[3] O.-B. Tysnes and A. Storstein, “Epidemiology of Parkinson’s disease,” *J. Neural Transm.*, vol. 124, no. 8, pp. 901–905, Aug. 2017, doi: 10.1007/s00702-017-1686-y.

[4] D. K. Simon, C. M. Tanner, and P. Brundin, “Parkinson Disease Epidemiology, Pathology, Genetics, and Pathophysiology,” *Clin. Geriatr. Med.*, vol. 36, no. 1, pp. 1–12, Feb. 2020, doi: 10.1016/j.cger.2019.08.002.

[5] S. Cerri, L. Mus, and F. Blandini, “Parkinson’s Disease in Women and Men: What’s the Difference?,” *J. Park. Dis.*, vol. 9, no. 3, pp. 501–515, 2019, doi: 10.3233/JPD-191683.

[6] M. Picillo, A. Nicoletti, V. Fetoni, B. Garavaglia, P. Barone, and M. T. Pellecchia, “The relevance of gender in Parkinson’s disease: a review,” *J. Neurol.*, vol. 264, no. 8, pp. 1583–1607, Aug. 2017, doi: 10.1007/s00415-016-8384-9.

[7] A. Samii, J. G. Nutt, and B. R. Ransom, “Parkinson’s disease,” *Lancet Lond. Engl.*, vol. 363, no. 9423, pp. 1783–1793, May 2004, doi: 10.1016/S0140-6736(04)16305-8.

[8] P. M. A. Antony, N. J. Diederich, R. Krüger, and R. Balling, “The hallmarks of Parkinson’s disease,” *FEBS J.*, vol. 280, no. 23, pp. 5981–5993, 2013, doi: 10.1111/febs.12335.

[9] A. Lee and R. M. Gilbert, “Epidemiology of Parkinson Disease,” *Neurol. Clin.*, vol. 34, no. 4, pp. 955–965, Nov. 2016, doi: 10.1016/j.ncl.2016.06.012.

[10] E. Tolosa, G. Wenning, and W. Poewe, “The diagnosis of Parkinson’s disease,” *Lancet Neurol.*, vol. 5, no. 1, pp. 75–86, Jan. 2006, doi: 10.1016/S1474-4422(05)70285-4.

[11] R. B. Postuma *et al.*, “MDS clinical diagnostic criteria for Parkinson’s disease,” *Mov. Disord. Off. J. Mov. Disord. Soc.*, vol. 30, no. 12, pp. 1591–1601, Oct. 2015, doi: 10.1002/mds.26424.

[12] R. Balestrino and A. H. V. Schapira, “Parkinson disease,” *Eur. J. Neurol.*, vol. 27, no. 1, pp. 27–42, Jan. 2020, doi: 10.1111/ene.14108.

[13] S. G. Reich and J. M. Savitt, “Parkinson’s Disease,” *Med. Clin. North Am.*, vol. 103, no. 2, pp. 337–350, Mar. 2019, doi: 10.1016/j.mcna.2018.10.014.

[14] B. R. Bloem, M. S. Okun, and C. Klein, “Parkinson’s disease,” *Lancet Lond. Engl.*, vol. 397, no. 10291, pp. 2284–2303, Jun. 2021, doi: 10.1016/S0140-6736(21)00218-X.

[15] J. Ohnmacht, P. May, L. Sinkkonen, and R. Krüger, “Missing heritability in Parkinson’s disease: the emerging role of non-coding genetic variation,” *J. Neural Transm. Vienna Austria 1996*, vol. 127, no. 5, pp. 729–748, May 2020, doi: 10.1007/s00702-020-02184-0.

[16] P. Kolber and R. Krüger, “Gene-environment interaction and Mendelian randomisation,” *Rev. Neurol. (Paris)*, vol. 175, no. 10, pp. 597–603, Dec. 2019, doi: 10.1016/j.neurol.2019.04.010.

[17] K. R. Kumar, A. Djarmati-Westenberger, and A. Grünewald, “Genetics of Parkinson’s disease,” *Semin. Neurol.*, vol. 31, no. 5, pp. 433–440, Nov. 2011, doi: 10.1055/s-0031-1299782.

[18] D. Guadagnolo, M. Piane, M. R. Torrisi, A. Pizzuti, and S. Petrucci, “Genotype-Phenotype Correlations in Monogenic Parkinson Disease: A Review on Clinical and Molecular Findings,” *Front. Neurol.*, vol. 12, p. 648588, 2021, doi: 10.3389/fneur.2021.648588.

[19] C. Klein and A. Westenberger, “Genetics of Parkinson’s Disease,” *Cold Spring Harb. Perspect. Med.*, vol. 2, no. 1, p. a008888, Jan. 2012, doi: 10.1101/cshperspect.a008888.

[20] A. Ascherio and M. A. Schwarzschild, “The epidemiology of Parkinson’s disease: risk factors and prevention,” *Lancet Neurol.*, vol. 15, no. 12, pp. 1257–1272, Nov. 2016, doi: 10.1016/S1474-4422(16)30230-7.

[21] D. W. Dickson, “Neuropathology of Parkinson disease,” *Parkinsonism Relat. Disord.*, vol. 46 Suppl 1, pp. S30–S33, Jan. 2018, doi: 10.1016/j.parkreldis.2017.07.033.

[22] L. V. Kalia and A. E. Lang, “Parkinson’s disease,” *Lancet Lond. Engl.*, vol. 386, no. 9996, pp. 896–912, Aug. 2015, doi: 10.1016/S0140-6736(14)61393-3.

[23] M. A. Thenganatt and J. Jankovic, “Parkinson disease subtypes,” *JAMA Neurol.*, vol. 71, no. 4, pp. 499–504, Apr. 2014, doi: 10.1001/jamaneurol.2013.6233.

[24] M. G. Spillantini, A. Divane, and M. Goedert, “Assignment of human alpha-synuclein (SNCA) and beta-synuclein (SNCB) genes to chromosomes 4q21 and 5q35,” *Genomics*, vol. 27, no. 2, pp. 379–381, May 1995, doi: 10.1006/geno.1995.1063.

[25] S. Nakajo, K. Tsukada, K. Omata, Y. Nakamura, and K. Nakaya, “A new brain-specific 14-kDa protein is a phosphoprotein. Its complete amino acid sequence and evidence for phosphorylation,” *Eur. J. Biochem.*, vol. 217, no. 3, pp. 1057–1063, Nov. 1993, doi: 10.1111/j.1432-1033.1993.tb18337.x.

[26] Y. Shibasaki, D. A. Baillie, D. St Clair, and A. J. Brookes, “High-resolution mapping of SNCA encoding alpha-synuclein, the non-A beta component of Alzheimer’s disease amyloid precursor, to human chromosome 4q21.3-->q22 by fluorescence in situ hybridization,” *Cytogenet. Cell Genet.*, vol. 71, no. 1, pp. 54–55, 1995, doi:

10.1159/000134061.

[27] A. Iwai *et al.*, “The precursor protein of non-A beta component of Alzheimer’s disease amyloid is a presynaptic protein of the central nervous system,” *Neuron*, vol. 14, no. 2, pp. 467–475, Feb. 1995, doi: 10.1016/0896-6273(95)90302-x.

[28] R. Jakes, M. G. Spillantini, and M. Goedert, “Identification of two distinct synucleins from human brain,” *FEBS Lett.*, vol. 345, no. 1, pp. 27–32, May 1994, doi: 10.1016/0014-5793(94)00395-5.

[29] G. S. Withers, J. M. George, G. A. Banker, and D. F. Clayton, “Delayed localization of synelfin (synuclein, NACP) to presynaptic terminals in cultured rat hippocampal neurons,” *Brain Res. Dev. Brain Res.*, vol. 99, no. 1, pp. 87–94, Mar. 1997, doi: 10.1016/s0165-3806(96)00210-6.

[30] S. Yu *et al.*, “Extensive nuclear localization of alpha-synuclein in normal rat brain neurons revealed by a novel monoclonal antibody,” *Neuroscience*, vol. 145, no. 2, pp. 539–555, Mar. 2007, doi: 10.1016/j.neuroscience.2006.12.028.

[31] E. Kontopoulos, J. D. Parvin, and M. B. Feany, “Alpha-synuclein acts in the nucleus to inhibit histone acetylation and promote neurotoxicity,” *Hum. Mol. Genet.*, vol. 15, no. 20, pp. 3012–3023, Oct. 2006, doi: 10.1093/hmg/ddl243.

[32] S. Xu *et al.*, “Oxidative stress induces nuclear translocation of C-terminus of alpha-synuclein in dopaminergic cells,” *Biochem. Biophys. Res. Commun.*, vol. 342, no. 1, pp. 330–335, Mar. 2006, doi: 10.1016/j.bbrc.2006.01.148.

[33] H. Schell, T. Hasegawa, M. Neumann, and P. J. Kahle, “Nuclear and neuritic distribution of serine-129 phosphorylated alpha-synuclein in transgenic mice,” *Neuroscience*, vol. 160, no. 4, pp. 796–804, Jun. 2009, doi: 10.1016/j.neuroscience.2009.03.002.

[34] X. Liu *et al.*, “Alpha-synuclein functions in the nucleus to protect against hydroxyurea-induced replication stress in yeast,” *Hum. Mol. Genet.*, vol. 20, no. 17, pp. 3401–3414, Sep. 2011, doi: 10.1093/hmg/ddr246.

[35] S. Gonçalves and T. F. Outeiro, “Assessing the subcellular dynamics of alpha-synuclein using photoactivation microscopy,” *Mol. Neurobiol.*, vol. 47, no. 3, pp. 1081–1092, Jun. 2013, doi: 10.1007/s12035-013-8406-x.

[36] R. Pinho *et al.*, “Nuclear localization and phosphorylation modulate pathological effects of alpha-synuclein,” *Hum. Mol. Genet.*, vol. 28, no. 1, pp. 31–50, Jan. 2019, doi: 10.1093/hmg/ddy326.

[37] K. Beyer, “Alpha-synuclein structure, posttranslational modification and alternative splicing as aggregation enhancers,” *Acta Neuropathol. (Berl.)*, vol. 112, no. 3, pp. 237–251, Sep. 2006, doi: 10.1007/s00401-006-0104-6.

[38] A. Villar-Piqué, T. Lopes da Fonseca, and T. F. Outeiro, “Structure, function and

toxicity of alpha-synuclein: the Bermuda triangle in synucleinopathies," *J. Neurochem.*, vol. 139 Suppl 1, pp. 240–255, Oct. 2016, doi: 10.1111/jnc.13249.

[39] R. Bussell and D. Eliezer, "Effects of Parkinson's disease-linked mutations on the structure of lipid-associated alpha-synuclein," *Biochemistry*, vol. 43, no. 16, pp. 4810–4818, Apr. 2004, doi: 10.1021/bi036135+.

[40] S. Chandra, X. Chen, J. Rizo, R. Jahn, and T. C. Südhof, "A broken alpha -helix in folded alpha -Synuclein," *J. Biol. Chem.*, vol. 278, no. 17, pp. 15313–15318, Apr. 2003, doi: 10.1074/jbc.M213128200.

[41] C. C. Jao, A. Der-Sarkissian, J. Chen, and R. Langen, "Structure of membrane-bound alpha-synuclein studied by site-directed spin labeling," *Proc. Natl. Acad. Sci. U. S. A.*, vol. 101, no. 22, pp. 8331–8336, Jun. 2004, doi: 10.1073/pnas.0400553101.

[42] M. Bisaglia, E. Schievano, A. Caporale, E. Peggion, and S. Mammi, "The 11-mer repeats of human alpha-synuclein in vesicle interactions and lipid composition discrimination: a cooperative role," *Biopolymers*, vol. 84, no. 3, pp. 310–316, 2006, doi: 10.1002/bip.20440.

[43] W. S. Davidson, A. Jonas, D. F. Clayton, and J. M. George, "Stabilization of alpha-synuclein secondary structure upon binding to synthetic membranes," *J. Biol. Chem.*, vol. 273, no. 16, pp. 9443–9449, Apr. 1998, doi: 10.1074/jbc.273.16.9443.

[44] D. L. Fortin, M. D. Troyer, K. Nakamura, S. Kubo, M. D. Anthony, and R. H. Edwards, "Lipid rafts mediate the synaptic localization of alpha-synuclein," *J. Neurosci. Off. J. Soc. Neurosci.*, vol. 24, no. 30, pp. 6715–6723, Jul. 2004, doi: 10.1523/JNEUROSCI.1594-04.2004.

[45] K. Uéda *et al.*, "Molecular cloning of cDNA encoding an unrecognized component of amyloid in Alzheimer disease," *Proc. Natl. Acad. Sci. U. S. A.*, vol. 90, no. 23, pp. 11282–11286, Dec. 1993, doi: 10.1073/pnas.90.23.11282.

[46] B. I. Giasson, I. V. Murray, J. Q. Trojanowski, and V. M. Lee, "A hydrophobic stretch of 12 amino acid residues in the middle of alpha-synuclein is essential for filament assembly," *J. Biol. Chem.*, vol. 276, no. 4, pp. 2380–2386, Jan. 2001, doi: 10.1074/jbc.M008919200.

[47] D. Eliezer, E. Kutluay, R. Bussell, and G. Browne, "Conformational properties of alpha-synuclein in its free and lipid-associated states," *J. Mol. Biol.*, vol. 307, no. 4, pp. 1061–1073, Apr. 2001, doi: 10.1006/jmbi.2001.4538.

[48] M. S. Nielsen, H. Vorum, E. Lindersson, and P. H. Jensen, "Ca2+ binding to alpha-synuclein regulates ligand binding and oligomerization," *J. Biol. Chem.*, vol. 276, no. 25, pp. 22680–22684, Jun. 2001, doi: 10.1074/jbc.M101181200.

[49] T. D. Kim, S. R. Paik, and C.-H. Yang, "Structural and functional implications of C-terminal regions of alpha-synuclein," *Biochemistry*, vol. 41, no. 46, pp. 13782–13790,

Nov. 2002, doi: 10.1021/bi026284c.

[50] S. Kanda, J. F. Bishop, M. A. Eglitis, Y. Yang, and M. M. Mouradian, “Enhanced vulnerability to oxidative stress by alpha-synuclein mutations and C-terminal truncation,” *Neuroscience*, vol. 97, no. 2, pp. 279–284, 2000, doi: 10.1016/s0306-4522(00)00077-4.

[51] R. A. Crowther, R. Jakes, M. G. Spillantini, and M. Goedert, “Synthetic filaments assembled from C-terminally truncated alpha-synuclein,” *FEBS Lett.*, vol. 436, no. 3, pp. 309–312, Oct. 1998, doi: 10.1016/s0014-5793(98)01146-6.

[52] P. H. Weinreb, W. Zhen, A. W. Poon, K. A. Conway, and P. T. Lansbury, “NACP, a protein implicated in Alzheimer’s disease and learning, is natively unfolded,” *Biochemistry*, vol. 35, no. 43, pp. 13709–13715, Oct. 1996, doi: 10.1021/bi961799n.

[53] F.-X. Theillet *et al.*, “Structural disorder of monomeric α-synuclein persists in mammalian cells,” *Nature*, vol. 530, no. 7588, pp. 45–50, Feb. 2016, doi: 10.1038/nature16531.

[54] J. Burré, “The Synaptic Function of α-Synuclein,” *J. Park. Dis.*, vol. 5, no. 4, pp. 699–713, 2015, doi: 10.3233/JPD-150642.

[55] F. Cheng, G. Vivacqua, and S. Yu, “The role of α-synuclein in neurotransmission and synaptic plasticity,” *J. Chem. Neuroanat.*, vol. 42, no. 4, pp. 242–248, Dec. 2011, doi: 10.1016/j.jchemneu.2010.12.001.

[56] S. Cockcroft, “Signalling roles of mammalian phospholipase D1 and D2,” *Cell. Mol. Life Sci. CMLS*, vol. 58, no. 11, pp. 1674–1687, Oct. 2001, doi: 10.1007/PL00000805.

[57] J. M. Jenco, A. Rawlingson, B. Daniels, and A. J. Morris, “Regulation of phospholipase D2: selective inhibition of mammalian phospholipase D isoenzymes by alpha- and beta-synucleins,” *Biochemistry*, vol. 37, no. 14, pp. 4901–4909, Apr. 1998, doi: 10.1021/bi972776r.

[58] B.-H. Ahn *et al.*, “alpha-Synuclein interacts with phospholipase D isozymes and inhibits pervanadate-induced phospholipase D activation in human embryonic kidney-293 cells,” *J. Biol. Chem.*, vol. 277, no. 14, pp. 12334–12342, Apr. 2002, doi: 10.1074/jbc.M110414200.

[59] S. Bellani, V. L. Sousa, G. Ronzitti, F. Valtorta, J. Meldolesi, and E. Chieregatti, “The regulation of synaptic function by alpha-synuclein,” *Commun. Integr. Biol.*, vol. 3, no. 2, pp. 106–109, Mar. 2010, doi: 10.4161/cib.3.2.10964.

[60] N. Ostrerova *et al.*, “alpha-Synuclein shares physical and functional homology with 14-3-3 proteins,” *J. Neurosci. Off. J. Soc. Neurosci.*, vol. 19, no. 14, pp. 5782–5791, Jul. 1999, doi: 10.1523/JNEUROSCI.19-14-05782.1999.

[61] N. M. Bonini and B. I. Giasson, “Snaring the function of alpha-synuclein,” *Cell*, vol. 123, no. 3, pp. 359–361, Nov. 2005, doi: 10.1016/j.cell.2005.10.017.

[62] J. Burré, M. Sharma, T. Tsetsenis, V. Buchman, M. R. Etherton, and T. C. Südhof, “Alpha-synuclein promotes SNARE-complex assembly in vivo and in vitro,” *Science*, vol. 329, no. 5999, pp. 1663–1667, Sep. 2010, doi: 10.1126/science.1195227.

[63] J. T. Bendor, T. P. Logan, and R. H. Edwards, “The function of α-synuclein,” *Neuron*, vol. 79, no. 6, pp. 1044–1066, Sep. 2013, doi: 10.1016/j.neuron.2013.09.004.

[64] A. Sidhu, C. Wersinger, and P. Vernier, “alpha-Synuclein regulation of the dopaminergic transporter: a possible role in the pathogenesis of Parkinson’s disease,” *FEBS Lett.*, vol. 565, no. 1–3, pp. 1–5, May 2004, doi: 10.1016/j.febslet.2004.03.063.

[65] R. G. Perez, J. C. Waymire, E. Lin, J. J. Liu, F. Guo, and M. J. Zigmond, “A role for alpha-synuclein in the regulation of dopamine biosynthesis,” *J. Neurosci. Off. J. Soc. Neurosci.*, vol. 22, no. 8, pp. 3090–3099, Apr. 2002, doi: 10.1523/JNEUROSCI.22-08-03090.2002.

[66] R. E. Drolet, B. Behrouz, K. J. Lookingland, and J. L. Goudreau, “Substrate-mediated enhancement of phosphorylated tyrosine hydroxylase in nigrostriatal dopamine neurons: evidence for a role of alpha-synuclein,” *J. Neurochem.*, vol. 96, no. 4, pp. 950–959, Feb. 2006, doi: 10.1111/j.1471-4159.2005.03606.x.

[67] D. Kirik *et al.*, “Parkinson-like neurodegeneration induced by targeted overexpression of alpha-synuclein in the nigrostriatal system,” *J. Neurosci. Off. J. Soc. Neurosci.*, vol. 22, no. 7, pp. 2780–2791, Apr. 2002, doi: 10.1523/JNEUROSCI.22-07-02780.2002.

[68] C. Wersinger and A. Sidhu, “Attenuation of dopamine transporter activity by alpha-synuclein,” *Neurosci. Lett.*, vol. 340, no. 3, pp. 189–192, Apr. 2003, doi: 10.1016/s0304-3940(03)00097-1.

[69] J. C. Bridi and F. Hirth, “Mechanisms of α-Synuclein Induced Synaptopathy in Parkinson’s Disease,” *Front. Neurosci.*, vol. 12, p. 80, 2018, doi: 10.3389/fnins.2018.00080.

[70] S. Chandra *et al.*, “Double-knockout mice for alpha- and beta-synucleins: effect on synaptic functions,” *Proc. Natl. Acad. Sci. U. S. A.*, vol. 101, no. 41, pp. 14966–14971, Oct. 2004, doi: 10.1073/pnas.0406283101.

[71] J. M. George, H. Jin, W. S. Woods, and D. F. Clayton, “Characterization of a novel protein regulated during the critical period for song learning in the zebra finch,” *Neuron*, vol. 15, no. 2, pp. 361–372, Aug. 1995, doi: 10.1016/0896-6273(95)90040-3.

[72] K. Petersen, O. F. Olesen, and J. D. Mikkelsen, “Developmental expression of α-synuclein in rat hippocampus and cerebral cortex,” *Neuroscience*, vol. 91, no. 2, pp. 651–659, Jun. 1999, doi: 10.1016/S0306-4522(98)00596-X.

[73] L. Stefanis, “α-Synuclein in Parkinson’s disease,” *Cold Spring Harb. Perspect. Med.*, vol. 2, no. 2, p. a009399, Feb. 2012, doi: 10.1101/cshperspect.a009399.

[74] I. C. Brás, M. Xylaki, and T. F. Outeiro, “Mechanisms of alpha-synuclein toxicity: An

update and outlook," *Prog. Brain Res.*, vol. 252, pp. 91–129, 2020, doi: 10.1016/bs.pbr.2019.10.005.

[75] M. H. Polymeropoulos *et al.*, "Mutation in the alpha-synuclein gene identified in families with Parkinson's disease," *Science*, vol. 276, no. 5321, pp. 2045–2047, Jun. 1997, doi: 10.1126/science.276.5321.2045.

[76] R. Krüger *et al.*, "AlaSOPro mutation in the gene encoding α-synuclein in Parkinson's disease," *Nat. Genet.*, vol. 18, no. 2, Art. no. 2, Feb. 1998, doi: 10.1038/ng0298-106.

[77] J. J. Zarranz *et al.*, "The new mutation, E46K, of alpha-synuclein causes Parkinson and Lewy body dementia," *Ann. Neurol.*, vol. 55, no. 2, pp. 164–173, Feb. 2004, doi: 10.1002/ana.10795.

[78] S. Appel-Cresswell *et al.*, "Alpha-synuclein p.H50Q, a novel pathogenic mutation for Parkinson's disease," *Mov. Disord. Off. J. Mov. Disord. Soc.*, vol. 28, no. 6, pp. 811–813, Jun. 2013, doi: 10.1002/mds.25421.

[79] S. Lesage *et al.*, "G51D α-synuclein mutation causes a novel parkinsonian-pyramidal syndrome," *Ann. Neurol.*, vol. 73, no. 4, pp. 459–471, Apr. 2013, doi: 10.1002/ana.23894.

[80] P. Pasanen *et al.*, "Novel α-synuclein mutation A53E associated with atypical multiple system atrophy and Parkinson's disease-type pathology," *Neurobiol. Aging*, vol. 35, no. 9, p. 2180.e1–5, Sep. 2014, doi: 10.1016/j.neurobiolaging.2014.03.024.

[81] P. Flagmeier *et al.*, "Mutations associated with familial Parkinson's disease alter the initiation and amplification steps of α-synuclein aggregation," *Proc. Natl. Acad. Sci. U. S. A.*, vol. 113, no. 37, pp. 10328–10333, Sep. 2016, doi: 10.1073/pnas.1604645113.

[82] D. F. Lázaro *et al.*, "Systematic comparison of the effects of alpha-synuclein mutations on its oligomerization and aggregation," *PLoS Genet.*, vol. 10, no. 11, p. e1004741, Nov. 2014, doi: 10.1371/journal.pgen.1004741.

[83] M. G. Spillantini, "Parkinson's disease, dementia with Lewy bodies and multiple system atrophy are α-synucleinopathies," *Parkinsonism Relat. Disord.*, vol. 5, no. 4, pp. 157–162, Dec. 1999, doi: 10.1016/S1353-8020(99)00031-0.

[84] W. Marui *et al.*, "Progression and staging of Lewy pathology in brains from patients with dementia with Lewy bodies," *J. Neurol. Sci.*, vol. 195, no. 2, pp. 153–159, Mar. 2002, doi: 10.1016/s0022-510x(02)00006-0.

[85] H. Braak, K. Del Tredici, U. Rüb, R. A. I. de Vos, E. N. H. Jansen Steur, and E. Braak, "Staging of brain pathology related to sporadic Parkinson's disease," *Neurobiol. Aging*, vol. 24, no. 2, pp. 197–211, 2003, doi: 10.1016/s0197-4580(02)00065-9.

[86] M. Vilar *et al.*, "The fold of alpha-synuclein fibrils," *Proc. Natl. Acad. Sci. U. S. A.*, vol. 105, no. 25, pp. 8637–8642, Jun. 2008, doi: 10.1073/pnas.0712179105.

[87] T. F. Outeiro *et al.*, "Formation of toxic oligomeric alpha-synuclein species in living

cells," *PloS One*, vol. 3, no. 4, p. e1867, Apr. 2008, doi: 10.1371/journal.pone.0001867.

[88] H. L. Roberts and D. R. Brown, "Seeking a mechanism for the toxicity of oligomeric α-synuclein," *Biomolecules*, vol. 5, no. 2, pp. 282–305, Mar. 2015, doi: 10.3390/biom5020282.

[89] D. P. Karpinar *et al.*, "Pre-fibrillar alpha-synuclein variants with impaired beta-structure increase neurotoxicity in Parkinson's disease models," *EMBO J.*, vol. 28, no. 20, pp. 3256–3268, Oct. 2009, doi: 10.1038/emboj.2009.257.

[90] B. Winner *et al.*, "In vivo demonstration that alpha-synuclein oligomers are toxic," *Proc. Natl. Acad. Sci. U. S. A.*, vol. 108, no. 10, pp. 4194–4199, Mar. 2011, doi: 10.1073/pnas.1100976108.

[91] E. Rockenstein *et al.*, "Accumulation of oligomer-prone α-synuclein exacerbates synaptic and neuronal degeneration in vivo," *Brain J. Neurol.*, vol. 137, no. Pt 5, pp. 1496–1513, May 2014, doi: 10.1093/brain/awu057.

[92] R. Sharon, I. Bar-Joseph, M. P. Frosch, D. M. Walsh, J. A. Hamilton, and D. J. Selkoe, "The formation of highly soluble oligomers of alpha-synuclein is regulated by fatty acids and enhanced in Parkinson's disease," *Neuron*, vol. 37, no. 4, pp. 583–595, Feb. 2003, doi: 10.1016/s0896-6273(03)00024-2.

[93] K. E. Paleologou *et al.*, "Detection of elevated levels of soluble alpha-synuclein oligomers in post-mortem brain extracts from patients with dementia with Lewy bodies," *Brain J. Neurol.*, vol. 132, no. Pt 4, pp. 1093–1101, Apr. 2009, doi: 10.1093/brain/awn349.

[94] R. F. Roberts, R. Wade-Martins, and J. Alegre-Abarrategui, "Direct visualization of alpha-synuclein oligomers reveals previously undetected pathology in Parkinson's disease brain," *Brain J. Neurol.*, vol. 138, no. Pt 6, pp. 1642–1657, Jun. 2015, doi: 10.1093/brain/awv040.

[95] K. C. Luk *et al.*, "Pathological α-synuclein transmission initiates Parkinson-like neurodegeneration in nontransgenic mice," *Science*, vol. 338, no. 6109, pp. 949–953, Nov. 2012, doi: 10.1126/science.1227157.

[96] M. Masuda-Suzukake *et al.*, "Prion-like spreading of pathological α-synuclein in brain," *Brain J. Neurol.*, vol. 136, no. Pt 4, pp. 1128–1138, Apr. 2013, doi: 10.1093/brain/awt037.

[97] A. Recasens *et al.*, "Lewy body extracts from Parkinson disease brains trigger α-synuclein pathology and neurodegeneration in mice and monkeys," *Ann. Neurol.*, vol. 75, no. 3, pp. 351–362, Mar. 2014, doi: 10.1002/ana.24066.

[98] V. R. Osterberg, K. J. Spinelli, L. J. Weston, K. C. Luk, R. L. Woltjer, and V. K. Unni, "Progressive aggregation of alpha-synuclein and selective degeneration of lewy

inclusion-bearing neurons in a mouse model of parkinsonism," *Cell Rep.*, vol. 10, no. 8, pp. 1252–1260, Mar. 2015, doi: 10.1016/j.celrep.2015.01.060.

[99] R. A. Bodner *et al.*, "Pharmacological promotion of inclusion formation: a therapeutic approach for Huntington's and Parkinson's diseases," *Proc. Natl. Acad. Sci. U. S. A.*, vol. 103, no. 11, pp. 4246–4251, Mar. 2006, doi: 10.1073/pnas.0511256103.

[100] M. Tanaka, Y. M. Kim, G. Lee, E. Junn, T. Iwatsubo, and M. M. Mouradian, "Aggresomes formed by alpha-synuclein and synphilin-1 are cytoprotective," *J. Biol. Chem.*, vol. 279, no. 6, pp. 4625–4631, Feb. 2004, doi: 10.1074/jbc.M310994200.

[101] K. A. Conway, S. J. Lee, J. C. Rochet, T. T. Ding, R. E. Williamson, and P. T. Lansbury, "Acceleration of oligomerization, not fibrillization, is a shared property of both alpha-synuclein mutations linked to early-onset Parkinson's disease: implications for pathogenesis and therapy," *Proc. Natl. Acad. Sci. U. S. A.*, vol. 97, no. 2, pp. 571–576, Jan. 2000, doi: 10.1073/pnas.97.2.571.

[102] S. Sahay, D. Ghosh, P. K. Singh, and S. K. Maji, "Alteration of Structure and Aggregation of α-Synuclein by Familial Parkinson's Disease Associated Mutations," *Curr. Protein Pept. Sci.*, vol. 18, no. 7, pp. 656–676, 2017, doi: 10.2174/1389203717666160314151706.

[103] R. Rott *et al.*, "Monoubiquitylation of alpha-synuclein by seven in absentia homolog (SIAH) promotes its aggregation in dopaminergic cells," *J. Biol. Chem.*, vol. 283, no. 6, pp. 3316–3328, Feb. 2008, doi: 10.1074/jbc.M704809200.

[104] P. Krumova *et al.*, "Sumoylation inhibits alpha-synuclein aggregation and toxicity," *J. Cell Biol.*, vol. 194, no. 1, pp. 49–60, Jul. 2011, doi: 10.1083/jcb.201010117.

[105] H. Vicente Miranda and T. F. Outeiro, "The sour side of neurodegenerative disorders: the effects of protein glycation," *J. Pathol.*, vol. 221, no. 1, pp. 13–25, May 2010, doi: 10.1002/path.2682.

[106] T. Bartels, N. C. Kim, E. S. Luth, and D. J. Selkoe, "N-alpha-acetylation of α-synuclein increases its helical folding propensity, GM1 binding specificity and resistance to aggregation," *PloS One*, vol. 9, no. 7, p. e103727, 2014, doi: 10.1371/journal.pone.0103727.

[107] R. Hodara *et al.*, "Functional consequences of alpha-synuclein tyrosine nitration: diminished binding to lipid vesicles and increased fibril formation," *J. Biol. Chem.*, vol. 279, no. 46, pp. 47746–47753, Nov. 2004, doi: 10.1074/jbc.M408906200.

[108] H. Fujiwara *et al.*, "alpha-Synuclein is phosphorylated in synucleinopathy lesions," *Nat. Cell Biol.*, vol. 4, no. 2, pp. 160–164, Feb. 2002, doi: 10.1038/ncb748.

[109] S. Tenreiro, K. Eckermann, and T. F. Outeiro, "Protein phosphorylation in neurodegeneration: friend or foe?," *Front. Mol. Neurosci.*, vol. 7, p. 42, 2014, doi: 10.3389/fnmol.2014.00042.

[110] H. Vicente Miranda *et al.*, “Glycation potentiates α-synuclein-associated neurodegeneration in synucleinopathies,” *Brain J. Neurol.*, vol. 140, no. 5, pp. 1399–1419, May 2017, doi: 10.1093/brain/awx056.

[111] M. J. Benskey, R. G. Perez, and F. P. Manfredsson, “The contribution of alpha synuclein to neuronal survival and function - Implications for Parkinson’s disease,” *J. Neurochem.*, vol. 137, no. 3, pp. 331–359, May 2016, doi: 10.1111/jnc.13570.

[112] W. D. Parker, S. J. Boyson, and J. K. Parks, “Abnormalities of the electron transport chain in idiopathic Parkinson’s disease,” *Ann. Neurol.*, vol. 26, no. 6, pp. 719–723, Dec. 1989, doi: 10.1002/ana.410260606.

[113] A. H. V. Schapira, J. M. Cooper, D. Dexter, J. B. Clark, P. Jenner, and C. D. Marsden, “Mitochondrial Complex I Deficiency in Parkinson’s Disease,” *J. Neurochem.*, vol. 54, no. 3, pp. 823–827, 1990, doi: 10.1111/j.1471-4159.1990.tb02325.x.

[114] N. Hattori, M. Tanaka, T. Ozawa, and Y. Mizuno, “Immunohistochemical studies on complexes I, II, III, and IV of mitochondria in Parkinson’s disease,” *Ann. Neurol.*, vol. 30, no. 4, pp. 563–571, Oct. 1991, doi: 10.1002/ana.410300409.

[115] W.-W. Li *et al.*, “Localization of alpha-synuclein to mitochondria within midbrain of mice,” *Neuroreport*, vol. 18, no. 15, pp. 1543–1546, Oct. 2007, doi: 10.1097/WNR.0b013e3282f03db4.

[116] S. J. Chinta, J. K. Mallajosyula, A. Rane, and J. K. Andersen, “Mitochondrial α-synuclein accumulation impairs complex I function in dopaminergic neurons and results in increased mitophagy in vivo,” *Neurosci. Lett.*, vol. 486, no. 3, pp. 235–239, Dec. 2010, doi: 10.1016/j.neulet.2010.09.061.

[117] L. Devi, V. Raghavendran, B. M. Prabhu, N. G. Avadhani, and H. K. Anandatheerthavarada, “Mitochondrial import and accumulation of alpha-synuclein impair complex I in human dopaminergic neuronal cultures and Parkinson disease brain,” *J. Biol. Chem.*, vol. 283, no. 14, pp. 9089–9100, Apr. 2008, doi: 10.1074/jbc.M710012200.

[118] K. Nakamura *et al.*, “Direct membrane association drives mitochondrial fission by the Parkinson disease-associated protein alpha-synuclein,” *J. Biol. Chem.*, vol. 286, no. 23, pp. 20710–20726, Jun. 2011, doi: 10.1074/jbc.M110.213538.

[119] L. J. Martin *et al.*, “Parkinson’s disease alpha-synuclein transgenic mice develop neuronal mitochondrial degeneration and cell death,” *J. Neurosci. Off. J. Soc. Neurosci.*, vol. 26, no. 1, pp. 41–50, Jan. 2006, doi: 10.1523/JNEUROSCI.4308-05.2006.

[120] A. Siddiqui *et al.*, “Selective binding of nuclear alpha-synuclein to the PGC1alpha promoter under conditions of oxidative stress may contribute to losses in mitochondrial

function: implications for Parkinson's disease," *Free Radic. Biol. Med.*, vol. 53, no. 4, pp. 993–1003, Aug. 2012, doi: 10.1016/j.freeradbiomed.2012.05.024.

[121] J. M. Chambers and R. A. Wingert, "PGC-1α in Disease: Recent Renal Insights into a Versatile Metabolic Regulator," *Cells*, vol. 9, no. 10, p. 2234, Oct. 2020, doi: 10.3390/cells9102234.

[122] R. Betarbet *et al.*, "Intersecting pathways to neurodegeneration in Parkinson's disease: effects of the pesticide rotenone on DJ-1, alpha-synuclein, and the ubiquitin-proteasome system," *Neurobiol. Dis.*, vol. 22, no. 2, pp. 404–420, May 2006, doi: 10.1016/j.nbd.2005.12.003.

[123] B. I. Giasson *et al.*, "Oxidative damage linked to neurodegeneration by selective alpha-synuclein nitration in synucleinopathy lesions," *Science*, vol. 290, no. 5493, pp. 985–989, Nov. 2000, doi: 10.1126/science.290.5493.985.

[124] V. M. Pozo Devoto *et al.*, "αSynuclein control of mitochondrial homeostasis in human-derived neurons is disrupted by mutations associated with Parkinson's disease," *Sci. Rep.*, vol. 7, no. 1, p. 5042, Jul. 2017, doi: 10.1038/s41598-017-05334-9.

[125] H. D. E. Booth, W. D. Hirst, and R. Wade-Martins, "The Role of Astrocyte Dysfunction in Parkinson's Disease Pathogenesis," *Trends Neurosci.*, vol. 40, no. 6, pp. 358–370, Jun. 2017, doi: 10.1016/j.tins.2017.04.001.

[126] K. Badanjak, S. Fixemer, S. Smajić, A. Skupin, and A. Grünewald, "The Contribution of Microglia to Neuroinflammation in Parkinson's Disease," *Int. J. Mol. Sci.*, vol. 22, no. 9, p. 4676, Apr. 2021, doi: 10.3390/ijms22094676.

[127] N. Hishikawa, Y. Hashizume, M. Yoshida, and G. Sobue, "Widespread occurrence of argyrophilic glial inclusions in Parkinson's disease," *Neuropathol. Appl. Neurobiol.*, vol. 27, no. 5, pp. 362–372, Oct. 2001, doi: 10.1046/j.1365-2990.2001.00345.x.

[128] K. Wakabayashi, S. Hayashi, M. Yoshimoto, H. Kudo, and H. Takahashi, "NACP/alpha-synuclein-positive filamentous inclusions in astrocytes and oligodendrocytes of Parkinson's disease brains," *Acta Neuropathol. (Berl.)*, vol. 99, no. 1, pp. 14–20, Jan. 2000, doi: 10.1007/pl00007400.

[129] V. Grozdanov and K. M. Danzer, "Release and uptake of pathologic alpha-synuclein," *Cell Tissue Res.*, vol. 373, no. 1, pp. 175–182, Jul. 2018, doi: 10.1007/s00441-017-2775-9.

[130] K. J. Ahn, S. R. Paik, K. C. Chung, and J. Kim, "Amino acid sequence motifs and mechanistic features of the membrane translocation of alpha-synuclein," *J. Neurochem.*, vol. 97, no. 1, pp. 265–279, Apr. 2006, doi: 10.1111/j.1471-4159.2006.03731.x.

[131] H.-J. Lee, J.-E. Suk, E.-J. Bae, J.-H. Lee, S. R. Paik, and S.-J. Lee, "Assembly-

dependent endocytosis and clearance of extracellular alpha-synuclein," *Int. J. Biochem. Cell Biol.*, vol. 40, no. 9, pp. 1835–1849, 2008, doi: 10.1016/j.biocel.2008.01.017.

[132] H.-J. Lee, S. Patel, and S.-J. Lee, "Intravesicular localization and exocytosis of alpha-synuclein and its aggregates," *J. Neurosci. Off. J. Soc. Neurosci.*, vol. 25, no. 25, pp. 6016–6024, Jun. 2005, doi: 10.1523/JNEUROSCI.0692-05.2005.

[133] L. Alvarez-Erviti *et al.*, "Lysosomal dysfunction increases exosome-mediated alpha-synuclein release and transmission," *Neurobiol. Dis.*, vol. 42, no. 3, pp. 360–367, Jun. 2011, doi: 10.1016/j.nbd.2011.01.029.

[134] C. Bliederhaeuser *et al.*, "Age-dependent defects of alpha-synuclein oligomer uptake in microglia and monocytes," *Acta Neuropathol. (Berl.)*, vol. 131, no. 3, pp. 379–391, Mar. 2016, doi: 10.1007/s00401-015-1504-2.

[135] K. M. Danzer *et al.*, "Exosomal cell-to-cell transmission of alpha synuclein oligomers," *Mol. Neurodegener.*, vol. 7, p. 42, Aug. 2012, doi: 10.1186/1750-1326-7-42.

[136] E. Emmanouilidou *et al.*, "Cell-produced alpha-synuclein is secreted in a calcium-dependent manner by exosomes and impacts neuronal survival," *J. Neurosci. Off. J. Soc. Neurosci.*, vol. 30, no. 20, pp. 6838–6851, May 2010, doi: 10.1523/JNEUROSCI.5699-09.2010.

[137] S. Abounit *et al.*, "Tunneling nanotubes spread fibrillar α-synuclein by intercellular trafficking of lysosomes," *EMBO J.*, vol. 35, no. 19, pp. 2120–2138, Oct. 2016, doi: 10.15252/embj.201593411.

[138] B. V. Dieriks, T. I.-H. Park, C. Fourie, R. L. M. Faull, M. Dragunow, and M. A. Curtis, "α-synuclein transfer through tunneling nanotubes occurs in SH-SY5Y cells and primary brain pericytes from Parkinson's disease patients," *Sci. Rep.*, vol. 7, p. 42984, Feb. 2017, doi: 10.1038/srep42984.

[139] N. Braidy *et al.*, "Uptake and mitochondrial dysfunction of alpha-synuclein in human astrocytes, cortical neurons and fibroblasts," *Transl. Neurodegener.*, vol. 2, no. 1, p. 20, Oct. 2013, doi: 10.1186/2047-9158-2-20.

[140] A. Hoffmann *et al.*, "Alpha-synuclein activates BV2 microglia dependent on its aggregation state," *Biochem. Biophys. Res. Commun.*, vol. 479, no. 4, pp. 881–886, Oct. 2016, doi: 10.1016/j.bbrc.2016.09.109.

[141] C. Kim *et al.*, "Neuron-released oligomeric α-synuclein is an endogenous agonist of TLR2 for paracrine activation of microglia," *Nat. Commun.*, vol. 4, p. 1562, 2013, doi: 10.1038/ncomms2534.

[142] V. Lindström *et al.*, "Extensive uptake of α-synuclein oligomers in astrocytes results in sustained intracellular deposits and mitochondrial damage," *Mol. Cell. Neurosci.*,

vol. 82, pp. 143–156, Jul. 2017, doi: 10.1016/j.mcn.2017.04.009.

[143] J. F. Reyes, N. L. Rey, L. Bousset, R. Melki, P. Brundin, and E. Angot, “Alpha-synuclein transfers from neurons to oligodendrocytes,” *Glia*, vol. 62, no. 3, pp. 387–398, Mar. 2014, doi: 10.1002/glia.22611.

[144] F. Loria *et al.*, “α-Synuclein transfer between neurons and astrocytes indicates that astrocytes play a role in degradation rather than in spreading,” *Acta Neuropathol. (Berl.)*, vol. 134, no. 5, pp. 789–808, Nov. 2017, doi: 10.1007/s00401-017-1746-2.

[145] H.-J. Lee *et al.*, “Direct transfer of alpha-synuclein from neuron to astroglia causes inflammatory responses in synucleinopathies,” *J. Biol. Chem.*, vol. 285, no. 12, pp. 9262–9272, Mar. 2010, doi: 10.1074/jbc.M109.081125.

[146] J. Rostami *et al.*, “Human Astrocytes Transfer Aggregated Alpha-Synuclein via Tunneling Nanotubes,” *J. Neurosci. Off. J. Soc. Neurosci.*, vol. 37, no. 49, pp. 11835–11853, Dec. 2017, doi: 10.1523/JNEUROSCI.0983-17.2017.

[147] H. Scheiblich *et al.*, “Microglia jointly degrade fibrillar alpha-synuclein cargo by distribution through tunneling nanotubes,” *Cell*, vol. 184, no. 20, pp. 5089-5106.e21, Sep. 2021, doi: 10.1016/j.cell.2021.09.007.

[148] X.-L. Gu, C.-X. Long, L. Sun, C. Xie, X. Lin, and H. Cai, “Astrocytic expression of Parkinson’s disease-related A53T alpha-synuclein causes neurodegeneration in mice,” *Mol. Brain*, vol. 3, p. 12, Apr. 2010, doi: 10.1186/1756-6606-3-12.

[149] M. V. Sofroniew and H. V. Vinters, “Astrocytes: biology and pathology,” *Acta Neuropathol. (Berl.)*, vol. 119, no. 1, pp. 7–35, Jan. 2010, doi: 10.1007/s00401-009-0619-8.

[150] M. Kumar, N. T. P. Nguyen, M. Milanese, and G. Bonanno, “Insights into Human-Induced Pluripotent Stem Cell-Derived Astrocytes in Neurodegenerative Disorders,” *Biomolecules*, vol. 12, no. 3, p. 344, Feb. 2022, doi: 10.3390/biom12030344.

[151] E. M. Legault, J. Bouquety, and J. Drouin-Ouellet, “Disease Modeling of Neurodegenerative Disorders Using Direct Neural Reprogramming,” *Cell. Reprogramming*, vol. 24, no. 5, pp. 228–251, Oct. 2022, doi: 10.1089/cell.2021.0172.

[152] M. X. Doss and A. Sachinidis, “Current Challenges of iPSC-Based Disease Modeling and Therapeutic Implications,” *Cells*, vol. 8, no. 5, p. 403, Apr. 2019, doi: 10.3390/cells8050403.

[153] M. Oksanen *et al.*, “PSEN1 Mutant iPSC-Derived Model Reveals Severe Astrocyte Pathology in Alzheimer’s Disease,” *Stem Cell Rep.*, vol. 9, no. 6, pp. 1885–1897, Dec. 2017, doi: 10.1016/j.stemcr.2017.10.016.

[154] T. Palm *et al.*, “Rapid and robust generation of long-term self-renewing human neural stem cells with the ability to generate mature astroglia,” *Sci. Rep.*, vol. 5, p. 16321, Nov. 2015, doi: 10.1038/srep16321.

[155] L. Magistrelli, E. Contaldi, and C. Comi, “The Impact of SNCA Variations and Its Product Alpha-Synuclein on Non-Motor Features of Parkinson’s Disease,” *Life Basel Switz.*, vol. 11, no. 8, p. 804, Aug. 2021, doi: 10.3390/life11080804.

[156] H. Phatnani and T. Maniatis, “Astrocytes in neurodegenerative disease,” *Cold Spring Harb. Perspect. Biol.*, vol. 7, no. 6, p. a020628, Apr. 2015, doi: 10.1101/cshperspect.a020628.

[157] M. T. Hayes, “Parkinson’s Disease and Parkinsonism,” *Am. J. Med.*, vol. 132, no. 7, pp. 802–807, Jul. 2019, doi: 10.1016/j.amjmed.2019.03.001.

[158] T. Stoddard-Bennett and R. Reijo Pera, “Treatment of Parkinson’s Disease through Personalized Medicine and Induced Pluripotent Stem Cells,” *Cells*, vol. 8, no. 1, p. 26, Jan. 2019, doi: 10.3390/cells8010026.

[159] F. Vasile, E. Dossi, and N. Rouach, “Human astrocytes: structure and functions in the healthy brain,” *Brain Struct. Funct.*, vol. 222, no. 5, pp. 2017–2029, Jul. 2017, doi: 10.1007/s00429-017-1383-5.

[160] I. Miyazaki and M. Asanuma, “Neuron-Astrocyte Interactions in Parkinson’s Disease,” *Cells*, vol. 9, no. 12, p. 2623, Dec. 2020, doi: 10.3390/cells9122623.

[161] M. Pons-Espinal, L. Blasco-Agell, and A. Consiglio, “Dissecting the non-neuronal cell contribution to Parkinson’s disease pathogenesis using induced pluripotent stem cells,” *Cell. Mol. Life Sci. CMLS*, vol. 78, no. 5, pp. 2081–2094, Mar. 2021, doi: 10.1007/s00018-020-03700-x.

[162] B. A. Barres, “The mystery and magic of glia: a perspective on their roles in health and disease,” *Neuron*, vol. 60, no. 3, pp. 430–440, Nov. 2008, doi: 10.1016/j.neuron.2008.10.013.

[163] M. M. Halassa, T. Fellin, and P. G. Haydon, “The tripartite synapse: roles for gliotransmission in health and disease,” *Trends Mol. Med.*, vol. 13, no. 2, pp. 54–63, Feb. 2007, doi: 10.1016/j.molmed.2006.12.005.

[164] A. Araque, V. Parpura, R. P. Sanzgiri, and P. G. Haydon, “Tripartite synapses: glia, the unacknowledged partner,” *Trends Neurosci.*, vol. 22, no. 5, pp. 208–215, May 1999, doi: 10.1016/s0166-2236(98)01349-6.

[165] G. R. J. Gordon, S. J. Mulligan, and B. A. MacVicar, “Astrocyte control of the cerebrovasculature,” *Glia*, vol. 55, no. 12, pp. 1214–1221, Sep. 2007, doi: 10.1002/glia.20543.

[166] C. Iadecola and M. Nedergaard, “Glial regulation of the cerebral microvasculature,” *Nat. Neurosci.*, vol. 10, no. 11, pp. 1369–1376, Nov. 2007, doi: 10.1038/nn2003.

[167] R. C. Koehler, R. J. Roman, and D. R. Harder, “Astrocytes and the regulation of cerebral blood flow,” *Trends Neurosci.*, vol. 32, no. 3, pp. 160–169, Mar. 2009, doi: 10.1016/j.tins.2008.11.005.

[168] R. Occhipinti, E. Somersalo, and D. Calvetti, “Astrocytes as the glucose shunt for glutamatergic neurons at high activity: an in silico study,” *J. Neurophysiol.*, vol. 101, no. 5, pp. 2528–2538, May 2009, doi: 10.1152/jn.90377.2008.

[169] J. E. Beevers, T. M. Caffrey, and R. Wade-Martins, “Induced pluripotent stem cell (iPSC)-derived dopaminergic models of Parkinson’s disease,” *Biochem. Soc. Trans.*, vol. 41, no. 6, pp. 1503–1508, Dec. 2013, doi: 10.1042/BST20130194.

[170] P. McGonigle and B. Ruggeri, “Animal models of human disease: challenges in enabling translation,” *Biochem. Pharmacol.*, vol. 87, no. 1, pp. 162–171, Jan. 2014, doi: 10.1016/j.bcp.2013.08.006.

[171] L. H. Goetz and N. J. Schork, “Personalized medicine: motivation, challenges, and progress,” *Fertil. Steril.*, vol. 109, no. 6, pp. 952–963, Jun. 2018, doi: 10.1016/j.fertnstert.2018.05.006.

[172] H. J. Kim and B. Jeon, “How close are we to individualized medicine for Parkinson’s disease?,” *Expert Rev. Neurother.*, vol. 16, no. 7, pp. 815–830, Jul. 2016, doi: 10.1080/14737175.2016.1182021.

[173] G. Blattner, A. Cavazza, A. J. Thrasher, and G. Turchiano, “Gene Editing and Genotoxicity: Targeting the Off-Targets,” *Front. Genome Ed.*, vol. 2, p. 613252, 2020, doi: 10.3389/fgeed.2020.613252.

[174] P. Malatesta, I. Appolloni, and F. Calzolari, “Radial glia and neural stem cells,” *Cell Tissue Res.*, vol. 331, no. 1, pp. 165–178, Jan. 2008, doi: 10.1007/s00441-007-0481-8.

[175] M. R. Freeman, “Specification and morphogenesis of astrocytes,” *Science*, vol. 330, no. 6005, pp. 774–778, Nov. 2010, doi: 10.1126/science.1190928.

[176] R. Kanski, M. E. van Strien, P. van Tijn, and E. M. Hol, “A star is born: new insights into the mechanism of astrogenesis,” *Cell. Mol. Life Sci. CMLS*, vol. 71, no. 3, pp. 433–447, Feb. 2014, doi: 10.1007/s00018-013-1435-9.

[177] A. S. Gauthier *et al.*, “Control of CNS cell-fate decisions by SHP-2 and its dysregulation in Noonan syndrome,” *Neuron*, vol. 54, no. 2, pp. 245–262, Apr. 2007, doi: 10.1016/j.neuron.2007.03.027.

[178] Y. Sun *et al.*, “Neurogenin promotes neurogenesis and inhibits glial differentiation by independent mechanisms,” *Cell*, vol. 104, no. 3, pp. 365–376, Feb. 2001, doi: 10.1016/s0092-8674(01)00224-0.

[179] T. Takizawa *et al.*, “DNA methylation is a critical cell-intrinsic determinant of astrocyte differentiation in the fetal brain,” *Dev. Cell*, vol. 1, no. 6, pp. 749–758, Dec. 2001, doi: 10.1016/s1534-5807(01)00101-0.

[180] P.-Y. Cheng *et al.*, “Interplay between SIN3A and STAT3 mediates chromatin conformational changes and GFAP expression during cellular differentiation,” *PloS*

One, vol. 6, no. 7, p. e22018, 2011, doi: 10.1371/journal.pone.0022018.

[181] Y. Hirabayashi *et al.*, “Polycomb limits the neurogenic competence of neural precursor cells to promote astrogenic fate transition,” *Neuron*, vol. 63, no. 5, pp. 600–613, Sep. 2009, doi: 10.1016/j.neuron.2009.08.021.

[182] B. Cebolla and M. Vallejo, “Nuclear factor-I regulates glial fibrillary acidic protein gene expression in astrocytes differentiated from cortical precursor cells,” *J. Neurochem.*, vol. 97, no. 4, pp. 1057–1070, May 2006, doi: 10.1111/j.1471-4159.2006.03804.x.

[183] K. Irmady, S. Zechel, and K. Unsicker, “Fibroblast growth factor 2 regulates astrocyte differentiation in a region-specific manner in the hindbrain,” *Glia*, vol. 59, no. 5, pp. 708–719, May 2011, doi: 10.1002/glia.21141.

[184] H. Asano, M. Aonuma, T. Sanosaka, J. Kohyama, M. Namihira, and K. Nakashima, “Astrocyte differentiation of neural precursor cells is enhanced by retinoic acid through a change in epigenetic modification,” *Stem Cells Dayt. Ohio*, vol. 27, no. 11, pp. 2744–2752, Nov. 2009, doi: 10.1002/stem.176.

[185] M. Namihira *et al.*, “Committed neuronal precursors confer astrocytic potential on residual neural precursor cells,” *Dev. Cell*, vol. 16, no. 2, pp. 245–255, Feb. 2009, doi: 10.1016/j.devcel.2008.12.014.

[186] A. Chandrasekaran, H. X. Avci, M. Leist, J. Kobolák, and A. Dinnyés, “Astrocyte Differentiation of Human Pluripotent Stem Cells: New Tools for Neurological Disorder Research,” *Front. Cell. Neurosci.*, vol. 10, p. 215, 2016, doi: 10.3389/fncel.2016.00215.

[187] J. Tiihonen *et al.*, “Neurobiological roots of psychopathy,” *Mol. Psychiatry*, vol. 25, no. 12, Art. no. 12, Dec. 2020, doi: 10.1038/s41380-019-0488-z.

[188] M. Magistri *et al.*, “A comparative transcriptomic analysis of astrocytes differentiation from human neural progenitor cells,” *Eur. J. Neurosci.*, vol. 44, no. 10, pp. 2858–2870, Nov. 2016, doi: 10.1111/ejn.13382.

[189] Y. Zhang *et al.*, “Purification and Characterization of Progenitor and Mature Human Astrocytes Reveals Transcriptional and Functional Differences with Mouse,” *Neuron*, vol. 89, no. 1, pp. 37–53, Jan. 2016, doi: 10.1016/j.neuron.2015.11.013.

[190] A. T. Marvian, D. J. Koss, F. Aliakbari, D. Morshedi, and T. F. Outeiro, “In vitro models of synucleinopathies: informing on molecular mechanisms and protective strategies,” *J. Neurochem.*, vol. 150, no. 5, pp. 535–565, Sep. 2019, doi: 10.1111/jnc.14707.

[191] P.-O. Fernagut and M.-F. Chesselet, “Alpha-synuclein and transgenic mouse models,” *Neurobiol. Dis.*, vol. 17, no. 2, pp. 123–130, Nov. 2004, doi: 10.1016/j.nbd.2004.07.001.

[192] J. L. Badger, O. Cordero-Llana, E. M. Hartfield, and R. Wade-Martins, “Parkinson’s disease in a dish - Using stem cells as a molecular tool,” *Neuropharmacology*, vol. 76 Pt A, pp. 88–96, Jan. 2014, doi: 10.1016/j.neuropharm.2013.08.035.

[193] J. M. Baena-Montes, S. Avazzadeh, and L. R. Quinlan, “α-synuclein pathogenesis in hiPSC models of Parkinson’s disease,” *Neuronal Signal.*, vol. 5, no. 2, p. NS20210021, Jun. 2021, doi: 10.1042/NS20210021.

[194] K. Singh Dolt, F. Hammachi, and T. Kunath, “Modeling Parkinson’s disease with induced pluripotent stem cells harboring α-synuclein mutations,” *Brain Pathol. Zurich Switz.*, vol. 27, no. 4, pp. 545–551, Jul. 2017, doi: 10.1111/bpa.12526.

[195] H. Braak, M. Sastre, and K. Del Tredici, “Development of alpha-synuclein immunoreactive astrocytes in the forebrain parallels stages of intraneuronal pathology in sporadic Parkinson’s disease,” *Acta Neuropathol. (Berl.)*, vol. 114, no. 3, pp. 231–241, Sep. 2007, doi: 10.1007/s00401-007-0244-3.

[196] J. N. Le Grand, L. Gonzalez-Cano, M. A. Pavlou, and J. C. Schwamborn, “Neural stem cells in Parkinson’s disease: a role for neurogenesis defects in onset and progression,” *Cell. Mol. Life Sci. CMLS*, vol. 72, no. 4, pp. 773–797, Feb. 2015, doi: 10.1007/s00018-014-1774-1.

[197] C. A. Morato Torres, Z. Wassouf, F. Zafar, D. Sastre, T. F. Outeiro, and B. Schüle, “The Role of Alpha-Synuclein and Other Parkinson’s Genes in Neurodevelopmental and Neurodegenerative Disorders,” *Int. J. Mol. Sci.*, vol. 21, no. 16, p. 5724, Aug. 2020, doi: 10.3390/ijms21165724.

[198] V. Ghiglieri, V. Calabrese, and P. Calabresi, “Alpha-Synuclein: From Early Synaptic Dysfunction to Neurodegeneration,” *Front. Neurol.*, vol. 9, p. 295, 2018, doi: 10.3389/fneur.2018.00295.

[199] P. Garcia-Reitboeck *et al.*, “Endogenous alpha-synuclein influences the number of dopaminergic neurons in mouse substantia nigra,” *Exp. Neurol.*, vol. 248, pp. 541–545, Oct. 2013, doi: 10.1016/j.expneurol.2013.07.015.

[200] L. M. A. Oliveira *et al.*, “Elevated α-synuclein caused by SNCA gene triplication impairs neuronal differentiation and maturation in Parkinson’s patient-derived induced pluripotent stem cells,” *Cell Death Dis.*, vol. 6, no. 11, p. e1994, Nov. 2015, doi: 10.1038/cddis.2015.318.

[201] A. Matejuk and R. M. Ransohoff, “Crosstalk Between Astrocytes and Microglia: An Overview,” *Front. Immunol.*, vol. 11, p. 1416, 2020, doi: 10.3389/fimmu.2020.01416.

[202] I. D. Vainchtein and A. V. Molofsky, “Astrocytes and Microglia: In Sickness and in Health,” *Trends Neurosci.*, vol. 43, no. 3, pp. 144–154, Mar. 2020, doi: 10.1016/j.tins.2020.01.003.

[203] M. K. Jha, M. Jo, J.-H. Kim, and K. Suk, “Microglia-Astrocyte Crosstalk: An Intimate

Molecular Conversation," *The Neuroscientist*, vol. 25, no. 3, pp. 227–240, Jun. 2019, doi: 10.1177/1073858418783959.

[204] Y. Shinozaki *et al.*, "Transformation of Astrocytes to a Neuroprotective Phenotype by Microglia via P2Y1 Receptor Downregulation," *Cell Rep.*, vol. 19, no. 6, pp. 1151–1164, May 2017, doi: 10.1016/j.celrep.2017.04.047.

[205] S. A. Liddelow *et al.*, "Neurotoxic reactive astrocytes are induced by activated microglia," *Nature*, vol. 541, no. 7638, pp. 481–487, Jan. 2017, doi: 10.1038/nature21029.

[206] D. Béraud *et al.*, "α-Synuclein Alters Toll-Like Receptor Expression," *Front. Neurosci.*, vol. 5, p. 80, 2011, doi: 10.3389/fnins.2011.00080.

[207] E. F. Garland, I. J. Hartnell, and D. Boche, "Microglia and Astrocyte Function and Communication: What Do We Know in Humans?," *Front. Neurosci.*, vol. 16, p. 824888, 2022, doi: 10.3389/fnins.2022.824888.

[208] J. Rostami *et al.*, "Crosstalk between astrocytes and microglia results in increased degradation of α-synuclein and amyloid-β aggregates," *J. Neuroinflammation*, vol. 18, no. 1, p. 124, Jun. 2021, doi: 10.1186/s12974-021-02158-3.

[209] P. K. Peterson, S. Hu, J. Salak-Johnson, T. W. Molitor, and C. C. Chao, "Differential production of and migratory response to beta chemokines by human microglia and astrocytes," *J. Infect. Dis.*, vol. 175, no. 2, pp. 478–481, Feb. 1997, doi: 10.1093/infdis/175.2.478.

[210] M. V. Sofroniew, "Molecular dissection of reactive astrogliosis and glial scar formation," *Trends Neurosci.*, vol. 32, no. 12, pp. 638–647, Dec. 2009, doi: 10.1016/j.tins.2009.08.002.

[211] C. Escartin *et al.*, "Reactive astrocyte nomenclature, definitions, and future directions," *Nat. Neurosci.*, vol. 24, no. 3, pp. 312–325, Mar. 2021, doi: 10.1038/s41593-020-00783-4.

[212] M. V. Sofroniew, "Astrogliosis," *Cold Spring Harb. Perspect. Biol.*, vol. 7, no. 2, p. a020420, Nov. 2014, doi: 10.1101/cshperspect.a020420.

[213] M. V. Sofroniew, "Astrocyte Reactivity: Subtypes, States, and Functions in CNS Innate Immunity," *Trends Immunol.*, vol. 41, no. 9, pp. 758–770, Sep. 2020, doi: 10.1016/j.it.2020.07.004.

[214] Y.-Y. Fan and J. Huo, "A1/A2 astrocytes in central nervous system injuries and diseases: Angels or devils?," *Neurochem. Int.*, vol. 148, p. 105080, Sep. 2021, doi: 10.1016/j.neuint.2021.105080.

[215] T. Shabab, R. Khanabdali, S. Z. Moghadamtousi, H. A. Kadir, and G. Mohan, "Neuroinflammation pathways: a general review," *Int. J. Neurosci.*, vol. 127, no. 7, pp. 624–633, Jul. 2017, doi: 10.1080/00207454.2016.1212854.

[216] W.-C. Huang and M.-C. Hung, “Beyond NF-κB activation: nuclear functions of IκB kinase α,” *J. Biomed. Sci.*, vol. 20, no. 1, p. 3, Jan. 2013, doi: 10.1186/1423-0127-20-3.

[217] M. Karin and Y. Ben-Neriah, “Phosphorylation meets ubiquitination: the control of NF-[kappa]B activity,” *Annu. Rev. Immunol.*, vol. 18, pp. 621–663, 2000, doi: 10.1146/annurev.immunol.18.1.621.

[218] D. Baltimore, “NF-κB is 25,” *Nat. Immunol.*, vol. 12, no. 8, pp. 683–685, Jul. 2011, doi: 10.1038/ni.2072.

[219] T. Liu, L. Zhang, D. Joo, and S.-C. Sun, “NF-κB signaling in inflammation,” *Signal Transduct. Target. Ther.*, vol. 2, p. 17023, Jul. 2017, doi: 10.1038/sigtrans.2017.23.

[220] R. Schreck and P. A. Baeuerle, “NF-kappa B as inducible transcriptional activator of the granulocyte-macrophage colony-stimulating factor gene,” *Mol. Cell. Biol.*, vol. 10, no. 3, pp. 1281–1286, Mar. 1990, doi: 10.1128/mcb.10.3.1281-1286.1990.

[221] T.-W. Liu, C.-M. Chen, and K.-H. Chang, “Biomarker of Neuroinflammation in Parkinson’s Disease,” *Int. J. Mol. Sci.*, vol. 23, no. 8, p. 4148, Apr. 2022, doi: 10.3390/ijms23084148.

[222] J. Sancéau, T. Kaisho, T. Hirano, and J. Wietzerbin, “Triggering of the human interleukin-6 gene by interferon-gamma and tumor necrosis factor-alpha in monocytic cells involves cooperation between interferon regulatory factor-1, NF kappa B, and Sp1 transcription factors,” *J. Biol. Chem.*, vol. 270, no. 46, pp. 27920–27931, Nov. 1995, doi: 10.1074/jbc.270.46.27920.

[223] S. Giridharan and M. Srinivasan, “Mechanisms of NF-κB p65 and strategies for therapeutic manipulation,” *J. Inflamm. Res.*, vol. 11, pp. 407–419, 2018, doi: 10.2147/JIR.S140188.

[224] X.-Y. Xiong, Y. Tang, and Q.-W. Yang, “Metabolic changes favor the activity and heterogeneity of reactive astrocytes,” *Trends Endocrinol. Metab.*, vol. 33, no. 6, pp. 390–400, Jun. 2022, doi: 10.1016/j.tem.2022.03.001.

[225] J. L. Robb, N. A. Hammad, P. G. Weightman Potter, J. K. Chilton, C. Beall, and K. L. J. Ellacott, “The metabolic response to inflammation in astrocytes is regulated by nuclear factor-kappa B signaling,” *Glia*, vol. 68, no. 11, pp. 2246–2263, 2020, doi: 10.1002/glia.23835.

[226] D. Pamies *et al.*, “Neuroinflammatory Response to TNFα and IL1β Cytokines Is Accompanied by an Increase in Glycolysis in Human Astrocytes In Vitro,” *Int. J. Mol. Sci.*, vol. 22, no. 8, p. 4065, Apr. 2021, doi: 10.3390/ijms22084065.

[227] M. G. Vander Heiden *et al.*, “Evidence for an alternative glycolytic pathway in rapidly proliferating cells,” *Science*, vol. 329, no. 5998, pp. 1492–1499, Sep. 2010, doi: 10.1126/science.1188015.

[228] B. Zhou, Y.-X. Zuo, and R.-T. Jiang, “Astrocyte morphology: Diversity, plasticity, and role in neurological diseases,” *CNS Neurosci. Ther.*, vol. 25, no. 6, pp. 665–673, Jun. 2019, doi: 10.1111/cns.13123.

[229] H. Tomimoto, I. Akiguchi, H. Wakita, T. Suenaga, S. Nakamura, and J. Kimura, “Regressive changes of astroglia in white matter lesions in cerebrovascular disease and Alzheimer’s disease patients,” *Acta Neuropathol. (Berl.)*, vol. 94, no. 2, pp. 146–152, Aug. 1997, doi: 10.1007/s004010050686.

[230] H. Qiao *et al.*, “Alpha-synuclein induces microglial migration via PKM2-dependent glycolysis,” *Int. J. Biol. Macromol.*, vol. 129, pp. 601–607, May 2019, doi: 10.1016/j.ijbiomac.2019.02.029.

[231] M. Somayaji, Z. Lanseur, S. J. Choi, D. Sulzer, and E. V. Mosharov, “Roles for α-Synuclein in Gene Expression,” *Genes*, vol. 12, no. 8, Art. no. 8, Aug. 2021, doi: 10.3390/genes12081166.

[232] J. Nunnari and A. Suomalainen, “Mitochondria: in sickness and in health,” *Cell*, vol. 148, no. 6, pp. 1145–1159, Mar. 2012, doi: 10.1016/j.cell.2012.02.035.

[233] I. Vercellino and L. A. Sazanov, “The assembly, regulation and function of the mitochondrial respiratory chain,” *Nat. Rev. Mol. Cell Biol.*, vol. 23, no. 2, pp. 141–161, Feb. 2022, doi: 10.1038/s41580-021-00415-0.

[234] S. Marchi *et al.*, “Mitochondrial and endoplasmic reticulum calcium homeostasis and cell death,” *Cell Calcium*, vol. 69, pp. 62–72, Jan. 2018, doi: 10.1016/j.ceca.2017.05.003.

[235] I. Lopez-Fabuel *et al.*, “Complex I assembly into supercomplexes determines differential mitochondrial ROS production in neurons and astrocytes,” *Proc. Natl. Acad. Sci.*, vol. 113, no. 46, pp. 13063–13068, Nov. 2016, doi: 10.1073/pnas.1613701113.

[236] K. McAvoy and H. Kawamata, “Glial mitochondrial function and dysfunction in health and neurodegeneration,” *Mol. Cell. Neurosci.*, vol. 101, p. 103417, Dec. 2019, doi: 10.1016/j.mcn.2019.103417.

[237] G. Faustini, F. Bono, A. Valerio, M. Pizzi, P. Spano, and A. Bellucci, “Mitochondria and α-Synuclein: Friends or Foes in the Pathogenesis of Parkinson’s Disease?,” *Genes*, vol. 8, no. 12, p. 377, Dec. 2017, doi: 10.3390/genes8120377.

[238] Y.-M. Jeon, Y. Kwon, M. Jo, S. Lee, S. Kim, and H.-J. Kim, “The Role of Glial Mitochondria in α-Synuclein Toxicity,” *Front. Cell Dev. Biol.*, vol. 8, p. 548283, 2020, doi: 10.3389/fcell.2020.548283.

[239] A. Gokoolparsadh *et al.*, “Transcriptional response to mitochondrial protease IMMP2L knockdown in human primary astrocytes,” *Biochem. Biophys. Res. Commun.*, vol. 482, no. 4, pp. 1252–1258, Jan. 2017, doi: 10.1016/j.bbrc.2016.12.024.

[240] O. Gakh, P. Cavadini, and G. Isaya, “Mitochondrial processing peptidases,”

Biochim. Biophys. Acta BBA - Mol. Cell Res., vol. 1592, no. 1, pp. 63–77, Sep. 2002, doi: 10.1016/S0167-4889(02)00265-3.

[241] A. Subramanian *et al.*, “Gene set enrichment analysis: A knowledge-based approach for interpreting genome-wide expression profiles,” *Proc. Natl. Acad. Sci.*, vol. 102, no. 43, pp. 15545–15550, Oct. 2005, doi: 10.1073/pnas.0506580102.

[242] K. Nakamura, “α-Synuclein and mitochondria: partners in crime?,” *Neurother. J. Am. Soc. Exp. Neurother.*, vol. 10, no. 3, pp. 391–399, Jul. 2013, doi: 10.1007/s13311-013-0182-9.

[243] E. M. Rocha, B. De Miranda, and L. H. Sanders, “Alpha-synuclein: Pathology, mitochondrial dysfunction and neuroinflammation in Parkinson’s disease,” *Neurobiol. Dis.*, vol. 109, no. Pt B, pp. 249–257, Jan. 2018, doi: 10.1016/j.nbd.2017.04.004.

[244] R. C. Scarpulla, “Metabolic control of mitochondrial biogenesis through the PGC-1 family regulatory network,” *Biochim. Biophys. Acta*, vol. 1813, no. 7, pp. 1269–1278, Jul. 2011, doi: 10.1016/j.bbamcr.2010.09.019.

7. Appendix

7.1 Manuscript IV

frontiers in Cell and Developmental Biology

ORIGINAL RESEARCH
published: 05 November 2021
doi: 10.3389/fcell.2021.740758

iPSC-Derived Microglia as a Model to Study Inflammation in Idiopathic Parkinson's Disease

*Katja Badanjak[1], Patrycja Mulica[1], Semra Smajic[1], Sylvie Delcambre[1], Leon-Charles Tranchevent[1], Nico Diederich[2], Thomas Rauen[3], Jens C. Schwamborn[1], Enrico Glaab[1], Sally A. Cowley[4], Paul M. A. Antony[1,5], Sandro L. Pereira[1], Carmen Venegas[1] and Anne Grünewald[1,6]**

[1] Luxembourg Centre for Systems Biomedicine, University of Luxembourg, Luxembourg, Luxembourg, [2] Centre Hospitalier de Luxembourg (CHL), Luxembourg, Luxembourg, [3] Department of Cell and Developmental Biology, Max Planck Institute for Molecular Biomedicine, Münster, Germany, [4] James Martin Stem Cell Facility, Sir William Dunn School of Pathology, University of Oxford, Oxford, United Kingdom, [5] Disease Modeling and Screening Platform (DMSP), Luxembourg Institute of Systems Biomedicine, University of Luxembourg and Luxembourg Institute of Health, Luxembourg, Luxembourg, [6] Institute of Neurogenetics, University of Lübeck, Lübeck, Germany

OPEN ACCESS

Edited by:
Andreas Hermann, University Hospital Rostock, Germany

Reviewed by:
Qian Chen, Warren Alpert Medical School of Brown University, United States
Björn Spittau, Bielefeld University, Germany

***Correspondence:**
Anne Grünewald
anne.gruenewald@uni.lu

Specialty section:
This article was submitted to Stem Cell Research, a section of the journal Frontiers in Cell and Developmental Biology

Received: *13 July 2021*
Accepted: *08 October 2021*
Published: *05 November 2021*

Citation:
Badanjak K, Mulica P, Smajic S, Delcambre S, Tranchevent L-C, Diederich N, Rauen T, Schwamborn JC, Glaab E, Cowley SA, Antony PMA, Pereira SL, Venegas C and Grünewald A (2021) iPSC-Derived Microglia as a Model to Study Inflammation in Idiopathic Parkinson's Disease. Front. Cell Dev. Biol. 9:740758. doi: 10.3389/fcell.2021.740758

Parkinson's disease (PD) is a neurodegenerative disease with unknown cause in the majority of patients, who are therefore considered "idiopathic" (IPD). PD predominantly affects dopaminergic neurons in the substantia nigra pars compacta (SNpc), yet the pathology is not limited to this cell type. Advancing age is considered the main risk factor for the development of IPD and greatly influences the function of microglia, the immune cells of the brain. With increasing age, microglia become dysfunctional and release pro-inflammatory factors into the extracellular space, which promote neuronal cell death. Accordingly, neuroinflammation has also been described as a feature of PD. So far, studies exploring inflammatory pathways in IPD patient samples have primarily focused on blood-derived immune cells or brain sections, but rarely investigated patient microglia *in vitro*. Accordingly, we decided to explore the contribution of microglia to IPD in a comparative manner using, both, iPSC-derived cultures and postmortem tissue. Our meta-analysis of published RNAseq datasets indicated an upregulation of *IL10* and *IL1B* in nigral tissue from IPD patients. We observed increased expression levels of these cytokines in microglia compared to neurons using our single-cell midbrain atlas. Moreover, *IL10* and *IL1B* were upregulated in IPD compared to control microglia. Next, to validate these findings *in vitro*, we generated IPD patient microglia from iPSCs using an established differentiation protocol. IPD microglia were more readily primed as indicated by elevated *IL1B* and *IL10* gene expression and higher mRNA and protein levels of NLRP3 after LPS treatment. In addition, IPD microglia had higher phagocytic capacity under basal conditions—a phenotype that was further exacerbated upon stimulation with LPS, suggesting an aberrant microglial function. Our results demonstrate the significance of microglia as the key player in the neuroinflammation process in IPD. While our study highlights the importance of microglia-mediated inflammatory signaling in IPD, further investigations will be needed to explore particular disease mechanisms in these cells.

Keywords: microglia, iPSC, neuroinflammation, idiopathic Parkinson's disease, disease modeling

INTRODUCTION

Parkinson's disease (PD) is an age-related, multifactorial disorder, resulting in the demise of dopaminergic neurons in the substantia nigra pars compacta (SNpc) of the midbrain, which subsequently leads to motor difficulties, tremor, and postural instability in affected individuals (Pang et al., 2019). While there is a genetic component to the disease, with 10% of all cases carrying a mutation in one of the causal PD genes, 90% of patients are deemed idiopathic.

The majority of studies published to date describe molecular mechanisms centered around α-synuclein aggregation, mitochondrial dysfunction, dysregulated autophagy flux, and neuroinflammation as the underlying causes of PD (Wang et al., 2015; Maiti et al., 2017). Interestingly, all of these processes are also affected by aging, which leads to functional decline, both at the physiological and molecular level. Thus, it is not surprising that aging is considered a major risk factor for the development of PD (Jin et al., 2020).

Additionally, "inflammaging" is a novel term coined to define basal, low-level inflammation during adult life that, with time, turns into a destructive, pathological process. On the one hand, lower levels of inflammation are considered to have a positive outcome on the overall cellular state. On the other hand, during prolonged inflammation, beneficial mechanisms of defense start to wear off while damaging insults increase. This phenomenon might explain why seemingly low-grade inflammatory occurrences can have a significant negative impact on health in older individuals (Calabrese et al., 2018).

Inflammation is one of the hallmarks of PD and it is propagated mostly through microglia cells, which are responsible for the innate immune defense of the brain. Early brain tissue studies showed an upregulation of microglial cells in the SNpc and higher expression of human major histocompatibility complex class II (MHC-II) molecules, while in human serum and cerebrospinal fluid (CSF), increased concentrations of cytokines such as IL-1β, IL-6, TNF-α, IL-2, IL-18, and, IL-10 were detected (Nagatsu and Sawada, 2005; Brodacki et al., 2008; Long-Smith et al., 2009; Collins et al., 2012; Wang et al., 2015; Badanjak et al., 2021). In line with these results, our own immunohistochemistry and single-nuclei transcriptomic analyses in postmortem midbrain tissue revealed an increase in abundance and a decrease in the complexity of microglia in IPD tissue, suggestive of an activated state. Moreover, patient microglia presented a disease-specific gene expression signature, indicating a significant role of these cells in the pathogenesis of the movement disorder (Smajić et al., 2020). Also, most recently, genes of the IFN-γ signaling pathway were found to be dysregulated in IPD patients (Magalhaes et al., 2021).

One of the most commonly implicated inflammatory pathways in PD is the inflammasome pathway (Chao et al., 2014; Sebastian-Valverde and Pasinetti, 2020; Yan et al., 2020). The NOD-, LRR-, and pyrin domain-containing protein 3 (NLRP3) is by far the most studied inflammasome, the main function of which is the clearance of pathogens. NLRP3 is a cytosolic sensor of intracellular and extracellular stimuli such as damage-associated and pathogen-associated molecular patterns (DAMPs and PAMPs, respectively). Two signals are necessary to fully activate this pathway, a priming signal and an activation signal. The priming signal is characterized by the upregulation of *IL1B* and *NLRP3* expression, while the secondary signal is characterized by the release of mature cytokines (Swanson et al., 2019). Underlining the relevance of the NLRP3 inflammasome, IL-1β has been associated with disease pathogenesis in multiple PD biomarker studies (Koprich et al., 2008; Su et al., 2008; Nakahira et al., 2011; Gillardon et al., 2012; Pike et al., 2021).

In our current study, we investigated inflammation markers in different models of IPD. First, we explored available RNAseq transcriptomic datasets from postmortem midbrain tissues to assess the expression of key cytokines in IPD. Next, we differentiated microglia from iPSC from IPD and control donors to test whether these cells can mirror the phenotypes observed in the brain. We detected elevated levels of *IL1B* and *IL10* in whole tissue or single cell RNAseq datasets from IPD nigral or midbrain sections. Indicative of the fidelity of iPSC-derived cellular PD models, both *IL1B* and *IL10* were also upregulated in patient microglia upon lipopolysaccharide (LPS) treatment. This coincided with increased protein abundance of NLRP3 in these cells, further implicating the inflammasome in the pathogenesis of PD.

MATERIALS AND METHODS

Bulk RNA Cytokine Expression Analysis

To profile the expression of cytokines in human SN tissue, we used a differential expression meta-analysis of publicly available case-control transcriptomics datasets, including only SN samples, as previously described (Glaab and Schneider, 2015). This provided meta-analysis Z-scores and FDR significance scores for candidate genes of interest (see **Supplementary Table 1**).

Postmortem Single-Nuclei RNA Sequencing of Human Midbrain

To analyze cytokine expression in a single-cell landscape, in this study, we used our previously published snRNAseq dataset from five IPD and six control postmortem midbrain tissues (GSE157783). The normalization, sample integration and cell clustering were performed using *Seurat* (version 3.1.5) in R 4.0.0., as described in Smajić et al. (2020).

The gene expression analysis was performed in neuronal and microglial clusters derived from our snRNAseq dataset (Smajić et al., 2020). For each of the two clusters, pseudobulk populations were created by merging all cells in the cluster from every individual in order to present the overall expression of cytokines. Then, the expression was presented as a sum of expressions of each individual cell and displayed in a bar plot using *"ggplot2"* and *"gg.gap"* packages. The cytokine expression in microglia was shown in both conditions using the *"DotPlot"* function.

Differentiation of Human iPSCs Into Microglia

An IPD patient as well as an age- and gender-matched control (both female, age: 68; IPD patient AAO: 60), who donated skin biopsies for the study, gave written and informed consent. Skin fibroblasts were reprogrammed into iPSCs as previously described (Arias-Fuenzalida et al., 2017). The study was approved by the Comité National d'Ethique de Recherche Luxembourg (CNER, vote 201411/05 V1.3). iPSCs were maintained in mTeSR™1 complete medium (StemCell Technologies). Microglia were differentiated from iPSCs following an established protocol (van Wilgenburg et al., 2013; Haenseler et al., 2017). In brief, embryoid bodies (EBs) were generated from iPSCs in mTeSR Plus (STEMCELL Technologies) supplemented with 50 ng/ml BMP-4 (Invitrogen), 50 ng/ml VEGF (Invitrogen) and 20 ng/ml SCF (Miltenyi). On day 4, EBs were transferred to a low attachment 6-well plate and were replenished with fresh EB media. On day 7, the medium was changed to X-VIVO 15 (Lonza) supplemented with 25 ng/ml IL-3 (Invitrogen), 100 ng/ml M-CSF (Invitrogen), 2 mM Glutamax (Gibco), 1% P/S (Gibco) and 0.055 mM β-mercaptoethanol (Gibco) and the EBs were transferred to T75 flasks (factories). These conditions promoted the generation of macrophage precursors. The factories were kept in culture for up to 6–8 months and macrophage precursors were harvested regularly. Terminal differentiation was achieved by culturing macrophage precursors in advanced DMEM/F12 supplemented with N2, Glutamax, P/S, β-mercaptoethanol, 100 ng/ml IL-34 (Peprotech) and 10 ng/ml GM-CSF (Peprotech). During all steps of the differentiation, cells were incubated at 37°C, 5% CO_2.

Microglia Treatments

Microglia were seeded into 6-well plates at a density of 1 × 10^6 cells/well. Upon treatment with 100 ng/ml LPS (Thermo Fisher Scientific 00-4976-93) for 3 h, cells were subjected to protein and RNA extractions. For functional analyses, microglia were seeded into 96-well glass-bottom plates at a density of 25,000 cells/well. Cells were treated with 50,000 Zymosan bioparticles (Thermo Fisher Scientific) per well for 45 min. After, cells were subjected to fixation (described in more detail below).

RNA Isolation and Quantitative PCR

RNA was isolated from microglia using the RNeasy RNA isolation kit (Qiagen, 74106) following the manufacturer's instructions for direct RNA extraction from the plate. cDNA was synthesized from 200 ng of RNA using the SuperScript™ III Reverse Transcriptase (Invitrogen, 18080044). Quantitative PCR (qPCR) was performed using iQ SYBR Green (Biorad, 170-8885). The PCR reaction was run on a LightCycler 480 (Roche). The samples were denatured for 5 min at 95°C. Amplification ran over 45 cycles with a denaturation step of 10 s at 95°C, primer annealing of 10 s at 60°C, and elongation of 10 s at 75°C. The expression of *IL1B*, *IL10*, *LRRK2*, and *NLRP3* was normalized to the expression of the housekeeping gene *ACTB*.

Western Blotting

Total protein from microglia cultures were extracted directly from the plate, using ice cold RIPA buffer (Pierce) supplemented with 1X Protease/phosphatase Inhibitor Cocktail (Thermo Fisher Scientific). The whole well was washed multiple times, on ice, and the lysate suspension was transferred to an Eppendorf tube and vortexed for 20 s followed by incubation on ice for 20 min. The samples were centrifuged at 21,130 g for 20 min at 4°C. The protein concentration of the cell lysates was measured using a bicinchoninic acid assay using Pierce™ BCA protein kit (Thermo Fisher Scientific) following the manufacturer's instructions.

Cell lysates were denatured in a loading buffer at 95°C for 5 min prior to loading on the gels. Proteins were then separated on NuPAGE 4–12% Bis-Tris gels (Invitrogen) in NuPAGE MES Running Buffer (NP0002) and transferred on a 0.2 µm nitrocellulose membrane. Membranes were blocked with 5% milk in TBS supplemented with Tween-20 (TBST, 10 mM Tris-HCl, 150 mM NaCl, 0.1% Tween-20, pH 8.0) for 1 h at RT. Thereafter, membranes were incubated overnight at 4°C with the following primary antibodies: 1:1,000 anti-NLRP3 (D4D8T, Cell Signaling), 1:500 anti-LRRK2 (75–188, UC Davis), 1:10,000 anti-β-actin (A1978, Sigma). On the next day, membranes were washed three times in TBST and incubated with the respective secondary antibodies for 1 h at RT. Immunoreactivity was detected by enhanced chemiluminescence reaction (ECL select Western blotting detection reagent, GE Healthcare) or near-infrared detection (Odyssey, Li-COR).

Immunocytochemistry and Image Analysis

IPSCs and microglia were fixed in 4% PFA (Thermo Fisher Scientific, Alfa Aesar J61899) for 15 min and washed twice with PBS (Westburg, LO BE17-513F). The cells were permeabilized and blocked in PBS containing 0.25% Triton X-100 and 1% BSA for 1 h at RT followed by overnight incubation with primary antibodies: anti-Nanog (3580S, Bioke), anti-Sox2 (sc-365823, Santa Cruz), anti-Oct4 (ab19857, Abcam), anti-Iba1 (ab5076, Abcam), anti-P2RY12 (APR-020-F, Alomone labs). On the next day, cells were washed and incubated with the corresponding secondary antibodies. Thereafter, another three washing steps with PBS were completed and Hoechst was used as a counterstain at 0.1 mg/ml for 15 min in PBS. To mount the cover slips onto slides, Prolong Antifade mounting media (Thermo Fisher Scientific) was used. Acquisition of microglia images was performed using a Zeiss LSM 710 and Yokogawa CV8000 microscope, and images of iPSC were acquired with a Zeiss Axio Imager M2. All acquired images were normalized for secondary-only antibody control, to confirm specificity of the signal observed.

For quantitative image analysis, custom code was implemented using MATLAB 2020a, and computations were performed using the High-Performance Computing (HPC) infrastructure of the University of Luxembourg (Varrette et al., 2014). Briefly, the "ZymosanAreaByIba1Area" is the ratio between Zymosan positive pixels and Iba1 positive pixels per

field of view. Furthermore, the mean abundance of Iba1 has been quantified as ratio of Iba1 area per nuclei count. The underlying MATLAB code is available upon request.

Statistics

All experiments carried out using iPSC-derived microglia were performed with 3–4 biological replicates. The data was normalized by the average of values per replicate. For statistical analyses, GraphPad Prism software (version 9) was used. To evaluate the presence of outliers, we used the ROUT test. Two-way ANOVA was used for grouped values. Differences were considered significant (*) when p-values were below 0.05.

RESULTS

Idiopathic Postmortem Midbrain Tissue Is Exhibiting Increased Cytokine Gene Expression

Studies implicating inflammatory cytokines in PD have been mostly conducted on neurotoxin and genetic animal models, or by analyzing peripheral blood samples and CSF from PD patients (Badanjak et al., 2021). To further confirm if these findings are indeed occurring in the brain of IPD patients, we analyzed available transcriptomic datasets. The transcriptomics data of human IPD and control SN revealed a significant increase in *IL1B* and *IL10* expression in the patient tissue ($FDR = 0.023$; $FDR = 0.0067$, respectively) (**Figure 1A** and **Supplementary Table 1**). A recent study showed that inflammation is not only mediated by microglia but can also be observed in neurons from an IPD mouse model (Panicker et al., 2020). In order to understand whether the detected immune signatures in the human SN are also cell-type specific, we examined our midbrain snRNAseq dataset to obtain an insight into transcriptional changes with single-cell resolution. We confirmed that the expression of cytokines is specific to microglia (**Figure 1B**). Further analysis of the microglia population revealed higher expression and a larger percentage of expressing cells in IPD compared to control tissue (**Figure 1C** and **Supplementary Table 2**).

Characterization of iPSC-Derived Microglia Model

IPD patient and control microglia were generated using an established protocol (van Wilgenburg et al., 2013; Haenseler et al., 2017; **Figure 2A**). The available iPSC lines were characterized by immunostaining with the stem cell markers Nanog, Sox2 and Oct4 (**Figure 2B**). Differentiation of iPSCs into microglia was achieved with the addition of multiple factors throughout the differentiation process (**Figure 2A**) to mimic microglia development in the human embryo. The microglial identity of cells was confirmed by positive expression of Iba1 and purinergic receptor (P2RY12) (**Figure 2C**). Comparable Iba1 areas per nuclei suggest that the disease status of the investigated lines did not have an impact on the differentiation procedure (**Figure 2D**). Additionally, we wanted to functionally characterize microglia cells by treating them with Zymosan bioparticles and assessing their phagocytic ability. While both control and IPD microglia were able to phagocyte the bioparticles, IPD microglia had a higher capacity (mean: 0.02493, $SD = 0.02472$) compared to control microglia (mean: 0.01606, $SD = 0.01304$; ANOVA: $^{***}p = 0.0004$). Furthermore, although the mean phagocytic capacity after LPS treatment was not significantly different between untreated and treated cells, IPD microglia had a significantly higher uptake of Zymosan particles compared to control cells upon addition of LPS (CTR/LPS mean: 0.01897, $SD = 0.01695$; IPD/LPS mean: 0.02683, $SD = 0.02835$; ANOVA: $^{**}p = 0.0070$) (**Figure 3**).

Upregulation of NOD-, LRR- and Pyrin Domain-Containing Protein 3 Inflammasome Components in Idiopathic Microglia

To test the transferability of our findings from postmortem single-nuclei transcriptomics to live cells, we investigated the gene expression of *IL1B* and *IL10* in iPSC-derived IPD microglia. Moreover, we quantified the mRNA and protein levels of the NLRP3 inflammasome, the inflammatory pathway most associated with chronic inflammation in PD. The priming step in inflammasome assembly is frequently mimicked by LPS

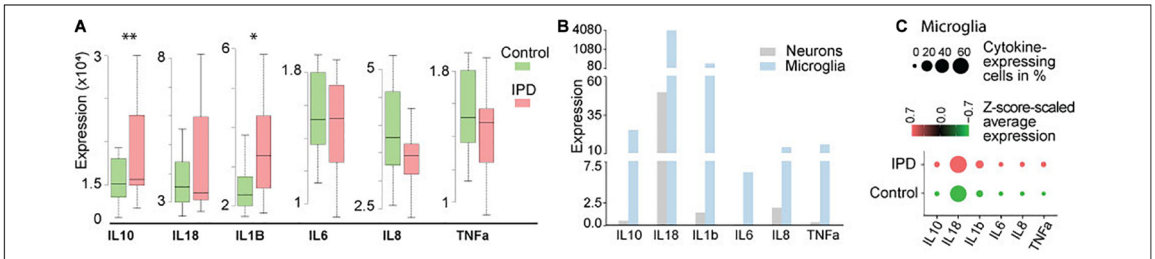

FIGURE 1 | Cytokine expression in bulk RNA-seq and single-nuclei RNA-seq datasets. **(A)** Bulk analysis of SN tissue displays higher expression of *IL1B* and *IL10* in IPD ($FDR = 0.023$; $FDR = 0.0067$). **(B)** Single-nuclei analysis of the human midbrain shows that the overall expression of cytokines is higher in microglia (3903 cells) than in neurons (5314 cells). **(C)** Cytokines are expressed in a large number of IPD and control microglia. Z-score-scaled average expression per cluster shows higher levels in IPD compared to control microglia. "*DotPlot*" function (Seurat package) was used to visualize expression and percentage of cytokine-expressing cells. $^{*}p < 0.05$; $^{**}p < 0.01$; IPD, idiopathic PD.

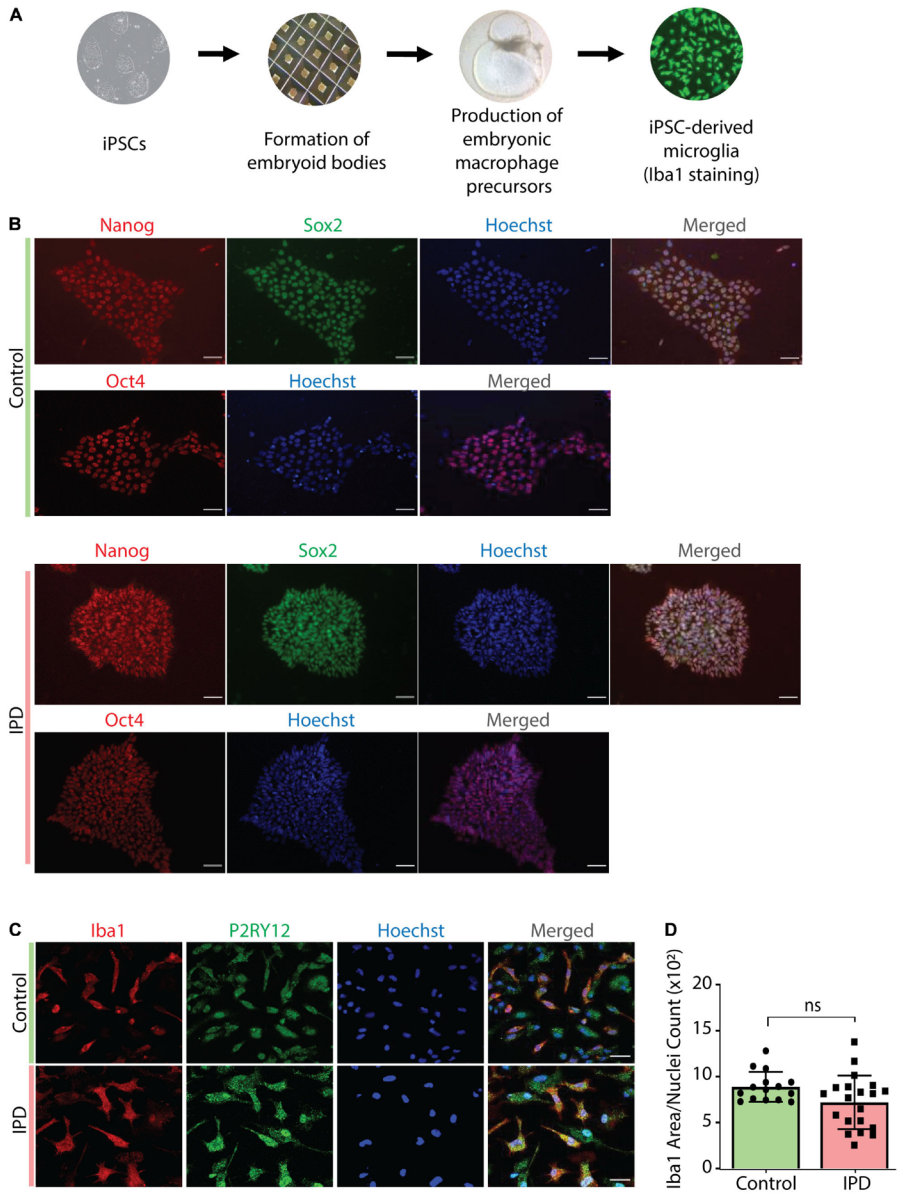

FIGURE 2 | Characterization of cellular models used in the study. **(A)** Overview of the protocol used to derive microglia from iPSCs. **(B)** Immunostaining with Nanog, Sox-2 and Oct-4, coupled with nuclear staining with Hoechst, confirmed the iPSC identity of our cells. Scale bar, 50 μm. **(C)** Terminally differentiated microglia were confirmed to express the microglia-specific markers Iba1 and P2RY12. Scale bar, 30 μm. **(D)** Quantification of data from **(C)**; no difference in Iba1 protein levels (Iba1 area was normalized for nuclei count); IPD, idiopathic PD; CTR, healthy control.

treatment (McKee and Coll, 2020). At baseline, IPD and control microglia did not show significant differences (data not shown). However, upon LPS treatment, the expression levels of *IL1B* and *IL10* increased significantly in both conditions compared to the respective untreated cells (*IL1B* CTR/LPS fold mean: 1.558, $SD = 0.117$; ANOVA: $^{**}p = 0.0098$; IPD/LPS fold mean: 3.880, $SD = 0.323$; ANOVA: $^{****}p < 0.0001$; *IL10* CTR/LPS fold mean: 3.409, $SD = 0.342$, ANOVA: $^{****}p < 0.0001$; IPD/LPS

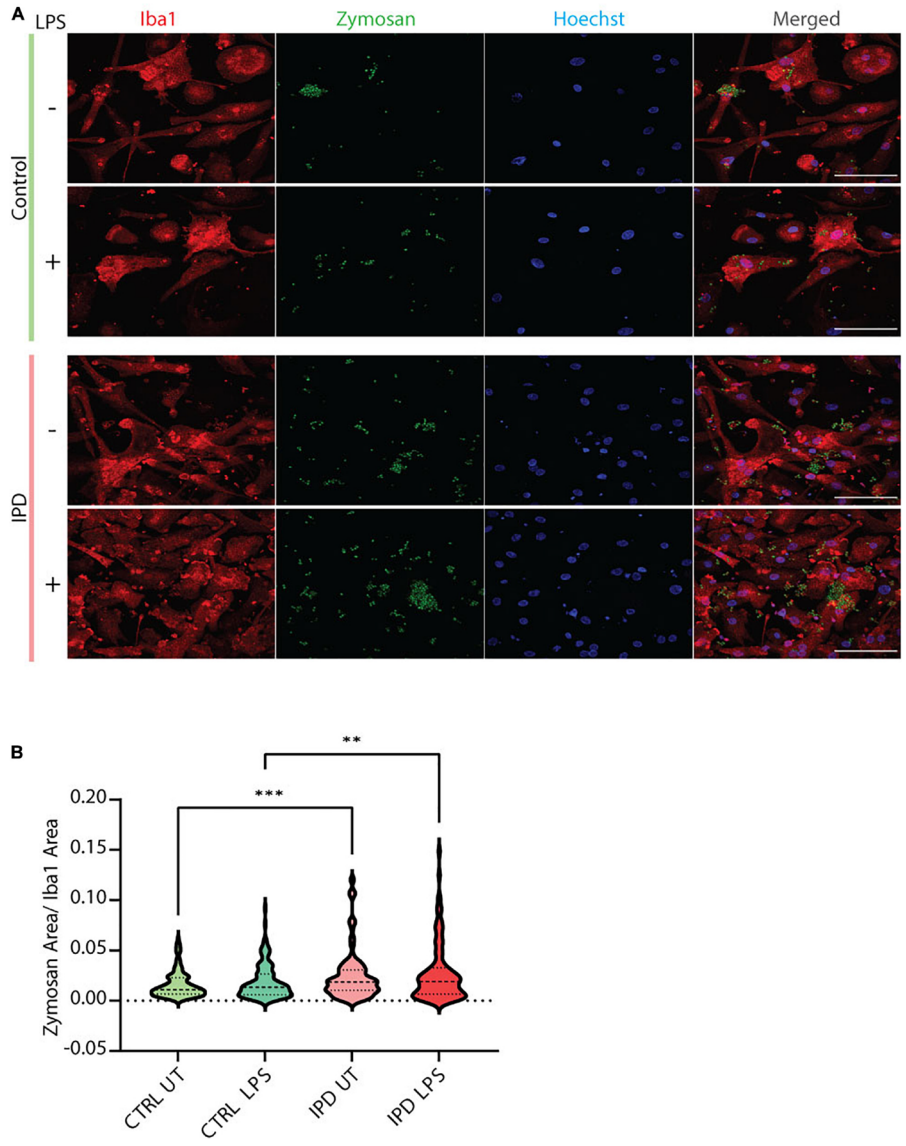

FIGURE 3 | Functional assessment of iPSC-derived microglia. **(A)** Representative immunostaining showing the functional ability of cultured control and IPD microglia treated with Zymosan bioparticles. Scale bar, 50 μm. **(B)** Quantification of data from **(A)**; IPD microglia have higher phagocytic capacity (Zymosan area was normalized for Iba1 area) compared to control cells. $^{**}p < 0.01$; $^{***}p < 0.001$; IPD, idiopathic PD; CTRL, healthy control.

fold mean: 7.717, $SD = 0.530$, ANOVA: $^{****}p < 0.0001$). When comparing the treatment response between both conditions, IPD microglia showed significantly higher *IL1B* and *IL10* expressions fold changes compared to control cells (*IL1B* LPS mean: 2.719, $SD = 1.642$; ANOVA: $^{****}p < 0.0001$; *IL10* LPS mean: 5.563, $SD = 3.047$, ANOVA: $^{****}p < 0.0001$). Additionally, when investigating *NLRP3* expression, only IPD microglia showed a significant upregulation upon LPS treatment, compared to both untreated IPD cells (*NLRP3* IPD/LPS fold mean: 3.984, $SD = 0.250$; ANOVA: $^{****}p < 0.0001$) and to LPS-treated healthy microglia (*NLRP3* LPS mean: 2.627, $SD = 1.918$; ANOVA: $^{****}p < 0.0001$) (**Figure 4A**).

Furthermore, NLRP3 protein levels corroborated the gene expression results. Again, both control and IPD microglia had significantly higher NLRP3 protein levels upon LPS addition compared to their respective basal levels (CTR/LPS fold mean:

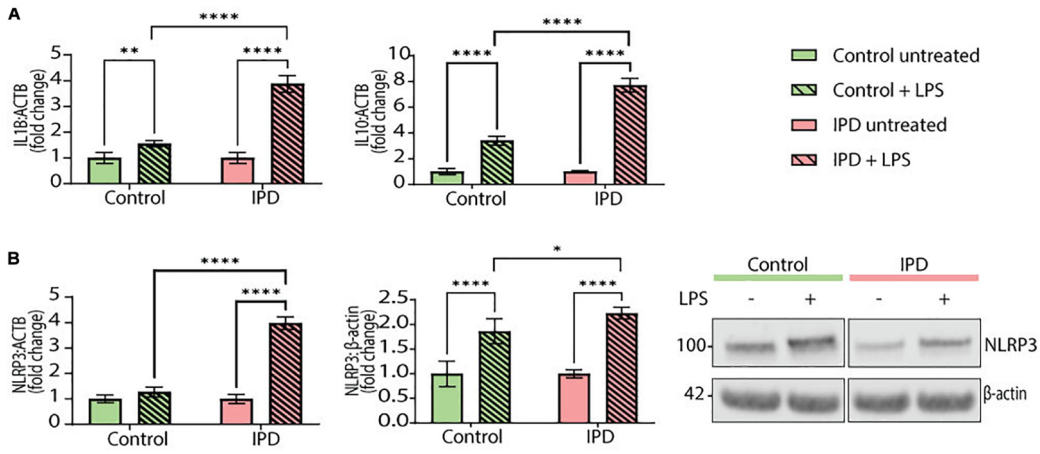

FIGURE 4 | Inflammatory phenotype and LRRK2 levels in iPSC-derived microglia. **(A)** *IL1B* and *IL10* gene expression (normalized to *ACTB*) in control and IPD microglia; a quantitative PCR showed higher gene expressions of *IL1B* and *IL10* in IPD compared to control cells upon priming with LPS (100 ng/ml). Values are represented as fold changes of untreated cells. **(B)** NLRP3 mRNA and protein levels (normalized to *ACTB* and β-actin, respectively) are increased in IPD microglia compared to control cells upon priming with LPS (100 ng/ml). Values are represented as fold change of untreated cells. $^{*}p < 0.05$; $^{**}p < 0.01$; $^{****}p < 0.0001$; IPD, idiopathic PD, NLRP3, NOD-, LRR-, and pyrin domain-containing protein 3.

1.866, $SD = 0.254$; IPD/LPS fold mean: 2.231, SD = 0.115; ANOVA: $^{****}p < 0.0001$). However, when comparing across conditions, IPD microglia showed a significant upregulation compared to treated control glia (LPS mean: 2.048, $SD = 0.2585$; ANOVA: $^{*}p = 0.0416$) (**Figure 4B**).

Downregulation of Leucine-Rich Repeat Kinase 2 Upon Lipopolysaccharide Treatment in Idiopathic Microglia

Leucine-rich repeat kinase 2 (LRRK2) is a protein implicated in both the idiopathic and genetic forms of PD. It is highly expressed in cells of the immune system and associated with immune disorders (Van Limbergen et al., 2009; Umeno et al., 2011) as well as infectious diseases (Zhang et al., 2009; Weindel et al., 2020). Its pathogenic effects have been extensively studied in the context of LRRK2-PD and in some instances in IPD. Basal levels of *LRRK2* expression were significantly downregulated in IPD microglia (CTR mean: 1.355, $SD = 0.136$; IPD mean: 0.929, $SD = 0.244$; ANOVA: $^{*}p = 0.0226$), while control cells had significantly lower expression upon LPS treatment (CTR mean: 1.355, $SD = 0.136$; CTR/LPS mean: 0.915, $SD = 0.178$; ANOVA: $^{*}p = 0.0186$) (**Figure 5A**). Furthermore, we investigated LRRK2 protein levels in our iPSC-derived microglia and saw a non-significant downregulation in untreated IPD microglia compared to controls (CTR mean: 1.332, $SD = 0.257$; IPD mean: 0.615, $SD = 0.425$; ANOVA: $p = 0.0593$). Moreover, after stimulating the cells with LPS, IPD microglia had significantly less LRRK2 protein compared to LPS-treated control glia (CTR/LPS mean: 1.649, $SD = 0.391$; IPD/LPS mean: 0.402, $SD = 0.215$; ANOVA: $^{**}p = 0.0036$) (**Figure 5B**).

DISCUSSION

Although the majority of PD cases suffer from the idiopathic form of the movement disorder, the cause of neurodegeneration in these individuals has not been extensively investigated. Genome wide association studies (GWAS) identified over 40 PD risk loci, the majority of which overlaps with known autosomal dominant PD genes, most notably *SNCA* and *LRRK2*, while other studies revealed the presence of heterozygous variants in autosomal recessively inherited PD genes (Simón-Sánchez et al., 2009; Nalls et al., 2014; Zeng et al., 2018; Germer et al., 2019; Lai et al., 2020). The main difficulty scientists are facing when studying IPD is the heterogeneous nature of the disease, which is further exacerbated by a plethora of environmental and epigenetic influences.

Inflammation has been considered a hallmark of PD since the late 1980's, when an upregulation of reactive microglia was first seen in patient brain tissue samples (McGeer et al., 1988). Positron emission tomography (PET) imaging dyes, which allow visualizing activated microglia *in vivo* over time, have been tested as biomarkers for disease progression (Gerhard et al., 2006; Terada et al., 2016; Roussakis and Piccini, 2018). Unfortunately, however, the findings from PET studies have not been successfully transferred to the clinic and the exact molecular mechanisms triggering neuroinflammation in PD currently remain elusive.

Thus, in this study, we investigated patient-derived microglia to explore the inflammatory component of IPD. First, we made use of publicly available transcriptomic data from nigral postmortem tissue to assess the expression of different cytokines in IPD patients compared to age-matched controls. Previous reports established certain secreted cytokines as reliable biomarkers in serum and plasma of PD patients, among them

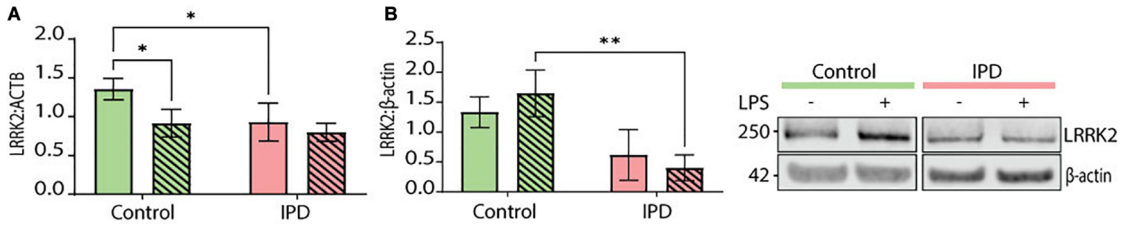

FIGURE 5 | LRRK2 levels in iPSC-derived microglia. **(A)** IPD microglia have a significant decrease of *LRRK2* expression at basal level (normalized to *ACTB*). **(B)** IPD microglia show a significant downregulation of total LRRK2 protein levels (normalized to β-actin) compared to control cells upon LPS treatment only. $^{*}p < 0.05$; $^{**}p < 0.01$; IPD, idiopathic PD; LRRK2, Leucine-rich repeat kinase 2.

IL-1β, IL-18, IL-6, IL-10, IL-8, TNF-α (Nagatsu et al., 2000; Brodacki et al., 2008; Qin et al., 2016). In line with these studies, our meta-analysis of published brain SNpc case-control transcriptomics datasets indicated elevated levels of *IL10* and *IL1B* in IPD patients.

To explore the cellular origin of this upregulation in IPD, we made use of our previously generated snRNAseq dataset from midbrain IPD and control tissue. Multiple cytokines, including *IL10* and *IL1B*, were predominantly expressed in microglia. This is in accordance with microglia acting as the main player of the immune system in the CNS. Moreover, in the same published dataset, we observed an increase in the microglia number as well as morphological alterations, indicative of an activated state, in IPD patients (Smajić et al., 2020). Next, to corroborate our findings from homogenized SN tissue, we investigated whether any of the aforementioned cytokines show an IPD-specific expression pattern in microglia. While we observed an increase in the expression of all investigated candidates in the patient compared to control cells, the levels of *IL10*, *IL18*, and *IL1B* were the most abundant.

Albeit informative, these postmortem results may be confounded by the fact that they only represent the molecular situation during the latest stage of the disease. Thus, to study inflammatory phenotypes and pathways in an *in vitro* IPD model, we differentiated microglia from control and patient-derived iPSCs using a published protocol (van Wilgenburg et al., 2013; Haenseler et al., 2017). While cultured IPD microglia did not show altered morphology (data not shown), we observed elevated phagocytosis in these cells indicative of overactive immune function. Phagocytosis is an integral part of microglial homeostatic function, and is not only involved in the recognition of self and non-self threats, but also in the engulfment of synaptic elements and the pruning process. Furthermore, enhanced and uncontrolled clearance is contributing to synaptic degeneration. Indeed, multiple PD studies showed loss of presynaptic terminals and synaptic changes in PD patient compared to control brains (Delva et al., 2020; Matuskey et al., 2020). It is also worth noting that disrupting the phagocytic ability of mouse glia was sufficient to rescue the neuronal degeneration phenotype observed in these animals after LPS injection (Bodea et al., 2014). Since we observed the differences in phagocytosis already at basal level, one may speculate that the genetic background in IPD glia contributes to the development of the disease. However, it is still unclear whether overactive, defective or perturbed uptake triggers PD pathogenesis (Janda et al., 2018).

To further validate our findings from postmortem tissue, we analyzed different inflammasome components in the iPSC-derived microglia cultures. IPD microglia were more reactive after priming with LPS, as indicated by enhanced expressions of *IL1B* and *IL10*, and higher mRNA and protein levels of NLRP3 compared to treated control cells. Higher levels of *IL1B* and NLRP3 in IPD microglia indicate a stronger priming step, which is necessary for downstream inflammasome activation and immune response. While we are the first to show NLRP3 dysregulation in iPSC-derived IPD microglia, our results are in agreement with findings from genetic PD models. Specifically, α-synuclein fibrils were shown to induce NLRP3 activation, and loss of the PD-associated protein Parkin triggered the release of mitoDAMPs into the cytosol, which in turn activated the NLRP3 inflammasome in mice (Zhong et al., 2016; Gordon et al., 2018; Ji et al., 2020; Pike et al., 2021). Moreover, NLRP3 was shown to regulate *IL10* levels in mice macrophages, with *IL10* production being decreased in NLRP3$^{-/-}$ mice (Gurung et al., 2015; Kobayashi et al., 2016). This is consistent with our observation of *IL10* and *NLRP3* co-regulation. In line with a biomarker study in serum, IPD patients had higher levels of IL-10 compared to healthy individuals (Rentzos et al., 2009). Furthermore, while the relationship of IL-1β and IL-10 has not been extensively studied in the context of PD, there are reports showing that, under inflammatory conditions, IL-10 selectively inhibits the release of IL-1β (Sun et al., 2019). Patient-derived microglia will be a useful model to explore the molecular mechanisms linking IL-10 and IL-1β in PD in more detail.

Further of interest with regard to inflammation in genetic but also IPD is the kinase LRRK2. Affected individuals harboring mutations in LRRK2 closely mirror the clinical picture of IPD patients (Tolosa et al., 2020) with kinase activity dysregulation being a shared feature of both forms of the disease. Due to its high abundance in immune cells, researchers have speculated that LRRK2 may be crucially involved in the regulation of neuroinflammatory processes (Gardet et al., 2010; Di Maio et al., 2018; Fyfe, 2018). Studies investigating *LRRK2* expression in IPD brain tissue showed a significant downregulation in dopaminergic neurons, which may contribute to the pathology

of the movement disorder (Simunovic et al., 2009; Sharma et al., 2011; Yılmazer et al., 2021). In agreement with these reports, we detected significantly reduced *LRRK2* expression and a trend toward lower LRRK2 protein abundance in IPD patient microglia at baseline. Inflammatory insults exacerbated this phenotype, leading to a further reduction in LRRK2 protein levels in the IPD patient-derived cells. However, the exact pathways connecting LRRK2 downregulation to microglia dysfunction in IPD warrant further investigation.

Taken together, inspired by published biomarker studies, we investigated inflammatory phenotypes in different models of IPD. In both, nigral and midbrain RNAseq datasets, we observed a disease-specific upregulation of *IL10* and *IL1B*. Furthermore, from our postmortem single-cell results, we derived that this overexpression predominantly stems from microglia. Next, to test whether we could reproduce this phenotype in a dish, we generated iPSC-derived IPD microglia. Further implicating *IL10* and *IL1B*, in IPD, the expression of these cytokines was also enhanced in patient microglia upon LPS treatment. Finally, we identified an upregulation of NLRP3 on RNA and protein level, corroborating our findings concerning *IL10* and *IL1B*. However, in light of the variability of sporadic PD, our results from a small sample may only be representative for a subset of IPD cases, warranting validation studies in larger cohorts. Moreover, while our study highlights the relevance of microglia in IPD, further experiments will be needed to decipher the exact pathways triggering neuroinflammation in sporadic PD patients.

DATA AVAILABILITY STATEMENT

The datasets presented in this study can be found in online repositories. The names of the repository/repositories and accession number(s) can be found below: https://www.ncbi.nlm.nih.gov/geo/, GSE157783; https://www.ncbi.nlm.nih.gov/geo/, GSE8397.

ETHICS STATEMENT

Patients gave written and informed consent. The study was approved by the Comité National d'Ethique de Recherche Luxembourg (CNER, vote 201411/05 V1.3).

AUTHOR CONTRIBUTIONS

SAC provided training in iPSC-derived microglia. KB, PM, SD, and SLP collected the data. KB, PM, SS, L-CT, PMAA, and EG performed the analysis. KB, PM, SS, PMAA, CV, and AG wrote the manuscript, which was reviewed by all authors. CV and AG conceived the study. ND, TR, and JCS contributed to the establishment of fibroblast cultures and iPSC generation from patient and control cells. AG acquired funding for the study and was in charge of direction and planning of the study.

FUNDING

KB was supported by the Luxembourg National Research Fund (FNR) through the PRIDE15/10907093/CriTiCS grant. SS and PM received funding from the FNR within the framework of the PARK-QC DTU (PRIDE17/12244779/PARK-QC). TR was supported by the EU Joint Programme—Neurodegenerative Disease Research (JPND) project 3DPD. CV was supported by the FNR through the C20/BM/14548100 CORE Junior grant. AG was awarded an FNR ATTRACT career development grant (Model IPD, FNR9631103). Moreover, AG and JCS were supported by the FNR as part of the National Centre of Excellence in Research on Parkinson's disease (NCER-PD, FNR/NCER13/BM/11264123).

ACKNOWLEDGMENTS

We would like to thank Jane Vowles and Cathy Browne from the University of Oxford for sharing their expertise and giving us valuable in-person training on iPSC-derived microglia protocol. In addition, we would like to express our gratitude to Anna-Lena Hallmann and Hans R. Schöler from the Max Planck Institute for Molecular Biomedicine for reprogramming fibroblasts into iPSCs.

SUPPLEMENTARY MATERIAL

The Supplementary Material for this article can be found online at: https://www.frontiersin.org/articles/10.3389/fcell.2021.740758/full#supplementary-material

REFERENCES

Arias-Fuenzalida, J., Jarazo, J., Qing, X., Walter, J., Gomez-Giro, G., Nickels, S. L., et al. (2017). FACS-Assisted CRISPR-Cas9 Genome Editing Facilitates Parkinson's Disease Modeling. *Stem Cell Rep.* 9, 1423–1431. doi: 10.1016/j.stemcr.2017.08.026

Badanjak, K., Fixemer, S., Smajić, S., Skupin, A., and Grünewald, A. (2021). The Contribution of Microglia to Neuroinflammation in Parkinson's Disease. *Int. J. Mol. Sci.* 22:ijms22094676. doi: 10.3390/ijms22094676

Bodea, L.-G., Wang, Y., Linnartz-Gerlach, B., Kopatz, J., Sinkkonen, L., Musgrove, R., et al. (2014). Neurodegeneration by activation of the microglial complement-phagosome pathway. *J. Neurosci.* 34, 8546–8556. doi: 10.1523/JNEUROSCI.5002-13.2014

Brodacki, B., Staszewski, J., Toczyłowska, B., Kozłowska, E., Drela, N., Chalimoniuk, M., et al. (2008). Serum interleukin (IL-2, IL-10, IL-6, IL-4), TNFalpha, and INFgamma concentrations are elevated in patients with atypical and idiopathic parkinsonism. *Neurosci. Lett.* 441, 158–162. doi: 10.1016/j.neulet.2008.06.040

Calabrese, V., Santoro, A., Monti, D., Crupi, R., Di Paola, R., Latteri, S., et al. (2018). Aging and Parkinson's Disease: Inflammaging, neuroinflammation and biological remodeling as key factors in pathogenesis. *Free Radic. Biol. Med.* 115, 80–91. doi: 10.1016/j.freeradbiomed.2017.10.379

Chao, Y., Wong, S. C., and Tan, E. K. (2014). Evidence of inflammatory system involvement in Parkinson's disease. *Biomed Res. Int.* 2014:308654.

Collins, L. M., Toulouse, A., Connor, T. J., and Nolan, Y. M. (2012). Contributions of central and systemic inflammation to the pathophysiology of Parkinson's

disease. *Neuropharmacology* 62, 2154–2168. doi: 10.1016/j.neuropharm.2012.01.028

Delva, A., Van Weehaeghe, D., Koole, M., Van Laere, K., and Vandenberghe, W. (2020). Loss of Presynaptic Terminal Integrity in the Substantia Nigra in Early Parkinson's Disease. *Mov. Disord.* 35, 1977–1986.

Di Maio, R., Hoffman, E. K., Rocha, E. M., Keeney, M. T., Sanders, L. H., De Miranda, B. R., et al. (2018). LRRK2 activation in idiopathic Parkinson's disease. *Sci. Transl. Med.* 10:aar5429. doi: 10.1126/scitranslmed.aar5429

Fyfe, I. (2018). Familial PD gene involved in idiopathic disease. *Nat. Rev. Neurol.* 14:508.

Gardet, A., Benita, Y., Li, C., Sands, B. E., Ballester, I., Stevens, C., et al. (2010). LRRK2 is involved in the IFN-gamma response and host response to pathogens. *J. Immunol.* 185, 5577–5585. doi: 10.4049/jimmunol.1000548

Gerhard, A., Pavese, N., Hotton, G., Turkheimer, F., Es, M., Hammers, A., et al. (2006). In vivo imaging of microglial activation with [11C](R)-PK11195 PET in idiopathic Parkinson's disease. *Neurobiol. Dis.* 21, 404–412. doi: 10.1016/j.nbd.2005.08.002

Germer, E. L., Imhoff, S., Vilariño-Güell, C., Kasten, M., Seibler, P., Brüggemann, N., et al. (2019). The Role of Rare Coding Variants in Parkinson's Disease GWAS Loci. *Front. Neurol.* 10:1284. doi: 10.3389/fneur.2019.01284

Gillardon, F., Schmid, R., and Draheim, H. (2012). Parkinson's disease-linked leucine-rich repeat kinase 2(R1441G) mutation increases proinflammatory cytokine release from activated primary microglial cells and resultant neurotoxicity. *Neuroscience* 208, 41–48. doi: 10.1016/j.neuroscience.2012.02.001

Glaab, E., and Schneider, R. (2015). Comparative pathway and network analysis of brain transcriptome changes during adult aging and in Parkinson's disease. *Neurobiol. Dis.* 74, 1–13. doi: 10.1016/j.nbd.2014.11.002

Gordon, R., Albornoz, E. A., Christie, D. C., Langley, M. R., Kumar, V., Mantovani, S., et al. (2018). Inflammasome inhibition prevents α-synuclein pathology and dopaminergic neurodegeneration in mice. *Sci. Transl. Med.* 10:aah4066. doi: 10.1126/scitranslmed.aah4066

Gurung, P., Li, B., Subbarao Malireddi, R. K., Lamkanfi, M., Geiger, T. L., and Kanneganti, T.-D. (2015). Chronic TLR Stimulation Controls NLRP3 Inflammasome Activation through IL-10 Mediated Regulation of NLRP3 Expression and Caspase-8 Activation. *Sci. Rep.* 5:14488. doi: 10.1038/srep14488

Haenseler, W., Sansom, S. N., Buchrieser, J., Newey, S. E., Moore, C. S., Nicholls, F. J., et al. (2017). A Highly Efficient Human Pluripotent Stem Cell Microglia Model Displays a Neuronal-Co-culture-Specific Expression Profile and Inflammatory Response. *Stem Cell Rep.* 8, 1727–1742. doi: 10.1016/j.stemcr.2017.05.017

Janda, E., Boi, L., and Carta, A. R. (2018). Microglial Phagocytosis and Its Regulation: A Therapeutic Target in Parkinson's Disease? *Front. Mol. Neurosci.* 11:144. doi: 10.3389/fnmol.2018.00144

Ji, Y.-J., Wang, H.-L., Yin, B.-L., and Ren, X.-Y. (2020). Down-regulation of DJ-1 Augments Neuroinflammation via Nrf2/Trx1/NLRP3 Axis in MPTP-induced Parkinson's Disease Mouse Model. *Neuroscience* 442, 253–263. doi: 10.1016/j.neuroscience.2020.06.001

Jin, H., Gu, H.-Y., Mao, C.-J., Chen, J., and Liu, C.-F. (2020). Association of inflammatory factors and aging in Parkinson's disease. *Neurosci. Lett.* 736:135259. doi: 10.1016/j.neulet.2020.135259

Kobayashi, M., Usui, F., Karasawa, T., Kawashima, A., Kimura, H., Mizushina, Y., et al. (2016). NLRP3 Deficiency Reduces Macrophage Interleukin-10 Production and Enhances the Susceptibility to Doxorubicin-induced Cardiotoxicity. *Sci. Rep.* 6:26489. doi: 10.1038/srep26489

Koprich, J. B., Reske-Nielsen, C., Mithal, P., and Isacson, O. (2008). Neuroinflammation mediated by IL-1beta increases susceptibility of dopamine neurons to degeneration in an animal model of Parkinson's disease. *J. Neuroinflamm.* 5:8. doi: 10.1186/1742-2094-5-8

Lai, D., PhD, Alipanahi, B., PhD, Fontanillas, P., PhD, et al. (2020). Genome-wide association studies of LRRK2 modifiers of Parkinson's disease. *Ann. Neurol.* 90, 76–88. doi: 10.1101/2020.12.14.20224378

Long-Smith, C. M., Sullivan, A. M., and Nolan, Y. M. (2009). The influence of microglia on the pathogenesis of Parkinson's disease. *Prog. Neurobiol.* 89, 277–287. doi: 10.1016/j.pneurobio.2009.08.001

Magalhaes, J., Tresse, E., Ejlerskov, P., Hu, E., Liu, Y., Marin, A., et al. (2021). PIAS2-mediated blockade of IFN-β signaling: a basis for sporadic Parkinson disease dementia. *Mol. Psychiatry* 2021:01207–w. doi: 10.1038/s41380-021-01207-w

Maiti, P., Manna, J., and Dunbar, G. L. (2017). Current understanding of the molecular mechanisms in Parkinson's disease: Targets for potential treatments. *Transl. Neurodegener.* 6:28.

Matuskey, D., Tinaz, S., Wilcox, K. C., Naganawa, M., Toyonaga, T., Dias, M., et al. (2020). Synaptic Changes in Parkinson Disease Assessed with in vivo Imaging. *Ann. Neurol.* 87, 329–338. doi: 10.1002/ana.25682

McGeer, P. L., Itagaki, S., Boyes, B. E., and McGeer, E. G. (1988). Reactive microglia are positive for HLA-DR in the substantia nigra of Parkinson's and Alzheimer's disease brains. *Neurology* 38, 1285–1291. doi: 10.1212/wnl.38.8.1285

McKee, C. M., and Coll, R. C. (2020). NLRP3 inflammasome priming: A riddle wrapped in a mystery inside an enigma. *J. Leukoc. Biol.* 108, 937–952. doi: 10.1002/JLB.3MR0720-513R

Nagatsu, T., and Sawada, M. (2005). Inflammatory process in Parkinson's disease: role for cytokines. *Curr. Pharm. Des.* 11, 999–1016. doi: 10.2174/1381612053381620

Nagatsu, T., Mogi, M., Ichinose, H., and Togari, A. (2000). Cytokines in Parkinson's disease. *J. Neural Transm. Suppl.* 2000, 143–151.

Nakahira, K., Haspel, J. A., Rathinam, V. A. K., Lee, S.-J., Dolinay, T., Lam, H. C., et al. (2011). Autophagy proteins regulate innate immune responses by inhibiting the release of mitochondrial DNA mediated by the NALP3 inflammasome. *Nat. Immunol.* 12, 222–230. doi: 10.1038/ni.1980

Nalls, M. A., Pankratz, N., Lill, C. M., Do, C. B., Hernandez, D. G., Saad, M., et al. (2014). Large-scale meta-analysis of genome-wide association data identifies six new risk loci for Parkinson's disease. *Nat. Genet.* 46, 989–993.

Pang, S. Y.-Y., Ho, P. W.-L., Liu, H.-F., Leung, C.-T., Li, L., Chang, E. E. S., et al. (2019). The interplay of aging, genetics and environmental factors in the pathogenesis of Parkinson's disease. *Transl. Neurodegener.* 8:23.

Panicker, N., Kam, T.-I., Neifert, S., Hinkle, J., Mao, X., Karuppagounder, S., et al. (2020). NLRP3 inflammasome activation in dopamine neurons contributes to neurodegeneration in Parkinson's Disease. *FASEB J.* 34, 1–1.

Pike, A. F., Varanita, T., Herrebout, M. A. C., Plug, B. C., Kole, J., Musters, R. J. P., et al. (2021). α-Synuclein evokes NLRP3 inflammasome-mediated IL-1β secretion from primary human microglia. *Glia* 69, 1413–1428. doi: 10.1002/glia.23970

Qin, X.-Y., Zhang, S.-P., Cao, C., Loh, Y. P., and Cheng, Y. (2016). Aberrations in Peripheral Inflammatory Cytokine Levels in Parkinson Disease: A Systematic Review and Meta-analysis. *JAMA Neurol.* 73, 1316–1324. doi: 10.1001/jamaneurol.2016.2742

Rentzos, M., Nikolaou, C., Andreadou, E., Paraskevas, G. P., Rombos, A., Zoga, M., et al. (2009). Circulating interleukin-10 and interleukin-12 in Parkinson's disease. *Acta Neurol. Scand.* 119, 332–337. doi: 10.1111/j.1600-0404.2008.01103.x

Roussakis, A.-A., and Piccini, P. (2018). Molecular Imaging of Neuroinflammation in Idiopathic Parkinson's Disease. *Int. Rev. Neurobiol.* 141, 347–363. doi: 10.1016/bs.irn.2018.08.009

Sebastian-Valverde, M., and Pasinetti, G. M. (2020). The NLRP3 Inflammasome as a Critical Actor in the Inflammaging Process. *Cells* 9:cells9061552. doi: 10.3390/cells9061552

Sharma, S., Bandopadhyay, R., Lashley, T., Renton, A. E. M., Kingsbury, A. E., Kumaran, R., et al. (2011). LRRK2 expression in idiopathic and G2019S positive Parkinson's disease subjects: a morphological and quantitative study. *Neuropathol. Appl. Neurobiol.* 37, 777–790. doi: 10.1111/j.1365-2990.2011.01187.x

Simón-Sánchez, J., Schulte, C., Bras, J. M., Sharma, M., Gibbs, J. R., Berg, D., et al. (2009). Genome-wide association study reveals genetic risk underlying Parkinson's disease. *Nat. Genet.* 41, 1308–1312.

Simunovic, F., Yi, M., Wang, Y., Macey, L., Brown, L. T., Krichevsky, A. M., et al. (2009). Gene expression profiling of substantia nigra dopamine neurons: further insights into Parkinson's disease pathology. *Brain* 132, 1795–1809. doi: 10.1093/brain/awn323

Smajić, S., Prada-Medina, C. A., Landoulsi, Z., Dietrich, C., Jarazo, J., Henck, J., et al. (2020). Single-cell sequencing of the human midbrain reveals glial activation and a neuronal state specific to Parkinson's disease. *bioRxiv* [Preprint]. doi: 10.1101/2020.09.28.20202812

Su, X., Maguire-Zeiss, K. A., Giuliano, R., Prifti, L., Venkatesh, K., and Federoff, H. J. (2008). Synuclein activates microglia in a model of Parkinson's

disease. *Neurobiol. Aging* 29, 1690–1701. doi: 10.1016/j.neurobiolaging.2007.04.006

Sun, Y., Ma, J., Li, D., Li, P., Zhou, X., Li, Y., et al. (2019). Interleukin-10 inhibits interleukin-1β production and inflammasome activation of microglia in epileptic seizures. *J. Neuroinflamm.* 16:66. doi: 10.1186/s12974-019-1452-1

Swanson, K. V., Deng, M., and Ting, J. P.-Y. (2019). The NLRP3 inflammasome: molecular activation and regulation to therapeutics. *Nat. Rev. Immunol.* 19, 477–489. doi: 10.1038/s41577-019-0165-0

Terada, T., Yokokura, M., Yoshikawa, E., Futatsubashi, M., Kono, S., Konishi, T., et al. (2016). Extrastriatal spreading of microglial activation in Parkinson's disease: a positron emission tomography study. *Ann. Nucl. Med.* 30, 579–587. doi: 10.1007/s12149-016-1099-2

Tolosa, E., Vila, M., Klein, C., and Rascol, O. (2020). LRRK2 in Parkinson disease: challenges of clinical trials. *Nat. Rev. Neurol.* 16, 97–107.

Umeno, J., Asano, K., Matsushita, T., Matsumoto, T., Kiyohara, Y., Iida, M., et al. (2011). Meta-analysis of published studies identified eight additional common susceptibility loci for Crohn's disease and ulcerative colitis. *Inflamm. Bowel Dis.* 17, 2407–2415. doi: 10.1002/ibd.21651

Van Limbergen, J., Wilson, D. C., and Satsangi, J. (2009). The genetics of Crohn's disease. *Annu. Rev. Genomics Hum. Genet.* 10, 89–116.

van Wilgenburg, B., Browne, C., Vowles, J., and Cowley, S. A. (2013). Efficient, long term production of monocyte-derived macrophages from human pluripotent stem cells under partly-defined and fully-defined conditions. *PLoS One* 8:e71098. doi: 10.1371/journal.pone.0071098

Varrette, S., Bouvry, P., Cartiaux, H., and Georgatos, F. (2014). "Management of an academic HPC cluster: The UL experience," in *2014 International Conference on High Performance Computing Simulation (HPCS)*, (Bologna: HPCS), 959–967.

Wang, Q., Liu, Y., and Zhou, J. (2015). Neuroinflammation in Parkinson's disease and its potential as therapeutic target. *Transl. Neurodegener.* 4:19.

Weindel, C. G., Bell, S. L., Vail, K. J., West, K. O., Patrick, K. L., and Watson, R. O. (2020). LRRK2 maintains mitochondrial homeostasis and regulates innate immune responses to Mycobacterium tuberculosis. *Elife* 9:51071. doi: 10.7554/eLife.51071

Yan, Y.-Q., Fang, Y., Zheng, R., Pu, J.-L., and Zhang, B.-R. (2020). NLRP3 Inflammasomes in Parkinson's disease and their Regulation by Parkin. *Neuroscience* 446, 323–334. doi: 10.1016/j.neuroscience.2020.08.004

Yılmazer, S., Candaş, E., Genç, G., Alaylıoğlu, M., Şengül, B., Gündüz, A., et al. (2021). Low Levels of LRRK2 Gene Expression are Associated with LRRK2 SNPs and Contribute to Parkinson's Disease Progression. *Neuromol. Med.* 23, 292–304. doi: 10.1007/s12017-020-08619-x

Zeng, X.-S., Geng, W.-S., Jia, J.-J., Chen, L., and Zhang, P.-P. (2018). Cellular and Molecular Basis of Neurodegeneration in Parkinson Disease. *Front. Aging Neurosci.* 10:109. doi: 10.3389/fnagi.2018.00109

Zhang, F.-R., Huang, W., Chen, S.-M., Sun, L.-D., Liu, H., Li, Y., et al. (2009). Genomewide association study of leprosy. *N. Engl. J. Med.* 361, 2609–2618.

Zhong, Z., Umemura, A., Sanchez-Lopez, E., Liang, S., Shalapour, S., Wong, J., et al. (2016). NF-κB Restricts Inflammasome Activation via Elimination of Damaged Mitochondria. *Cell* 164, 896–910. doi: 10.1016/j.cell.2015.12.057

Conflict of Interest: The authors declare that the research was conducted in the absence of any commercial or financial relationships that could be construed as a potential conflict of interest.

Publisher's Note: All claims expressed in this article are solely those of the authors and do not necessarily represent those of their affiliated organizations, or those of the publisher, the editors and the reviewers. Any product that may be evaluated in this article, or claim that may be made by its manufacturer, is not guaranteed or endorsed by the publisher.

Copyright © 2021 Badanjak, Mulica, Smajic, Delcambre, Tranchevent, Diederich, Rauen, Schwamborn, Glaab, Cowley, Antony, Pereira, Venegas and Grünewald. This is an open-access article distributed under the terms of the Creative Commons Attribution License (CC BY). The use, distribution or reproduction in other forums is permitted, provided the original author(s) and the copyright owner(s) are credited and that the original publication in this journal is cited, in accordance with accepted academic practice. No use, distribution or reproduction is permitted which does not comply with these terms.

Supplementary Table 1. Gene expression analysis of human IPD and control SN transcriptome.

Gene symbol	Z-score	FDR
IL1B	2.273739646	0.022981645
IL6	-0.293008563	0.769515607
IL10	2.710259928	0.00672305
IL18	1.512416069	0.13042805
IL8	1.290107048	0.197013493
TNF	-0.37382918	0.708531408

Supplementary Table 2. Gene expression analysis in IPD and control microglia of the human midbrain single-cell transcriptome.

Gene symbol	Average expression	Percent expressed	cluster_id
IL1B	0.325002368	5.55967383	Microglia_IPD
IL6	0.003882633	0.11119348	Microglia_IPD
IL18	3.170897328	63.45441067	Microglia_IPD
TNF	0.011861339	0.48183840	Microglia_IPD
IL10	0.015103408	0.70422535	Microglia_IPD
IL8	0.014423550	0.29651594	Microglia_IPD
IL1B	0.306312685	2.98755187	Microglia_Control
IL6	0.002964900	0.08298755	Microglia_Control
IL18	3.089786862	59.33609959	Microglia_Control
TNF	0.000000000	0.00000000	Microglia_Control
IL10	0.007378525	0.24896266	Microglia_Control
IL8	0.002578054	0.08298755	Microglia_Control

7.2 Manuscript V

Check for updates

RESEARCH ARTICLE

Parkin Deficiency Impairs Mitochondrial DNA Dynamics and Propagates Inflammation

Kobi Wasner, PhD,[1] Semra Smajic, MSc,[1] Jenny Ghelfi, BSc,[1] Sylvie Delcambre, PhD,[1] Cesar A. Prada-Medina, PhD,[2] Evelyn Knappe, MSc,[3] Giuseppe Arena, PhD,[1] Patrycja Mulica, MSc,[1] Gideon Agyeah, MSc,[1] Aleksandar Rakovic, PhD,[3] Ibrahim Boussaad, PhD,[1,4] Katja Badanjak, MSc,[1] Jochen Ohnmacht, PhD,[1,5] Jean-Jacques Gérardy, BSc,[6] Masashi Takanashi, MD,[7] Joanne Trinh, PhD,[3] Michel Mittelbronn, MD,[1,6,8,9] Nobutaka Hattori, MD, PhD,[7] Christine Klein, MD,[3] Paul Antony, PhD,[1,4] Philip Seibler, PhD,[3] Malte Spielmann, MD,[2,10] Sandro L. Pereira, PhD,[1,7] and Anne Grünewald, PhD[1,3*]

[1]*Luxembourg Centre for Systems Biomedicine, University of Luxembourg, Esch-sur-Alzette*
[2]*Max Planck Institute for Molecular Genetics, Berlin, Germany*
[3]*Institute of Neurogenetics, University of Lübeck, Lübeck, Germany*
[4]*Disease Modeling and Screening Platform, Luxembourg Centre of Systems Biomedicine, University of Luxembourg & Luxembourg Institute of Health, Luxembourg*
[5]*Department of Life Science and Medicine, University of Luxembourg, Esch-sur-Alzette, Luxembourg*
[6]*National Center of Pathology, Laboratoire National de Santé, Dudelange, Luxembourg*
[7]*Department of Neurology, Juntendo University, Tokyo, Japan*
[8]*Luxembourg Center of Neuropathology, Dudelange, Luxembourg*
[9]*Department of Cancer Research, Luxembourg Institute of Health, Luxembourg, Luxembourg*
[10]*Institute of Human Genetics, University of Lübeck, Lübeck, Germany*

ABSTRACT: Background: Mutations in the E3 ubiquitin ligase parkin cause autosomal recessive Parkinson's disease (PD). Together with PTEN-induced kinase 1 (*PINK1*), parkin regulates the clearance of dysfunctional mitochondria. New mitochondria are generated through an interplay of nuclear- and mitochondrial-encoded proteins, and recent studies suggest that parkin influences this process at both levels. In addition, parkin was shown to prevent mitochondrial membrane permeability, impeding mitochondrial DNA (mtDNA) escape and subsequent neuroinflammation. However, parkin's regulatory roles independent of mitophagy are not well described in patient-derived neurons.

Objectives: We sought to investigate parkin's role in preventing neuronal mtDNA dyshomeostasis, release, and glial activation at the endogenous level.

Methods: We generated induced pluripotent stem cell (iPSC)–derived midbrain neurons from PD patients with parkin (*PRKN*) mutations and healthy controls. Live-cell imaging, proteomic, mtDNA integrity, and gene expression analyses were employed to investigate mitochondrial biogenesis and genome maintenance. To assess neuroinflammation, we performed single-nuclei RNA sequencing in postmortem tissue and quantified interleukin expression in mtDNA/lipopolysaccharides (LPS)-treated iPSC-derived neuron–microglia co-cultures.

Results: Neurons from patients with *PRKN* mutations revealed deficits in the mitochondrial biogenesis pathway, resulting in mtDNA dyshomeostasis. Moreover, the energy sensor sirtuin 1, which controls mitochondrial biogenesis and clearance, was downregulated in parkin-deficient cells. Linking mtDNA disintegration to neuroinflammation, in postmortem midbrain with *PRKN* mutations, we confirmed mtDNA dyshomeostasis and detected an upregulation of microglia overexpressing proinflammatory cytokines. Finally, parkin-deficient neuron–microglia co-cultures elicited an enhanced immune response when exposed to mtDNA/LPS.

Conclusions: Our findings suggest that parkin coregulates mitophagy, mitochondrial biogenesis, and mtDNA maintenance pathways, thereby protecting midbrain neurons from neuroinflammation and degeneration.
© 2022 The Authors. *Movement Disorders* published by Wiley Periodicals LLC on behalf of International Parkinson and Movement Disorder Society

Key Words: Parkinson's disease; mitochondrial DNA; induced pluripotent stem cells; parkin; neuroinflammation

This is an open access article under the terms of the Creative Commons Attribution-NonCommercial-NoDerivs License, which permits use and distribution in any medium, provided the original work is properly cited, the use is non-commercial and no modifications or adaptations are made.

***Correspondence to:** Dr. Anne Grünewald, Luxembourg Centre for Systems Biomedicine, University of Luxembourg, 6 Avenue du Swing, L-4367 Belvaux. E-mail: anne.gruenewald@uni.lu

Semra Smajic and Jenny Ghelfi contributed equally.

Relevant conflicts of interest/financial disclosures: The authors report no conflicts of interest.

Received: 22 December 2021; **Revised:** 7 March 2022; **Accepted:** 27 March 2022

Published online 23 April 2022 in Wiley Online Library (wileyonlinelibrary.com). DOI: 10.1002/mds.29025

Introduction

Dopaminergic neurons (DANs) of the substantia nigra pars compacta (SNpc) in the midbrain are critically involved in the regulation of movement.[1] Loss of DANs results in clinical motor disturbances of patients with Parkinson's disease (PD)—the second most common neurodegenerative disorder.[2] Although the underlying biological mechanisms causing neuronal loss are still under investigation, mitochondrial dysfunction has been well implicated in PD pathology.[3]

The majority of patients with PD are sporadic, with individuals manifesting the disease at ≥65 years of age. The remainder are caused by genetic mutations, of which many are linked to mitochondrial dysfunction. Roughly 50% of patients with early-onset PD harbor mutations in parkin (*PRKN*).[2,4]

PRKN encodes the E3 ubiquitin ligase parkin—an established regulator of mitochondrial clearance.[5] However, parkin's substrates are involved in several fundamental cellular processes. For instance, parkin targets parkin-interacting substrate (PARIS)—an inhibitor of the mitochondrial biogenesis regulator peroxisome gamma coactivator 1-alpha (PGC1-α).[6] Moreover, *PRKN* overexpression in cell models revealed an association with the mitochondrial genome and a direct interaction with mitochondral transcription factor A (TFAM)—the main transcription factor of mitochondrial DNA (mtDNA).

mtDNA has gained recent interest as a determinant of aging and age-associated diseases, including PD.[7] Improper mtDNA maintenance has been shown to allow its escape from the mitochondrial compartment, triggering an immune response.[8,9] This phenomenon was furthermore demonstrated in parkin-knockout (KO) "mutator" mice, which harbor an error-prone version of DNA polymerase γ (POLG). These animals show elevated extracellular mtDNA levels and cyclic GMP-AMP synthase (cGAS)-stimulator of interferon genes (STING) signaling under stress conditions.[10] However, parkin's involvement in these cellular processes has yet to be investigated in patient-derived neurons.

To explore the role of parkin in mtDNA maintenance endogenously, we generated induced pluripotent stem cell (iPSC)–derived midbrain neurons from patients with PD with biallelic *PRKN* mutations. We found that parkin-deficient neurons exhibit impaired mitochondrial biogenesis, mtDNA dynamics, and increased cytosolic mtDNA levels. Parkin knockdown during mutagenic stress mirrored these phenotypes and evidenced upregulations of the cGAS protein and extracellular mtDNA. Moreover, treatment with lipopolysaccharides (LPS) and mtDNA elicited a stronger inflammatory response in *PRKN*-mutant compared with control neuron–microglia co-cultures. Finally, single-nuclei RNA sequencing (snRNAseq) of postmortem midbrain sections from a patient with *PRKN*-PD revealed microgliosis and proinflammatory signaling. Our findings elucidate novel parkin-regulated mitophagy-independent mechanisms contributing toward mitochondrial quality control. We show that parkin coordinates mitochondrial biogenesis and mtDNA maintenance and is essential to prevent neuroinflammation and neurodegeneration.

Materials and Methods

Generation of iPSCs was performed as described,[11] and DANs and microglia were derived using established protocols.[12-14] To isolate tyrosine hydroxylase (TH)–positive cells, iPSC-derived neurons were subjected to fluorescence-activated cell sorting (FACS) using an adapted protocol.[15] Production of lentiviral vectors expressing short hairpin RNA (shRNA) against human *PRKN* or a control plasmid was performed as described.[16] SH-SY5Y neuroblastoma cells were treated with 200 μM cobalt chloride ($CoCl_2$).[17] Nicotinamide adenine dinucleotide:nicotinamide adenine dinucleotide hydrogen (NAD^+:NADH) ratios were determined using a kit (Sigma, St. Louis, MO). Respiratory chain complex I (CI) and citrate synthase activities were assessed in mitochondrial fractions by means of spectrophotometry.[18,19] Isolated extracellular mtDNA was quantified using a Digital PCR System (Applied Biosystems, Waltham, MA) and TaqMan probes specific for mitochondrially encoded NADH:ubiquinone oxidoreductase core subunit 1 (*MT-ND1*) and beta-2-microglobulin (*B2M*).[20,21] Polar metabolites from 30 day-old neurons were extracted and then derivatized and measured as published.[22] All experiments using iPSC-derived neurons and SH-SY5Y cells were performed with at least three biological replicates. Unpaired two-tailed Student's *t* tests or one-way analysis of variance followed by post hoc Tukey tests were used to determine statistical significance ($P < 0.05$).

Midbrain sections were immunostained, and TH-positive neurons were isolated through laser capture microdissection (LCM) using the PALM MicroBeam (Zeiss, Oberkochen, Germany).[20] Nuclei isolation, snRNAseq, and data analysis of the *PRKN*-mutant midbrain was carried out as described.[23]

A detailed description of the materials and methods can be found in the supplement.

Results

Parkin Deficiency Impairs Mitochondrial Biogenesis in the Neurons of Patients with PD

We generated iPSC-derived midbrain neurons from healthy controls and *PRKN* mutation carriers (Fig. S1A, B), which lack the parkin protein (Fig. S1C). Furthermore, we employed SH-SY5Y wild-type (WT) and

15318257, 2022, 7, Downloaded from https://movementdisorders.onlinelibrary.wiley.com/doi/10.1002/mds.29025 by Cochrane Luxembourg, Wiley Online Library on [29/03/2023]. See the Terms and Conditions (https://onlinelibrary.wiley.com/terms-and-conditions) on Wiley Online Library for rules of use; OA articles are governed by the applicable Creative Commons License

isogenic parkin-KO cells, which were generated using clustered regularly interspaced short palindromic repeats and CRISPR-associated protein 9 (CRISPR/Cas9) technology (Fig. S1D).

Parkin targets a plethora of proteins,[24] with mounting evidence supporting regulatory roles in diverse cellular mechanisms beyond mitophagy. Given that mitophagy and mitochondrial biogenesis are tightly linked to preserve bioenergetic homeostasis,[25] we sought to investigate possible alterations in mitochondrial biogenesis in our models. Previous research demonstrated that parkin overexpression enhances mitochondrial biogenesis through PGC1-α, either directly or via PARIS, its transcriptional repressor.[6,26,27] We found significantly lower levels of PGC1-α protein in parkin-deficient neurons and SH-SY5Y cells compared with controls (Fig. 1A,B). Interestingly, neither cell model showed differences in the PARIS protein under basal conditions (Fig. 1A,C).

Conversely, parkin deficiency substantially reduced sirtuin 1 (SIRT1) levels (Fig. 1A,D), an NAD^+-dependent energy sensor acting on mitochondrial biogenesis through regulation of PGC1-α gene expression and protein deacetylation.[28,29] Moreover, in parkin-deficient neurons, we detected higher lactate:pyruvate ratios (Fig. 1E), which suggests a lack of free NAD^+ based on the chemical equilibrium principle.[30]

PGC1-α regulates the transcription of nuclear respiratory factors (NRFs), which in turn mediates gene expressions of mtDNA transcription factors and replication activators TFAM and mitochondrial transcription factor B2 (TFB2M).[31] In agreement with reduced PGC1-α abundance, we found that parkin deficiency resulted in decreased NRF1 protein levels (Fig. 1A,F) and reduced *TFAM* and *TFB2M* expression (Fig. 1G, H). In addition, we detected significantly downregulated mRNA levels of twinkle mtDNA helicase (*TWNK*), a factor mainly involved in mtDNA replication (Fig. 1I).

Parkin Influences mtDNA Dynamics and Respiratory Chain Function

Mitochondrial biogenesis may be defined as the division and growth of preexisting mitochondria and is accomplished by the import of nuclear-encoded proteins and transcription and replication of the mitochondrial genome, which contains genes encoding subunits

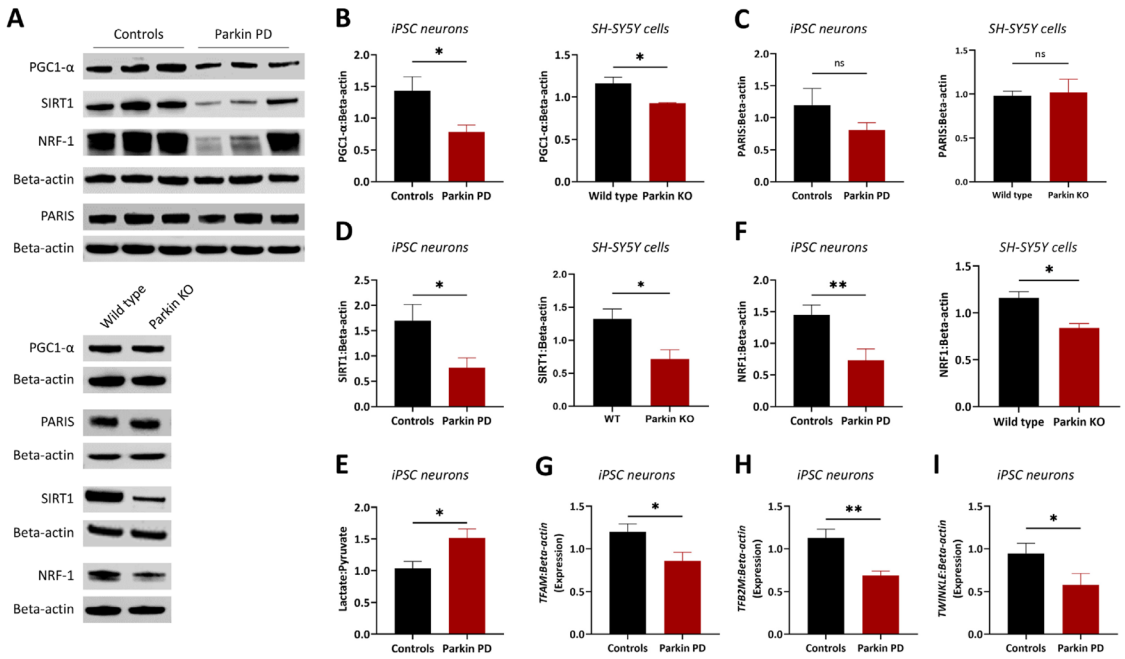

FIG. 1. Mitochondrial biogenesis is impaired in parkin-deficient cells. (**A**) Representative cropped Western blot images of total cell lysates from induced pluripotent stem cell (iPSC)–derived neurons from controls and patients with parkin-associated Parkinson's disease (Parkin PD) as well as wild-type and parkin-knockout (KO) SH-SY5Y neuroblastoma cells. (**B**-**E**) Quantifications from (**A**) peroxisome gamma coactivator 1-alpha (PGC1-α) (**B**), parkin-interacting substrate (PARIS) (**C**), sirtuin 1 (SIRT1) (**D**) and nuclear respiratory factor 1 (NRF1) (**F**) protein levels normalized to beta-actin. (**E**) Lactate-to-pyruvate ratios served as a proxy measure for free nicotinamide adenine dinucleotide:nicotinamide adenine dinucleotide hydrogen (NAD^+/NADH) ratios. (**G**-**I**) Quantitative polymerase chain reaction (qPCR) was used to quantify gene expression of mitochondrial transcription factor A (*TFAM*) (**G**), mitochondrial transcription factor B2 (*TFB2M*) (**H**) and twinkle mtDNA helicase (*TWNK*) (**I**) in iPSC-derived neurons from controls and patients with parkin-associated PD normalized to beta-actin. Data are presented as the mean ± SEM. SEM = standard error of the mean, $^*P < 0.05$, $^{**}P < 0.01$; ns = not significant as determined by Student's *t* test.

15318257, 2022, 7, Downloaded from https://movementdisorders.onlinelibrary.wiley.com/doi/10.1002/mds.29025 by Cochrane Luxembourg, Wiley Online Library on [29/03/2023]. See the Terms and Conditions (https://onlinelibrary.wiley.com/terms-and-conditions) on Wiley Online Library for rules of use; OA articles are governed by the applicable Creative Commons License

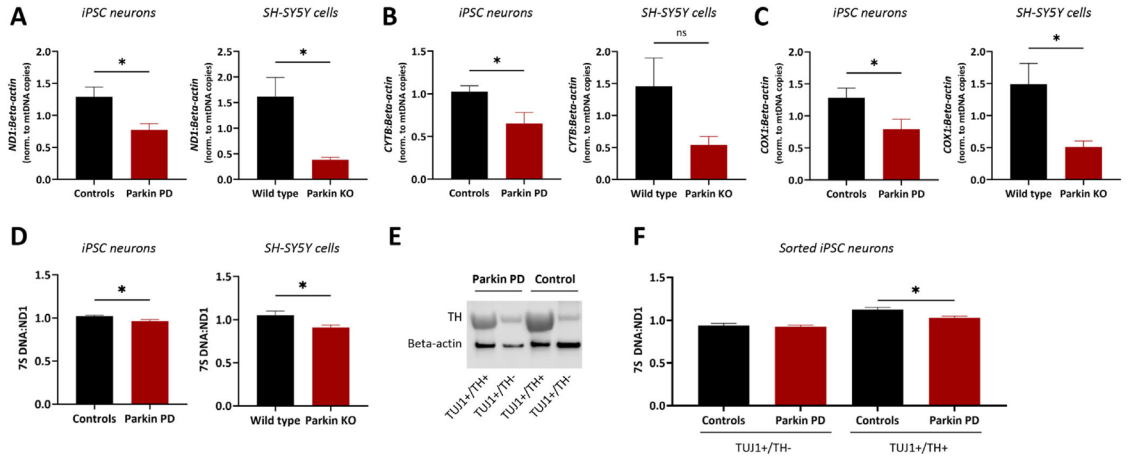

FIG. 2. Parkin influences mitochondrial DNA (mtDNA) dynamics. (**A**-**C**) Quantitative polymerase chain reaction (qPCR) was used to measure expression of mtDNA-encoded genes NADH:ubiquinone oxidoreductase core subunit 1 (*ND1*) (**A**), cytochrome B (*CYTB*) (**B**), and (**C**) cytochrome C oxidase I *(COX1)* in induced pluripotent stem cell (iPSC)–derived neurons from controls and Parkinson's disease patients with mutations in parkin (Parkin PD) and wild-type and parkin-knockout (KO) SH-SY5Y neuroblastoma cells. Gene expression was normalized to beta-actin and mtDNA copy number. (**D**) A multiplex real-time polymerase chain reaction (RT-PCR) assay was used to quantify transcription-associated 7S DNA per mtDNA molecule (with probes targeting *ND1*) in iPSC-derived neurons and SH-SY5Y cells. (**E, F**) Neuronal cultures from three controls and three *PRKN* mutation carriers were sorted using the pan-neuronal marker β-Tubulin 3 (TUJ1) and the dopaminergic neuron (DAN) marker tyrosine hydroxylase (TH) and subjected to Western blotting and RT-PCR analyses. (**E**) Representative cropped Western blotting images of TH and TUJ1 protein abundances in sorted control and patient neurons. (**F**) TUJ1/TH double-positive iPSC-derived neurons were separated from TUJ1-positive/TH-negative neurons derived from controls and patients with *PRKN* mutations. The resulting cell populations underwent multiplex RT-PCR to quantify the abundance of 7S DNA per mtDNA molecule (with a probe targeting *ND1*). RT-PCR results are from two technical replicates. n = 3 biological replicates; data are presented as the mean ± SEM; SEM = standard error of the mean, $^*P < 0.05$, ns = not significant as determined by Student's *t* test.

of the electron transport chain (ETC).[32] Our experiments suggest decreases in nuclear-encoded factors controlling mitochondrial biogenesis. We next sought to assess mtDNA dynamics by measuring the expression of mtDNA-encoded genes. The expression of mitochondrially encoded NADH:ubiquinone oxidoreductase core subunit 1 (*MT-ND1*), mitochondrially encoded cythochrome B (*MT-CYTB*), and mitochondrially encoded cytochrome C oxidase I (*MT-COX1*) (encoding subunits of complexes I, III, and IV, respectively) per mtDNA molecule was significantly downregulated in our parkin-deficient models (Fig. 2A–C). In line with this, both parkin-deficient iPSC-derived neurons and SH-SY5Y cells showed diminished 7S DNA: *MT-ND1* ratios, suggestive of fewer transcription initiation events (Fig. 2D).[20] Moreover, we used FACS to isolate TH-positive neurons and found that the 7S DNA phenotype is specific to DANs (Fig. 2E,F).

Because parkin overexpression was reported to enhance the selective removal of mitochondria harboring deleterious mtDNA mutations,[33] we explored the abundance of somatic major arc deletions. By contrast, we did not find differences between groups (data not shown). We further evaluated the mtDNA copy number and detected significantly higher mtDNA levels in parkin-deficient cells using both real-time polymerase chain reaction (RT-PCR) (Fig. 3A) and immunocytochemistry (Fig. 3B). Finally, we assessed respiratory chain function in SH-SY5Y cells and found that parkin-KO cells exhibited significantly reduced CI activity compared with WT cells (Fig. 3C). These results suggest that although parkin deficiency leads to an accumulation of mtDNA molecules, it also hinders the mtDNA transcription process, which likely contributes to ETC dysfunction.

Parkin Mitigates Cytosolic mtDNA Infiltration

Consistent with its evolutionary bacterial origin, mtDNA has been identified as a damage-associated molecular pattern (DAMP). Cytosolic mtDNA molecules can activate the innate immune system via the cGAS-STING pathway.[8] Implicating mtDNA release in the pathogenesis of *PRKN*-PD, our previous research showed increased levels of circulating cell-free mtDNA (ccf-mtDNA) and inflammatory cytokines in serum from *PRKN* mutation carriers.[34] Several mechanisms have been proposed to facilitate mtDNA release into the cytosol, including TFAM depletion.[8] We next confirmed that reduced *TFAM* gene expression detected in parkin-deficient neurons resulted in diminished TFAM (protein):mtDNA ratios (Fig. 3D, Fig. S2A). TFAM also acts as a packaging factor compacting the mtDNA molecule to form the mitochondrial nucleoid, and disruption of this process is associated with mtDNA extrusion from mitochondria. To investigate if impaired TFAM:mtDNA ratios coupled to disrupted mtDNA

15318257, 2022, 7, Downloaded from https://movementdisorders.onlinelibrary.wiley.com/doi/10.1002/mds.29025 by Cochrane Luxembourg, Wiley Online Library on [29/03/2023]. See the Terms and Conditions (https://onlinelibrary.wiley.com/terms-and-conditions) on Wiley Online Library for rules of use; OA articles are governed by the applicable Creative Commons License

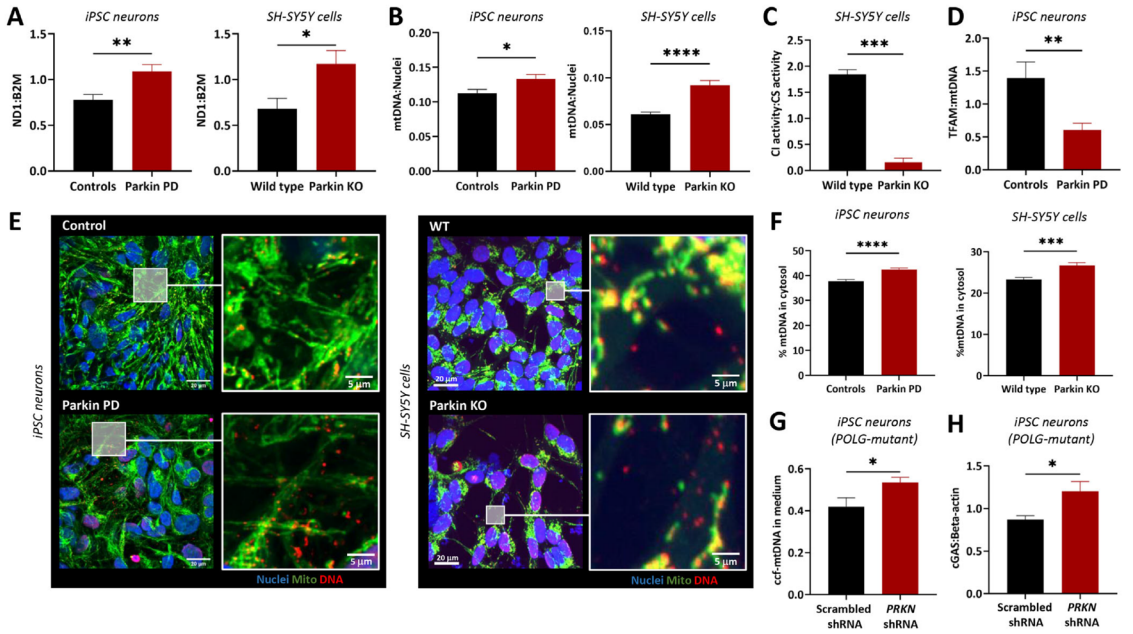

FIG. 3. Parkin attenuates cytosolic mitochondrial DNA (mtDNA) infiltration at baseline and extracellular mtDNA release during mutagenic stress. (**A**) A real-time polymerase chain reaction (RT-PCR) assay was used to quantify mtDNA copy number (with a probe targeting NADH:ubiquinone oxidoreductase core subunit 1 [*ND1*]) relative to the nuclear single copy gene beta-1-microglobulin (*B2M*) in induced pluripotent stem cell (iPSC)–derived neurons and SH-SY5Y neuroblastoma cells in healthy controls and patients with parkin-associated Parkinson's disease (Parkin PD) as well as wild-type (WT) and parkin-knockout (KO) SH-SY5Y cells. (**B**) Immunocytochemistry analysis of mtDNA copy number in iPSC-derived neurons and SH-SY5Y cells. Copy number was determined by mtDNA volume:nuclei volume. (**C**) Quantification of mitochondrial complex I activity normalized to citrate synthase activity in SH-SY5Y cells. (**D**) Quantification of mitochondrial transcription factor A (TFAM) protein abundance normalized to mtDNA copy number in iPSC-derived neurons. (**E**) Representative cropped immunocytochemistry images used to assess mtDNA subcellular location by targeting mtDNA, nuclei (Hoechst 33342), the mitochondrial marker translocase of outer mitochondrial membrane 20 (TOM20) and cytosol (high content screening CellMask Orange Stain [ThermoFisher Scientific, Waltham, MA]). (**F**) Analysis of mtDNA localization in iPSC-derived neurons and SH-SY5Y cells from (**E**). Percentage of mtDNA in cytosol was calculated by dividing the mtDNA volume outside mitochondria by total mtDNA volume. (**G**) Extracellular circulating cell-free mtDNA (ccf-mtDNA) in medium from polymerase γ (POLG)–mutant iPSC-derived neurons transduced with scrambled or *PRKN* short hairpin RNA (shRNA). Quantification by means of multiplex digital PCR (dPCR) targeting the mtDNA fragment *ND1* and the nuclear single-copy gene *B2M*. ccf-mtDNA was calculated as the ratio of extracellular *ND1* normalized to extracellular *B2M* copies to the sum of intra- and extracellular *ND1* normalized by their respective intra- and extracellular *B2M* copies. (**H**) cyclic GMP-AMP synthase (cGAS)-stimulator of interferon genes (STING) signaling in *POLG*-mutant iPSC-derived neurons transduced with scrambled or *PRKN* shRNA. Quantification of cGAS protein levels relative to beta-actin from Figure S2E. n = 3 or 5 biological replicates; data are presented as the mean ± SEM; SEM = standard error of the mean, $^{*}P < 0.05$, $^{**}P < 0.01$, $^{***}P < 0.001$, $^{****}P < 0.0001$ as determined by Student's *t* test.

dynamics could result in elevated mtDNA release, we assessed the subcellular localization of mtDNA molecules with an imaging approach. Indeed, patient neurons and parkin-KO SH-SY5Y cells harbored significantly more mtDNA molecules in the cytosol compared with controls (Fig. 3E,F). This mtDNA shift from mitochondria to the cytosol was independently validated by applying an RT-PCR approach to cellular fractions from control and parkin-KO SH-SY5Y cells (Fig. S2B).

Hypoxic Conditions Mirror mtDNA Phenotypes Observed in Parkin-Deficient Cells

To test our hypothesis of metabolic remodeling as the underlying cause of mtDNA dyshomeostasis in *PRKN*-PD, we exposed WT SH-SY5Y cells to the hypoxia-inducing agent $CoCl_2$.[17] $CoCl_2$ treatment triggered an upregulation of the hypoxia-inducible factor 1-α (Fig. 4A) and a shift from oxidative phosphorylation to glycolysis as indicated by increased NAD^+:NADH ratios (Fig. 4B). In line with the cellular function of SIRT1, the protein was less abundant under hypoxic conditions (Fig. 4A,C). We then investigated the SIRT1 target PGC1-α, which was also downregulated in $CoCl_2$-treated cells (Fig. 4A,D). To explore the impact of PGC1-α depletion on mtDNA maintenance, we next determined the protein levels of NRF1 and TFAM, which were both downregulated in response to $CoCl_2$ exposure (Fig. 4A,E,F). In addition, the treatment reduced the 7S DNA:*MT-ND1* ratio (Fig. 4G) and *MT-ND1* mRNA levels (Fig. 4H).

15318257, 2022, 7, Downloaded from https://movementdisorders.onlinelibrary.wiley.com/doi/10.1002/mds.29025 by Cochrane Luxembourg, Wiley Online Library on [29/03/2023]. See the Terms and Conditions (https://onlinelibrary.wiley.com/terms-and-conditions) on Wiley Online Library for rules of use; OA articles are governed by the applicable Creative Commons License

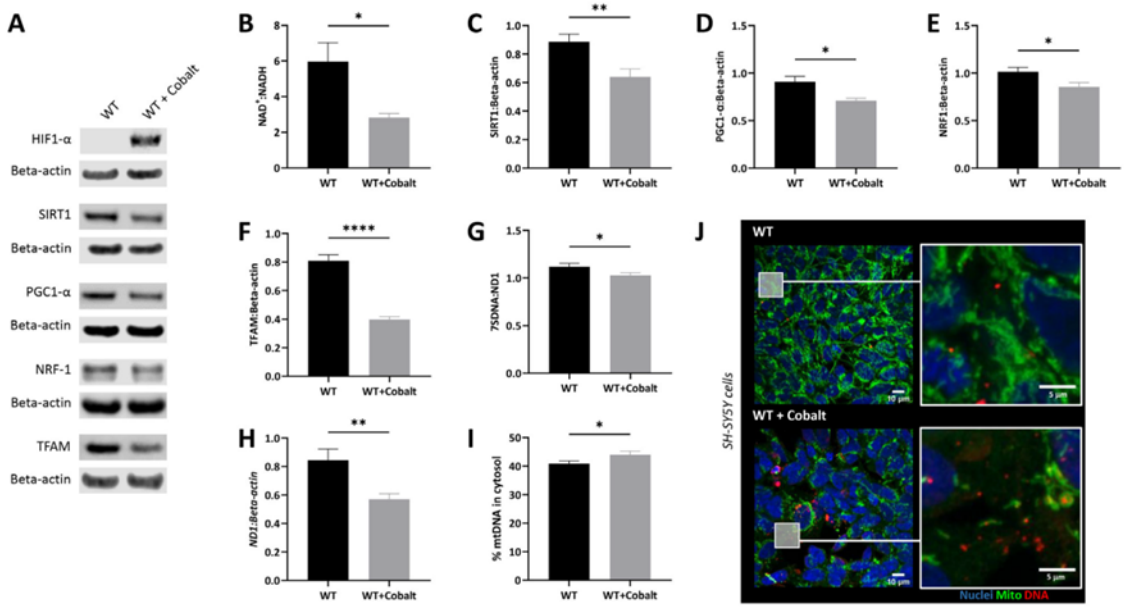

FIG. 4. Hypoxia-mediated metabolic alterations induce mitochondrial DNA (mtDNA) dyshomeostasis. (**A**) Representative cropped Western blot images of total cell lysates from untreated and cobalt chloride ($CoCl_2$)-treated wild-type (WT) SH-SY5Y neuroblastoma cells. (**B**) Nicotinamide adenine dinucleotide:nicotinamide adenine dinucleotide hydrogen (NAD^+/NADH) ratios measured in cellular extracts from untreated and $CoCl_2$-treated WT SH-SY5Y cells. Quantifications from (**A**) sirtuin 1 (SIRT1) (**C**), peroxisome gamma coactivator 1-alpha (PGC1-α) (**D**), nuclear respiratory factor 1 (NRF1) (**E**), mitochondrial transcription factor A (TFAM) (**F**) protein levels normalized to Beta-actin. (**G**) Real-time polymerase chain reaction quantification of transcription-associated 7S DNA per mtDNA molecule. (**H**) qPCR was used to quantify gene expression of the mtDNA gene NADH:ubiquinone oxidoreductase core subunit 1(*ND1*). (**I**) Analysis of mtDNA localization in untreated and $CoCl_2$-treated WT SH-SY5Y cells (**J**). Percentage of mtDNA in cytosol was calculated by dividing the mtDNA volume outside mitochondria by total mtDNA volume. (**J**) Representative cropped immunocytochemistry images used to assess mtDNA subcellular location by targeting mtDNA, nuclei (Hoechst 33342), the mitochondrial marker translocase of outer mitochondrial membrane 20 (TOM20), and cytosol (high content screening CellMask Orange Stain [ThermoFisher Scientific, Waltham, MA]). n ≤ 3 biological replicates; data are presented as the mean ± SEM; SEM = standard error of the mean, $^*P < 0.05$, $^{**}P < 0.01$, $^{****}P < 0.0001$ as determined by Student's *t* test.

Finally, we tested whether the $CoCl_2$-induced metabolic shift was sufficient to trigger mtDNA release. Indeed, high-throughput imaging revealed elevated cytosolic mtDNA levels in treated SH-SY5Y cells (Fig. 4I,J). These data indicate that metabolic impairments can interfere with mtDNA dynamics.

Mutagenic Stress Exacerbates Parkin-Mediated Mitochondrial Biogenesis and mtDNA Transcription Deficits

Next, we further explored the downstream effects of parkin deficiency–induced mtDNA dyshomeostasis. Although we observed an increase of cytosolic mtDNA in parkin-mutant neurons, this mtDNA release from the mitochondria was not accompanied by an upregulation of extracellular mtDNA or immune-related factors (Fig. S2C,D), which may be explained by the inability of iPSC-derived cultures to model age-associated phenotypes such as inflammation.[35] To overcome the rejuvenation-associated limitations of iPSC-derived neurons, we adapted a mitochondrial aging strategy from mice. Recently, an innovative mouse strain was generated that, contrary to most established rodent PD models, recapitulates motor phenotypes during the short lifetime of the animals.[10] To simulate mitochondrial aging, parkin-KO mice were crossed with animals harboring an error-prone version of POLG, which causes mtDNA mutagenic stress. The resulting parkin-KO "mutator" mice showed increased serum levels of ccf-mtDNA and inflammatory cytokines mediated by cGAS-STING signaling.[9] Inspired by this work, we differentiated iPSCs from a patient with compound-heterozygous mutations in *POLG* and subjected the resulting neurons to shRNA to reduce parkin expression (Fig. S3A).

Compared with *POLG*-mutant cells transduced with scrambled shRNA, parkin shRNA reduced 7S DNA:*MT-ND1* ratios (Fig. S3B) and showed significantly lower levels of mitochondrial biogenesis factors PGC1-α and NRF1 (Fig. S3A,C,D), strengthening our findings in *PRKN*-mutant neurons. Next, we quantified ccf-mtDNA in the extracellular medium and found a

15318257, 2022, 7, Downloaded from https://movementdisorders.onlinelibrary.wiley.com/doi/10.1002/mds.29035 by Cochrane Luxembourg, Wiley Online Library on [29/03/2023]. See the Terms and Conditions (https://onlinelibrary.wiley.com/terms-and-conditions) on Wiley Online Library for rules of use; OA articles are governed by the applicable Creative Commons License

significant upregulation, suggesting that parkin reduction in the presence of mtDNA stress elevated the release of mtDNA from mitochondria into the extracellular space (Fig. 3G). Furthermore, we found an increase in protein abundance of the cytosolic DNA sensor cGAS (Fig. 3H). Finally, we assessed the expression of key cytokines that were previously shown to be upregulated in serum from parkin-KO "mutator" mice and patients with *PRKN* mutations in response to cGas/STING signaling.[9] By contrast, RT-PCR analyses still revealed very low levels of interleukin 6 (*IL6*) and interleukin-1-beta (*IL1B*) in any of the investigated neurons (Fig. S3E), likely attributed to the absence of microglia in the cultures.

mtDNA Maintenance Impairments Propagate Neuroinflammation in *PRKN*-PD Tissue

Although iPSC-derived neurons allow the study of parkin-related mitochondrial functions, the cultures do not reflect the cellular diversity of the midbrain. Recent publications implicate glia-mediated inflammation in the pathogenesis of *PRKN*-associated PD.[9,34] In light of these findings, we next used postmortem tissue from a patient with PD with compound-heterozygous *PRKN* mutations and two healthy controls to assess the extent and possible consequences of mtDNA disintegration in a more comprehensive environment (Fig. 5A).

We first sought to validate our findings concerning mtDNA maintenance in human brain tissue. We

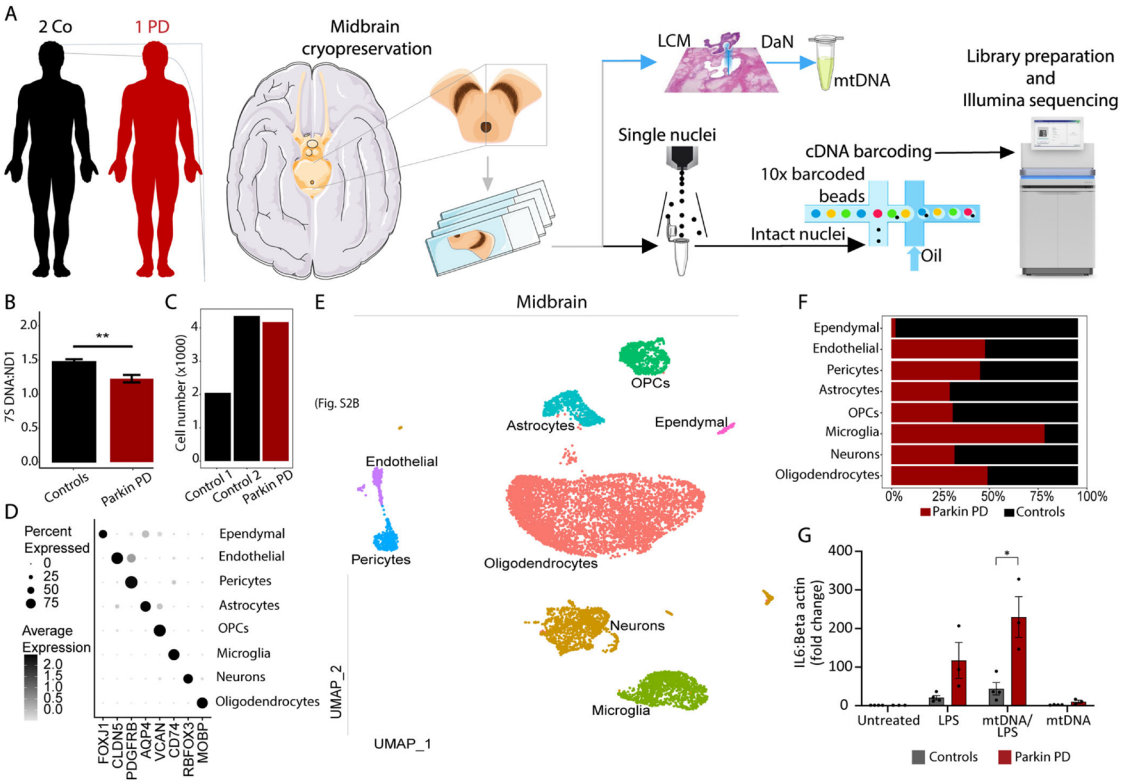

FIG. 5. Cell-type differences in human *PRKN*-mutant and control midbrains. (**A**) Handling of the midbrain tissue for single-cell studies. Midbrain sections were used for (1) laser capture microdissection (LCM) of dopaminergic neurons (DAN) and (2) nuclei isolation, 10X Genomics platform processing, and Illumina sequencing. (**B**) 7S DNA:mitochondrially encoded NADH:ubiquinone oxidoreductase core subunit 1 (7SDNA:*MT-ND1*) ratios quantified via multiplex real-time polymerase chain reaction from single postmortem DANs of the substantia nigra pars compacta. (**C**) Number of nuclei per sample. The analyzed population is composed of 4173 *PRKN*-mutant nuclei and 6405 control nuclei, making a population of 10,578 nuclei. (**D**) Representative cell-type specific marker genes. (**E**) The population of 10,578 nuclei projected onto a uniform manifold approximation and projection (UMAP) space. (**F**) Percentage of *PRKN*-mutant and control cell-type specific nuclei. (**G**) Fold change of interleukin 6 (*IL6*) expression at baseline (NT = nontreated) or after treatment with mitochondrial DNA (mtDNA), lipopolysaccharides (LPS), or both. n = 3 patients and n = 4 controls; data are presented as the mean ± SEM; SEM = standard error of the mean, *P < 0.05, **P < 0.01, ns = not significant as determined by two-way analysis of variance and Sidak's multiple comparisons test. Co = healty control subjects, PD/Parkin PD = Parkinson's disease patient with mutations in parkin, OPCs = oligodendrocyte precursor cells, *FOXj1* = forkhead box J1, *CLDN5* = claudin 5, *PDGFRB* = platelet derived growth factor receptor beta, *AQP4* = aquaporin 4, *VCAN* = versican, *RBFOX3* = RNA binding fox-1 homolog 3, *MOBP* = myelin associated oligodendrocyte basic protein.

15318257, 2022, 7, Downloaded from https://movementdisorders.onlinelibrary.wiley.com/doi/10.1002/mds.29025 by Cochrane Luxembourg, Wiley Online Library on [29/03/2023]. See the Terms and Conditions (https://onlinelibrary.wiley.com/terms-and-conditions) on Wiley Online Library for rules of use; OA articles are governed by the applicable Creative Commons License

applied LCM to midbrain tissue to isolate single neuromelanin- and TH-positive neurons (n = 10 per sample) from the SNpc, which were then subjected to RT-PCR. In line with our previous results, we found significantly reduced 7S DNA:*MT-ND1* ratios in postmortem patient DANs (Fig. 5B). However, we did not detect any differences in mtDNA deletion levels or in mtDNA copy number (data not shown).

Next, to determine whether *PRKN* mutation carriers suffer from neuroinflammation, we performed snRNAseq from postmortem ventral midbrain sections (Fig. 5A). A total of 10,578 high-quality nuclei (patient = 4173, controls = 2047 and 4358) were projected into two dimensions with the uniform manifold approximation and projection (UMAP) algorithm (Fig. 5C,E). We found eight major cell types including neurons and glial cells (Fig. 5D,E). Each cell cluster was annotated based on the expression of marker genes (Fig. 5D, Table S1). The most abundant cell type making ≈52.5% of the midbrain population are oligodendrocytes, followed by neurons (≈14.6%), microglia (≈11.6%), oligodendrocyte precursor cells (≈7.3%), and astrocytes (≈6.6%). Residual abundances were detected for other cell types. To assess neuroinflammation, we first compared cell density distributions in UMAP and observed a large increase in the microglial population and a decreased fraction of neurons and astrocytes (Fig. 5F) in the *PRKN*-mutant midbrain. Our results confirm the alteration in glial cell populations in the *PRKN* mutation carriers reported previously.[36] This shift infers an incorrect immune response, which likely leads to neuroinflammation. The resulting decrease of the *PRKN* midbrain neuronal population (Fig. 5F) compared with controls may be a trigger or downstream effect of the aforementioned immune response. Furthermore, the proinflammatory cytokines *IL1B* and tumor necrosis factor (*TNF)* were differentially expressed and upregulated in *PRKN*-mutant microglia compared with controls (Table S2). Accordingly, the immune response pathways, primarily the interleukin signaling pathways, were most perturbed in microglia from the *PRKN* mutation carrier (Tables S3 and S4).

Finally, to assess the causal link between mtDNA dyshomeostasis and neuroinflammation in *PRKN*-associated PD, we generated iPSC-derived neuron–microglia co-cultures from controls and patients with *PRKN* mutations and exposed them to LPS, mtDNA isolated from patients with *PRKN*-PD, or both. The composition of the co-cultures with regard to DANs and microglia was not affected by the different treatments (Fig. S4A,B). Moreover, stimulation by mtDNA or LPS alone did not reveal any differences in the expression of cytokines in cells lacking parkin. However, when mtDNA was added as a secondary trigger after LPS priming, we observed that patient-derived co-cultures showed a greater response in the expression of *IL6* (Fig. 5G). Although *IL1B* was equally upregulated after LPS/mtDNA treatment, the difference between *PRKN*-PD and control co-cultures was not significant (Fig. S4C).

Discussion

Using a multimodal approach, we explored novel mechanisms of mitochondrial quality control exerted by parkin. Although most parkin studies focused on its role in mitochondrial clearance, the wide range of parkin substrates suggests that the protein functions in cellular processes beyond mitophagy.[24] Thus, we decided to investigate the mitochondrial biogenesis and mtDNA maintenance pathways in parkin-deficient cells.

Mitochondrial biogenesis is synchronized in the nucleus, with PGC1-α acting as the master regulator.[27] Studies found a direct interaction between parkin and PGC1-α,[27] whereas others have shown an interaction with PARIS—a PGC1-α transcriptional repressor.[6] In the current study, parkin-depleted cells showed reduced PGC1-α protein levels while the abundance of PARIS remained unchanged, insinuating an alternative mechanism of PGC1-α reduction. We looked upstream and found that the SIRT1 protein was reduced in parkin-deficient cells. *PGC1-α* gene expression and protein deacetylation is regulated by the NAD^+-dependent energy sensor SIRT1.[28,29] Moreover, our and a published metabolic study in parkin-deficient neurons revealed increased lactate:pyruvate ratios, suggesting lower levels of freely accessible NAD^+ as a result of metabolic remodeling from oxidative phosphorylation to glycolysis.[30,37]

PGC1-α can activate the NRFs, which control the expression of the mitochondrial transcription factors *TFAM* and *TFB2M*.[31] Our gene expression and protein analyses confirmed disruptions of this pathway at each level in cells lacking parkin. The sole semiautonomous organelle of human cells, mitochondria, encompass their own system to coordinate mtDNA transcription, replication, translation, and repair. Because of its dynamic nature and proximity to the ETC, mtDNA maintenance is exceptionally important for ensuring homogeneity and preventing the expansion of aberrant mtDNA molecules. Studies in mitotically active parkin-overexpressing cells have shown a direct interaction of parkin with TFAM and an association with the mitochondrial genome.[26,38]

Focusing on mtDNA integrity, we found significantly less 7S DNA per mtDNA molecule in iPSC-derived neurons, SH-SY5Y cells, and postmortem DANs lacking parkin. This is in agreement with previous findings in postmortem DANs isolated from patients with idiopathic PD (IPD).[20] The D-loop region of the

15318257, 2022, 7, Downloaded from https://movementdisorders.onlinelibrary.wiley.com/doi/10.1002/mds.29025 by Cochrane Luxembourg, Wiley Online Library on [29/03/2023]. See the Terms and Conditions (https://onlinelibrary.wiley.com/terms-and-conditions) on Wiley Online Library for rules of use; OA articles are governed by the applicable Creative Commons License

mitochondrial genome serves as the initiation site for its replication and transcription. The synthesis of 7S DNA in the D-loop is stimulated by TFAM, consistent with evidence showing that elevated TFAM matrix levels increase the rate of 7S DNA synthesis.[39] Indeed, calculating TFAM:mtDNA ratios, parkin-deficient neurons exhibited a significant reduction. Moreover, we observed decreased mtDNA gene expression that coincided with diminished ETC CI activity in parkin-KO SH-SY5Y cells. Of note, we previously reported ETC CI impairments in iPSC-derived neurons from our *PRKN*-mutant samples.[40] Interestingly, experiments in purified TH-positive neurons from patients with *PRKN* mutations highlighted that the 7S DNA phenotype is more pronounced in DANs, suggesting a link between mtDNA homeostasis and dopamine signaling. Because of their high energy requirements and the autoxidation properties of the neurotransmitter, DANs are particularly vulnerable to metabolic changes.[41,42] Interestingly, hypoxic conditions mimicked the mtDNA phenotypes observed in parkin-deficient cells. These findings further strengthened our hypothesis that a shift from oxidative phosphorylation to glycolysis triggers mtDNA dyshomeostasis in the absence of parkin.

Beyond alterations in the mitochondrial biogenesis pathway, we detected elevated mtDNA copy numbers but diminished TFAM abundance per mitochondrial genome in parkin-deficient neurons. TFAM reduction has previously been shown to allow mtDNA to escape from mitochondria into the cytosol, where it is recognized by the cytosolic DNA sensor cGAS, provoking activation of an innate immune response.[8] Indeed, we observed that neurons from patients with PD and parkin-KO SH-SY5Y cells incur higher levels of mtDNA in the cytosolic compartment compared with controls. We also quantified mtDNA molecules in the extracellular medium of our cellular samples, yet we did not detect any differences compared with controls or increases in inflammatory cytokines.

However, keeping in mind that reprogramming of postnatal cells can cause artificial rejuvenation,[35] we burdened parkin-deficient cells with mitochondrial mutagenic stress—a normal aging phenomenon[43]—to investigate mtDNA release and inflammation. To create a neuronal aging model of *PRKN*-PD, we adopted an approach by Pickrell and colleagues who crossed parkin-KO with *POLG*-mutant mice.[10] These animals exhibited levodopa-reversible motor deficits, a selective loss of nigral DANs, impaired mtDNA dynamics, and cGas/STING-mediated inflammation.[9,10] Accordingly, we generated iPSC-derived midbrain neurons from a patient with Alper's disease with compound-heterozygous *POLG* mutations and subjected the cultures to either scramble or parkin shRNA. Parkin knockdown in *POLG*-mutant neurons replicated the 7S DNA phenotype as well as disruptions of the mitochondrial biogenesis pathway. In addition, we detected elevated ccf-mtDNA levels in the cellular medium and an increase in cGAS protein abundance. In agreement with previous results in parkin-KO "mutator" mice, this suggests that parkin depletion combined with mitochondrial mutagenic stress triggers the release of mtDNA into the cytosol and extracellular space in patient neurons.

Microglia are considered the resident innate immune cells in the brain, which can be activated by various DAMPs. The lack of microglial cells in our neuronal cultures may explain the inability to detect inflammation in our samples. We therefore decided to use postmortem tissue from a patient with compound-heterozygous *PRKN*-PD and controls to investigate a potential link between parkin dysfunction and neuroinflammation using snRNAseq. Our results showed a strong infiltration of microglia in the *PRKN*-mutant midbrain and an upregulation of the proinflammatory cytokines *IL1B* and *TNF*. This dysregulation resulted in the perturbation of immune and oxidative stress response pathways.

To additionally evaluate the extent of the microglia phenotype in *PRKN*-PD, we made use of our recently published single-cell data set of five patients with IPD and six controls.[23] Comparing the cell-type distribution across the three groups (Fig. S5A-D), the *PRKN*-mutant midbrain showed an even larger percentage of microglia than the IPD tissue samples (Fig. S5D). Moreover, the expression of microglia activation markers heat shock protein 90 alpha family class A member 1 (*HSP90AA1*) and *IL1B* was the highest in the *PRKN*-mutant cell population (Fig. S5E). Thus, despite the limitation of examining brain tissue from a single mutant case, this cross-comparison further supports a role for microglia in the pathogenesis of *PRKN*-PD.

With regard to the distribution of other glial cells, we detected a reduction in astrocytes in *PRKN*-PD (Fig. S4D), which is in line with previous observations in the *PRKN*-mutant midbrain.[36] The resulting lack of astroglial neuron support likely perpetuates the inflammatory phenotypes in *PRKN*-PD as indicated by elevated expression of the astrocyte activation marker cluster of differentiation 44 (*CD44*) (Fig. S5F). Interestingly, despite lower overall astrocyte numbers, *CD44* levels in *PRKN*-PD astrocytes were even higher than in IPD astrocytes (Fig. S5F). Although additional rare *PRKN*-mutant midbrain samples need to be studied in the future, our snRNAseq analysis, which also considered our published results from IPD cases, provides valuable insights into the cell-type composition and transcriptomic landscape of the *PRKN*-PD midbrain.

Finally, to assess whether mtDNA dyshomeostasis and inflammation are causally linked in *PRKN*-PD, we generated iPSC-derived neuron–microglia co-cultures from controls and patients with *PRKN* mutations, which were treated with mtDNA isolated from *PRKN*-mutant cells. Our results showed that, when added as a secondary stimulus to LPS priming, mtDNA caused *IL6* overexpression

15318257, 2022, 7, Downloaded from https://movementdisorders.onlinelibrary.wiley.com/doi/10.1002/mds.29025 by Cochrane Luxembourg, Wiley Online Library on [29/03/2023]. See the Terms and Conditions (https://onlinelibrary.wiley.com/terms-and-conditions) on Wiley Online Library for rules of use; OA articles are governed by the applicable Creative Commons License

in cells lacking parkin, suggesting that parkin deficiency renders cells more responsive to proinflammatory stimuli.

Taken together, our study highlights parkin's involvement in mtDNA maintenance and supports a link between mtDNA dyshomeostasis and inflammation in human cellular models of PD. In iPSC-derived cultures from patients with *PRKN* mutations, we observed that mtDNA transcription-associated 7S DNA is preferentially depleted in DANs. This TFAM deficiency-mediated phenotype is likely the consequence of SIRT1 depletion and inactivation in response to a lack of free NAD^+ in the absence of parkin. However, the origin of the mitochondrial energy deficit in *PRKN*-mutant neurons currently remains elusive. Interestingly, recent studies suggest that parkin deficiency can be a driver of altered mitochondrial metabolism. Either via its function in mitochondrial clearance or through translational control of nuclear-encoded ETC mRNAs,[5,26] the mutant protein could trigger the respiratory complex impairments detected in patient neurons. With SIRT1 acting as a connector between cell metabolism, mitophagy, and biogenesis pathways, further research will be needed to determine the exact sequence of events triggering mitochondrial dysfunction in parkin-deficient DANs.[44] Moreover, additional analyses in iPSC-derived co-culture systems should aim at the identification of the immune signaling pathways activated in microglia in response to neuronal release of mitochondrial DAMPs, including mtDNA. Such investigations will pave the way for innovative anti-inflammatory treatment approaches in PD.

Acknowledgments: We express our gratitude to the tissue donors and their families for their generous participation. Postmortem tissue for this study was provided by the Newcastle Brain Tissue Resource and Juntendo University. Moreover, Prof. Dr. Doug Turnbull (Wellcome Trust Centre for Mitochondrial Research, Newcastle University) kindly provided fibroblasts for the study from a patient with Alper's disease. We are grateful to Thea Maria Van Wüllen (Luxembourg Centre for Systems Biomedicine) and Carola Dietrich (Max-Planck-Institute for Human Molecular Genetics, Berlin) for their assistance in postmortem sample preparation for single-cell RNA sequencing. We thank Nassima Ouzren and Ursula Heins-Marroquin for optimizing protocols for experiments used in the study. In addition, the authors thank Dr. Christian Jäger and Xiangyi Dong from the Luxembourg Centre for Systems Biomedicine Metabolomics Platform for the generation of metabolomics data. Finally, this project was supported by the Imaging Facility and the Disease Modelling and Screening Platform, Luxembourg Centre for Systems Biomedicine, University of Luxembourg, and Luxembourg Institute of Health, Luxembourg. Open access funding enabled and organized by Projekt DEAL.

Data Availability Statement

Raw data for the midbrain tissue sample from the *PRKN* mutation carrier is available in the GEO with accession number GSE166790. Raw data for the two control samples were previously sequenced used in this study are available in the GEO with the accession number GSE157783 (data sets: C2-GSM4774937, C3-GSM4774938). Other data are available upon request.

References

1. Panigrahi B, Martin KA, Li Y, et al. Dopamine Is Required for the Neural Representation and Control of Movement Vigor. Cell 2015; 162(6):1418–1430. https://doi.org/10.1016/j.cell.2015.08.014
2. Lücking CB, Dürr A, Bonifati V, et al. Association between early-onset Parkinson's disease and mutations in the parkin gene. N Engl J Med 2000;342(21):1560–1567. https://doi.org/10.1056/NEJM200005253422103
3. Grünewald A, Kumar KR, Sue CM. New insights into the complex role of mitochondria in Parkinson's disease. Prog Neurobiol 2019; 177:73–93. https://doi.org/10.1016/j.pneurobio.2018.09.003
4. Kitada T, Asakawa S, Hattori N, et al. Mutations in the parkin gene cause autosomal recessive juvenile parkinsonism. Nature 1998; 392(6676):605–608. https://doi.org/10.1038/33416
5. Narendra D, Tanaka A, Suen DF, Youle RJ. Parkin is recruited selectively to impaired mitochondria and promotes their autophagy. J Cell Biol 2008;183(5):795–803. https://doi.org/10.1083/jcb.200809125
6. Shin JH, Ko HS, Kang H, et al. PARIS (ZNF746) repression of PGC-1α contributes to neurodegeneration in Parkinson's disease. Cell 2011;144(5):689–702. https://doi.org/10.1016/j.cell.2011.02.010
7. Chocron ES, Munkácsy E, Pickering AM. Cause or casualty: The role of mitochondrial DNA in aging and age-associated disease. Biochim Biophys Acta Mol Basis Dis 2019;1865(2):285–297. https://doi.org/10.1016/j.bbadis.2018.09.035
8. West AP, Khoury-Hanold W, Staron M, et al. Mitochondrial DNA stress primes the antiviral innate immune response. Nature 2015; 520(7548):553–557. https://doi.org/10.1038/nature14156
9. Sliter DA, Martinez J, Hao L, et al. Parkin and PINK1 mitigate STING-induced inflammation. Nature 2018;561(7722):258–262. https://doi.org/10.1038/s41586-018-0448-9
10. Pickrell AM, Huang CH, Kennedy SR, et al. Endogenous Parkin Preserves Dopaminergic Substantia Nigral Neurons following Mitochondrial DNA Mutagenic Stress. Neuron 2015;87(2):371–381. https://doi.org/10.1016/j.neuron.2015.06.034
11. Seibler P, Graziotto J, Jeong H, Simunovic F, Klein C, Krainc D. Mitochondrial Parkin recruitment is impaired in neurons derived from mutant PINK1 induced pluripotent stem cells. J Neurosci Off J Soc Neurosci. 2011;31(16):5970–5976. https://doi.org/10.1523/JNEUROSCI.4441-10.2011
12. Kriks S, Shim JW, Piao J, et al. Dopamine neurons derived from human ES cells efficiently engraft in animal models of Parkinson's disease. Nature 2011;480(7378):547–551. https://doi.org/10.1038/nature10648
13. Haenseler W, Sansom SN, Buchrieser J, et al. A Highly Efficient Human Pluripotent Stem Cell Microglia Model Displays a Neuronal-Co-culture-Specific Expression Profile and Inflammatory Response. Stem Cell Rep 2017;8(6):1727–1742. https://doi.org/10.1016/j.stemcr.2017.05.017
14. Reinhardt P, Glatza M, Hemmer K, et al. Derivation and expansion using only small molecules of human neural progenitors for neurodegenerative disease modeling. PloS One 2013;8(3):e59252. https://doi.org/10.1371/journal.pone.0059252
15. Sandor C, Robertson P, Lang C, et al. Transcriptomic profiling of purified patient-derived dopamine neurons identifies convergent perturbations and therapeutics for Parkinson's disease. Hum Mol Genet 2017;26(3):552–566. https://doi.org/10.1093/hmg/ddw412
16. Arena G, Cissé MY, Pyrdziak S, et al. Mitochondrial MDM2 Regulates Respiratory Complex I Activity Independently of p53. Mol Cell 2018;69(4):594–609.e8. https://doi.org/10.1016/j.molcel.2018.01.023
17. Vengellur A, LaPres JJ. The role of hypoxia inducible factor 1alpha in cobalt chloride induced cell death in mouse embryonic fibroblasts. Toxicol Sci Off J Soc Toxicol 2004;82(2):638–646. https://doi.org/10.1093/toxsci/kfh278
18. McCormack JG. Mitochondria. A practical approach; Edited by V M Darley-Usmar, D Rickwood and M T Wilson. pp 340. IRL Press, Oxford. 1987. £29 or £18 (pbk) ISBN 1-85221-034-6 or 033-8 (pbk). Biochem Educ 1988;16(2):118. https://doi.org/10.1016/0307-4412(88)90107-0

15318257, 2022, 7, Downloaded from https://movementdisorders.onlinelibrary.wiley.com/doi/10.1002/mds.29025 by Cochrane Luxembourg, Wiley Online Library on [29/03/2023]. See the Terms and Conditions (https://onlinelibrary.wiley.com/terms-and-conditions) on Wiley Online Library for rules of use; OA articles are governed by the applicable Creative Commons License

19. Delcambre S, Ghelfi J, Ouzren N, et al. Mitochondrial Mechanisms of LRRK2 G2019S Penetrance. Front Neurol 2020;11:881. https://doi.org/10.3389/fneur.2020.00881
20. Grünewald A, Rygiel KA, Hepplewhite PD, Morris CM, Picard M, Turnbull DM. Mitochondrial DNA Depletion in Respiratory Chain-Deficient Parkinson Disease Neurons. Ann Neurol 2016;79(3):366–378. https://doi.org/10.1002/ana.24571
21. Rygiel KA, Grady JP, Taylor RW, Tuppen HAL, Turnbull DM. Triplex real-time PCR--an improved method to detect a wide spectrum of mitochondrial DNA deletions in single cells. Sci Rep 2015;5:9906. https://doi.org/10.1038/srep09906
22. Meiser J, Delcambre S, Wegner A, et al. Loss of DJ-1 impairs antioxidant response by altered glutamine and serine metabolism. Neurobiol Dis 2016;89:112–125. https://doi.org/10.1016/j.nbd.2016.01.019
23. Smajić S, Prada-Medina CA, Landoulsi Z, et al. Single-cell sequencing of human midbrain reveals glial activation and a Parkinson-specific neuronal state. Brain J Neurol. Published online December 17 2021;awab446. https://doi.org/10.1093/brain/awab446
24. Sarraf SA, Raman M, Guarani-Pereira V, et al. Landscape of the PARKIN-dependent ubiquitylome in response to mitochondrial depolarization. Nature 2013;496(7445):372–376. https://doi.org/10.1038/nature12043
25. Palikaras K, Lionaki E, Tavernarakis N. Balancing mitochondrial biogenesis and mitophagy to maintain energy metabolism homeostasis. Cell Death Differ 2015;22(9):1399–1401. https://doi.org/10.1038/cdd.2015.86
26. Kuroda Y, Mitsui T, Kunishige M, et al. Parkin enhances mitochondrial biogenesis in proliferating cells. Hum Mol Genet 2006;15(6):883–895. https://doi.org/10.1093/hmg/ddl006
27. Zheng L, Bernard-Marissal N, Moullan N, et al. Parkin functionally interacts with PGC-1α to preserve mitochondria and protect dopaminergic neurons. Hum Mol Genet 2017;26(3):582–598. https://doi.org/10.1093/hmg/ddw418
28. Cantó C, Auwerx J. PGC-1alpha, SIRT1 and AMPK, an energy sensing network that controls energy expenditure. Curr Opin Lipidol 2009;20(2):98–105. https://doi.org/10.1097/MOL.0b013e328328d0a4
29. Amat R, Planavila A, Chen SL, Iglesias R, Giralt M, Villarroya F. SIRT1 controls the transcription of the peroxisome proliferator-activated receptor-gamma Co-activator-1alpha (PGC-1alpha) gene in skeletal muscle through the PGC-1alpha autoregulatory loop and interaction with MyoD. J Biol Chem 2009;284(33):21872–21880. https://doi.org/10.1074/jbc.M109.022749
30. Williamson DH, Lund P, Krebs HA. The redox state of free nicotinamide-adenine dinucleotide in the cytoplasm and mitochondria of rat liver. Biochem J 1967;103(2):514–527. https://doi.org/10.1042/bj1030514
31. Gleyzer N, Vercauteren K, Scarpulla RC. Control of mitochondrial transcription specificity factors (TFB1M and TFB2M) by nuclear respiratory factors (NRF-1 and NRF-2) and PGC-1 family coactivators. Mol Cell Biol 2005;25(4):1354–1366. https://doi.org/10.1128/MCB.25.4.1354-1366.2005
32. Jornayvaz FR, Shulman GI. Regulation of mitochondrial biogenesis. Essays Biochem 2010;47:69–84. https://doi.org/10.1042/bse0470069
33. Suen DF, Narendra DP, Tanaka A, Manfredi G, Youle RJ. Parkin overexpression selects against a deleterious mtDNA mutation in heteroplasmic cybrid cells. Proc Natl Acad Sci U S A 2010;107(26):11835–11840. https://doi.org/10.1073/pnas.0914569107
34. Borsche M, König IR, Delcambre S, et al. Mitochondrial damage-associated inflammation highlights biomarkers in PRKN/PINK1 parkinsonism. Brain J Neurol 2020;143(10):3041–3051. https://doi.org/10.1093/brain/awaa246
35. Mertens J, Paquola ACM, Ku M, et al. Directly Reprogrammed Human Neurons Retain Aging-Associated Transcriptomic Signatures and Reveal Age-Related Nucleocytoplasmic Defects. Cell Stem Cell 2015;17(6):705–718. https://doi.org/10.1016/j.stem.2015.09.001
36. Kano M, Takanashi M, Oyama G, et al. Reduced astrocytic reactivity in human brains and midbrain organoids with PRKN mutations. NPJ Park Dis 2020;6(1):33. https://doi.org/10.1038/s41531-020-00137-8
37. Okarmus J, Havelund JF, Ryding M, et al. Identification of bioactive metabolites in human iPSC-derived dopaminergic neurons with PARK2 mutation: Altered mitochondrial and energy metabolism. Stem Cell Rep. 2021;16(6):1510–1526. https://doi.org/10.1016/j.stemcr.2021.04.022
38. Rothfuss O, Fischer H, Hasegawa T, et al. Parkin protects mitochondrial genome integrity and supports mitochondrial DNA repair. Hum Mol Genet 2009;18(20):3832–3850. https://doi.org/10.1093/hmg/ddp327
39. Gensler S, Weber K, Schmitt WE, et al. Mechanism of mammalian mitochondrial DNA replication: import of mitochondrial transcription factor A into isolated mitochondria stimulates 7S DNA synthesis. Nucleic Acids Res 2001;29(17):3657–3663. https://doi.org/10.1093/nar/29.17.3657
40. Zanon A, Kalvakuri S, Rakovic A, et al. SLP-2 interacts with Parkin in mitochondria and prevents mitochondrial dysfunction in Parkin-deficient human iPSC-derived neurons and Drosophila. Hum Mol Genet 2017;26(13):2412–2425. https://doi.org/10.1093/hmg/ddx132
41. LaVoie MJ, Hastings TG. Dopamine quinone formation and protein modification associated with the striatal neurotoxicity of methamphetamine: evidence against a role for extracellular dopamine. J Neurosci Off J Soc Neurosci 1999;19(4):1484–1491.
42. Graves SM, Xie Z, Stout KA, et al. Dopamine metabolism by a monoamine oxidase mitochondrial shuttle activates the electron transport chain. Nat Neurosci 2020;23(1):15–20. https://doi.org/10.1038/s41593-019-0556-3
43. Reeve A, Simcox E, Turnbull D. Ageing and Parkinson's disease: why is advancing age the biggest risk factor? Ageing Res Rev 2014;14:19–30. https://doi.org/10.1016/j.arr.2014.01.004
44. Agarwal E, Goldman AR, Tang HY, et al. A cancer ubiquitome landscape identifies metabolic reprogramming as target of Parkin tumor suppression. Sci Adv 2021;7(35):eabg7287. https://doi.org/10.1126/sciadv.abg7287

Supporting Data

Additional Supporting Information may be found in the online version of this article at the publisher's web-site.

15318257, 2022, 7, Downloaded from https://movementdisorders.onlinelibrary.wiley.com/doi/10.1002/mds.29025 by Cochrane Luxembourg, Wiley Online Library on [29/03/2023]. See the Terms and Conditions (https://onlinelibrary.wiley.com/terms-and-conditions) on Wiley Online Library for rules of use; OA articles are governed by the applicable Creative Commons License

Supplement

Parkin deficiency impairs mitochondrial DNA dynamics and propagates inflammation

Kobi Wasner, PhD[1], Semra Smajic, MSc[1]*, Jenny Ghelfi, BSc[1]*, Sylvie Delcambre, PhD[1], Cesar A. Prada-Medina, PhD[2], Evelyn Knappe, MSc[3], Giuseppe Arena, PhD[1], Patrycja Mulica, MSc[1], Gideon Agyeah, MSc[1], Aleksandar Rakovic, PhD[3], Ibrahim Boussaad, PhD[1,9], Katja Badanjak, MSc[1], Jochen Ohnmacht, PhD[1,8], Jean-Jacques Gérardy, BSc[5], Masashi Takanashi, MD[4], Joanne Trinh, PhD[3], Michel Mittelbronn, MD,[1,5-8], Nobutaka Hattori, MD, PhD[4], Christine Klein, MD[3], Paul Antony, PhD[1,9], Philip Seibler, PhD[3], Malte Spielmann, MD[2,10], Sandro L. Pereira, PhD[1,7], and Anne Grünewald, PhD[1,3]

*These authors contributed equally.

1 Luxembourg Centre for Systems Biomedicine, University of Luxembourg, Esch-sur-Alzette, Luxembourg

2 Max Planck Institute for Molecular Genetics, Berlin, Germany

3 Institute of Neurogenetics, University of Lübeck, Lübeck, Germany

4 Department of Neurology, Juntendo University, Tokyo, Japan

5 National Center of Pathology, Laboratoire National de Santé, Dudelange, Luxembourg

6 Luxembourg Center of Neuropathology, Dudelange, Luxembourg

7 Department of Oncology, Luxembourg Institute of Health, Luxembourg, Luxembourg

8 Department of Life Science and Medicine, University of Luxembourg, Esch-sur-Alzette, Luxembourg

9 Disease Modelling and Screening Platform, Luxembourg Centre of Systems Biomedicine, University of Luxembourg & Luxembourg Institute of Health, Luxembourg

10 Institute of Human Genetics, University of Lübeck, Lübeck, Germany

Corresponding author:

Anne Grünewald, Ph.D., Luxembourg Centre for Systems Biomedicine, University of Luxembourg, 6 avenue du Swing, L-4367 Belvaux, Luxembourg, phone: (+352) 46 66 44 9793, e-mail: anne.gruenewald@uni.lu

List of content

1. Supplementary methods

1.1. Cell culture

1.1.1. Generation of small molecule neural precursor cells (smNPCs)

smNPCs were cultured and expanded in N2B27 medium - Neurobasal (Gibco)/DMEM-F12 (Gibco) 50:50 with 1% B27 lacking vitamin A (ThermoFisher), 0.5% N2 (Life Technologies), 1% penicillin-streptomycin (ThermoFisher) and 1% 200 mM glutamine (Westburg) - supplemented with 3 µM CHIR 99021 (Sigma), 150 µM ascorbic acid (AA) (Sigma) and 0.5 µM purmorphamine (Sigma). The medium was changed every second day.

1.1.2. Generation of midbrain neurons

To initiate neuronal differentiation, smNPCs were counted using the Countess II FL Automated Cell Counter (ThermoFisher) and seeded onto Matrigel-coated (Corning) 6-well plates in N2/B27 medium supplemented with 1 µM purmorphamine, 200 µM ascorbic acid (AA) and 100 ng FGF8 (PeproTech) for 8 days. For the next 2 days, cells were cultured in N2/B27 medium with 0.5 µM purmorphamine and 200 µM AA. For the remainder of the differentiation (22 days), cells were maintained in Maturation medium: N2/B27 supplemented with 200 µM AA, 500 µM dibutyryl-cAMP (Applichem), 1 ng/mL TGF-β3 (Peprotech), 10 ng/mL GDNF (Peprotech) and 20 ng/mL BDNF (PeproTech). The medium was changed every second day.

1.1.3. Generation of induced pluripotent stem cells (iPSCs)

Skin fibroblasts obtained from an Alper's disease patient with *POLG* mutations (Fig. S1A) were reprogrammed into iPSCs using the Epi5^{TM} Episomal iPSC Reprogramming Kit (ThermoFisher) according to the manufacturer's instructions. Briefly, fibroblasts were maintained in DMEM supplemented with 10% FBS and 1% Penicillin-Streptomycin. Once 75-90% confluent, fibroblasts were washed with PBS (Gibco) and detached by adding 0.05% Trypsin/EDTA (ThermoFisher) for 5 min at 37°C. Cells were then collected and counted using the Countess II FL Automated Cell Counter. Next, 1 x 10^7 cells were removed, centrifuged at 200 x g for 5 min and transduced with Epi5™ Reprogramming Vectors and Epi5™ p53 & EBNA Vectors using the Amaxa Nucleofector I (Lonza) with 3 pulses at 1650 V for 10 ms. After transfection, cells were seeded onto irritated mouse embryonic fibroblasts and cultured

in mTeSR™ 1 complete medium (STEMCELL Technologies). The medium was changed every day. After ~1 month, iPSC colonies were picked based on their stem-cell-like morphology and expanded on Matrigel-coated plates. The generation of smNPCs and midbrain neurons was performed identically as described for iPSCs from Parkin mutation carriers.

1.1.4. Generation of isogenic Parkin-knockout neuroblastoma cells

Parkin knockout neuroblastoma (SH-SY5Y) cells were generated using an RNA-guided CRISPR/Cas9 endonuclease. For this, SH-SY5Y cells were transiently cotransfected with plasmids expressing either a human codon-optimized Cas9 (hCas9 was a gift from George Church [Addgene plasmid # 41815]) and a guide RNA (gRNA_Cloning Vector was a gift from George Church [Addgene plasmid # 41824]) containing a 19-base long sequence that matches the human *PRKN* target sequence 5'- GTGGTTGCTAAGCGACAGG -3'. Upon transfection, cells were re-suspended in growth medium, counted and plated onto Petri dishes at a density of 1 cell/cm2. Cells were grown until they formed distinct, monoclonal colonies. The colonies were scraped off, transferred into different wells of a 6-well plate, and propagated to obtain enough material for the DNA extraction for Sanger sequencing. We identified one clonal cell line carrying a homozygous mutation c.100_101insC (p.Q34PfsX5) in the *PRKN* gene resulting in a premature stop codon, further leading to nonsense-mediated decay. To induce hypoxia, SH-SY5Y cells were plated onto a 6-well plate at a density of 1.1 million cells/well and, the following day, treated for 24h with 200 µM $CoCl_2$ (Merck, C8661) in MOPS (ROTH, 6979.2) buffer.

1.2. Parkin silencing

For Parkin knockdown, the lentiviral pLKO.1 vector (Addgene) was used to express short hairpin RNA (shRNA) against human Parkin (Sense: ccggCCAGTAGCTTTGCACCTGATTctcgagAATCAGGTGCAAAGCTACTGGttttttg).[1] The MISSION pLKO.1-puro Non-Mammalian shRNA control Plasmid DNA (Sigma), targeting no known mammalian genes, was used as negative control for lentiviral transduction (Sense: CCGGCAACAAGATGAAGAGCACCAACTC-GAGTTGGTGCTCTTCATCTTGTTGTTTTT). Lentiviral constructs, as well as 2nd generation packaging plasmids (psPAX2, pMD2G), were transfected in HEK293T cells by calcium phosphate precipitation in the presence of 25 µM

chloroquine. HEK293T cell culture medium, containing the respective lentiviral particles, were harvested 48 hrs post-transfection, passed through 0.45 µM filters and used to transduce target cells overnight, in presence of 8 µg/mL Polybrene.

1.3. Generation and treatment of iPSC-derived neuron-microglia co-cultures

DANs and microglia cells were generated according to previously described protocols.[2-4] At day 92 of neuronal differentiation, $4x10^5$ microglia precursor cells were plated onto corresponding cell lines of neurons leading to their maturation. Equal amounts of both cell types were co-cultured for 35 days before treatment with LPS (100 ng/mL) for 3 hours and mtDNA (300 ng) for 1 hour. A mixture of mtDNA extracted from all *PRKN*-mutant patients was used.

1.4. Immunocytochemistry

SH-SY5Y cells, iPSC-derived smNPCs and midbrains neurons were fixed in 4% paraformaldehyde for 15 min at room temperature and then washed three times in PBS (Gibco). Cells were then permeabilized in the blocking buffer (1% bovine serum albumin [Sigma], 0.25% Triton-X 100 [Sigma] in PBS) for 1 hr at room temperature. Cells were then stained overnight at 4°C with primary antibodies in blocking buffer. For smNPCs, cells received antibodies against Nestin (R&D Systems, MAB1259), Pax6 (BioLegend, 901301) and Musashi (Abcam, ab21628). For neurons, cells were subjected to several combinations of antibodies (depending upon the experiment) against TUBB3 (BioLegend, 801202), tyrosine hydroxylase (Sigma T8700), DNA (Progen AC-30-10), TOM20 (Santa Cruz SC-17764). The next day, cells were washed three times in PBS and then stained with fluorescent secondary antibodies in blocking buffer for 1h at room temperature. Cells were then washed three times in PBS, and incubated with Hoechst 33342 (ThermoFisher) for 10 min. For the assessment of mtDNA release into the cytosol, cells were incubated for 30 minutes at room temperature with HCS CellMask™ Orange stain (ThermoFisher) prior to the nuclear staining and following the manufacturer's indications. Images were taken using a 20X objective (for smNPCs) or 40X objective (for neurons) using the Zeiss Axio Imager 2 microscope, or 60X objective for neurons and SH-SY5Y cells on the Cell Voyager CV8000 high-content screening confocal microscope (Yokogawa Electric Corporation).

1.5. Western blotting

Antibodies used in the study: Parkin (Santa Cruz sc-32282), SIRT1 (Abcam ab32441), PGC1-α (Novus Biologicals NBP1-04676), NRF1 (Abcam ab175932), NRF2 (Cell Signaling abe1047), VDAC (Abcam ab14734), LC3A/B (Cell Signaling, 4108), TFAM (Abcam ab47517), TUBB3 (Tuj1) (BioLegend 801202), tyrosine hydroxylase (Sigma T8700), cGAS (Santa Cruz sc-515777) and beta-actin (Sigma A1978).

1.6. Metabolite extraction and metabolomics analysis

Metabolites from 35d-old neurons were extracted using a Methanol/Water-Chloroform mix. Neurons were seeded in 12-well plates at day 25 of differentiation and then maintained for 5 days. Cells were washed once with 0.9% NaCl (Sigma). Metabolism was quenched with 200 µL ice-cold methanol (Roth). 80 µL of 4°C water was added and the plate was placed on an orbital shaker for 10 min at 4°C. The mixture was transferred to a tube containing 100 µL of ice-cold chloroform (Roth) and then shaken on a thermomixer at 4°C for 5 min. An additional 100 µL of ice-cold chloroform and 4°C water were added. The samples were then vortexed and centrifuged for 5 min at 21000 x g, 4°C. 125 µL of the upper phase were transferred to a glass vial and dried in a vacuum centrifuge. Samples were capped and kept at -80°C until measurement.

Polar metabolites were derivatized and measured by GC-MS using an Agilent 7890B GC coupled to an Agilent 5977A Mass Selective Detector (Agilent Technologies) following an established method. The MetaboliteDetector software package (Version 3.220180913) was used for mass spectrometry (MS) data post processing and quantification. NAD^+:NADH ratios were determined using the colorimetric NAD/NADH Quantification Kit from Sigma following the manufacturer's instructions.

1.7. Mitochondrial extraction

SH-SY5Y cells were resuspended and washed in homogenization buffer (HB) (10 mM Tris, pH 7.4, 1 mM EDTA, 250 mM Sucrose) with protease and phosphatase inhibitors (Halt Protease & Phosphatase inhibitor cocktail). After washing the pellet at 4000 x g for 5 min at 4°C, fresh HB was added and the pellet was homogenized for 1 min on ice

using a pellet pestle (Sigma). Homogenates were then centrifuged at 1500 x g for 10 min at 4°C and the supernatant was removed. After two washing steps in HB, mitochondria were pelleted by centrifugation at 8000 x g for 10 min.

1.8. NADH-COQ1 reductase assay

To measure complex I activity, mitochondrial homogenates were subjected to three freeze/thaw cycles in HB buffer and then placed in buffer containing 20 mM K^+Phosphate buffer (sodium phosphate (VWR), magnesium chloride (Sigma), 150 µM NADH (Sigma), 1 mM potassium cyanide (Sigma), and bovine serum albumin (BSA) (Sigma)) followed by an additional three freeze/thaw cycles. Samples were then placed into a 96-well plate (Greiner Bio-One) and kinetic measurement was evaluated at 340 nm using the Biotek Cytation 5 plate reader (Biotek). We first measured baseline activity for 3 min, then added 50 µM ubiquinone (Sigma) and measured kinetics for 10 min, and finally added 10 µM rotenone (Abcam) and measured for 10 min.

1.9. Citrate synthase assay

The citrate synthase assay was performed on the same mitochondrial extracts as in the NADH-COQ1 assay. Here, we followed a modified protocol based on Coore *et al.*[5] First, we subjected mitochondria to three freeze/thaw cycles in HB buffer and then added a buffer containing 100 mM Tris (Sigma), 100 µM acetyl CoA (Sigma), 100 µM DTNB (Sigma) and 0.1% Triton X (Sigma), followed by three more freeze/thaw cycles. The samples were then added to a 96-well plate (Greiner Bio-One) and kinetic measurement was performed at 412 nm in the BioTek Cytation 5 plate reader (BioTek) at baseline for 3.5 min. We then added 100 µM oxaloacetic acid (Sigma) and measured for an additional 10 min.

1.10. Quantitative PCR analyses

1.10.1. MtDNA integrity and copy number analyses

DNA was extracted using the QIAmp DNA Mini Kit (Qiagen) following the manufacturer's instructions. Transcription and copy number were measured using a real-time polymerase chain reaction (RT-PCR) method on the LightCycler

480 (Roche) with TaqMan probes for *D-loop, MT-ND1*, *MT-ND4,* and the nuclear single copy gene *B2M* as described.[6,7]

1.10.2. Digital PCR

DNA was quantified using a digital PCR (dPCR) assay with TaqMan probes specific for *MT-ND1* and *B2M*. dPCR was executed using the QuantStudio 3D Digital PCR System (Applied Biosystems) as published.[6, 7]

1.10.3. RNA extraction and quantitative PCR

RNA was prepared by using the RNeasy Mini Kit (Qiagen). RNA was then reverse-transcribed into cDNA using SuperScript III Reverse Transcriptase (ThermoFisher) and measured via RT-PCR using iQ SYBR Green Supermix (Biorad) on the LightCycler 480. Primer sequences are summarized in Table S5.

1.11. Laser capture microdissection

Frozen sections were fixed with 4% paraformaldehyde for 10 min and then washed in distilled water for 10 min. After three 5 min washes in TBST buffer, a TH primary antibody (Merck) was applied for 1 hr at room temperature. After three more washes, a secondary antibody (Santa Cruz) was applied for 30 min at room temperature. Following more washing, sections were incubated with DAB (Millipore) and 3% H2O2 for 4 min at room temperature and then washed in distilled water for 5 min. Single TH-positive neurons were isolated through laser capture microdissection (LCM) using the PALM MicroBeam (Zeiss) and captured in 15 µL of lysis buffer (50 mM Tris-HCl, pH 8.5, 1 mM EDTA, 0.5% Tween-20, 200 ng/mL proteinase K), centrifuged for 10 min at 20,000 x g at 4°C and then incubated for 3 hr at 55°C and 10 min at 95°C.

1.12. Single-nuclei RNA sequencing (snRNAseq) and data analysis

1.12.1. Tissue processing

Eight sections of the *PRKN*-mutant brain were pooled together for nuclei isolation. Tissue was collected in cold lysis buffer (10 mM Tris-HCl, 10 mM NaCl, 3 mM MgCl2, 0.1% NonidetTM P40). The resulting tissue suspension was

filtered and pelleted by centrifugation. Pellets were washed with 'nuclei wash and resuspension buffer' (1xPBS, 1% BSA, 0.2 U/µL RNase inhibitor) and then filtered and re-pelleted. Next, pelleted nuclei were incubated in DAPI solution (1.5 µM DAPI in 1x PBS) for 5 min prior to FACS-sorting. After dissociation, the nuclei suspension was subjected to FACS-sorting with FACSDiva Cell Sorter (BD Biosciences). Single DAPI-positive nuclei were sorted. To sequence harvested nuclei and prepare cDNA libraries, the Chromium Next GEM Single Cell 3'Kit v3.1 was used. The quality of resulting cDNA was assessed with the Agilent 2100 Bioanalyzer System.

1.12.2. Sequencing and data analysis

Sequencing was performed via Illumina NovaSeq 600-S2. Resulting data was processed identically to controls.[8] Briefly, after sequencing, the quantification of transcripts and filtering FASTQ files were produced from raw base call outputs with the Cell Ranger (10X Genomics) *mkfastq* pipeline v.3.0. Further, with the Cell Ranger (10X Genomics) count pipeline v.3.0 with default parameters, we obtained a gene-barcode UMI count matrix per sample. Considering that nuclei rather than cells were sequenced, we utilized the Cell Ranger recommended variation of the human reference transcriptome (hg38), which also annotates introns as exons. Only barcodes with more than 1500 UMIs and 1000 genes were included. Moreover, only those with less than 10% of mitochondrial-encoded and 10% ribosomal encoded genes were kept. Only genes detected in more than three barcodes were retained and ribosomal and mitochondrial-encoded genes were removed. With Scrubblet57, possible multiplet barcodes were identified, and such were kept with an estimated duplet score smaller than 0.15.

To determine the cell types comprising human midbrain tissue samples, we pooled the samples in a single embedding following the Seurat v3 integration workflow.[9] The top 4000 most variable genes were identified with *SelectIntegrationFeatures*, and used to determine the between-sample cell-anchors with *FindIntegrationAnchors*. The *IntegrateData* function was used to build a centered expression matrix, which was further used for principal component analysis. After, the Shared Nearest Neighbor (SNN) cell graph was built with the top 25 principal components and then clustered using the Louvain algorithm (resolution = 1.5) with the *FindClusters* function. With the FindAllMarkers function we detected the marker genes (expressed in minimally 25% of the cluster) for each cluster by using the default 'wilcox' test. With such top marker genes, each cell cluster was cell-type annotated. To

identify the differentially expressed genes in microglia, *FindMarkers* function with *logfc.threshold=0.25* and *min.pct=0.05* was used to compare microglia clusters between control and Parkin conditions. This list of differentially expressed genes was further utilized in pathway enrichment analysis with MetaCore software.

2. Supplementary figures

A

Disease Status	Sample	Sex	Age of Sampling	AAO	Gene	Mutation
Healthy	Control 1	M	39	N/A	N/A	N/A
Healthy	Control 2	F	37	N/A	N/A	N/A
Healthy	Control 3	M	40	N/A	N/A	N/A
Parkinson's disease	Parkin-PD 1	M	58	43	*PRKN*	c.1072Tdel (hom)
Parkinson's disease	Parkin-PD 2	M	57	15	*PRKN*	delEx4; + c.924C>T
Parkinson's disease	Parkin-PD 3	F	41	37	*PRKN*	del Ex1;c.924C>T
Alpers' disease	POLG	M	1 month	Birth	*POLG*	c.1399G>A; c.2740A>C

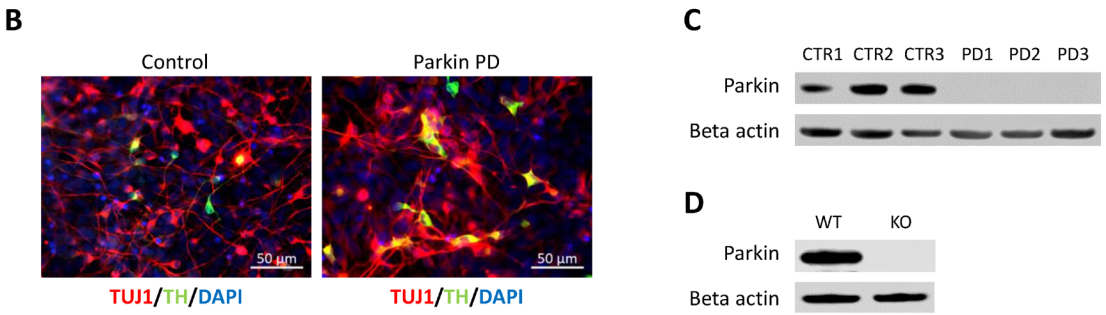

Figure S1 Derivation and characterization of iPSC-derived midbrain neurons and SH-SY5Y cells. (A) Overview of patients and controls included in the *in vitro* part of the study. **(B)** iPSC-derived neurons were stained for the neuronal marker TUJ1 and the catecholamine rate limiting enzyme tyrosine hydroxylase (TH). Images were taken using a 40x objective. **(C)** Parkin protein abundance in iPSC-derived patient and control neurons. Protein was extracted and subjected to Western blotting analysis using anti-Parkin and anti-beta-actin antibodies. Representative cropped images are shown. **(D)** Parkin protein abundance in control and isogenic Parkin-knockout SH-SY5Y cells. Representative cropped images are shown.

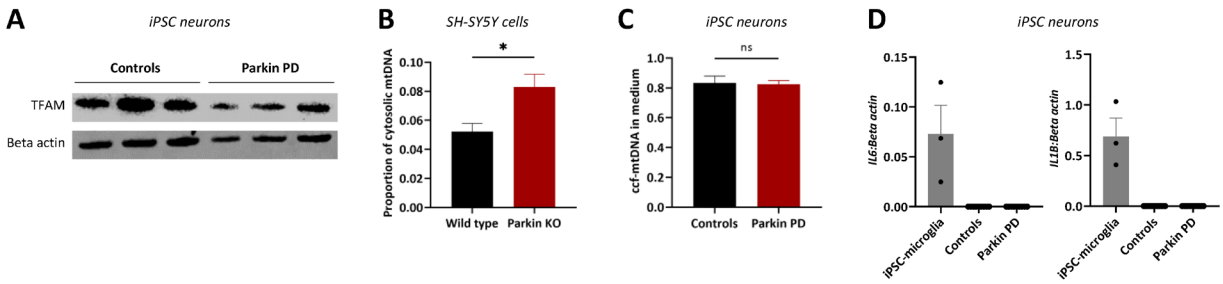

Figure S2 MtDNA dynamics and inflammation in PRKN-mutant and control iPSC-derived neurons. (A) Representative cropped Western blot images of TFAM and beta-actin. **(B)** Quantification of mtDNA in cytosolic and mitochondrial fractions from Parkin-PD and control iPSC-derived neurons. mtDNA levels were quantified by means of real-time PCR targeting the mtDNA fragment *ND1* and the nuclear single copy gene *B2M*. The proportion of cytosolic mtDNA normalized to cytosolic *B2M* copies was calculated relative to the total amount of cellular mtDNA copies. **(C)** Extracellular ccf-mtDNA in medium from Parkin-PD and control iPSC-derived neurons. Quantification by means of multiplex dPCR with probes against *ND1* and *B2M*. The proportion of extracellular *ND1* normalized to extracellular *B2M* copies was calculated relative to the total amount of mtDNA copies present in the medium and cells. **(D)** *IL6* and *IL1B* gene expression. *IL6* and *IL1B* levels were measured relative to the house-keeping gene *Beta-actin*. *IL6* and *IL1B* expression in iPSC-derived control microglia served as a positive control. n = 3 or 5 biological replicates, data are presented as the mean ± SEM; **P* < 0.05, ***P* < 0.01, ns = not significant as determined by student's t-test.

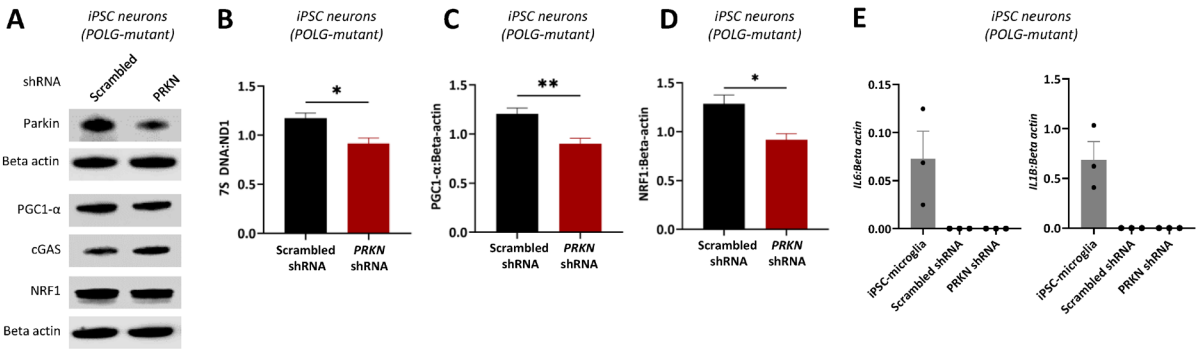

Figure S3 MtDNA dynamics and inflammation in iPSC-derived neurons from a compound-heterozygous POLG mutation carrier transduced with scrambled or PRKN shRNA. (A) Representative cropped images of Western blot membranes of whole cell lysates. Cells were harvested 5 days post transduction and subjected to Western blot analysis. **(B)** Quantification of 7S-associated transcription via multiplex RT-PCR. mtDNA transcription initiation events were determined by calculating the 7S DNA:ND1 ratios. **(C)** Quantification of PGC1-α protein levels relative to Beta-actin from (A). **(D)** Quantification of NRF1 protein levels relative to Beta-actin from (A). **(E)** *IL6* and *IL1B* gene expression in *POLG*-mutant iPSC-derived neurons transduced with scrambled or *RRKN* shRNA. *IL6* and *IL1B* levels were measured relative to *Beta-actin*. *IL6* and *IL1B* expression in iPSC-derived control microglia served as a positive control. n = 3 or 5 biological replicates, data are presented as the mean ± SEM; **P* < 0.05, ***P* < 0.01, as determined by student's t-test.

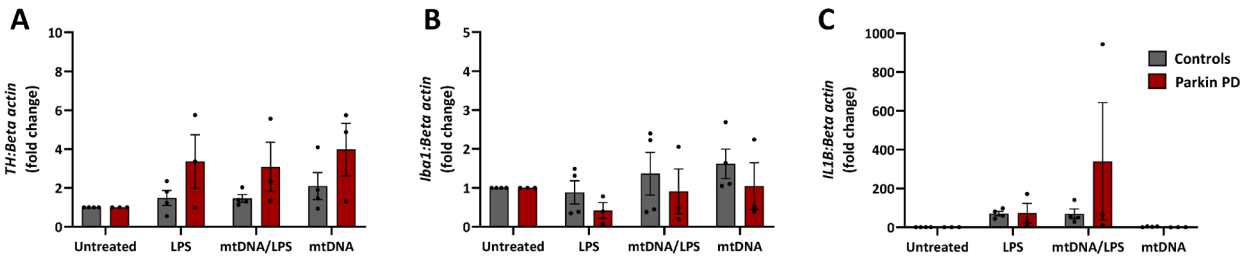

Figure S4 Expression of neuronal, microglial and inflammatory marker genes in PRKN-PD and control neuron-microglia co-cultures. (A) Dopaminergic neuron abundances in co-cultures. Expression of *TH* was measured relative to *Beta-actin* by means of qPCR. This assessment did not reveal significant differences between lines and treatments. **(B)** Microglia abundance in co-cultures. Quantifying the expression of the microglial marker gene *Iba1* relative to the house-keeping gene *Beta-actin* by qPCR did not show differences between investigated lines and treatments. **(C)** Pro-inflammatory cytokine analysis. Quantitative gene expression analysis of *IL1B* relative to *Beta-actin* revealed a non-significant upregulation in *PRKN*-PD co-cultures after co-treatment with LPS and mtDNA.

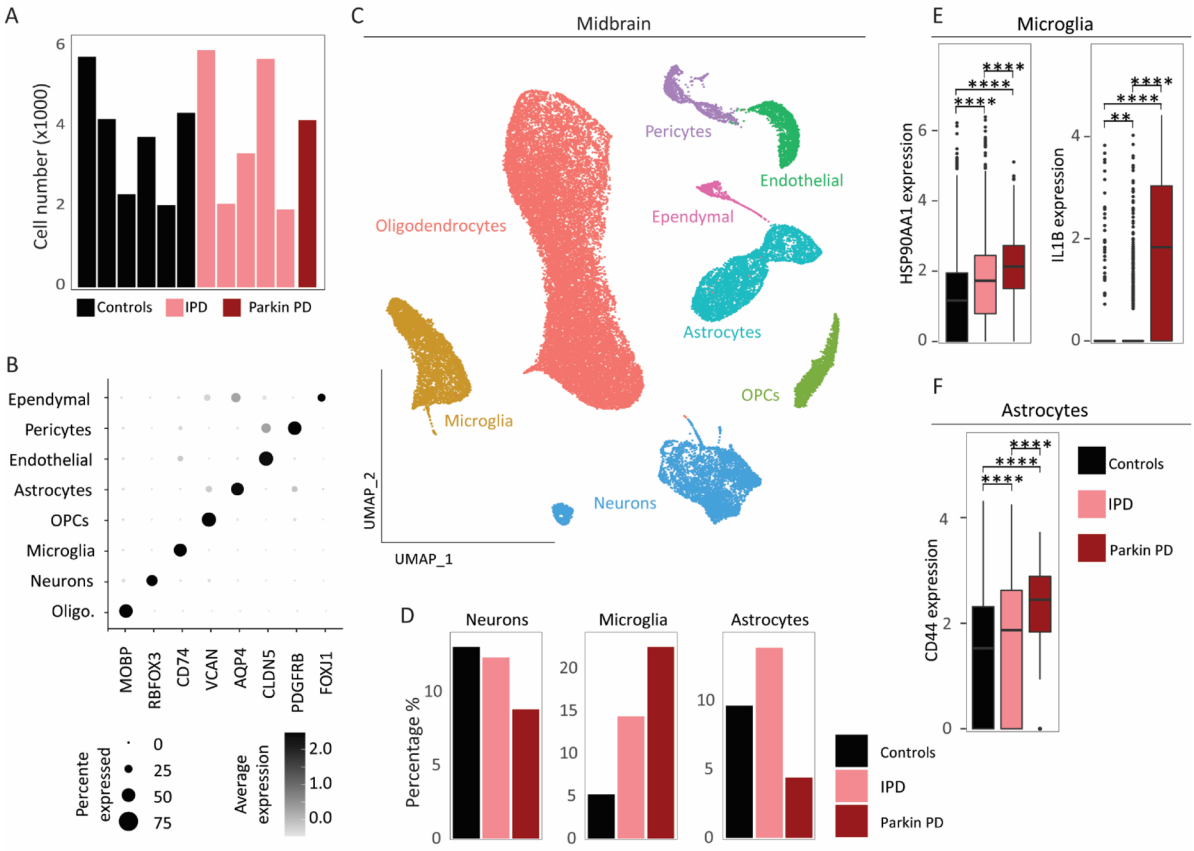

Figure S5 PRKN-mutant midbrain single-nuclei transcriptome comparison with six healthy controls and five idiopathic Parkinson's disease (IPD) cases. (A) Number of nuclei per sample. **(B)** Cell-type specific marker genes. **(C)** UMAP representation of 45.608 nuclei from *PRKN*-mutant, control and IPD midbrain samples. **(D)** Percentage of *PRKN*-mutant, control and IPD neuronal, astrocytic and microglia nuclei. **(E)** *CD44* gene expression in astrocytes in *PRKN*-mutant, control and IPD samples. **(F)** *HSP90AA1* and *IL1B* gene expression in microglia in *PRKN*-mutant, control and IPD samples.

3. Supplementary tables

Table S1 Marker genes for cell clusters

Table S2 Differentially expressed genes in *PRKN*-mutant midbrain microglia

Table S3 *PRKN*-mutant midbrain microglia; upregulated pathways

Table S4 *PRKN*-mutant midbrain microglia; downregulated pathways

(Tables S2-4 were submitted as csv files)

Table S5 Sequences of primers used in the study

Gene	Forward	Reverse
Beta-actin	5' - CGAGGACTTTGATTGCACATTGTT	5' - TGGGGTGGCTTTTAGGATGG
MT-ND1	5'- ATACCCACACCCACCCAAGAAC	5'- GGTTTGAGGGGGAATGCTGGA
MT-CYTB	5'- CTGATCCTCCAAATCACCACAG	5'- GCGCCATTGGCGTGAAGGTA
MT-COX1	5'-GGAGCAGGAACAGGTTGAACAG	5'-GTTGTGATGAAATTGATGGC
TFAM	5'-AAGATTCCAAGAAGCTAAGGGTGA	5'-CAGAGTCAGACAGATTTTTCCAGT
TFB2M	5'-TCTGGCAATTAGCTTGTGAG	5'-CTTACGCTTTGGGTTTTCCA
Twinkle	5'-ATTGTAGAAGGACGTGGACG	5'-TGCAGAGCTCACTCTAGGTG

4. References

1. Arena G, Cissé MY, Pyrdziak S, et al. Mitochondrial MDM2 Regulates Respiratory Complex I Activity Independently of p53. *Mol Cell*. 2018;69(4):594-609.e8. doi:10.1016/j.molcel.2018.01.023

1. Kriks S, Shim JW, Piao J, et al. Dopamine neurons derived from human ES cells efficiently engraft in animal models of Parkinson's disease. *Nature*. 2011;480(7378):547-551. doi:10.1038/nature10648

2. Haenseler W, Sansom SN, Buchrieser J, et al. A Highly Efficient Human Pluripotent Stem Cell Microglia Model Displays a Neuronal-Co-culture-Specific Expression Profile and Inflammatory Response. *Stem Cell Rep*. 2017;8(6):1727-1742. doi:10.1016/j.stemcr.2017.05.017

3. Reinhardt P, Glatza M, Hemmer K, et al. Derivation and expansion using only small molecules of human neural progenitors for neurodegenerative disease modeling. *PloS One*. 2013;8(3):e59252. doi:10.1371/journal.pone.0059252

4. Coore HG, Denton RM, Martin BR, Randle PJ. Regulation of adipose-tissue pyruvate dehydrogenase by insulin and other hormones. *Biochem J*. 1971;125(1):115-127

5. Grünewald A, Rygiel KA, Hepplewhite PD, Morris CM, Picard M, Turnbull DM. Mitochondrial DNA Depletion in Respiratory Chain-Deficient Parkinson Disease Neurons. *Ann Neurol*. 2016;79(3):366-378. doi:10.1002/ana.24571

6. Rygiel KA, Grady JP, Taylor RW, Tuppen HAL, Turnbull DM. Triplex real-time PCR--an improved method to detect a wide spectrum of mitochondrial DNA deletions in single cells. *Sci Rep*. 2015;5:9906. doi:10.1038/srep09906

7. Smajić S, Prada-Medina CA, Landoulsi Z, et al. Single-cell sequencing of human midbrain reveals glial activation and a Parkinson-specific neuronal state. *Brain*. Published online December 17, 2021:awab446. doi:10.1093/brain/awab446

8. Stuart T, Butler A, Hoffman P, et al. Comprehensive Integration of Single-Cell Data. *Cell*. 2019;177(7):1888-1902.e21. doi:10.1016/j.cell.2019.05.031